

2nd International Workshop on Dynamics in Viscous Liquids

Mainz, April 9-12, 2006

Programme

Organization

Gerald Hinze, Jürgen Horbach and Wolfgang Paul

Table of Contents

Organizational Information

Welcome	5
Organization	6
Map of conference location	7
List of lunch sites	8
Bus information	8

Programme

Timeline	9
Session Schedule	10

Abstracts

Abstracts of oral contributions	17
Abstracts of poster contributions	67

List of participants

121

Welcome

We welcome you all in Mainz to the 2nd International Workshop on Dynamics in Viscous Liquids.

This second workshop follows up on the scientific scope set by the first one in Munich in 2004. It aims to provide a forum for discussions on the dynamics in viscous liquids for scientists addressing this problem for different materials and with different perspectives. A central topic will again be viscous dynamics accompanying the glass transition in materials ranging from metallic and oxidic glass formers, to molecular systems, colloids and polymers. Universal as well as specific properties will be discussed from the experimental as well as the theoretical perspective. A special emphasis will also be laid on the non-equilibrium response of glass forming systems. Another topic will be viscous slowing down due to complexity of the architecture of the materials building blocks, e.g., reptation in polymers or living polymers of sulphur.

Being encouraged by the predominantly positive experience from the Munich workshop, we kept the special organizational structure of this workshop series. There will be no invited talks or key note lectures. Instead, all of the programme was put together during a meeting of the Programme Committee in November 2005. The decisions were made solely on the basis of the extended abstracts collected in this booklet, that had been submitted before. We are deeply indebted to the members of the Programme Committee for their careful work. We are also grateful to the participants of this workshop who again have sent in a large number of excellent contributions.

The programme has been laid out to allow for intensive discussions. There are no parallel sessions and all talks have a length of only 20 minutes including questions, aiming to stimulate further discussions of the presented topics during the breaks. All posters will be put up for the complete time of the meeting and there is ample time for discussions at the poster contributions.

The workshop takes place in the lecture hall P1 of the Philosophicum at the Johannes Gutenberg-University in Mainz. We are grateful to the Johannes Gutenberg-University for supporting this workshop. We also gratefully acknowledge financial help by the EU Network of Excellence SOFTCOMP (Soft Matter Composites) and by the collaborative research projects SFB TR6 and SFB 625 funded by the German Science Foundation.

We wish all of you an inspiring meeting filled with lively discussions and a pleasant stay in Mainz.

Programme Committee

J. Colmenero	Universidad del Pais Vasco, San Sebastian, Spain
L. Cugliandolo	Ecole Normale Supérieure, Paris, France
W. Götze	Technische Universität, München, Germany
W. Kob	Université Montpellier II, Montpellier, France
W. Poon	The University of Edinburgh, Edinburgh, UK
K. Samwer	Georg-August-Universität, Göttingen, Germany
H. Sillescu	Johannes Gutenberg-Universität, Mainz, Germany
A. Sokolov	University of Akron, Akron, USA
G. Szamel	Colorado State University, Fort Collins, USA

Organization

G. Hinze	Institut für Physikalische Chemie, Universität Mainz
J. Horbach	Institut für Physik, Universität Mainz
W. Paul	Institut für Physik, Universität Mainz

Conference Office

Institut für Physik
Johannes Gutenberg-Universität
Staudinger Weg 7
55099 Mainz

Phone: +49-6131-3923680
Fax: +49-6131-3925441
Email: visliqu@socrates.physik.uni-mainz.de

Conference Location

Philosophicum, Lecture Hall P1
Johannes Gutenberg-Universität
Jakob Welder Weg 18
55099 Mainz

List of lunch places on Campus

Restaurants

1. Ristorante Campus, Italian Restaurant next to the Mensa building
2. Taberna Academica, in the “Alte Mensa“ building at the forum of the university
3. Benno Wischmann house, next to the stadium of the university

Cafeterias of the university

1. in the Mensa building, top floor (the regular lines in the Mensa are only accessible if you have a special card of the Mainzer Studentenwerk)
2. in the ReWi building (house of law and economics) back towards main university entrance along Jakob Welder Weg
3. in the Philosophicum

Döner Kebab places

1. next to the lecture hall building called “Muschel“ on Becherweg
2. in the student housing “Inter I“ towards the Mensa on Jakob Welder Weg

Down town

If you prefer to take a bus down town, there are many possibilities.

Bus information

Going up to campus: In front of the Central Railway Station (Hbf) you will find the bus platform G. There are buses to **Friedrich-von-Pfeiffer-Weg**. You can take buses 54, 55, 58 and 68 (destination Lerchenberg, Finthen, Wackernheim and Klein-Winternheim, respectively). Other lines (6, 6A, 56, 57) go up to the university but pass only by the front entrance to the campus. If you have a hotel close to the dome or the Altstadt, buses 54 and 55 also leave from the stops “Höfchen“ and “Schillerplatz“.

Going into town: To reach the train station you can take any bus going into town from Friedrich-von-Pfeiffer-Weg or the campus entrance.

Programme Timeline

	Sunday		Monday	Tuesday	Wednesday
		09:00 -10:20	Session 3	Session 7	Session 10
		10:20 -10:50	Coffee and Discussions		
		10:50 -12:10	Session 4	Session 8	Session 11
12:30 -14:00	Registration & Welcome	12:10 -14:00	Lunch		
14:00 -15:20	Session 1	14:00 -15:20	Session 5	Poster	Session 12
15:20 -15:50	Coffee and Discussions	15:20 -15:50	Coffee & Discussions		
15:50 -17:30	Session 2	15:50 -17:20	Poster	Poster	
		17:20 -18:40	Session 6	Session 9	
		Evening		Conference Dinner	

Sunday Afternoon

12:30	Registration and Welcome
14:00-15:20	Session 1, Chairperson: D. Chandler
14:00	<u>Giulio Biroli</u> <i>Direct experimental evidence of a growing length scale escorting the glass transition</i>
14:20	<u>Ludovic Berthier</u>, <u>Giulio Biroli</u>, <u>Cristina Toninelli</u>, <i>Understanding the role of activated processes by controlling their strength</i>
14:40	<u>Gilles Tarjus</u>, <u>F. Sausset</u>, <u>P. Viot</u> <i>Geometric frustration and the glass transition: the Lennard-Jones liquid on a hyperbolic plane</i>
15:00	<u>Andreas Heuer</u>, <u>Aimorn Saksaengwijit</u> <i>Can the dynamics of silica be predicted from properties of the potential energy landscape</i>
15:20-15:50	Coffee and Discussions
15:50-17:30	Session 2, Chairperson: W. Kob
15:50	<u>David Reichman</u>, <u>Peter Mayer</u>, <u>Kunimasa Miyazaki</u> <i>Mode-Coupling Hierarchy: a Non-perturbative, Microscopic Approach to the Dynamics of Glass-Forming Liquids</i>
16:10	<u>Juan P. Garrahan</u>, <u>David Chandler</u> <i>Dynamical facilitation view of glass formers</i>
16:30	<u>Alexandre Lefevre</u> <i>Dynamical field theory for glass forming liquids, self-consistent resummations and time-reversal symmetry</i>
16:50	<u>Jean-Philip Bouchaud</u>, <u>Giulio Biroli</u> <i>On the Adam-Gibbs-Kirkpatrick-Thirumalai-Wolynes scenario for the viscosity increase in glasses</i>
17:10	<u>Andrea Cavagna</u> <i>Viscoelasticity and metastability limit in supercooled liquids</i>

Monday Morning

09:00-10:20 Session 3, Chairperson: C. Alba-Simionesco	
09:00	<u>Grant D. Smith</u>, Dmitry Bedrov <i>A Molecular Dynamics Simulation Study of the α and β Relaxation Processes in 1,4-Polybutadiene</i>
09:20	S.-H. Chong, M. Aichele, H. Meyer, M. Fuchs, <u>Jörg Baschnagel</u> <i>Structural and conformational dynamics of simulated glass-forming polymer melt</i>
09:40	<u>I.Sergueev</u>, U. van Bürck, A. I. Chumakov, T. Asthalter, R. Ruffer <i>The non-translational origin of the slow beta relaxation</i>
10:00	<u>Daniele Cangialosi</u>, Angel Alegria, Juan Colmenero <i>A thermodynamic approach to the fragility of glass-forming polymers</i>
10:20-10:50 Coffee and Discussions	
10:50-12:10 Session 4, Chairperson: W. Schirmacher	
10:50	<u>Andreas Meyer</u>, Florian Kargl, Emmanuel Longueteau <i>Mechanism of Ionic Transport in Viscous Sodium Borate Melts</i>
11:10	<u>Thomas Voigtmann</u>, Jürgen Horbach <i>Slow Dynamics and Fast Ion Diffusion in Sodium Silicates - Simulation and Mode-Coupling Theory</i>
11:30	<u>Michael Vogel</u> <i>The glass transition of polymer melts in the presence and the absence of ions: Multidimensional nuclear magnetic resonance and molecular dynamics simulation studies</i>
11:50	<u>Angel J. Moreno</u>, Juan Colmenero <i>Is there a high-order Mode Coupling transition in polymer blends?</i>
12:10-14:00 Lunch	

Monday Afternoon

14:00-15:20	Session 5, Chairperson: K. Binder
14:00	<u>R. Besseling</u>, A. B. Schofield, W. C. K. Poon, E. R. Weeks <i>Realtime 3D imaging of heterogeneities and yielding in a sheared colloidal glass</i>
14:20	<u>Francesca Ianni</u>, S. Gentilini, R. Di Leonardo, G. Ruocco <i>Liquid and solid phases in a soft glassy colloidal suspension under shear</i>
14:40	<u>Fathollah Varnik</u>, Oliver Henrich, Matthias Fuchs <i>Rheological response of a model glass: Theory versus computer simulation</i>
15:00	<u>Oliver Henrich</u>, Matthias Fuchs, Jérôme Crassous, Matthias Ballauf <i>Nonlinear Rheology of Colloidal Suspensions</i>
15:20-15:50	Coffee and Discussions
15:50-17:20	Poster
17:20-18:40	Session 6, Chairperson: M. Allen
17:20	<u>W. C. K. Poon</u>, K. N. Pham, G. Petekedis, S. U. Egelhaaf, D. Vlassopoulos, P. N. Pusey <i>Topological and bond yielding in colloidal glasses</i>
17:40	<u>Emanuela Zaccarelli</u>, I. Saika-Voivod, S. V. Buldyrev, A. J. Moreno, P. Tartaglia, F. Sciortino <i>Gel to glass transition in simulation of a valence-limited colloidal system</i>
18:00	<u>Emanuela Del Gado</u>, Walter Kob <i>Length scale dependent relaxation in colloidal gels</i>
18:20	<u>Matthias Fuchs</u> <i>Fluctuation dissipation relations in stationary states of interacting Brownian particles under shear</i>

Tuesday Morning

09:00-10:20 Session 7, Chairperson: J. Colmenero	
09:00	<u>Kurt Kremer</u>, L . Delle-Site, N. van der Vegt, B. Hess <i>Polymer Dynamics and Long Time Atomistic Trajectories</i>
09:20	<u>Jens-Uwe Sommer</u> <i>Topological Disorder, Large Scale Heterogeneities and Long Time Relaxation Behavior in Polymer Networks. Models and Monte Carlo Simulations</i>
09:40	S. Rastogi, D. R. Lippits, G. W. M. Peters, R. Graf, Y. Yao, <u>H. W. Spiess</u> <i>Structural and dynamic heterogeneity of polymer melts from melting polymer crystals</i>
10:00	<u>M. Zamponi</u>, A. Wischnewski, M. Monkenbusch, L . Willner, D. Richter, B. Farago <i>Anomalous diffusion in short chain polymer melts</i>
10:20-10:50 Coffee and Discussions	
10:50-12:10 Session 8, Chairperson: H. Schober	
10:50	<u>Horacio E. Castillo</u>, Azita Parsaeian <i>Spatial correlations of fluctuations in the aging dynamics of glasses</i>
11:10	Sylvain Mazoyer, Luca Cipelletti, <u>Laurence Ramos</u> <i>Origin of the slow dynamics and the aging of a soft glass</i>
11:30	<u>Roberta Angelini</u>, Giancarlo Ruocco <i>Inverse Melting, Underheating and Glass Transition</i>
11:50	<u>Gregor Diezemann</u> <i>Aging effects in trap models for glassy relaxation</i>
12:10-14:00 Lunch	

Tuesday Afternoon

14:00-15:20	Poster
15:20-15:50	Coffee and Discussions
15:50-17:20	Poster
17:20-18:40	Session 9, Chairperson: R. Schilling
17:20	<u>Thomas Franosch, Felix Höfling, Erwin Frey</u> <i>The Localization Transition of the 3D Lorentz Model and Continuum Percolation</i>
17:40	<u>Norio Kikuchi, Jürgen Horbach</u> <i>Dynamics of mobile particles in an immobile environment: Simulation of a binary Yukawa system</i>
18:00	<u>Vincent Krakoviack</u> <i>Mode-coupling theory for the liquid-glass transition of a fluid confined in a disordered porous matrix</i>
18:20	<u>Vakhtang Rostiashvili, A. Milchev, G. Migliorini, T. A. Vilgis</u> <i>Polymer chain in a quenched random medium: slow dynamics and ergodicity breaking</i>

Wednesday Morning

09:00-10:20	Session 10, Chairperson: C. Dreyfus
09:00	<u>Jeppe Dyre</u>, Niels Boye Olsen, T. Christensen <i>Elastic models for viscous liquids</i>
09:20	<u>Arantxa Arbe</u>, M. Tyagi, J. Colmenero, B. Frick, R. Stewart <i>Self-Confinement Effects in Extremely Diluted Polymer Blends</i>
09:40	<u>Giulio Monaco</u>, L. Crapanzano, R. Bellissent, W. Chrichton, D. Fioretto, M. Mezouar, F. Scarponi, R. Verbeni <i>Rubber-like dynamics in sulfur above the T_g-transition temperature</i>
10:00	<u>Ravinath Kausik</u>, Carlos Mattea, Rainer Kimmich, Nail Fatkullin, Nicola Hüsing <i>Emergence and establishment of the Corset Effect in mesoscopic polymer melt layers : A crossover from bulk to confined dynamics</i>
10:20-10:50	Coffee and Discussions
10:50-12:10	Session 11, Chairperson: T. Palberg
10:50	<u>Jose B. Caballero</u>, Antonio M. Puertas, M. E. Cates <i>Phase Diagram and Glass Transitions in Oppositely Charged Colloids</i>
11:10	<u>Hans-Joachim Schöpe</u> <i>Homogeneous nucleation kinetics of model charged sphere suspensions: a Different Route into the Glassy State?</i>
11:30	<u>Tullio Scopigno</u> <i>Infrared Photon correlation Spectroscopy: a novel experimental technique for investigation of dynamics in viscous liquids</i>
11:50	<u>Gurpreet S. Matharoo</u>, Subir K. Sarkar <i>Universality in the Vibrational Spectra of Amorphous Systems</i>
12:10-14:00	Lunch

Wednesday Afternoon

14:00-15:20	Session 12, Chairperson: U. Buchenau
14:00	A. Azzimani, C. Dreyfus, <u>R. M. Pick</u>, A. Taschin, P. Bartolini, R. Torre <i>A Transient Grating study of the molecular glass former m-toluidine to the vicinity of its glass transition temperature</i>
14:20	A. Nowaczyk, <u>B. Geil</u>, M. Winterlich, G. Hinze, G. Diezemann, R. Böhmer <i>Correlation of primary relaxations and high-frequency modes in supercooled liquids</i>
14:40	<u>Matthias Sperl</u> <i>Cole-Cole Dynamics in Molecular and Colloidal Liquids</i>
15:00	V. Bercu, M. Martinelli, C. A. Massa, L. A. Pardi, <u>D. Leporini</u> <i>The exponential distribution of the landscape energy-barriers and the fast dynamics of glassy polymers: evidences from high-field Electron Paramagnetic Resonance of molecular guests</i>

Direct experimental evidence of a growing lengthscale escorting the glass transition

Giulio Biroli*

Service de Physique Théorique Orme des Merisiers CEA Saclay, 91191 Gif sur Yvette Cedex, France

After decades of research, a clear picture of the glass transition phenomenon, a rather mundane observation, common to scores of different materials (molecular glasses, polymers, colloids) is still lacking. The conundrum is that the static structure of a glass is indistinguishable from that of the corresponding liquid, with no sign of increasing static correlation lengthscales escorting the glass transition. Numerical simulations performed well above the glass temperature, T_g , reveal instead the existence of a growing dynamic lengthscale [1] associated to dynamic heterogeneities [2]. This result has been obtained by measuring a “four-point” dynamic susceptibility $\chi_4(t)$, which quantifies the amplitude of spontaneous fluctuations around the average dynamics [1]. The susceptibility $\chi_4(t)$ typically presents a nonmonotonic time dependence with a peak centered at the liquid’s relaxation time [1]. The height of this peak is proportional to the volume within which correlated motion takes place. Experimentally, detecting spontaneous fluctuations of dynamic correlators remains an open challenge, since dynamic measurements have to be resolved both in space and time. However, clever experiments [2] have shown indirect evidences for a dynamic correlation lengthscale of about 5-20 molecular diameters at T_g , but its time and temperature dependences were not determined, a missing information crucial to ascertain its relation with the glass transition and contrasting different theoretical scenarii. In this talk we present [3] quantitative experimental evidence based on rigorous theoretical results that glass formation in molecular liquids and colloids is accompanied by at least one growing dynamic lengthscale.

The key idea is that induced fluctuations are more easily accessible experimentally than spontaneous ones, and can be related to one another by fluctuation-dissipation theorems. We introduce a new dynamic susceptibility defined as the response of a correlator $F(t)$ to a perturbing field x , $\chi_x(t) = \frac{\partial F(t)}{\partial x}$. We shall consider as perturbing field the control parameter for the glass transition: the temperature, T , for supercooled liquids and the packing fraction, φ , for colloidal hard spheres. We will show that linear response formalism allows one to relate $\chi_x(t)$ to dynamic correlations. Therefore, $\chi_x(t)$ is an experimentally accessible multi-point dynamic susceptibility that directly quantifies dynamic heterogeneity in glass-formers. We will show our experimental and numerical measures of $\chi_x(t)$ in two representative glass-formers: glycerol and

hard sphere colloids. Furthermore we will show using fluctuation theory that from $\chi_x(t)$ one can obtain a *rigorous* lower bound for $\chi_4(t)$. Our numerical simulations on a binary Lennard-Jones mixture suggest that this bound is actually saturated, and that it pro-

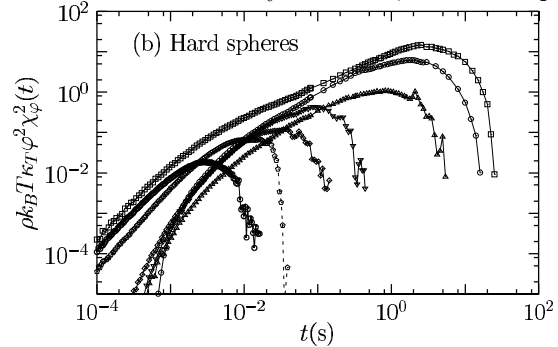


FIG. 1: Lower Bound (or estimate) of $\chi_4(t)$, for hard sphere colloids. The curves correspond to different packing fractions: from left to right, $\varphi = 0.18, 0.34, 0.42, 0.46, 0.49, 0.50$. In this case $\chi_4(t)$ measures the fluctuations of the normalized intermediate scattering function, F , for a wavevector close to the first peak of the static structure factor.

vides a good estimate in the regime of slow dynamics. The experimental estimate (or lower bound) of $\chi_4(t)$ is shown in Fig. 1 for hard sphere colloids. Assuming that correlators obey time-temperature superposition we obtain an estimate of the dynamic correlation length for many other glass-forming liquids too. Its variation with fragility will be presented and compared to available theoretical predictions. Finally, we will discuss the general relationship between length and time scales that follows from our theoretical results.

* Electronic address: biroli@cea.fr

- [1] H.C. Andersen, PNAS **102** 6686 (2005).
- [2] Ediger, M.D., *Annu. Rev. Phys. Chem.* **51**, 99-128 (2000).
- [3] L. Berthier, G. Biroli, J.-P. Bouchaud, L. Cipelletti, D. El Masri, D. L’Hôte, F. Ladieu, M. Pierno, *Direct experimental evidence of a growing lengthscale escorting the glass transition*, accepted for publication as a Report in Science.

Understanding the role of activated processes by controlling their strength

 Ludovic Berthier,^{1,*} Giulio Biroli,² and Cristina Toninelli²
¹*Laboratoire des Colloïdes, Verres et Nanomatériaux,*
Université Montpellier II and CNRS, 34095 Montpellier, France
²*Service de Physique Théorique Orme des Merisiers – CEA Saclay, 91191 Gif sur Yvette Cedex, France*

When dealing with theories describing the physics of supercooled liquids approaching the glass transition there is a clear temperature gap between the description offered by mode-coupling theory which is usually applied far above the glass temperature T_g , and more phenomenological approaches which describe the activated relaxation of liquids close to T_g .

All these approaches somehow claim to capture the correct physics. The common folklore says however that physics has a mean-field, non-activated character above the mode-coupling temperature T_c , and it becomes spatially heterogeneous and activated below T_c where new “physical processes” appear. In recent years, many detailed studies have shown that this view is most certainly incorrect: even above T_c the dynamics is spatially heterogeneous and activated processes are present. It is therefore not even clear how and when a mean-field mode-coupling description holds.

To understand this point we have devised a kinetically constrained lattice model where the strength of activated processes can be controlled by an external geometrical parameter, R . This is a standard spin facilitated model [1] where the lattice has locally the structure of a Bethe lattice, but for distances larger than R , it becomes an ordinary square lattice. In the limit of $R \rightarrow \infty$ the model lives on the Bethe lattice and exhibits a mode-coupling like singularity [2] at a finite temperature T_c while for $R = 1$ the model is a standard Fredrickson-Andersen model characterized by a zero-temperature critical point [3]. For finite R , the model smoothly interpolates between these two limiting behaviours and the singularity at T_c is avoided. The geometrical parameter R therefore allows us to control the strength of activated processes, and this opens the possibility to study their influence

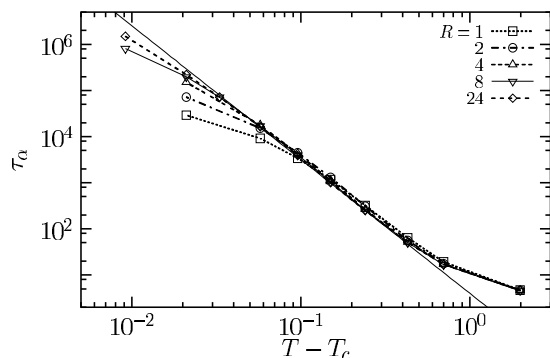


FIG. 1: Equilibrium relaxation timescales for various R in a representation where the power law $\tau_\alpha \sim (T - T_c)^{-\gamma}$ is a straight line. The strength of activated processes diminishes when R increases leading to a wider range of validity of a power law regime.

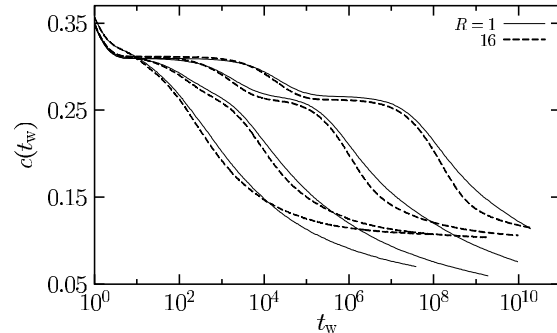


FIG. 2: Time decay of the energy density following a sudden quench from $T = \infty$ down to 4 different low temperatures decreasing from left to right. At large R the system remains blocked in some high energy “threshold” state while for smaller R deeper metastable states can be probed in an activated fashion.

on the glassy dynamics in some detail.

This is illustrated in Fig. 1 where equilibrium relaxation timescales are shown. For large R the dynamics resembles the one predicted by mode-coupling theory, and timescales diverge as a power law. The range of validity of this power law regime shrinks when R diminishes: the singularity is avoided because of activated processes.

A similar crossover is found in the aging regime following a sudden quench to low temperatures, see Fig. 2. The system follows the peculiar dynamics predicted from the mean-field studies [4] for large R but probes deeper and deeper metastable states in an activated manner for smaller R .

In this talk I will present the results obtained from extensive numerical studies of this model to study both the equilibrium dynamical slowing down upon decreasing temperature and the non-equilibrium aging regime. I will also discuss the consequences for our understanding of how activated processes appear and influence the dynamics of real supercooled liquids.

* Corresponding author: berthier@lcvn.univ-montp2.fr

- [1] G.H. Fredrickson and H.C. Andersen, Phys. Rev. Lett. **53**, 1244 (1984).
- [2] C. Toninelli, G. Biroli, and D.S. Fisher, Phys. Rev. Lett. **92**, 185504 (2004).
- [3] S. Whitelam, L. Berthier and J.P. Garrahan, Phys. Rev. Lett. **92**, 185705 (2004).
- [4] L.F. Cugliandolo and J. Kurchan, Phys. Rev. Lett. **71**, 173 (1993).

Geometric frustration and the glass transition: the Lennard-Jones liquid on a hyperbolic plane

G. Tarjus*, F. Sausset and P. Viot

LPTMC, University P. & M. Curie, 4 Place Jussieu, 75005 Paris, France

Geometric frustration, *i.e.* an incompatibility between extension of the local order preferred in a liquid and tiling of the whole space, has been proposed as a physical mechanism for explaining the glass transition and the phenomenology of supercooled liquids [1,2]. In this work we check the fundamentals of the frustration-based theoretical scenario by investigating, both by MD simulation and analytical means, what seems to be the simplest yet tractable frustrated liquid model: a Lennard-Jones fluid on a hyperbolic plane. Indeed, the 2-dimensional system of disks on a flat (Euclidean) plane is unfrustrated because the local hexagonal order can propagate in space to form a triangular lattice. Placing the system in hyperbolic geometry introduces frustration, whose strength is associated with the curvature of the hyperbolic plane.

We have generalized the standard MD algorithm (equations of motion and periodic boundary conditions) to hyperbolic geometry. This is the first time that such a study is undertaken. It allows an investigation of the dynamic and static properties of the model, both as a function of temperature (and density) and as a function of the degree of frustration, *i.e.* the curvature of space. We focus on the behavior of the diffusion constant and discuss the connection between "dynamic fragility" and frustration.

To relate the slowing down of motion as temperature decreases to microscopic characterizations of the frustration, we have studied the topological defects, point-like disclinations and dislocations, that are present in the liquid. This provides a means to describe the interplay between structure and dynamics.

Finally, we discuss the statistical mechanics of frustration and the way to derive a coarse-grained description of frustrated liquid systems that could provide a minimal theoretical model for studying real glassforming liquids.

* Corresponding author: tarjus@lptl.jussieu.fr

[1] G. Tarjus et al., *J. Phys.: Condensed Matter* **17**, (2005); cond-mat/0508267.

[2] D. Nelson, *Defects and Geometry in Condensed Matter Physics* (Cambridge University Press, Cambridge, 2001).

Can the dynamics of silica be predicted from properties of the potential energy landscape?

Andreas Heuer* and Aimorn Saksaengwijit

WWU Münster, Inst. f. Phys. Chemie, Corrensstr. 30, D-48149 Münster

The thermodynamics and dynamics of silica has been studied in great detail [1-3]. From knowledge of the configurational entropy on the one hand and the diffusion constant on the other hand it has been possible to check the prediction of the Adam-Gibbs relation [2,3]. Furthermore, it has been clearly seen that the potential energy landscape of silica displays a low-energy cutoff which is probably related to the network structure of silica because of the presence of amorphous low-energy states with a high local tetrahedral order [3,4]. In agreement with the case of the binary mixture Lennard-Jones (BMLJ) case the energy distribution of inherent structures of silica can be described as a Gaussian for energies above the cutoff. Complete information is presently available to express relevant thermodynamic quantities like the average energy in terms of properties of the potential energy landscape.

In recent years we have developed numerical techniques to characterize relevant properties of the potential energy landscape in a systematic way in order to improve the understanding of the long-range transport [5]. One key element in this analysis is the definition and identification of metabasins.

The goal of the present contribution is fourfold.

- (1) We check to which degree the properties of the potential energy landscape of silica are different as compared to the binary mixture Lennard Jones (BMLJ) system [6]. It turns out that the nature of the potential energy landscape, giving rise to local relaxation processes, is surprisingly similar for both systems. There is, however, one dramatic difference. The temperature-dependence of the escape rate from a low-energy configuration of silica is Arrhenius-like with an attempt frequency which is 10^5 times larger than typical microscopic frequency scales. In contrast, for the BMLJ system no significant variations of the attempt frequencies have been observed.
- (2) We analyze whether the observed transition of the Non-Arrhenius to Arrhenius temperature dependence [1] is only due to the cutoff in the potential energy landscape or whether it is also embedded in the local properties of the landscape. For example it is conceivable that the low-temperature relaxation is basically due to bond breaking events with a relatively well-defined activation energy which would then translate into the Arrhenius temperature dependence of macroscopic diffusion.

- (3) We formulate in general terms, how the macroscopic dynamics can be explained in terms of local processes. In particular it is clarified how the interplay of entropic and energetic aspects influences the local dynamics. The entropic contributions mainly stem from the multitude of high-energy states which the system has to cross to move from one low-energy (often defect-free) structure to another.
- (4) Having studied the characteristics of the potential energy landscape, we can identify a minimum set of parameters which characterize its relevant properties for the thermodynamics and the dynamics. Then we can answer for example the question how the degree of fragility is related to these parameters. Surprisingly, it turns out that silica is significantly more fragile than the BMLJ system, if artificially the cutoff of the potential energy landscape is removed by extending the gaussian distribution of states. Furthermore, a direct connection between the kinetic and the thermodynamic fragility can be formulated in terms of potential energy landscape parameters.

In summary, the macroscopic silica dynamics can be expressed in terms of the thermodynamics and the local properties of the potential energy landscape. This insight may be also relevant for other amorphous network-formers like water.

* Corresponding author: andheuer@uni-muenster.de

- [1] J. Horbach and W. Kob, Phys. Rev. B 60, 3169 (1999).
- [2] I. Saika-Voivod et al, Nature 412, 514 (2001).
- [3] I. Saika-Voivod et al, Phys. Rev. E 69, 041503 (2003).
- [4] A. Saksaengwijit et al, Phys. Rev. Lett. 93, 235701 (2004).
- [5] B. Doliwa, A. Heuer, Phys. Rev. E 67, 031506 (2003); 031506 (2003).
- [6] J. Reinisch, A. Heuer, Phys. Rev. Lett. 95, 155502 (2005).

The Mode-Coupling Hierarchy: a Non-perturbative, Microscopic Approach to the Dynamics of Glass-Forming Liquids.

**David Reichman, Peter Mayer, and Kunimasa Miyazaki
Columbia University, New York, NY 10027**

Idealized mode-coupling theory (IMCT) has been a remarkably useful first-principles approach that yields detailed predictions for various properties of supercooled liquids and colloidal suspensions [1]. It is well known that the IMCT predicts a glass transition at higher temperatures or lower densities than that observed in the laboratory. For non-Brownian systems, various versions of extended mode-coupling theories (EMCT) have been put forward as a means of describing the "hopping" motion that rounds off the transition predicted by the IMCT [2,3]. These theories invoke a coupling to the current modes. Recent work has pointed to some problems with various versions of EMCT. Simulations of Brownian systems (where the momentum current should not effectively couple to slow relaxation) have demonstrated that deviations from IMCT can be as large as they are in Newtonian systems [4]. Theoretical work has also cast doubt on the role of the current mode in EMCT [5,6]. In this talk I will discuss the microscopic foundation for a coupled hierarchy of mode-coupling equations [7]. The schematic version of this hierarchy contains essentially the same number of control parameters as the original schematic IMCT equation [8]. The hierarchy contains IMCT [1,8] and higher-order versions [9,10] as special cases. It is shown that the non-perturbative limit of this hierarchy produces a dynamics devoid of a sharp glass transition with an asymptotically exponential (as opposed to power-law) form of the relaxation time with respect to thermodynamic control parameters. The non-perturbative analysis of the hierarchy does not make use of the momentum mode, completely avoids any factorization approximation, and approximately employs all multi-linear products of slow (density) modes. Interestingly, many of the useful properties of the IMCT are approximately preserved. Comparison to simulation, and a discussion of the description of dynamic heterogeneity and the violation of the Stokes-Einstein relation will be briefly presented.

- [1]W. Gotze and L. Sjogren, Rep. Prog. Phys., 55, 241, (1992).
- [2]W. Gotze and L. Sjogren, Z. Phys. B, 65, 415, (1987).
- [3]S.P. Das and G. F. Mazenko, Phys. Rev. A 34, 2265, (1986).
- [4]G. Szamel and E. Flenner, Europhys. Lett. 67, 779 (2004).
- [5]A. Andreatov, G. Biroli, and A. Lefevre, cond-mat/0510699 (2005).
- [6]M.E. Cates and S. Ramaswamy "Do Current-Density Nonlinearities Cut Off the Glass Transition?" (to be submitted).
- [7]P. Mayer, K. Miyazaki and D.R. Reichman "The Mode-Coupling Hierarchy: a Non-perturbative, Microscopic Approach to the Dynamics of Glass-Forming Liquids" (to be submitted).
- [8]U. Bengtzelius, W. Gotze and A. Sjolander, J. Phys. C, 33, 5915 (1984).
- [9]G. Szamel, Phys. Rev. Lett., 90, 228301 (2003).
- [10] J.L. Wu, and J.S. Cao, Phys. Rev. Lett., 95, 078301, (2005).

Dynamical facilitation view of glass formers

Juan P. Garrahan¹ and David Chandler²

¹*School of Physics and Astronomy, University of Nottingham, Nottingham, NG7 2RD, UK*

²*Department of Chemistry, University of California, Berkeley, CA 94720-1460*

This presentation deals with the dynamic facilitation approach to the glass transition problem [1–7]. It focuses on the idea that the interesting structure in glass-forming systems is most easily identified in trajectory space, rather than configuration space. In contrast to mean-field approaches, dynamic facilitation naturally accounts for the dynamic heterogeneity of glass-forming materi-

als and related fluctuation phenomena such as transport decoupling. We will describe the connection between the so-called "glass transition" and order-disorder in the $d + 1$ dimensions of trajectory space, organizing phenomena according to scaling and universality classes. Various predictions from this viewpoint, some yet to be verified experimentally, will be discussed.

-
- [1] J. P. Garrahan and D. Chandler, *Phys. Rev. Lett.* **89**, 035704 (2002).
 [2] J. P. Garrahan and D. Chandler, *Proc. Natl. Acad. Sci. U. S. A.* **100**, 9710 (2003).
 [3] S. Whitelam, L. Berthier, and J. P. Garrahan, *Phys. Rev. Lett.* **92**, 185705 (2004).
 [4] Y. J. Jung, J. P. Garrahan, and D. Chandler, *Phys. Rev. E* **69**, 061205 (2004).
 [5] L. Berthier, D. Chandler, and J. P. Garrahan, *Europhys. Lett.* **69**, 320 (2005).
 [6] M. Merolle, J. P. Garrahan, and D. Chandler, *Proc. Natl. Acad. Sci. U. S. A.* **102**, 10837 (2005).
 [7] R. L. Jack, J. P. Garrahan, and D. Chandler, preprint 2005.

Dynamical field theory for glass forming liquids, self-consistent resummations and time-reversal symmetry [1]

Alexandre Lefèvre*

Service de Physique Théorique, CEA, CNRS URA 2306, Gif-sur-Yvette, France

We analyze the symmetries and the self-consistent perturbative approaches for dynamical field theories of glass forming liquids. We show that time-reversal symmetry is related to *nonlinear* fields transformations that leave the corresponding actions invariant. This nonlinearity makes perturbation theories problematic since they generically do not preserve time-reversal symmetry and in particular fluctuation-dissipation relations (FDR). We show how one can overcome this problem and set up symmetry preserving perturbation theories by introducing some auxiliary fields. We apply our results to the Mode-Coupling Theory (MCT) of the glass transition. We revisit previous field theory derivations of MCT equations [2] showing that they generically violates FDR. We obtain symmetry preserving mode-coupling equations for Brownian and Newtonian dynamics and discuss their advantages and drawbacks. An interesting phys-

ical result is that even in the presence of coupling between current and density the MCT transition is not cut-off.

This communication is based on work in collaboration with G. Biroli and A. Andreanov [1]. We are also deeply indebted to J.-P. Bouchaud for very useful discussions and his participation to the early stage of this work.

* Corresponding author: alexandre.lefevre@cea.fr

[1] A. Andreanov, G. Biroli and A. Lefèvre, *cond-mat/0510669* (2005).

[2] S. P. Das and G. F. Mazenko, *Phys. Rev. A* **34**, 2265 (1986); S. P. Das *Phys. Rev. A* **42**, 6116 (1990).

On the Adam-Gibbs-Kirkpatrick-Thirumalai-Wolynes scenario for the viscosity increase in glasses

J.P. Bouchaud* and G. Biroli

SPEC & SPhT, CEA-Saclay, Orme des Merisiers, 91191 Gif s/ Yvette, France

We reformulate the interpretation of the mean-field glass transition scenario for finite dimensional systems, proposed by Wolynes and collaborators. This allows us to establish clearly a temperature dependent length ξ^* above which the mean-field glass transition picture has to be modified, due to the existence of an exponentially large number of inherent states competing with a surface tension-like effect. We argue in favor of the mosaic state introduced by Wolynes and collaborators, which leads to the Adam-Gibbs relation between the viscosity and configurational entropy of glass forming liquids. Our argument is a mixture of thermodynamics and kinetics: small clusters of particles are thermodynamically frozen in low

energy states, whereas large clusters are kinetically frozen by large activation energies. The relevant average relaxation time is that of the smallest 'liquid' clusters. We show that the correlation between the value of the stretching exponent β and fragility are accounted for in this framework. Some predictions for the aging properties of glasses are outlined.

* Corresponding author: bouchaud@spec.saclay.cea.fr

Viscoelasticity and metastability limit in supercooled liquids

Andrea Cavagna*

National Institute for Condensed Matter (INFM) and National Research Council (CNR), Rome, Italy

A supercooled liquid is said to have a kinetic spinodal if a temperature T_{sp} exists below which the liquid relaxation time exceeds the crystal nucleation time. We revisit classical nucleation theory taking into account the viscoelastic response of the liquid to the formation of crystal nuclei and find that the kinetic spinodal is strongly influenced by elastic effects. We introduce a dimensionless parameter λ , which is essentially the ratio between the infinite frequency shear modulus and the enthalpy of fusion of the crystal. In systems where λ is larger than a critical value λ_c the metastability limit is totally suppressed, independently of the

surface tension. On the other hand, if $\lambda < \lambda_c$ a kinetic spinodal is present and the time needed to experimentally observe it scales as $\exp[\omega/(\lambda_c - \lambda)^2]$, where ω is roughly the ratio between surface tension and enthalpy of fusion.

* Corresponding author: Andrea.Cavagna@roma1.infn.it

A Molecular Dynamics Simulation Study of the α - and β -Relaxation Processes in 1,4-Polybutadiene

Grant D. Smith* and Dmitry Bedrov

Department of Materials Science and Engineering, University of Utah, Salt Lake City, Utah, USA

We have conducted molecular dynamics simulation studies of melts of 1,4-polybutadiene (PBD) using a quantum chemistry-based potential where the rotational energy barriers between conformational states have been reduced (LB-PBD model, where LB indicates lowered barrier). Segmental relaxation in the LB-PBD melts was investigated over a wide range of temperature by monitoring the decay of the torsional autocorrelation function (TACF). The decay of the TACF could not be well-represented by a single stretched (Kohlrausch-William-Watts) exponential, as shown in FIG. 1, indicating the presence of resolvable α - and β -relaxation processes even at the highest temperatures investigated. Mechanistically we found that the β -relaxation is due to large-scale conformational motions corresponding to all dihedrals visiting each conformational state (e.g., *gauche*⁺, *trans*, and *gauche*⁻), as shown in Fig. 2.

The β -relaxation process was observed to weaken with decreasing temperature due to an increasingly heterogeneous population of conformational states with

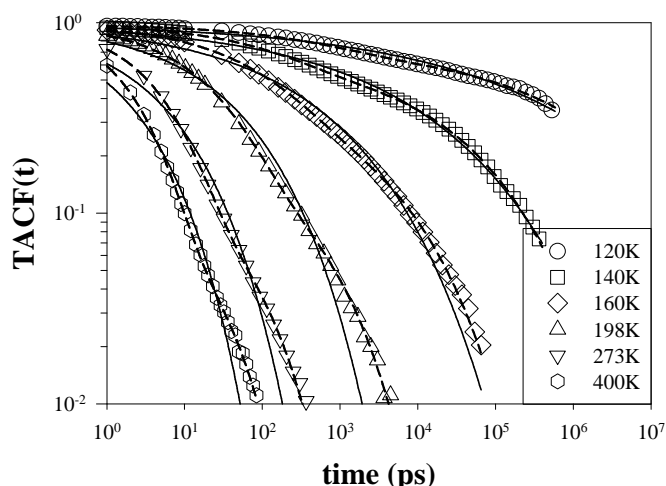


FIG 1. Torsional autocorrelation function for the LB-PBD melt showing fits of single stretched exponential function (solid lines) and a sum of two stretched exponential functions (dashed lines).

Complete segmental relaxation (α -relaxation) occurred on longer time scales over which all dihedrals are able to populate each conformational state with equilibrium probability, a process that requires cooperative motion of the matrix.

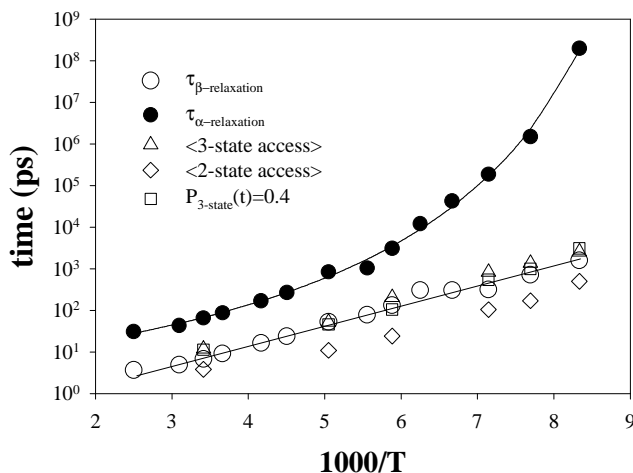


FIG. 2. Relaxation times for the α - and β -relaxation processes in the LB-PBD melt as a function of inverse temperature. Also shown are the average times required for dihedrals to access any two and all three conformational states.

decreasing temperature imposed by the matrix which biases conformations of individual dihedrals on time scales shorter than the α -relaxation time. The β -relaxation process was also found to broaden with decreasing temperature due to an increasingly broad distribution of times required for dihedrals to visit each conformational state.

* Corresponding author: gsmith2@gibbon.mse.utah.edu

Structural and conformational dynamics of simulated glass-forming polymer melts

 S.-H. Chong,¹ M. Aichele,^{2,3} H. Meyer,³ M. Fuchs,⁴ and J. Baschnagel^{3,*}
¹*Institute for Molecular Science, Okazaki, Japan*
²*Institut für Physik, Universität Mainz, Germany*
³*Institut Charles Sadron, Strasbourg, France*
⁴*Fachbereich Physik, Universität Konstanz, Germany*

We present results from MD simulations for the dynamics of nonentangled glass-forming polymer melts. The simulations are carried out at constant pressure with a bead-spring model where each chain contains $N = 10$ monomers [1]. The simulation results are quantitatively analyzed within the framework of a recent extension of idealized mode-coupling theory (MCT) to nonentangled polymer melts [2].

Our analysis does not rely on fits, but is based on the following procedure: We determine from the simulation the collective structure factor S_q and the monomer-resolved intrachain structure factors w_q^{ab} ($a, b = 1, \dots, N$) [3]. These quantities are the only input that the theory requires to predict the dynamics of the model. Predicted and simulated dynamics may then be compared.

Figure 1 shows an example of this comparison. The figure depicts the mean-square displacements (MSDs) of the monomers $g_M(t)$ and of chain's center of mass (CM) $g_C(t)$

$$g_M(t) = \frac{1}{N} \sum_{a=1}^N \langle [\vec{r}_a(t) - \vec{r}_a(0)]^2 \rangle, \quad (1)$$

$$g_C(t) = \langle [\vec{R}_s(t) - \vec{R}_s(0)]^2 \rangle.$$

Qualitatively, the MSDs display the following features: At short times, both the monomers and the CM move ballistically ($\sim t^2$). The regime of ballistic motion is succeeded by a ‘plateau regime’, where the MSDs increase only slowly with time. There, $g_M(t)$ is of the order of 10% of the monomer diameter. This reflects the temporary caging of a monomer by its neighbors. The plateau regime may thus be identified with the MCT β -process [2]. For longer times, $g_M(t) \sim t^x$ with $x \approx 0.63$, while $g_C(t)$ crosses over to final diffusion. The subdiffusive monomer-displacement can be attributed to chain connectivity; however, the value of the effective exponent x cannot be understood within the classical theory of polymer dynamics (i.e., the Rouse model; cf. e.g. [1]). Chain connectivity dominates the monomer dynamics until the MSD becomes comparable to the chain size, $g_M \sim R_e^2 \sim 12.3$, R_e being the chain's end-to-end distance. Then, final diffusion also sets in for the monomer motion, and we have $g_M(t) \propto g_C(t) = 6Dt$, where D is the diffusion coefficient of a chain.

In Fig. 1 the data are plotted versus Dt . This representation forces agreement between theory and simulation at late times. So, a fair assessment of the quality of the comparison can only be made in the β and early- α regimes. Here, the comparison reveals the following strengths and weaknesses: We find

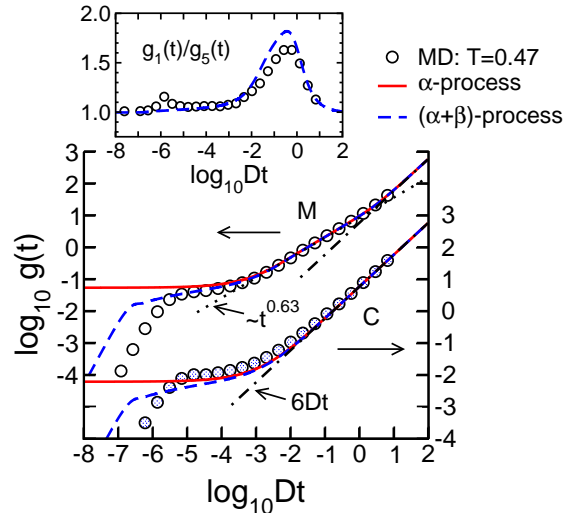


FIG. 1: Log-log plot of the monomer MSD $g_M(t)$ (left ordinate) and of the MSD $g_C(t)$ for the chain's center of mass (right ordinate) versus Dt . Here, D denotes the diffusion coefficient of a chain and $g_C(t)$ was shifted downward for clarity. The inset displays the ratio of the end-over-middle-monomer MSD, $g_1(t)/g_5(t)$. Circles refer to the simulation results obtained at $T = 0.47$ which is close to the critical glass temperature of MCT, $T_c \simeq 0.45$, for our model. The solid line shows the MCT α -master curve, while the dashed line also takes the MCT β -process into account (for a distance parameter of $\epsilon = (T_c - T)/T_c = -0.046$). The dash-dotted lines show the final diffusion, $6Dt$, and the dotted line indicates a connectivity-related effective power law ($\sim t^{0.63}$).

good agreement for the monomer dynamics. In particular, the theory correctly describes the motion of the end monomer relative to the MSD of the central monomer (see inset). Furthermore, it suggests that there should be deviations from pure Rouse behavior due to finite- N effects [2]; this rationalizes the effective power law $g_M(t) \sim t^{0.63}$. On the other hand, the agreement with the CM motion is not so satisfactory. Careful examination of Fig. 1 reveals that the theoretical $g_C(t)$ enters the diffusive regime earlier than the simulated one. We discuss possible origins of this deviation which is hitherto not understood.

* Corresponding author: baschnag@ics.u-strasbg.fr

- [1] J. Baschnagel and F. Varnik, *J. Phys.: Condens. Matter* **17**, R851 (2005).
- [2] S.-H. Chong and M. Fuchs, *Phys. Rev. Lett.* **88**, 185702 (2002).
- [3] M. Aichele, S.-H. Chong, J. Baschnagel, and M. Fuchs, *Phys. Rev. E* **69**, 061801 (2004).

The non-translational origin of the slow β relaxation.I. Sergueev,^{1,*} U. van B \ddot{u} reck,² A. I. Chumakov,¹ T. Asthalter,³ and R. R \ddot{u} ffer¹¹European Synchrotron Radiation Facility (ESRF), P.O. Box 220, F-38043 Grenoble, France²Physik-Department E13, Technische Universit \ddot{a} t M \ddot{u} ncchen, D-85748 Garching, Germany³Physikalische Chemie II, Universit \ddot{a} t Stuttgart, D-70569 Stuttgart, Germany

One of the unsolved questions of the glass physics is the origin of the secondary or slow β relaxation. One explanation of this process is based on a nonuniform glass structure. The process is attributed to faster molecular motions in those regions where the molecules are loosely packed, i.e. in the "islands of mobility". An alternative explanation assumes the decoupling of different molecular motions below crossover temperature T_c . Here, the slow β relaxation is explained as a certain type of motion, like side group motion or molecular rotation which remains active even when translational motion of the molecules has been frozen out.

The origin of the slow β relaxation might become clearer by analyzing its appearance for different kinds of molecular motion, e.g. translational and rotational motions. However, the methods which are mainly used to investigate slow β relaxation, dielectric spectroscopy and nuclear magnetic resonance, are directly sensitive to rotations alone. Neutron scattering, which could yield information also on microscopic translations, cannot reach the relevant time region. By contrast, M \ddot{o} ssbauer spectroscopy and Nuclear Forward Scattering (NFS) of Synchrotron Radiation which are sensitive to spatial motion on an atomic length scale cover a ns- μ s time window and allow to investigate dynamics below T_c . Additionally, they are sensitive to molecular rotation via hyperfine interactions between the nuclear spin and its surroundings. In order to separate two types of motion a new method, SR based Perturbed Angular Correlation (SRPAC) can be used which reveals only molecular rotation. Thus, the combination of NFS and SRPAC applied to the same object simultaneously allows one to separate rotational and translational molecular dynamics.

We applied NFS and SRPAC to investigate the dynamics of the organic glass formers toluene, dibutyl phthalate and orthoterphenyl using probe molecules of ferrocene enriched with the spectator ⁵⁷Fe. The ferrocene molecule has an iron atom in the center of mass between two cyclopentadienyl rings which produce an electric field gradient at the iron site and, correspondingly, split the nuclear level. Therefore, the iron atom is sensitive to both the center-of-mass translational motion of the probe molecules and their rotation.

In Fig. 1 we show the rotational relaxation rate and the diffusion coefficient of the probe molecules inserted in toluene. The diffusion coefficient here corresponds to the microscopical translational motion on the lengths scale of ~ 1 \AA . We compare our data with dielectric spectroscopy measurements on pure toluene whose dynamics is described by α and slow β relaxation branches [1]. In order to compare the rotational

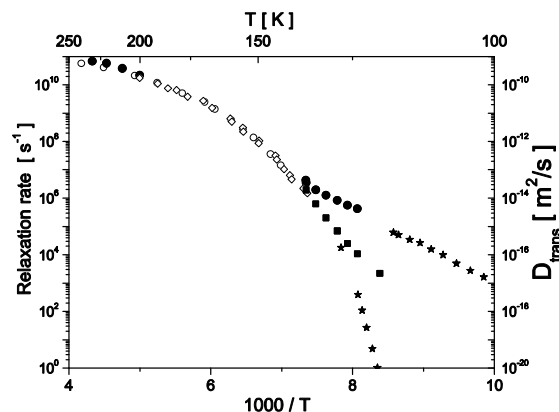


FIG. 1: Arrhenius plot of the relaxation variables in toluene. Left side scale: the rotational relaxation rate of the probe molecules (\bullet)(our data), the relaxation rate obtained by dielectric spectroscopy (\star) [1] and by NMR(\circ) [2]; right side scale: the diffusion coefficient of the probe molecules (\blacksquare)(our data) and the diffusion coefficient obtained by the ¹H static gradient technique (\diamond) [3]. Left and right side scales are adjusted to have the same value of the relaxation variables at high temperature.

relaxation rate, the diffusion coefficient and the dielectric spectroscopy data on an absolute scale we use complementary measurements of the diffusion coefficient [3] and of the relaxation rate [2] at high temperatures where all dynamical variables should have the same temperature dependence. The figure shows that the rotational relaxation rate of the probe molecules follows the line of the slow β relaxation. On the other hand, the diffusion coefficient which reveals a microscopical translational motion of the probe molecules follows the α relaxation branch. This means that on the time scale of slow β relaxation, the probe molecules are fixed in their positions. The same effect is observed for other investigated glass formers. This result support the concept of decoupling of the different modes of motion below the crossover temperature T_c and suggest an identification of the slow β relaxation with non-translational, possibly rotational molecular motion.

* Corresponding author: sergueev@esrf.fr

[1] A. Kudlik et al., Europhys.Lett. **40**, 649 (1997).

[2] E. Roessler and H. Sillescu, Chem. Phys. Lett. **112**, 94 (1984).

[3] G. Hinze and H. Sillescu, J. Chem. Phys. **104**, 314 (1996).

A thermodynamic approach to the fragility of glass-forming polymers

Daniele Cangialosi^{*1}, Angel Alegría², and Juan Colmenero^{1,2}

¹Fundacion Donostia International Physics Center, Paseo Manuel de Lardizabal 4, 20018 San Sebastián, Spain

²Departamento de Física de Materiales, Universidad del País Vasco (UPV/EHU) y Unidad de Física de Materiales Centro Mixto (CSIC-UPV/EHU), Facultad de Química, Apartado 1072, 20080 San Sebastián, Spain

The connection between the steepness of the relaxation time variation of the **a** process, the so-called dynamic fragility, with other properties of the glass-former, such as thermodynamic [1], vibrational [2] and mechanical properties [3], has been the subject of intense research in recent years.

In this contribution, we attempt to connect the dynamic fragility to thermodynamic properties for a large number of glass-forming polymers. To do this, we revisit the connection between the steepness of the relaxation time variation and thermodynamic properties starting from the AG equation [4]:

$$t = t_0 \exp \frac{C}{TS_{ex}} \quad (1)$$

Here the configurational entropy that appears in the AG theory is replaced by the entropy of the supercooled liquid in excess to the corresponding crystal. Though these two quantities are never the same, it has been shown that they are proportional and, therefore, equation (1) is still applicable.

The dynamic fragility can be defined as:

$$m_A = \frac{d \left[\ln(t(T)/t_0) / \ln(t(T_g)/t_0) \right]}{d(T_g/T)} \Bigg|_{T=T_g} \quad (2)$$

Insertion of equation (1) into equation (2) gives:

$$m_A = 1 + \frac{\Delta c_p(T_g)}{S_{ex}(T_g)} \quad (3)$$

In figure 1, the test of equation (3) is displayed for all investigated polymers. As can be seen, a correlation between dynamic fragility and thermodynamic properties is found for a certain group of polymers (filled circles), whereas it fails for another group of polymers (open triangles). In addition, we notice that polymers, for which equation (3) does not hold, have residual excess entropy at T_0 .

We have attributed the residual excess entropy at T_0 to the existence of all sorts of intra-molecular motions, not related to the **a** process and detectable through standard spectroscopic techniques. Therefore equation (3) modifies to:

$$m_A = 1 + \frac{\Delta c_p(T_g)}{S_{ex}(T_g) - S_{ex}(T_0)} = 1 + \frac{\Delta c_p(T_g)}{S_{ex,a}(T_g)} \quad (4)$$

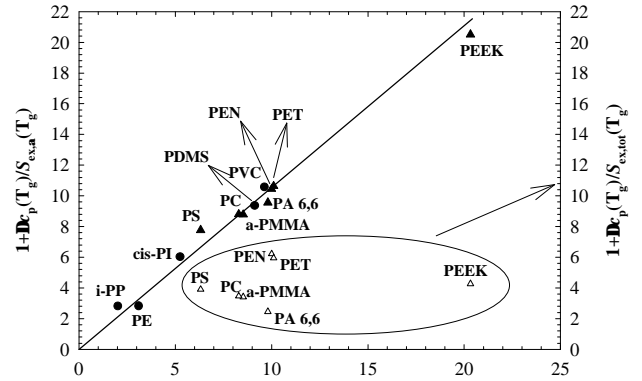


FIG. 1: Comparison between the experimental dynamic fragility and that obtained from the application of the AG equation. Filled circles correspond to polymers that verify equation (3) and open triangles to polymers for which equation (3) fails. Filled triangles correspond to polymers for which equation (4) was applied, i.e. after subtraction from the total excess entropy of the contribution unrelated to the **a** process.

The subtraction from the total excess entropy of the residual excess entropy at T_0 allows re-establishing a positive correlation between dynamic fragility and thermodynamic properties.

This means that the mere comparison between the dynamic fragility, a property exclusively related to the **a** process, and properties representative of the overall structure of the glass former, such as the excess entropy, the compressibility [3] and vibrational properties [2], may result in some inconsistencies. That may arise from the presence of contributions to the overall system properties not related to the **a** process, such as intra-molecular motions in glass-forming polymers.

* Daniele Cangialosi: swxcacad@sw.ehu.es

[1] K. Ito, C. T. Moynihan, and C. A. Angell, Nature 398, 492 (1999).

[2] T. Scopigno, G. Rocco, F. Sette, and G. Monaco, Science 302, 849 (2003).

[3] V. N. Novikov and A. V. Sokolov, Nature 431, 961 (2004).

[4] G. Adam and J. H. Gibbs, J. Chem. Phys. 43, 139 (1965).

Mechanism of Ionic Transport in Viscous Sodium Borate Melts

Andreas Meyer,* Florian Kargl, and Emmanuel Longueteau

Physik Department E13, Technische Universität München, 85747 Garching, Germany

We investigate the atomic motion in multicomponent oxidic melts with inelastic neutron scattering and dynamic light scattering in order to clarify the microscopic transport mechanisms. The high-resolution energy and momentum information emerging from inelastic neutron scattering experiments allows to study the interplay between structure, viscous flow and the atomic diffusion of particular components. In this context sodium borates are binary systems in the sense that long range atomic transport of sodium is faster by orders of magnitude as compared to the transport of the boron and oxygen atoms.

In multicomponent hard sphere like viscous metallic melts, where diffusion coefficients of the various components exhibit similar values above T_c , the relaxational dynamics is in quantitative agreement with the universal mode coupling scaling functions [1] and mixing effects only play a minor role for the mass transport [2]. In sodium borates the time scales for the Na α relaxation and the B-O network structural relaxation are separated. We used inelastic neutron scattering and dynamic light scattering to investigate the fast MCT β relaxation regime in sodium diborate and sodium tetra borate in order to address the question how far the relaxational dynamics in such a system can be described with universal mode coupling scaling functions.

In the low q -region incoherent neutron scattering on sodium is the dominant contribution to the signal, whereas around the first sharp diffraction peak at $q \approx 1.5 \text{ \AA}^{-1}$ coherent scattering on B and O dominates. Therefore, the q dependence of amplitude and time scale of a fast β relaxation process should display the coupling to the two distinct α relaxation processes. The dynamic susceptibility measured with depolarized light scattering does apparently not couple to the relaxational dynamics of the Na ions and does therefore only contain information on the B-O network relaxations.

Figure 1 shows density correlation functions obtained from inelastic neutron scattering on the neutron time-of-flight spectrometer of the new TU neutron source in Munich. The lines are fits with the mode coupling β scaling law. The full set of data can consistently be described with a temperature and q independent line shape parameter λ and a q independent cross over time t_σ as found in one component

viscous liquids. The amplitude h_q of the fast relaxation is found to be in phase with static structure factor for all q . h_q^2 plotted as a function of temperature extrapolates to one T_c value for all q .

Since toward small q the signal is dominated by incoherent scattering on the sodium atoms, the q dependence of the amplitude h_q shows that sodium contributes to the fast relaxation process. Therefore, the Na ion diffusion in sodium borates is prepared by a fast MCT β relaxation process. This conclusion is supported by the light scattering results: The susceptibility spectra do not exhibit a strong signal around the susceptibility minimum. As found in pure boron oxide [4] the contribution of the B-O network to the fast β relaxation as compared to the signal of the B-O peak is rather weak.

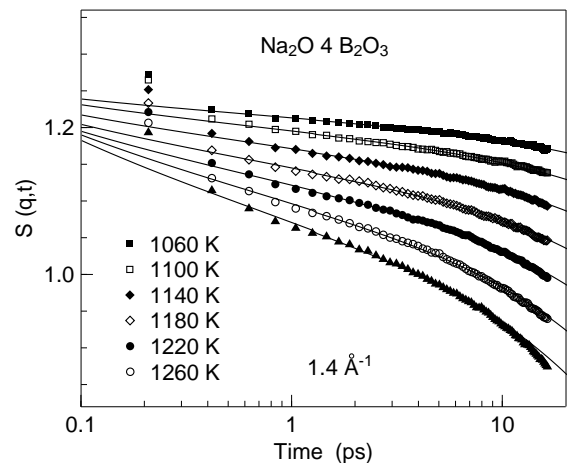


FIG. 1: Density correlation function of a viscous sodium tetra borate melt obtained from inelastic neutron scattering. The lines are fits with the β scaling function of mode coupling theory.

* Corresponding author: ameyer@ph.tum.de

[1] A. Meyer, Phys. Rev. B **66**, 134205 (2002).

[2] S. Mavila Chathoth, A. Meyer, H. Schober, F. Juranyi, Appl. Phys. Lett. **85**, 4881 (2004).

[3] F. Kargl, A. Meyer, M. M. Koza (submitted).

[4] A. Brodin et al, Phys. Rev. B **53**, 11511 (1996)

Slow Dynamics and Fast Ion Diffusion in Sodium Silicates: Simulation and Mode-Coupling Theory

Thomas Voigtmann^{1,*} and Jürgen Horbach²

¹*SUPA, School of Physics, The University of Edinburgh,
JCMB King's Buildings, Edinburgh EH9 3JZ, United Kingdom*

²*Institut für Physik, Johannes-Gutenberg-Universität Mainz, Staudinger Weg 7, 55099 Mainz, Germany*

We study the relation between structure and dynamics in sodium-silicate melts, $(\text{Na}_2\text{O})(\text{SiO}_2)_x$ (denoted NS_x), using molecular-dynamics (MD) computer simulations for the static structure information, and the mode-coupling theory of the glass transition (MCT) for calculating dynamical quantities. Of particular interest is the large time-scale separation observed (in experiment and MD simulations) between the fast sodium-ion diffusion and the slow silicon/oxygen tetrahedral-network relaxation; the latter often being orders of magnitude slower. The phenomenon is reproduced by the theory, thereby demonstrating that MCT provides a framework within which it is possible to explain the fast ion dynamics peculiar to these ion-conducting silicates. This furthermore gives rise to a number of MCT predictions about which features of the static structure factors are responsible for the observed phenomena, and what the qualitative change with varying sodium concentration is. The discussion of these predictions is the focus of this presentation.

In terms of a qualitative picture, preferential diffusion pathways in the Si-O network were proposed more than 20 years ago to be the cause of the high mobility of one of the mixtures' species. Recent MD simulation studies have indeed demonstrated the existence of such 'channels' [1], and they have, in connection with neutron-scattering experiments, linked them to a specific pre-peak feature in the partial static structure factors. This picture, however, remains on a qualitative level only.

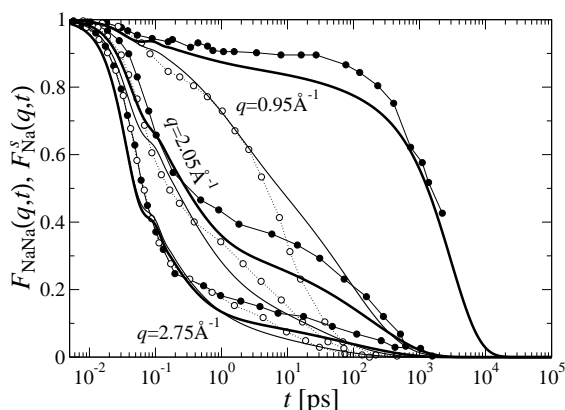


FIG. 1: Dynamic structure factors for sodium disilicate (NS_2) as calculated within MCT: thick solid lines represent the normalized sodium-sodium density correlator $F_{\text{NaNa}}(q, t)$, thin lines the sodium-self correlation function $F_{\text{Na}}^s(q, t)$ ($T_{\text{MCT}} = 3410 \text{ K}$). Filled and open circles are the corresponding MD data (Ref. [1]) for $T = T_{\text{MD}}$ such that the same degree of slowing down is observed.

Whether the presence of such intermediate-range order in the static structure is indeed the cause of (or at least intimately related to) the high mobility of the alkali ions, is the question we address. We have recently demonstrated [2], that MCT can be used to make qualitative, and sometimes quantitative statements about the fast-ion diffusion in sodium silicates. MCT provides an approximate equation for the time evolution of the dynamic structure factors, which we solve numerically for a number of NS_x models with different sodium concentration. The only input required is, in principle, the set of interatomic potentials, in the form of the static structure factors, which we take from computer simulation. The results are then tested against dynamical data obtained from MD simulations. In particular, the fact that sodium-self correlations decay much faster than all other dynamical correlation functions, and that this depends on the concentration of Na_2O in the system, is well reproduced (see Fig. 1). This fact is surprising, since the existence of preferential diffusion channels even in the static sense seems to imply that a description of fast-ion diffusion would require information beyond the two-particle-correlation level. Yet, the version of MCT we are using gives qualitatively correct results even without taking them into account.

Discussing previously unpublished calculations, we show what particular features of the partial structure factors are – within MCT – responsible for the fast-ion dynamics. In addition, the theory offers some analogy to the case of binary hard-sphere mixtures (arguably the simplest multi-component systems). There, once the sizes of the two species are sufficiently different, a similar phenomenon of decoupling between the respective time scales of tagged-particle relaxation occurs. In the MCT framework, it is connected to a continuous delocalization transition termed ‘type A transition’ that occurs in addition to the usual discontinuous ‘type B’ glass transition. We discuss, how far the analogy can be pushed, and in what sense the type A scenario of MCT yields an explanation for the fast-ion dynamics in sodium-silicate mixtures.

This work has been supported by the EPSRC (grant GR/S10377) and the Emmy Noether program of the DFG (grants Ho 2231/2-1/2 and Vo 1270/1-1).

* Corresponding author: tvoigtma@ph.ed.ac.uk

[1] J. Horbach, W. Kob, and K. Binder, Phys. Rev. Lett. **88**, 125502 (2002).

[2] Th. Voigtmann and J. Horbach, cond-mat/0508379.

The glass transition of polymer melts in the presence and the absence of ions: Multidimensional nuclear magnetic resonance and molecular dynamics simulation studies

Michael Vogel*

Institute of Physical Chemistry, University of Münster, Corrensstr. 30/36, 48149 Münster, Germany

NMR experiments and MD simulations proved well suited to study the segmental motion in polymer melts undergoing a glass transition. Here, we demonstrate that in particular a combined application provides detailed insights into polymer dynamics. Specifically, we use these methods to investigate polymers that can dissolve salts so as to compare properties of the α -process in the presence and the absence of ions. In polymer electrolytes, which are promising candidates for many applications in energy and information technologies, the segmental motion governs the ion transport and, hence, the electric conductivity of the material. Thus, understanding polymer dynamics in the presence of ions, i.e., of strong Coulomb interactions, is important from the viewpoints of both fundamental and applied science.

We use ^2H and ^{13}C NMR to measure multi-time correlation functions for polypropylene oxide (PPO) containing various amounts of the salt LiClO_4 . Then, the resonance frequency ω depends on the orientation of the polymer segment so that the molecular reorientation can be tracked by correlating the frequencies at several times in the experiment. We find that a Kohlrausch function, $\exp[-(t/\tau)^\beta]$, describes the correlation functions $F_2^{\text{cc}}(t_m; t_p) = \langle \cos[\omega(0)t_p] \cos[\omega(t)t_p] \rangle$ for all studied materials. An addition of salt slows down the α -process, consistent with a rise of the glass transition temperature T_g . Further, it leads to more stretched correlation functions, as indicated by a decrease of the stretching parameter from $\beta \approx 0.33$ to $\beta \approx 0.24$. The evolution time t_p in these experiments has a similar meaning as the scattering vector Q so that measurement of $F_2^{\text{cc}}(t_m; t_p)$ for various values of t_p provides detailed insights into the geometry of the segmental motion. For example, the t_p dependence of the corresponding mean correlation times $\langle \tau(t_p) \rangle$ can be used to determine the mean jump angle $\langle \gamma \rangle$ according to $\langle \tau(\infty) \rangle / \langle \tau(0) \rangle = 3/2 \sin^2 \langle \gamma \rangle$. In Fig. 1, we see that the mean jump angle in the polymer electrolyte $(\text{PPO})_6\text{-LiClO}_4$, where the ratio $\text{O}_{\text{PPO}}:\text{LiClO}_4$ is 6:1, is significantly smaller than in the neat melt, indicating that the freedom for the segmental reorientation is reduced due to interaction with ions.

Analysis of appropriate ^2H NMR three-time correlation functions shows that, for all studied materials, the non-exponentiality of the structural relaxation is due to existence of dynamical heterogeneities rather than to intrinsic non-exponentiality. In particular, the more pronounced stretching of $F_2^{\text{cc}}(t_m)$ for polymer electrolytes results in large parts from a broadening of the distribution of correlation times $G(\ln \tau)$. Measuring ^2H NMR four-time correlation functions, we find that the dynamical heterogeneities of all studied systems are short-lived, i.e., the rate exchange between fast and slow segments occurs on the same time scale as the reorientation

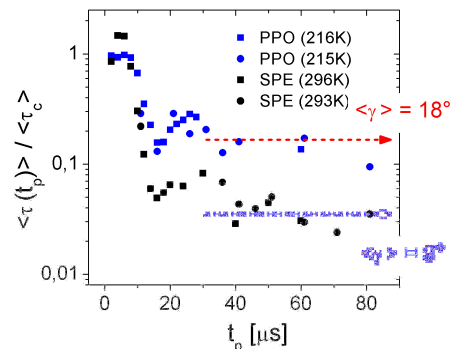


FIG. 1: Mean correlation times $\langle \tau(t_p) \rangle$ for PPO and $(\text{PPO})_6\text{-LiClO}_4$ (SPE) at the indicated temperatures. The values were normalized by the mean time constant $\langle \tau_c \rangle$, characterizing the correlation function $F_2^{\text{ss}}(t_m; t_p \rightarrow 0) = \langle \sin[\omega(0)t_p] \sin[\omega(t)t_p] \rangle$.

itself. This rules out the possibility that an addition of ions leads to micro-phase separation.

Furthermore, we perform MD simulations for PPO and polyethylene oxide (PEO), using atomistic force fields [1]. To demonstrate that the α -process in the polymer models is *spatially* heterogeneous, we show that highly mobile segments form clusters. Specifically, we identify the 5% most mobile oxygen atoms in a given time interval Δt and construct clusters by grouping neighboring mobile oxygen atoms into the same cluster. We find that the mean cluster size exhibits a maximum at times Δt that correspond to the early α -relaxation regime. Further, the height of this peak increases with decreasing T . Qualitatively similar results were reported for a bead-spring model of a polymer melt and for models of metallic liquids, silica and water, indicating that spatially heterogeneous dynamics is a key feature of glass forming systems. Moreover, we calculate NMR multi-time correlation functions from the MD trajectories. We find qualitative agreement between the computed data at high T /short times and the experimental data at low T /long times, suggesting that there are no fundamental changes of polymer dynamics over a wide T range. Thus, we can use the MD results to determine the individual contributions of different structural units to the NMR correlation functions and, hence, to obtain even more detailed insights. MD Simulations for polymer electrolytes based on PPO are underway.

* Corresponding author: mivogel@uni-muenster.de

[1] G.D. Smith, O. Borodin and D. Betrov, *J. Chem. Phys.* **A 102**, 10318 (1998); O. Borodin and G. D. Smith, *J. Chem. Phys.* **107**, 6801 (2003).

Is there a high-order Mode Coupling transition in polymer blends?

 Angel J. Moreno ^{*,1} and Juan Colmenero ^{1,2,3}
¹Donostia International Physics Center, Paseo Manuel de Lardizabal 4, 20018 San Sebastián, Spain.

²Dpto. de Física de Materiales, Universidad del País Vasco (UPV/EHU), Apdo. 1072, 20080 San Sebastián, Spain.

³Unidad de Física de Materiales, Centro Mixto CSIC-UPV, Apdo. 1072, 20080 San Sebastián, Spain.

The ideal Mode Coupling Theory (MCT) for the glass transition predicts a sharp transition from an ergodic to an arrested state at a given value of the control parameter. At the transition, the long-time limit of the density-density correlator $F(q, t)$ jumps from zero to a finite value, the critical non-ergodicity parameter, f_q . In the ergodic state close to a standard fold transition, $F(q, t)$ shows an initial decay to a plateau of height f_q , whose duration becomes longer as the transition is approached. At long times, $F(q, t)$ decays to zero. This second decay is well described by a power law expansion:

$$F(q, t) \approx f_q - h_q(t/\tau)^b + h_q^{(2)}(t/\tau)^{2b}, \quad (1)$$

where the dynamic exponent b is related to the so-called exponent parameter $1/2 \leq \lambda \leq 1$. High-order MCT transitions ($\lambda = 1$) occur at regions of the control parameter space where different caging mechanisms compete. Close to a high-order transition, or to a fold transition with $\lambda \lesssim 1$, $F(q, t)$ does not show a two-step decay. Instead, in an intermediate time interval, it is approximated by a logarithmic expansion:

$$F(q, t) \approx f_q - H_q \ln(t/\tau) + H_q^{(2)} \ln^2(t/\tau). \quad (2)$$

Polymer blends with components of very different mobilities are good candidates for showing the latter MCT scenario. Hence, the caging mechanism for the fast component might originate from the competition between bulk-like dynamics and confinement effects induced by the slow component. Motivated by these ideas, we have carried out simulations in a binary mixture of bead-spring chains, each component (A and B) having a different bead diameter ($\sigma_A = 1.6$, $\sigma_B = 1$). We have investigated, at constant packing fraction, the temperature, T , dependence of $F_{BB}(q, t)$ (i.e., B-B correlations) as a function of the fraction of the fast B-component, x_B .

Fig. 1 shows, for a given T and x_B , the q -dependence of $F_{BB}(q, t)$, as compared to the homopolymer case. The latter shows the standard behavior close to fold MCT transitions. Hence, the decay from the plateau is well described by Eq. (1), and f_q is modulated by the static structure factor (see Fig. 2). Rather different features are observed in the blend. Hence, the decay of $F_{BB}(q, t)$ is well described by Eq. (2), and in particular, logarithmic relaxation occurs over four time decades around $q \approx 4.8$, in agreement with MCT, which predicts lines in the control parameter space with $H_q^{(2)} = 0$. Another fulfilled prediction is the observed convex-to-concave crossover [1]. Moreover, f_q shows a nearly monotonic decay (see Fig. 2), very different from the homopolymer case. It is worthy of remark that these features

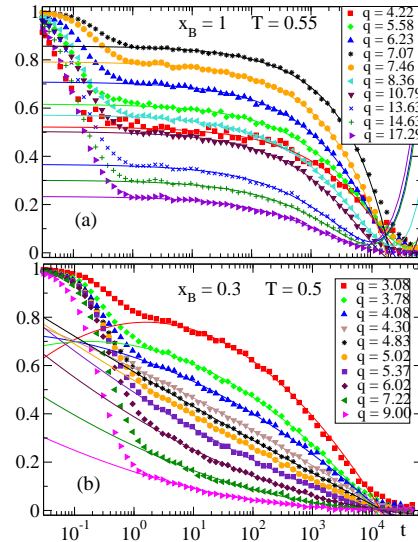


FIG. 1: q -dependence of $F_{BB}(q, t)$ at a given T for the homopolymer (a) and for $x_B = 0.3$ (b). Symbols are simulation data. Lines in panels (a) and (b) are respectively fits to Eqs. (1) and (2).

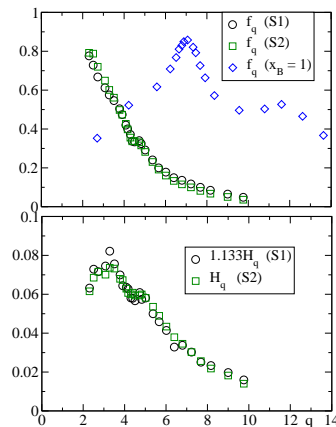


FIG. 2: Values of f_q and H_q , from fits of $F_{BB}(q, t)$ to Eq. (2). The state points are S1: $x_B = 0.3$; $T = 0.4$, and S2: $x_B = 0.3$; $T = 0.5$. The f_q for the homopolymer ($x_B = 1$, fit to Eq. (1)) is also shown for comparison.

are observed in a range $0.1 \lesssim x_B \lesssim 0.8$, suggesting that chain connectivity extends competition between bulk-like and confined-like dynamics over a wide range of blend compositions.

According to MCT, H_q factorizes as $H_q = C \tilde{h}_q$, where \tilde{h}_q only depends on q , and the q -independent term C depends on the state point. Hence, the H_q 's obtained for different state points close to transitions with $\lambda = 1$ or $\lambda \lesssim 1$ must be proportional, as it is demonstrated in Fig. 2.

* Corresponding author: wabmoesa@sq.ehu.es

[1] Recent atomistic simulations on the blend PMMA/PEO [Genix *et al.*, Phys. Rev. E 72, 031808 (2005)] show this feature for PEO, supporting the simple model here investigated.

Realtime 3D imaging of heterogeneities and yielding in sheared colloidal glasses

R. Besseling* and A.B. Schofield, and W.C.K. Poon
 School of Physics, University of Edinburgh, Edinburgh, EH9 3JZ, UK
 COSMIC, University of Edinburgh, Edinburgh, EH9 3JZ, UK

E.R. Weeks
 Physics Department, Emory University, Atlanta GA, USA

The evolution of the microstructure in sheared (colloidal) glasses and its relation to the rheological response is an area of intense current research, relevant both from a fundamental point of view as well as for technological applications. Recent theories of glassy rheology have emphasized the importance of local plastic deformations, while there is also considerable interest in the behavior of correlation functions under shear [1]. However, so far the full 3D structural evolution has only been addressed by numerical simulations, experiments being mostly limited to coarse grained (light scattering) information.

yielding transition from quasi-reversible shearing with sub-diffusive, mostly 'caged', particle displacements at small strain amplitude ($\lesssim 10\%$) to irreversible, diffusive behavior at larger strain. On the particle level, the caging (or cage breaking) and (ir)reversibility exhibit pronounced fluctuations, similar to recent simulations and predictions such as in the 'Shear Transformations Zone' theory. Some regions deform more reversibly than others and over time these regions change. In steady shear, we also find a marked heterogeneity in the topological changes over time. This is illustrated in Fig.1(a)-(c), displaying snapshots of a sheared glass at two different times t_0 , where the grey-scale indicates the change in each particle's local environment over different elapsed times. (measured by a function $\Delta^i(t_0, dt)$ based on bond order parameters [2]). As observed, the changes appear in clusters and are 'switched' on and off at different locations after subsequent strain increments.

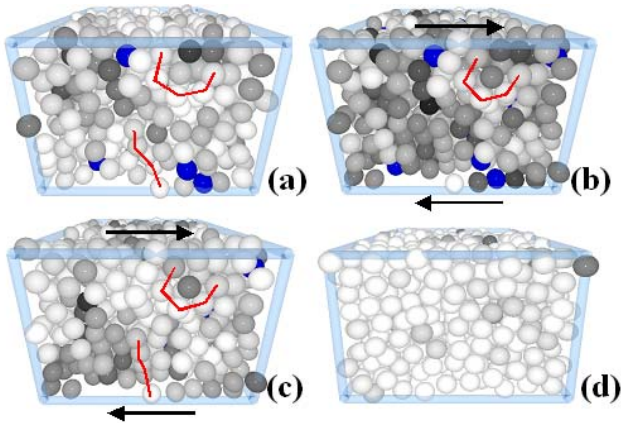


FIG. 1: (a)-(c) Snapshots of a colloidal glass in steady shear ($\dot{\gamma} = 0.0015s^{-1}$), (a) at $t_0 = 80s$ after starting the experiment. The grey-scale measures the change in local environment of each particle i in the *un-sheared* frame ($\propto \Delta^i(t_0, dt)$) over the past $dt = 40s$. (b) Structure at $t_0 = 120s$ and $dt = 80s$. (c) $t_0 = 120s$ and $dt = 40s$. Red lines connecting colloid centers show local deformations, arrows mark the shear direction. (d): For comparison, a quiescent glass, with $dt = 200s$, showing an essentially fixed topology.

Using ultra-fast Confocal Microscopy, we have succeeded to image and track the three-dimensional structural rearrangements in colloidal glasses both in oscillatory and steady shear, up to shear rates of $\dot{\gamma} \simeq 0.05s^{-1}$. Firstly, in oscillatory shear we observe a

We also show an anisotropy measured in the shear induced diffusion when strained beyond 'yielding', in contrast to results of simulations of metallic glasses under steady shear. Finally, using the time-dependent 3D particle coordinates, we extracted several correlation functions, providing direct experimental evidence for the speeding up of structural relaxation in a steadily sheared colloidal glass.

We like to acknowledge K. Pham, G. Petekidis, M.E. Cates and P. Pusey for useful discussions.

* Corresponding author: rbesseli@ph.ed.ac.uk

[1] M.L. Falk and J.S. Langer, Phys. Rev. E **57**, 7192 (1998); P. Sollich *et al.*, Phys. Rev. Lett. **78**, 2020 (1997); L. Berthier and J.L. Barrat, Phys. Rev. Lett. **89**, 095702 (2002).

[2] The parameter Δ^i for the change in local environment of particle i between time t and $t - dt$ is $\Delta^i(t, dt) = 1 - \sum_{m=-6}^{m=6} Q_{6,m}^i(t)Q_{6,m}^i(t - dt)^*$ with bond order parameters $Q_{6,m}$ as described in P.R. ten Wolde *et al.*, J. Chem. Phys **104**, 9932 (1996).

Liquid and solid phases in a soft glassy colloidal suspension under shear

F. Ianni,* S. Gentilini, R. Di Leonardo, and G. Ruocco
 CRS SOFT-INFM-CNR c/o Università di Roma "La Sapienza", I-00185, Roma, Italy.

When subjected to shear, many complex fluids such as colloidal suspensions, granular materials or emulsions, show a shear induced phase separation at low shear rates, characterized by the occurrence of two bands of different shear rate, parallel to the flow direction. In soft glassy systems, whose rheological behavior is determined by the competition between an intrinsic slow dynamics and the acceleration caused by the external flow, this shear-banding phenomena doesn't involve structural changes and can be entirely attributed to dynamical differences between the two bands.

In particular, through molecular dynamics simulations, [1] showed that a simple model of glassy material separates into a fluidized shear-band and an unsheared part at low shear rates (shear localization phenomena). The size of the sheared band is found to increase with the applied shear rate. By calculating the intermediate scattering function $\Phi_q(t)$ in the two bands, they found that in the jammed region the system behaves as a glassy solid as $\Phi_q(t)$ does not relax to zero, while in the sheared region the system behaves as a liquid. In this phase, $\Phi_q(t)$ exhibits a two-step relaxation and reflects the acceleration of the structural relaxation due to flow.

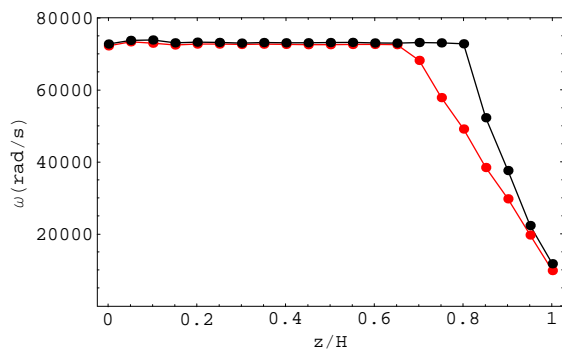


FIG. 1: Velocity profile probed at two different waiting times after the shear switching. The unsheared band size increases during the first hours. The angular velocity is here measured in arbitrary units.

An experimental microscopic counterpart investigating the shear localization phenomena is still rela-

tively poor. In our work, we study a colloidal sample of laponite in a cone-plane shear cell. The system is characterized by an aging dynamics which is significantly reduced by shear as soon as structural relaxation enters the timescale set by the inverse shear rate [2]. Shear localization has been observed on the system at low shear rates [3]. In order to study the system dynamics in the solid and liquid bands, we probe the intermediate scattering function of the colloidal particles through dynamic light scattering; while the possibility of choosing an heterodyne correlation scheme enables to access directly the detailed velocity profile. Thus, using the same technique, we contemporarily monitor the the two bands' appearance and evolution and their corresponding dynamics.

As soon as the sample is prepared, it is poured in the cell and a constant shear rate is applied. After a few minutes, an unsheared band forms, whose size increases with time (Fig. 1), reflecting the aging of the system under shear. After a few hours, the profile stop changing, and the aging dynamics seems to be stopped by the shear. During the whole experiment, slip on the still plane shows, which progressively increases with the waiting time.

By measuring the intermediate scattering function, a non relaxing correlation function is found in the unsheared region, confirming its solid nature, while a correlation function relaxing to zero is measured in the fluidized band, as found in [1]. However, contrarily to their results, the size of the unsheared band does not change as soon as the shear rate changes, as a long time is required for the system to reach the equilibrium configuration. A simple model is proposed to explain the described phenomenology.

* F. Ianni: francesca.ianni@phys.uniroma1.it

- [1] F. Varnik, L. Bocquet, J.-L. Barrat, L. Berthier, Phys. Rev. Lett. **90**, 095702 (2003).
 [2] R. Di Leonardo, F. Ianni, G. Ruocco, Phys. Rev. E **71**, 011505 (2005).
 [3] F. Pignon, A. Magnin, J.-M. Piau, J. Rheol. **40**, 573 (1996).

Rheological response of a model glass: Theory versus computer simulation

 Fathollah Varnik^{1*} and Oliver Henrich² and Matthias Fuchs²
¹Max-Planck Institut für Eisenforschung, Max-Planck Straße 1, 40237 Düsseldorf, Germany

²Fachbereich für Physik, Universität Konstanz, 78457 Konstanz, Germany

Steady state non linear rheology and dynamic yielding of a well established simple glass forming model [1] is studied via large scale molecular dynamics simulations. It is observed that the rheological response of the system changes qualitatively as the temperature is varied from the glassy phase toward the supercooled regime (see Fig. 1): In the supercooled state, the system response is marked by a shear thinning behavior [2] at high shear rates, $\dot{\gamma}$, followed by a cross over to linear response as $\dot{\gamma}$ approaches zero. In contrast to this behavior, a stress plateau forms in the glass in the limit of vanishing shear rate. This stress plateau is best developed for temperatures deep in the glassy phase extending over about three decades in shear rate. The onset of the stress plateau is then shifted toward progressively lower $\dot{\gamma}$ as the temperature is increased toward T_c , the ideal glass transition temperature of the model. This makes an estimate of the dynamic yield stress, $\sigma^+(T) \equiv \sigma(T; \dot{\gamma} \rightarrow 0)$, a difficult task for temperatures below but close to T_c .

Nevertheless, an estimate of $\sigma^+(T)$ is obtained by comparing the steady state shear stress for the two lowest simulated shear rates, namely $\dot{\gamma} = 10^{-5}$ and $\dot{\gamma} = 3 \times 10^{-6}$. As shown in Fig. 2, at temperatures below $T = 0.38$, practically the same shear stress is obtained for both choices of $\dot{\gamma}$ indicating the presence of a stress plateau. For these temperatures, the simulated shear stress at the shear rate of $\dot{\gamma} = 3 \times 10^{-6}$ is

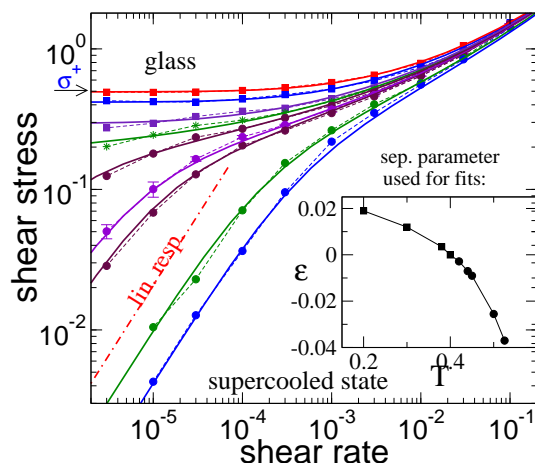


FIG. 1: Simulated shear stress versus shear rate for temperatures ranging from the glass (triangles) to the supercooled state (circles) (from bottom to top: $T=0.525, 0.5, 0.45, 0.44, 0.42, 0.4, 0.38, 0.3, 0.2$). The critical curve ($T_c = 0.4$) is denoted by stars. Solid lines are theoretical predictions within a schematic $F_{12}^{\dot{\gamma}}$ -mode coupling model [3]. A horizontal arrow points to the dynamic yield stress at $T = 0.2$. The inset shows the correspondance between temperature and the separation parameter, ϵ , used for theoretical curves.

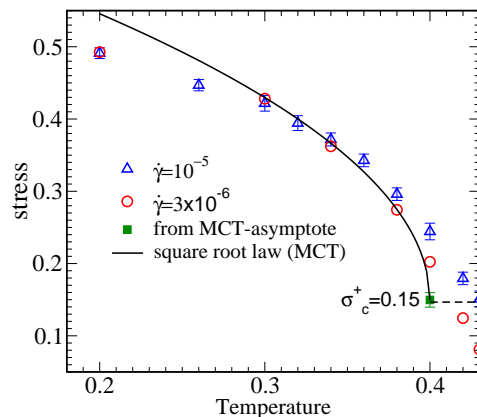


FIG. 2: Determination of dynamic yield stress and its temperature dependence (see text).

thus practically identical to the dynamic yield stress of the system (see circles in Fig. 2).

For $T > 0.38$, we make use of theoretical predictions based on the $F_{12}^{\dot{\gamma}}$ -model [3] (square). Note that the theory is able to describe the whole set of flow curves ($\sigma(\dot{\gamma})$ for *all* studied temperatures) by adjusting two parameters only; one parameter sets the time scale and the other the position of the ideal glass transition, T_c . This gives $T_c \approx 0.4$ and a critical dynamic yield stress of $\sigma_c^+ \equiv \sigma^+(T_c) \approx 0.15$ [3].

Above mentioned results on the dynamic yield stress allow an investigation of the temperature dependence of $\sigma^+(T)$. It is found that a square root law suggested by MCT [4], $\sigma^+(T) - \sigma_c^+ \propto |1 - T/T_c|^{0.5}$, describes well the variation of σ^+ with temperature in the glassy phase. Recalling that $\sigma^+(T_c) \approx 0.15$ and $\sigma^+(T > T_c) = 0$, our observations suggest the existence of a yield stress discontinuity at the ideal glass transition of our model.

FV was supported by the Deutsche Forschungsgemeinschaft (DFG) under the grant VA 205/1-1, OH by the DFG (in the international Graduate College 'Soft Matter'), and MF by the DFG Transregio-SFB TR6.

* Corresponding author: varnik@mpie.de

- [1] W. Kob and H. C. Andersen, Phys. Rev. E **51**, 4626 (1995); *ibid* **52**, 4134 (1995).
- [2] L. Berthier and J.-L. Barrat, J. Chem. Phys. **116**, 6228 (2002).
- [3] O. Henrich, F. Varnik, and M. Fuchs, J.Phys.: Condes. Matter **17**, 1 (2005).
- [4] M. Fuchs and M. E. Cates, Faraday Discuss. **123**, 267 (2003); Phys. Rev. Lett. **89**, 248304 (2002).

Nonlinear Rheology of Colloidal Suspensions

Oliver Henrich* and Matthias Fuchs

Fachbereich Physik, Universität Konstanz, D-78457 Konstanz, Germany

Jerôme Crassous and Matthias Ballauff

Physikalische Chemie I, Universität Bayreuth, D-95440 Bayreuth, Germany

A complete understanding of the nonlinear rheology for viscous liquids is still not available. Their rheological properties are often described and quantified with empirical relations. We aim to fill that gap with a first-principles approach that gives an explanation for the phenomenon of shear-thinning. The resulting theory is applied to steadily sheared dense colloidal fluids and glasses in plane Couette-flow.

Starting point is the microscopic Smoluchowski-equation with linear flow-profile whereas hydrodynamic interactions are not considered. Using the Zwanzig-Mori projection-operator formalism, an expression for the shear-stress in terms of an exact Green-Kubo type relation can be derived [1]. It can be evaluated by means of the mode-coupling approximation for the fluctuating forces. The underlying mechanism leading to shear-thinning in this approach is found to be a competition between the cage effect on the one hand and the decorrelation of memory due to shear-advection on the other hand.

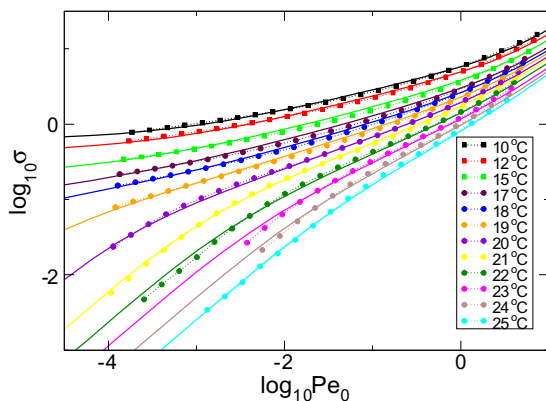


FIG. 1: Flow curve: shear-stress versus strain-rate. Between 15°C and 17°C the transition from a supercooled liquid to a yielding solid occurs. Solid lines give fits by eye to the experimental data with the extended Sjögren-model.

As a first step towards solving the microscopic theory we introduce gradually more and more complex schematic models. To account for the shearing extensions to well studied schematic models (F_{12} - and the Sjögren-model) were made. Comparisons of the theory with experimental data on thermosensitive core-shell latex particles [2] are shown. The experiments

were performed in the group of M. Ballauff, University of Bayreuth, Germany. Shear-thinning appears to be reasonably described in the experimental window by this newly developed model (Fig. 1). Additional information on quantities like the viscosity at zero and infinite shear-rate could be retrieved from the fits (Fig. 2). Predictions for the transient viscosity are also shown. Noteworthy hydrodynamic interactions can be included by a rescaling procedure of the high-shear viscosity.

We continue with a schematic model, in which negative vertices emerge upon shearing just like in the full microscopic calculation. Finally we proceed with 2D-calculations for structure and dynamics in the quiescent system that serve as a reference for the shear-induced effects.

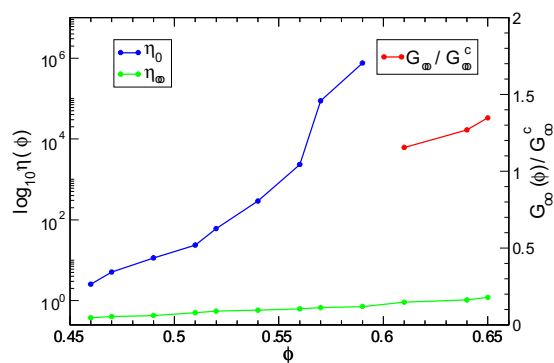


FIG. 2: Viscosity η_0 and η_{∞} at zero and infinite shear-rate.

OH was supported by the Deutsche Forschungsgemeinschaft (DFG) in the *International Graduate College "Soft Condensed Matter"*. MF was supported by the DFG *Transregio-SFB TR6*.

- * Corresponding author: oliver.henrich@uni-konstanz.de
- [1] M. Fuchs, M.E. Cates, Phys. Rev. Lett. **89**, 248304 (2002).
M. Fuchs, M.E. Cates, J. Phys.: Condens. Matter **17**, 1681 (2005).
- [2] J. Crassous, O. Henrich, M. Fuchs, M. Ballauff, *in preparation*

Topological and bond yielding in colloidal glasses

W. C. K. Poon,*⁽¹⁾ K. N. Pham,⁽¹⁾ G. Petekedis,⁽²⁾ S. U. Egelhaaf,⁽¹⁾
D. Vlassopoulos,⁽²⁾ P. N. Pusey⁽¹⁾

⁽¹⁾ SUPA, School of Physics, The University of Edinburgh, Kings Buildings, Mayfield Road, Edinburgh EH9 3JZ, UK.

⁽²⁾ Institute of Electronic Structure and Laser-FORTH, PO Box 1527, Heraklion 71110, Crete, Greece.

In a concentrated colloidal suspension in which the particles repel each other at contact, but also attract each other with a short-range attraction, two qualitatively distinct kinds of glasses are possible [1,2]. At no or low interparticle attraction, a repulsive glass exists, where non-ergodicity is due to crowding – each particle is trapped by a permanent cage of neighbours. At high enough interparticle attraction, however, glassiness is caused instead by interparticle bonds.

We have studied the non-linear rheology of repulsive and attractive colloidal glasses. The system consists of sterically-stabilised polymethylmethacrylate (PMMA) particles dispersed in decalin at volume fraction $\phi = 0.6$, with added random-coil linear polystyrene. The latter induces a short-range depletion attraction between the particles estimated to be about $19 k_B T$.

Oscillatory rheology was used to measure the storage and loss moduli (G' and G'' respectively) at the angular frequency of 1 rad/s. At low applied strain amplitudes, the repulsive and attractive glasses behave similarly, Fig. 1 a,b. G' is constant, and about an order of magnitude larger than G'' – the samples respond as elastic solids. At higher strain amplitudes, however, G' decreases in each case, until it becomes smaller than G'' – the samples yield and become liquid-like.

In detail, however, the two samples behave quite differently. The hard sphere glass, Fig. 1 a, basically yields in a single step, at a strain of just over 10%, where G'' also peaks [3]. In the attractive glass, however, we see that G' starts to decrease, and G'' first peaks, at the very low amplitude of about 2%; at the much higher strain of 40%, G' finally drops below G'' , and the latter peaks for a second time.

We interpret this finding as follows. Yielding in a hard-sphere glass is due to the breaking of local ‘cages’. In an attractive glass, however, interparticle bonds have to be broken first; this occurs at a low strain amplitude controlled by the range of the interparticle attraction. After bond breaking, the system is still very dense, and therefore local topological constraints remain to be overcome. When this finally happens, at a higher strain, the sample completely yields.

Interestingly, a lower volume fraction sample with about the same interparticle attraction and is also non-ergodic, Fig. 1 c, yields in a single step at low strain: after bond breaking, there are no cages to break any more, because the volume fraction is low enough.

Step strain measurements confirm this picture.

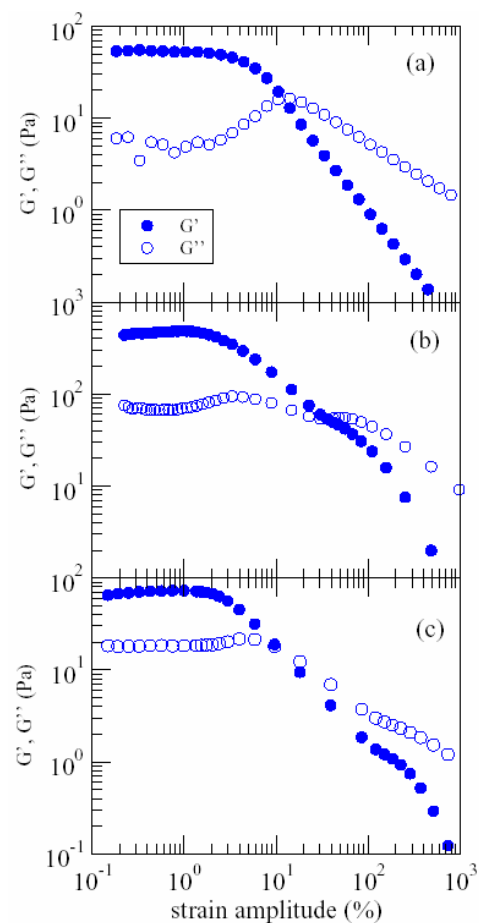


FIG. 1: Dynamic strain sweep measurements at frequency $\omega = 1$ rad/s for (a) a hard sphere glass at $\phi = 0.6$ (b) an attractive glass at $\phi = 0.6$ and (c) a colloidal gel at $\phi = 0.4$. Each graph shows the storage (G' , filled circles) and loss (G'' , open circles) moduli as functions of the strain amplitude.

* Corresponding author: w.poon@ed.ac.uk

[1] K. N. Pham et al., *Science* **296** (2002) 104

[2] K. A. Dawson et al., *Phys. Rev. E* **63** (2001) 011401

[3] G. Petekedis et al., *Phys. Rev. E* **66** (2002) 051402

Gel to glass transition in simulation of a valence-limited colloidal system

Emanuela Zaccarelli^{1,2*}

¹Dipartimento di Fisica and CNR-INFM-SOFT,
 Università di Roma 'La Sapienza', P.le A. Moro 2, I-00185, Roma, Italy and
²ISC-CNR, Via dei Taurini 19, I-00185, Roma, Italy

I. Saika-Voivod³, S. V. Buldyrev⁴, A. J. Moreno⁵, P. Tartaglia⁶ and F. Sciortino¹

³Department of Chemistry, University of Saskatchewan, Saskatoon, Saskatchewan, S7N 5C9

⁴Yeshiva University, Department of Physics, 500 W 185th Street New York, NY 10033, USA

⁵Donostia International Physics Center Paseo Manuel de Lardizabal 4 E-20018 San Sebastián, Spain and

⁶Dipartimento di Fisica and CNR-INFM-SMC,
 Università di Roma 'La Sapienza', P.le A. Moro 2, I-00185, Roma, Italy

We study via extensive numerical simulations a simple model for thermo-reversible colloidal gelation in which particles can form reversible bonds with a predefined maximum number of neighbors n_{\max} . We focus on a square-well interaction between particles with three and four maximally coordinated bonds, since in these two cases the low valency makes it possible to probe slow dynamics down to very low temperatures T [1]. By studying a large region of T and packing fractions ϕ we estimate the location of the liquid-gas phase separation spinodal and its precursors, i.e., iso- $S(0)$ lines. We also calculate iso-diffusivity lines, which are precursors of the locus of dynamic arrest, where the system is trapped in a disordered non-ergodic state. We find that there are two distinct arrest lines for the system: a *glass* line at high packing fraction, and a *gel* line at low ϕ and T . The former is rather vertical (ϕ -controlled), while the latter is rather horizontal (T -controlled) in the $(\phi - T)$ plane.

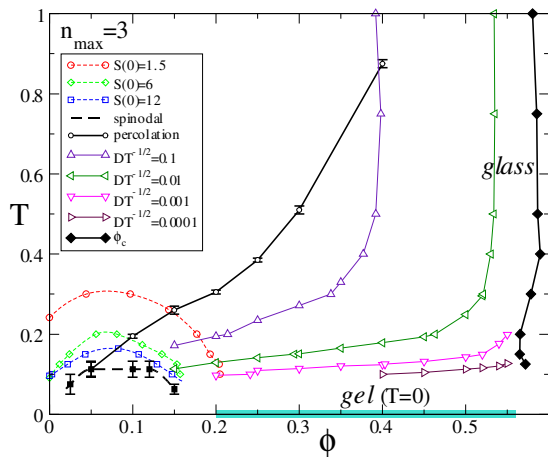


FIG. 1: Summary of the phase diagram for $n_{\max} = 3$. Spinodal, iso- $S(0)$ lines, iso-diffusivity lines, percolation line, extrapolated *glass* and *gel* lines are reported.

Dynamics on approaching the glass line is compatible with a power-law dependence on the distance from the glass line, while dynamics along isochores follows an activated (Arrhenius) dependence. In this way we estimate the locus of glass transition labeled as ϕ_c and of gel transition at $T = 0$. A summary of all these findings is reported in Fig. 1.

Typical signatures of dynamical arrest, such as the plateau in the mean squared displacement and the non-ergodicity parameter, are compared for the approach to the gel and the glass and found to be utterly different. At the same time, the gel can be always well distinguished from the so-called attractive glass. We complement the MD results with mode coupling theory calculations, using the numerical structure factors as input, and find that the theory satisfactorily predicts the glass line but fails in predicting the gel line.

Interestingly, we detect the presence of anomalous dynamics, such as subdiffusive behaviour for the mean squared displacement and logarithmic decay for the density correlation functions in the region where the gel-dynamics interferes with the glass dynamics. These findings are in analogy with the corresponding ones without limited-valency, where anomalous dynamics arises from the presence of a higher order MCT singularity [2], due to the competition of the attractive and repulsive glasses.

* Corresponding author: emanuela.zaccarelli@phys.uniroma1.it

- [1] E. Zaccarelli, S. V. Buldyrev, E. La Nave, A. J. Moreno, I. Saika-Voivod, F. Sciortino and P. Tartaglia Phys. Rev. Lett. **94**, 218301 (2005).
 [2] K. A. Dawson, G. Foffi, M. Fuchs, W. Götze, F. Sciortino, M. Sperl, P. Tartaglia, T. Voigtmann and E. Zaccarelli, Phys. Rev. E **63**, 11401 (2001).

Length scale dependent relaxation in colloidal gels

Emanuela Del Gado* and Walter Kob

*Dipartimento di Scienze Fisiche, Università di Napoli "Federico II", Italia and
Laboratoire de Colloïdes, Verres et Nanomatériaux, Université Montpellier II, France*

Although gels are ubiquitous in fundamental science, technological applications and also in our daily life, their structural and dynamical properties are not well understood. In contrast to other systems that show a slow relaxation, such as glass-forming liquids, the structure of gels is given by an open network that is thought to be responsible for the unusual dynamical properties of these systems.

Apart from the dramatic slowing down of the relaxation dynamics with increasing interaction strength between the particles, one finds a complex dependence of the dynamics on the length scale considered: The relaxation functions are often stretched and/or, most remarkably, compressed, i.e. the time correlators decay faster than an exponential. Due to the large variety of gel-forming systems (colloidal gels, chemical gels,...) it has so far not been possible to obtain a clear picture on which ones of these phenomena are universal and which ones are specific to just a subclass of these systems. The same is true for their theoretical description since various mechanisms have been proposed to rationalize certain observations from experiments or computer simulations, but so far no unifying picture has emerged yet. We present the re-

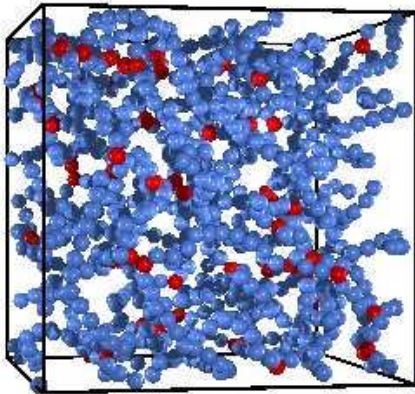


FIG. 1: Part of a configuration, a cube with side $L/2$, of the system at $T = 0.05$. The red particles are the bridging point of the gel network, with coordination number 3.

sults of a recent study based on a simple model that does indeed have the characteristics of (colloidal) gel-forming systems at a finite temperature. By means of molecular dynamics computer simulations, we investigate the gel formation from the equilibrium sol phase. At low volume fraction and low T particles are linked by long-living bonds and form an open percolating network (see Fig.1). Our results on the structural and dynamical properties [1, 2] shed some light on the mechanism that is responsible for the slow dynamics in these systems. In particular we show that the strong length scale dependence of the dynamics in gel forming systems is tightly related to the formation of the gel structure and is therefore a general feature. This study allows for the first time to investigate on a microscopic level the relaxation processes in the incipient gel and to understand why they must strongly depend on the length scale investigated. In our model the mesh-size of the incipient gel network corresponds to a crossover length between dramatically different relaxation processes, from stretched to compressed exponentials. Moreover our results link the super-exponential relaxation at low temperature to the motion of pieces of the incipient gel structure.

* Corresponding author: delgado@na.infn.it

[1] E. Del Gado and W. Kob, *Europhys. Lett.* (2005, *in press*; cond-mat/0507085.

[2] E. Del Gado and W. Kob, cond-mat/0510690.

Fluctuation dissipation relations in stationary states of interacting Brownian particles under shear

Matthias Fuchs*

Fachbereich Physik, Universit Konstanz, 78457 Konstanz, Germany

Colloidal dispersions exhibit slow structural dynamics at high concentrations. Thus they can easily be driven into stationary non-equilibrium states by shearing with already modest shear rates, as shearing breaks detailed balance. Steady state averages, like the shear stress, exhibit nonlinear behaviors (like power laws or discontinuities at non-equilibrium transitions), which can not be rationalised within linear response theory close to equilibrium.

Computer simulations of sheared Newtonian viscous liquids have shown that the stationary states are also characterized by anomalous time dependent fluctuation and response functions, which deal with small deviations of the system from the steady state. Especially a violation of the Fluctuation Dissipation Theorem (FDT), as had been predicted by spin glass theory, has been studied in detailed simulations by Berthier and Barrat [1]. The following observations were made on glassy states that exhibit ergodic dynamics only because of the external driving (viz. $T < T_{\text{glass}}$ and shear rate $\dot{\gamma} \neq 0$):

(i) For various quantities connected to the particle motion in the vorticity direction, viz. perpendicular to the shear plane, FDT is violated at long times:

$$\chi_f(t) = \begin{cases} \frac{-1}{k_B T} \frac{d}{dt} C_f(t) & \text{short times} \\ \frac{-1}{k_B T_{\text{eff}}} \frac{d}{dt} C_f(t) & \text{long times} \end{cases}$$

where the effective temperature T_{eff} , defined in the lower equation, is larger than the real one.

(ii) T_{eff} is independent on the variables studied.

(iii) T_{eff} agrees with the effective temperature found during the aging of the quiescent system.

This contribution shows that the recently developed mode coupling approach to sheared colloidal dispersions [2] includes violation of equilibrium FDT, and enables one to determine T_{eff} . Points (i) to (iii) will be discussed.

We start from the 'Smoluchowski equation', $\frac{\partial}{\partial t} \Psi = \Omega \Psi$, for the time-evolution of the N -Brownian particle distribution function $\Psi(\{\mathbf{r}_i\})$ under steady shearing, to calculate fluctuations, $C_f(t) = \langle \delta f^* e^{\Omega t} \delta f \rangle$ and susceptibilities, $\chi_f(t)$, where the latter give the linear deviation $\Delta f(t) = \int^t dt' \chi_f(t-t') h_f(t')$ when the potential energy is perturbed by $U \rightarrow U - f^* h_f(t)$ [2]. A generalized FDT holds also for non-equilibrium steady states [3]:

$$\chi_f(t) = \frac{-1}{k_B T} \frac{d}{dt} C_f(t) - \left\langle \sum_i \mathbf{j}_i \cdot \frac{\partial f^*}{\partial \mathbf{r}_i} e^{\Omega t} f \right\rangle, \quad (1)$$

yet its form differs from the one close to equilibrium, because the stationary distribution Ψ_s differs from the Gibbsian one [4], and because a stationary probability current, $\langle \mathbf{j} \rangle$, exists [2, 3], when detailed balance is broken.

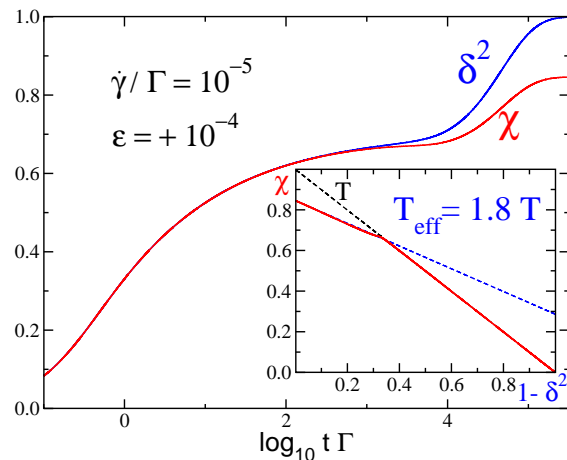


FIG. 1: The integrated response, $\int_0^t dt' \chi(t')$ (labeled χ), is compared to the (shifted) fluctuation, $1 - \Phi(t)$ (labeled δ^2), both calculated from the $F_{12}^{(\dot{\gamma})}$ -model for a yielding glassy state (see parameters given), and $\alpha = 0.015$. The inset shows the parametric plot of the integrated response as function of the fluctuation. At long times, the effective temperature $T_{\text{eff}} = 1.8T$ can be read off.

Equation (1) can serve as an exact starting point for approximations to test the concept of an effective temperature in sheared colloidal dispersions. Mode coupling approximations, and further simplifications to a schematic model, lead to the known sheared $F_{12}^{(\dot{\gamma})}$ -model [2], containing one correlator $\Phi(t)$, supplemented by the equation for the corresponding susceptibility ($k_B T = 1$ is chosen):

$$\chi(t) = -\frac{d}{dt} \Phi(t) - \alpha \dot{\gamma} \Phi(t), \quad (2)$$

where α is a new parameter. Figure 1 shows that this simple model can result in effective temperatures almost twice the real one.

This work builds on a cooperation with M. Cates, whom I thank for continuing helpful discussions. Support by the DFG via the SFB-TR 6 'Colloids in external fields' is also acknowledged.

-
- * Correspondence: matthias.fuchs@uni-konstanz.de
 [1] L. Berthier and J.-L. Barrat, J. Chem. Phys. **116**, 6228 (2002); and references therein.
 [2] M. Fuchs and M. E. Cates, Phys. Rev. Lett. **89**, 248304 (2002); Faraday Discuss. **123**, 267 (2003); J. Phys.: Condens. Matter **17**, 1681 (2005).
 [3] G. S. Agarwal, Z. Phys. **252**, 25 (1972).
 [4] G. Szamel, Phys. Rev. Lett. **93**, 178301 (2004).

Polymer Dynamics and Long Time Atomistic Trajectories

K. Kremer,* L. Delle Site, N. van der Vegt, and B. Hess

Max-Planck-Institute for Polymer Research, Theory Group, D-55128 Mainz, Germany

By a combination of coarse grained and atomistic simulations we follow the motion of highly entangled polymers for up to 10^{-5} sec. This allows to directly compare simulations with experiments, which address the microscopic structure and their consequences on the long time dynamics. Tests on the structure show, that n-scattering results on the local packing are well reproduced in detail. In combination with

a topological analysis, one is thus able to generate a rather comprehensive view on the dynamical properties of specific polymer melts by computer simulations.

* Corresponding author: k.kremer@mpip-mainz.mpg.de

Topological Disorder, Large Scale Heterogeneities and Long Time Relaxation Behavior in Polymer Networks. Models and Monte Carlo Simulations.

Jens-Uwe Sommer*

Institut de Chimie des Surfaces et Interfaces, CNRS, F-68057 Mulhouse, BP 2488, France

Large scale computer simulations allow for the first time to investigate the topological structure of networks formed by crosslinking polymer chains. Here, we present results from Monte Carlo simulations using the bond fluctuation model for different types of end-linked polymer networks both in the dry and in the swollen state, relaxed on large computational time scales.

By following the connectivity of monomers in the network structure a fractal dimension can be defined which characterizes the spatial extension of a connected part of the network with respect to the number of monomers contained therein. For all network structures we have studied, the latter displays a value of about four, valid up to a large spatial scale (usually the box size of the simulated system), thus indicating a *folded structure* of the polymer network in the dry state. Here, clusters of connected monomers interpenetrate each other on a length scale well beyond the extension of individual network strands [1, 2]. Further evidence for the folded substructure in dry polymer networks is obtained from the analysis of closed paths and the conformations of clusters of closely connected monomers.

The simulated networks are allowed to swell and relax in athermal (good) solvent and we analyze various properties such as the deformation of individual

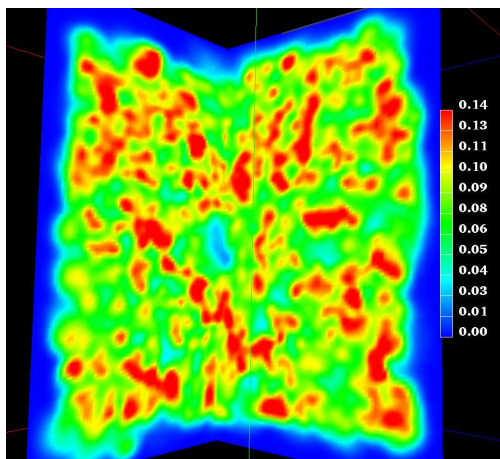


FIG. 1: Cut through the density distribution in a swollen end-linked network averaged over $4 \cdot 10^7$ MCS. The color legend gives the value of the monomer density and the box extension is 400 lattice units. The size of the frozen-in density heterogeneities are about one order of magnitude larger than the average extension of the network chains. Similar results are obtained from different types of networks such as bimodal end-linked networks and randomly crosslinked networks. Complementary results are obtained from the comparison of scattering functions between swollen networks and semi-dilute solutions at the same monomer concentrations.

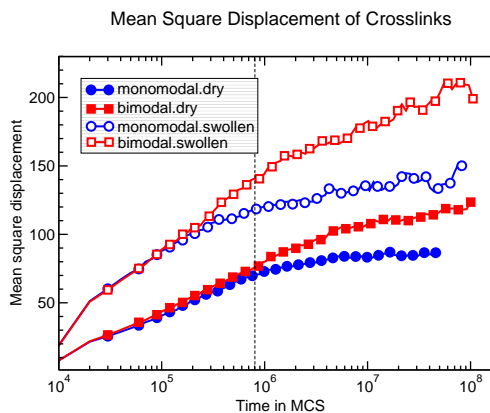


FIG. 2: The mean square displacement of crosslinks is displayed as a function of time in Monte Carlo steps. The dashed vertical line indicates the Rouse time for individual strands.

chains, the unfolding of clusters of connected chains, as well as the morphology and scattering properties of the swollen system. In Fig.1, density heterogeneities in a swollen, end-linked network are visualized. Here, the 3D density is averaged over a long simulation time to reveal frozen-in density fluctuations. The size of these heterogeneities exceeds the extension of individual chains by far and strongly supports the role of unfolding and desinterspersion mechanisms in the process of swelling. In accord with this result is the subaffine behavior of individual strands and of connected structures under swelling.

The analysis of the fluctuation dynamics of the network monomers reveals a long time tail which extends up to the longest simulated time scales (10^8 Monte Carlo steps), while the (Rouse) relaxation times of individual strands are at least two orders of magnitude smaller, see Fig.2. This indicates a cooperativity of many strands. The long time tails can be approximated by a logarithmic law. Further evidence for desinterspersion and long time relaxation processes in network structures is obtained from the analysis of segregation phenomena in crosslinked diblock copolymers and crosslinked polymer blends [2, 3].

* Electronic address: ju.sommer@uha.fr

- [1] J.-U. Sommer and S. Lay, *Macromolecules* **35**, 9832 (2002).
- [2] S. Lay, J.-U. Sommer and A. Blumen *J. Chem. Phys.* **110**, 12173 (1999).
- [3] S. Lay, J.-U. Sommer and A. Blumen *J. Chem. Phys.* **113**, 11355 (2000).

Structural and dynamic heterogeneity of polymer melts from melting polymer crystals

S. Rastogi[#], D. R. Lippits[#], G.W.M. Peters[#], R. Graf,⁺ Y. Yao,⁺ H.W. Spiess^{+,*}

[#]Eindhoven University of Technology, P.O. Box 513, 5600MB Eindhoven, The Netherlands,

⁺Max Planck Institute for Polymer Research, Ackermannweg 10, D-55128 Mainz, Germany

Usually in semi-crystalline polymers, like polyethylene (PE) containing amorphous and crystalline regions, the chains are intimately mixed. The resulting topological constraints (entanglements) in the amorphous regions limit the drawability in the solid-state. By controlled synthesis the number of entanglements can be reduced. Ultimately, crystals composed of single chains are feasible, where the chains are fully separated from each other. If such separation can be maintained in the melt a new melt state can be formed, Fig. 1, adapted from ref [1]. We show that upon slow heating such crystals form a heterogeneous melt with regions that are more entangled and the chains are mixed, and less entangled domains, composed of single chains.

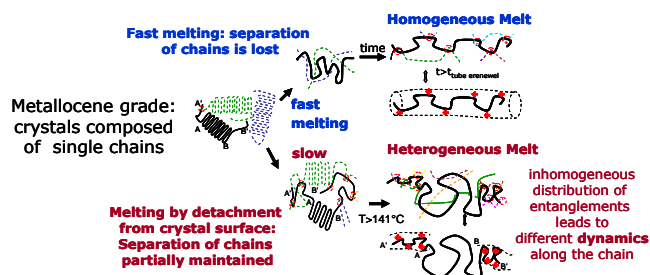


FIG. 1: Schematic view of creating a polymer melt with a heterogeneous distribution of entanglements [1]

Advanced NMR spectroscopy is applied to probe the local chain dynamics which is indicative for structural differences. It is able to detect dynamic heterogeneities in polymer melts, even if the dynamics in different regions are very similar, i.e. for melts with extremely low structural contrast [2]. Standard spin echo experiments probing, kHz motions via spin-spin (T_2) relaxation of the protons, already reveal pronounced differences. Fig. 2a shows T_2 relaxation for slow and fast heated melts of all three grades. In the commercial sample the T_2 relaxation is independent of the heating rate (0.2 K/min and 10 K/min). Hence, we designate such melts as 'homogeneous', meaning that entanglements are homogeneously distributed.

In contrast, the metallocene sample exhibits considerable differences in the relaxation behavior for different melting rates. The fast heated sample relaxes faster than the slowly heated sample. Using the different T_2 relaxations as a filter, thereby suppressing the less-mobile fractions of the melt, significant differences in the peak width are observed in the NMR spectrum of the metallocene melts, whereas the T_2 -filtered peak width of the commercial grade is independent of the heating rate and similar to the peak width of the fast

heated metallocene melt, Fig. 2b. The narrower peak of the slow heated melt indicates a higher local mobility in part of the sample. As the PE chains are chemically uniform, the different local dynamics originate from a heterogeneous melt structure.

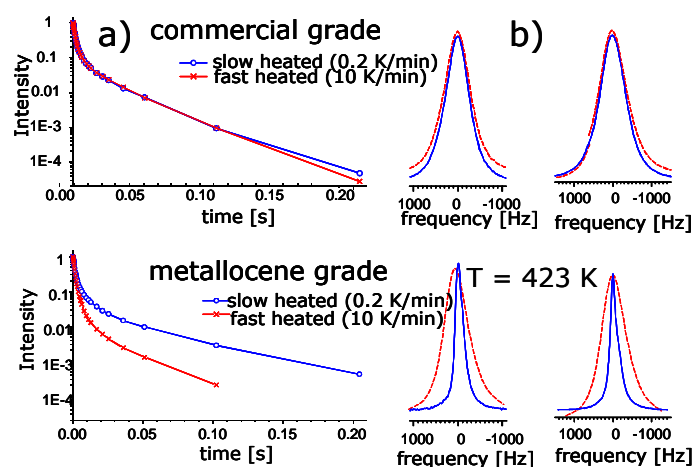


FIG. 2: Transverse NMR relaxation times and filtered NMR line shapes of different PE samples [1]

We attribute these findings to a new melt state in which the chain dynamics is altered, because the entanglements along the main chain are inhomogeneously distributed and located close to the chain ends. These constraints in the heterogeneous melt restrict the reptation of chains, required for homogenization of the entanglement distribution. This is even true after leaving the melt at temperatures as high as 180°C for several hours. Moreover, in the heterogeneous melt enhanced local mobility is found for part of the chain, but it apparently does not foster the overall cooperative motion required for chain reptation.

This new state of melt has both fundamental and technological implications, e.g., the long-lived heterogeneous melts exhibit decreased melt viscosity and enhanced drawability on crystallization. This concept may apply to polymers in general by controlling the synthesis route and the subsequent melting process.

* Corresponding author: spiess@mpip-mainz.mpg.de

[1] S. Rastogi et al. Nature Materials **4**, 635 (2005).
 [2] K. Schmidt-Rohr, H.W. Spiess, Phys. Rev. Lett. **66**, 3020 (1991).

Anomalous diffusion in short chain polymer melts

M. Zamponi,^{1,*} A. Wischnewski,¹ M. Monkenbusch,¹ L. Willner,¹ D. Richter,¹ and B. Farago²

¹Forschungszentrum Jülich, 52425 Jülich, Germany

²Institut Laue-Langevin, 38042 Grenoble, France

The dynamics of linear polymer chains in the melt depends strongly on the chain length: For short unentangled chains it is determined by a balance of viscous and entropic forces (Rouse dynamics), for long chains topological constraints are dominating. In the reptation model these topological constraints, stemming from entanglements of the chains with each other, are described by a virtual tube which follows the primitive path of the observed test chain. However, this definition means that a test chain with a length in the order of one entanglement distance can not be captured in a tube. This conclusion does not depend on the matrix properties and should hold even if the matrix chains are much longer than the test chain. Short chains below the entanglement weight are therefore expected to perform free Rouse motion.

Neutron spin echo (NSE) spectroscopy is a powerful tool to explore the different dynamic regimes in polymer melts on a microscopic scale. For short chains at low momentum transfers Q the center of mass diffusion dominates, internal modes are negligible. From the measured dynamic structure factor $S(Q, t)$ the center of mass mean squared displacement $\langle r^2 \rangle$ can then easily be extracted. We report on a systematic NSE study of different dispersed polyethylene mixtures.

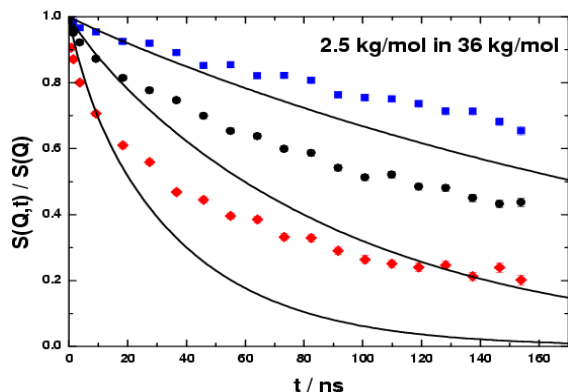


FIG. 1: Dynamic structure factor of a short labelled chain (2.5kg/mol) in a long chain matrix (36kg/mol) for three different momentum transfers. Lines are a fit with the Rouse model.

The dynamic structure factor of a series of short test chains of different length in the same long chain matrix shows significant deviations from the expected Rouse behavior (see fig. 1). Moreover anomalous behaviour in the time dependence of the center of mass mean squared displacement was found for all samples showing a clear subdiffusive regime (see fig. 2): The

expected free diffusion with a $\langle r^2 \rangle \sim t^1$ behaviour is only reached at long times, while at short times surprisingly a $t^{1/2}$ behaviour is found. The time at which this transition occurs increases with increasing chain length, but the data can be shifted onto one master curve by simply rescaling the time. For all the different chain lengths the transition to normal diffusion takes place at the same mean square displacement. This indicates that the observed deviations are independent of the length of the test chain and therefore reflect a property of the matrix chains which may be related to the tube diameter. This would imply that the short chains are captured in a tube, although their length is below or about the entanglement distance.

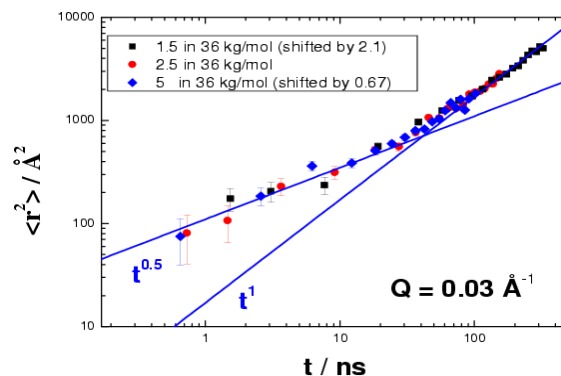


FIG. 2: Center of mass mean squared displacement of different short labelled chains in a long chain matrix (as indicated in the plot). Lines are guides for the eye

To further investigate this phenomenon the same short unentangled chains were measured in a matrix of their own molecular weight. Still discrepancies from the expected behaviour occur: Although qualitatively the dynamic structure factor displays free Rouse motion, the fitted diffusion constant is much smaller than expected. Again anomalous behaviour of the center of mass mean squared displacement for the different samples is found. However, the deviations are qualitatively different from what was observed in the long chain matrix. The deviations for the short chains in a short matrix may be explained by taken intermolecular interactions as discussed by Guenza [1] into account.

* Corresponding author: m.zamponi@fz-juelich.de
[1] M. Guenza, *Macromolecules* **35**, 2714 (2002).

Spatial correlations of fluctuations in the aging dynamics of glasses

Horacio E. Castillo* and Azita Parsaeian

Department of Physics and Astronomy, Ohio University, Athens, OH, 45701, USA

In this work we present the results of a detailed molecular dynamics simulation of the spatial correlations of fluctuations in the aging regime of a simple glass model. We study an 80:20 mixture of two kinds of particles (labeled A and B respectively), that interact via a Lennard-Jones (LJ) potential [1]. A system of 8000 particles is equilibrated at a temperature $T_0 = 5.0$, and then it is quenched by instantly changing the temperature of the thermal bath to $T = 0.4$, i.e. just below the glass transition temperature $T_g = 0.435$ [1]. The origin of times is taken at the instant of the quench. We average the results of 4000 runs performed under identical conditions. In order to probe the spatial correlations of the fluctuations, the following 4-point (2-time, 2-position) function is defined [2]:

$$g_4(\mathbf{r}, t, t_w) = \frac{1}{N\rho} \left\langle \sum_{jk} \delta(\mathbf{r} - \mathbf{r}_k(t_w) + \mathbf{r}_j(t_w)) \right. \\ \left. \times w(|\mathbf{r}_j(t) - \mathbf{r}_j(t_w)|) w(|\mathbf{r}_k(t) - \mathbf{r}_k(t_w)|) \right\rangle - \left\langle \frac{Q(t, t_w)}{N} \right\rangle^2$$

where $Q(t, t_w) = \sum_{i=1}^N w(|\mathbf{r}_i(t) - \mathbf{r}_i(t_w)|)$ and $w(|\mathbf{r}_1 - \mathbf{r}_2|)$ is an overlap function which is unity for $|\mathbf{r}_1 - \mathbf{r}_2| \leq a$ and zero otherwise. The parameter $a = 0.3 \sigma_{AA}$ represents an upper bound for the typical amplitude of the vibrational motion of the particles [2], i.e. the overlap function for a given particle is unity unless the particle has moved more than a typical vibrational lengthscale. By integrating the 4-point function over space the generalized 4-point density susceptibility χ_4 [2] is obtained: $\chi_4(t, t_w) = \beta \int d^3r g_4(\mathbf{r}, t, t_w)$ (Fig. 1).

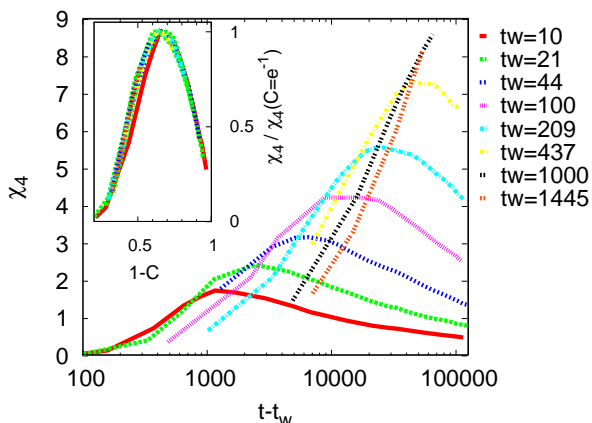


FIG. 1: Four point density susceptibility $\chi_4(t, t_w)$ as a function of $t - t_w$, for $t_w = 10, \dots, 1445$. *Inset*: Rescaled four point density susceptibility $\chi_4 / \chi_4(C = e^{-1})$, plotted as a function of $1 - C_{\text{global}}(t, t_w)$ for the same values of t_w .

For a fixed waiting time t_w , and as a function of $t - t_w$, χ_4 grows, reaches a peak, and then decreases towards zero. The time where the peak is reached and the value at the peak both increase

with t_w . Indeed, to a good approximation the peak is always achieved for a fixed value of the incoherent part of the intermediate scattering function $C_{\text{global}}(t, t_w)$. In fact our data are consistent with the scaling $\chi_4(t, t_w) = F(t_w) \chi_4^0(C(t, t_w))$, where $C = C(t, t_w) = C_{\text{global}}(t, t_w)$. By Fourier transforming the 4-point spatial function $g_4(\mathbf{r}, t, t_w)$, the dynamics structure factor $S_4(\mathbf{q}, t, t_w)$ can be obtained, and from it a dynamic correlation length can be extracted by fitting to the function

$$S_4(\mathbf{q}, t, t_w) = \frac{S_4(\mathbf{q} \rightarrow 0, t, t_w)}{1 + (|\mathbf{q}| \xi_4(t, t_w))^\gamma}. \quad (1)$$

It turns out that also $\xi_4(t, t_w)$ can be rescaled in the form $\xi_4(t, t_w) = G(t_w) \xi_4^0(C(t, t_w))$. In Fig. 2, we show that this rescaling is indeed successful, and that for fixed t_w , as $t - t_w$ (or $1 - C$) grows, the correlation length first grows and then reaches a plateau, but doesn't seem to decay to zero after that (in contrast to results previously reported for supercooled liquids [2]). The inset shows that the correlation length at a fixed value of the correlation $\xi_4(C = e^{-1})$ grows approximately linearly with $\ln(t_w)$ for two decades in t_w . This growth is similar to the one found in simulations in a 3D spin glass, and consistent with a theoretical picture based on the presence of local fluctuations in the age of the system [3].

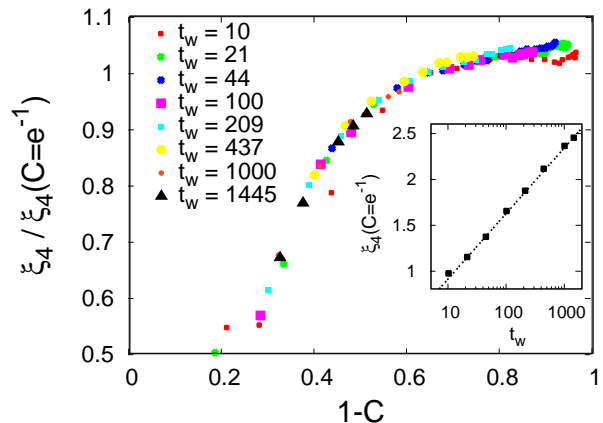


FIG. 2: Rescaled dynamic correlation length $\xi_4 / \xi_4(C = e^{-1})$ as a function of $1 - C_{\text{global}}(t, t_w)$ for $t_w = 10, \dots, 1445$. *Inset*: $\xi_4(C = e^{-1})$ as a function of t_w .

* Corresponding author: castilh@ohio.edu

- [1] W. Kob and J.-L. Barrat, Phys. Rev. Lett., **78**, 4581–4584, 1997.
- [2] N. Lacevic, F. W. Starr, T. B. Schroder and S. C. Glotzer, J. Chem. Phys. **119**, pp. 7372–7387, 2003.
- [3] H. E. Castillo, C. Chamon, L. F. Cugliandolo, J. L. Iguain and M. P. Kennett, Phys. Rev. B. **68**, 134442, 2003.

Origin of the slow dynamics and the aging of a soft glass

Sylvain Mazoyer, Luca Cipelletti, and Laurence Ramos*
 LCVN UMR CNRS-UM2 5587, Université Montpellier 2, 34095 Montpellier Cedex 5, France

The origin of the slow and non stationary dynamics exhibited by many glassy soft materials is still under debate. One emerging idea is that the slow dynamics be due to a series of rearrangements driven by the relaxation of internal stress built up at the transition from a fluid state to a solid state. However, in most cases the physical mechanisms responsible for these rearrangements remain unclear.

To investigate this issue, we study a compact arrangement of polydisperse elastic spheres (onions) [1]. Previous dynamic light scattering and linear rheology experiments have revealed a slow dynamics due to rearrangements of the onion texture over distance of the order of the onion size [2], with a characteristic time that increases with sample age, t_w . For the onions, the internal stresses built up at the transition from the fluid to the viscoelastic state result from a deformation of the local structure with respect to the ideal, relaxed configuration, which corresponds to perfectly spherical onions. We have shown that the system relaxes toward a less deformed configuration during aging [3]; thanks to time- and space-resolved light microscopy experiments, we now identify the driving force that makes rearrangements possible and derive a clear scenario of why the sample ages.

To follow the sample dynamics, we use Particle Imaging Velocimetry thereby measuring the displacement field between pairs of microscope images separated by a time lag τ . Surprisingly, we find that the driving mechanism that induces the rearrangements are the experimentally unavoidable fluctuations of the sample temperature T (of order $\pm 0.15^\circ\text{C}$ in our experiments). A raise (decrease) of T induces a dilation (contraction) of the sample along the x axis direction [4]. Temperature fluctuations thus result in the intermittent motion shown in fig. 1a, where we plot the age dependence of $\langle \delta R_x^2 \rangle$, the x component of the absolute mean square displacement (MSD) of the onions for $\tau = 15000$ sec (here and in the following $\langle \dots \rangle$ is a spatial average over the full displacement field). The peaks raise from a base line ≈ 0 (grey line), which corresponds to pairs of images taken (by chance) at nearly the same temperature. Figure 1b shows the MSD of the relative motion, $\langle \delta r_x^2 \rangle$. Similar peaks are observed, indicating that the deformation is not spatially homogeneous, but rather induces a local shear in the sample. More importantly, the peaks of $\langle \delta r_x^2 \rangle$ raise from a base line larger than zero. Therefore, the temperature-induced deformations lead to irreversible rearrangements: although the absolute displacement is zero for pairs of images taken at the same temperature, the relative displacement is finite. With age, the change in configuration due to these irreversible rearrangements decreases, as shown by the negative slope of the gray line in fig. 1b. Most likely, this aging stems from a decrease of the

frequency of the rearrangements and/or of the amplitude of the displacement field after a rearrangement. This is consistent with the intuitive picture of the most unstable local configurations being rapidly relaxed by the shear induced by the temperature fluctuations, leaving the sample in a configuration that is increasingly harder to relax. Finally, we mention that our microscopy results suggest that the displacement due to the rearrangements grows linearly with time. Such a “ballistic” motion is in agreement with previous dynamic light scattering experiments [2]; its physical origin remains an open issue.

As a concluding remark, we note that the dynamics of our (a priori undriven) soft glass bears similarities with that of driven systems such as colloidal suspensions under oscillatory mechanical shear stress and vibrated granular materials, with the temperature fluctuations-induced mechanical shear playing here the same role as an externally imposed stress or shear in driven systems.

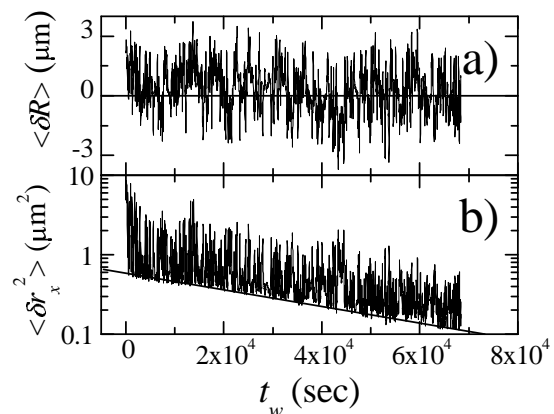


FIG. 1: Age dependence of the absolute ($\langle \delta R_x^2 \rangle$, a) and relative ($\langle \delta r_x^2 \rangle$, b) mean square displacement, measured for a lag $\tau = 15000$ sec. The displacement is due to the sample deformation induced by temperature fluctuations. The base line = 0 in a) (grey line) corresponds to a zero global displacement, which occurs whenever the temperature variation is 0. The finite base line in b) corresponds to irreversible rearrangements that persist even when the temperature variation is 0. Their amplitude decreases with time, leading to aging.

* Corresponding author: ramos@lcvn.univ-montp2.fr

- [1] L. Ramos *et al.*, Europhys. Lett. **66**, 888 (2004).
- [2] L. Ramos *et al.*, Phys. Rev. Lett. **87**, 245503 (2001).
- [3] L. Ramos *et al.*, Phys. Rev. Lett. **94**, 158301 (2005).
- [4] The deformation is uniaxial due to the geometry of the sample cell used in the experiment.

Inverse Melting, Underheating and Glass transition

Roberta Angelini* and Giancarlo Ruocco
 CNR-INFM CRS-SOFT Universit di Roma "La Sapienza", I-00185,Roma, Italy.

We present rheological measurements on a solution composed of α -cyclodextrine (α CD), water and 4-methylpyridine (4MP) as a function of the temperature in the range of 290 to 360 K and concentration. This solution when heated undergoes a reversible liquid-solid transition at a temperature which depends on the concentration of α CD. If further heated at temperatures above $\sim 370K$ the solid melts in the liquid state. A dynamic experiment has been performed with a rheometer RheoStress RS150 Haake using a stainless steel couette geometry cell. The instrument was used in oscillatory mode and in controlled stress (CS) configuration.

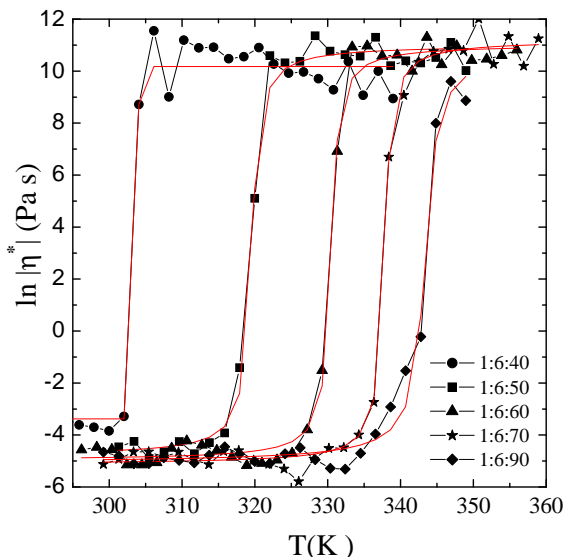


FIG. 1: Complex viscosity as a function of the temperature for different values of the concentration at the indicated molar ratios α CD: H_2O :4MPD measured in oscillatory mode at a frequency $\omega = 1.26 \text{ rad/s}$ as discussed in the text. A fit with a phenomenological function is reported on the data.

The dynamical complex viscosity η^* , the storage modulus G' and the loss modulus G'' related through the relation $G^* = G' + iG'' = i\omega\eta^*$ have been measured. An example of the measured curves is reported in Fig. 1 where the logarithm of the complex viscosity is plotted as a function of the temperature at a frequency $\omega = 1.26 \text{ rad/s}$ and at five different concentrations with molar ratio 1:6: x (α CD: H_2O :4MP) where $40 < x < 90$. The abrupt increase of several order of magnitude of the complex viscosity, underlines the presence of a transition which happens at higher temperatures as the concentration of 4MP increases. The limited temperature range accessible by the instrument did not allow to see the fall down of the viscosity at temperatures higher than $\sim 370K$ when the sample melts and comes back to the liquid phase.

Nevertheless preliminary measurements with a differential scanning calorimeter (DSC) allowed to detect this second transition. The phase diagram in Fig. 2 is obtained by plotting the measured transition temperatures as a function of the concentration. The ob-

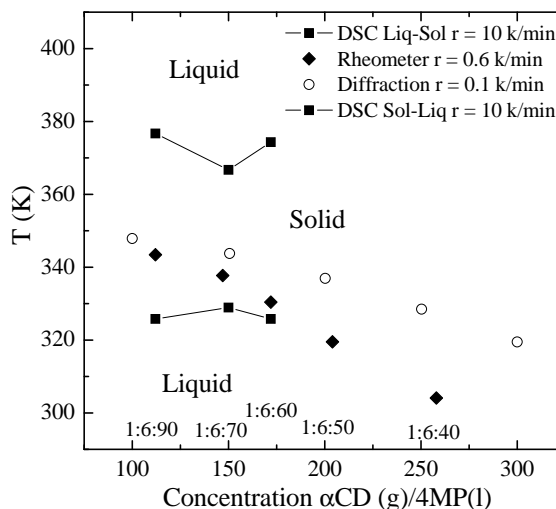


FIG. 2: Liquid-Solid transition temperature as a function of the concentration of α CD in 4MP. Diamonds: rheometric measurements in oscillatory mode as described in the text at heating rate $r=0.6 \text{ k/m}$; squares: DSC measurements at heating rate $r=10 \text{ k/m}$; open circles: quasielastic and elastic neutron measurements from reference [1] at heating rate $r=0.1 \text{ k/m}$

tained results (full symbols) are in agreement with what found in recent quasielastic and elastic neutron scattering measurements [1] (open circles). As shown in Fig. 2 a slight difference in the transition temperature is observed, it is due to the different applied heating rates and to a different content of water in solution. What observed is very intriguing, stimulates further studies on the the attracting phenomenon of the inverse melting [2] and suggests that at high heating rates on fast heating this solution, it can sustain a metastable liquid state, becoming a (disordered) solid at the glass transition temperature T_g . Underheating the liquid an inverse glass transition is observed. Further measurements as a function of the heating rate are also discussed.

* Corresponding author: roberta.angelini@phys.uniroma1.it

[1] M. Plazanet, C. Floare, M. R. Johnson, R. Schweins, H. P. Trommsdorff, J. Chem. Phys. **121**, 5031 (2004).
 [2] A. Lindsay Greer, Nature **404**, 134 (2000).

Aging effects in trap models for glassy relaxation

Gregor Diezemann*

Institut für Physikalische Chemie, Universität Mainz, Welderweg 11, 55099 Mainz, FRG

Aging effects in models for glassy relaxation have been investigated for a long time. Recently, particular attention has been paid to the violations of the fluctuation-dissipation theorem. This theorem relates the linear response of a sample to an external perturbation to the time-derivative of an correlation function. In out-of-equilibrium situations, however, strong violations are observed. These violations can be parameterized via the introduction of the so-called fluctuation-dissipation ratio (FDR), which in some cases can be used for the definition of an effective temperature.

It has been shown that for a stochastic dynamics described by a Markov process the response is not determined by time-derivatives of the correlation alone, but that an additional function, the so-called asymmetry, additionally enters the expression for the response [1]. This asymmetry vanishes in equilibrium but can have an important impact on the FDR in out-of equilibrium situations.

In the present contribution, I consider the aging behavior of the trap model [2]. For the model with an exponential distribution of trap energies it has been found that the FDR is not well suited for the definition of an effective temperature because it depends on the choice of the dynamical variables used to determine the correlation and the response.

If the model with a gaussian distribution of trap en-

ergies is analyzed instead, it is well known that all aging effects are of a transient nature [2]. This model is of interest because in canonical glasses the system also reaches equilibrium on (extremely) long time scales. Also in this case the response and the correlation strongly depend on the dynamical variable used for the calculation. The FDR for very short waiting times behaves differently for different variables. Only in the limit of long waiting times, the FDR approaches unity, as expected in equilibrium. Additionally, the relation to a waiting time dependent effective temperature that has been used recently in experimental investigations of glasses [3], will be discussed.

This work was supported by the DFG under Contract No. Di693/1-2.

* Corresponding author: diezeman@mail.uni-mainz.de

- [1] G. Diezemann; *Phys. Rev. E* **72** 011104 (2005)
- [2] C. Monthus and J.-P. Bouchaud; *J. Phys. A* **29** 3847 (1996)
- [3] T.S. Grigera and N.E. Israeloff; *Phys. Rev. Lett.* **83** 5038 (1999); L. Buisson, S. Ciliberto and A. Garcamartin; *Europhys. Lett.* **63** 603 (2003)

The Localization Transition of the 3D Lorentz Model and Continuum Percolation

Thomas Franosch,^{1,2,*} Felix Höfling,¹ and Erwin Frey²

¹Hahn-Meitner-Institut Berlin, Abteilung Theorie,
Glienicker Str. 100, D-14109 Berlin, Germany

²Arnold Sommerfeld Center and CeNS, Department of Physics,
Ludwig-Maximilians-Universität München, Theresienstr. 37, D-80333 München, Germany

The Lorentz model has served as a paradigm for transport in disordered media. The simplest variant of the Lorentz model consists of a structureless test particle moving according to Newton's laws in a d -dimensional array of identical obstacles. The latter are distributed randomly and independently in space and interact with the test particle via a hard-sphere repulsion. Consequently, the test particle explores a disordered environment of possibly overlapping regions of excluded volume. The only control parameter is the dimensionless obstacle density, $n^* := n\sigma^d$, where σ denotes the radius of the hard-core potential. At high densities, the model exhibits a localization transition, i. e., above a critical density, the particle is always trapped by the obstacles.

It has been conjectured that the dynamics close to the critical density can be mapped to the transport properties of continuum percolation ("Swiss cheese model"). The fractal nature of the void space between the overlapping spheres in the Lorentz model suggested to use a description in terms of an equivalent random resistor network model characterized by a power law distribution of the conductances [1–4]. Hence the physics is dominated by the narrow gaps the particle has to squeeze through.

We present extensive Molecular Dynamics simulation and provide the first unambiguous evidence for an intimate connection between the Lorentz model and continuum percolation [5]. We demonstrate the validity of a generalized dynamic scaling theory for the van Hove self-correlation function with two divergent length scales. In particular we provide accurate data for the mean-square displacement (MSD) for obstacle densities close to the transition, see Figure. Anomalous transport in the critical regime is found in a time window extending over more than five decades. The critical density nicely discriminates between the diffusive and localized phases. The exponent characterizing the subdiffusive behavior is in excellent agreement with the prediction of continuum percolation.

Approaching the critical density from below, the diffusion coefficient rapidly vanishes according to a power law which we confirm over five orders in magnitude. Similarly, the localization length increases critically by a factor of ten close to the transition. We identify a divergent cross-over length which is different from the usual correlation length of the percolating cluster. The presence of two divergent length scales manifests itself in a divergence for the non-Gaussian parameter close to the transition.

The quality of our data allows to go beyond determining critical exponents, and to give a full analysis of the dynamic scaling properties. Although good

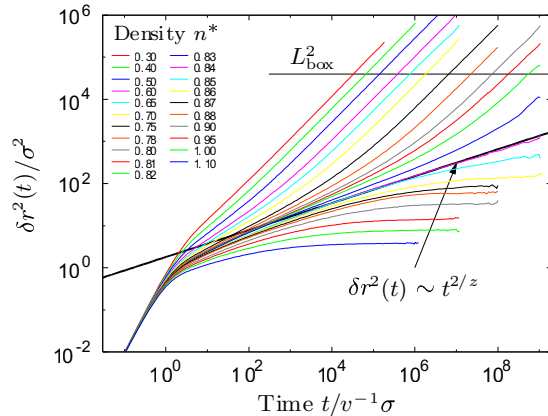


FIG. 1: MSD $\delta r^2(t)$ for various obstacle densities n^* varying from 0.30 (top) to 1.10 (bottom). The thick black line represents a power law, $\delta r^2(t) \sim t^{2/z}$ with $z = 6.25$.

overall agreement is found, we demonstrate the necessity to include the leading-order corrections to scaling. Correspondingly, we extend the dynamic scaling hypothesis by an irrelevant scaling field, and obtain considerable improvement of data collapse.

Considering a needle as tracer particle enriches the Lorentz problem by an additional orientational degree of freedom. This extension might serve as a minimal model for the dynamics of a semiflexible polymer in a biological polymer network. We present first results for the MSD and orientational correlation functions, which provide new insight into different mechanisms for slow dynamics.

* Corresponding author: thomas.franosch@physik.lmu.de

[1] J. Kertész, J. Phys. (Paris) **42**, L 393 (1981).
 [2] W. T. Elam, A. R. Kerstein, and J. J. Rehr, Phys. Rev. Lett. **52**, 1516 (1984).
 [3] B. I. Halperin, S. Feng, and P. N. Sen, Phys. Rev. Lett. **54**, 2391 (1985).
 [4] J. Machta and S. M. Moore, Phys. Rev. A **32**, 3164 (1985).
 [5] F. Höfling, T. Franosch, and E. Frey, cond-mat/0510442.

Dynamics of mobile particles in an immobile environment: Simulation of a binary Yukawa system

N. Kikuchi* and J. Horbach

Institut für Physik, Johannes Gutenberg-Universität Mainz, Staudinger Weg 7, D-55099 Mainz, Germany

The classical example of mobile particles in an immobile environment is the Lorentz gas model. It considers the transport of a particle through a matrix of fixed obstacles whereby particle and obstacles interact by a hard-sphere interaction. Control parameter of the model is the obstacle packing density η . At high values of η , a delocalization-localization transition occurs where the particle gets trapped by percolating clusters of obstacles.

In this work, we use molecular dynamics (MD) simulations to investigate a binary mixture of small and big charged particles that interact via a screened Coulomb (or Yukawa) potential. We find that the system undergoes another type of a delocalization-localization transition. The different scenario is as follows: the small particles become localized when the big particles crystallize. Now, the small particles move in a periodic potential formed by the crystalline arrangement of big particles. In contrast to the Lorentz gas, the localization is driven by a periodic potential energy landscape and not by a packing effect. Note that Yukawa mixtures of big and small particles can be realized experimentally by colloidal systems [1].

Our binary Yukawa system consists of $N_s = 820$ small and $N_b = 1640$ big particles. The size ratio between them is $\frac{\sigma_b}{\sigma_s} = 5$ (with σ_b and σ_s the diameter of the big and small particles, respectively). The Yukawa interactions are short-ranged with a screening length of $1/\kappa = 0.12\sigma_b$. Excluded volume interactions between the particles are modeled by a shifted Lennard-Jones (WCA) potential. In our investigation, we first equilibrated the system by a NVT simulation (here, temperature was kept constant by means of a stochastic collision algorithm). We then performed microcanonical molecular dynamics for the production runs. Newton's equations of motion were integrated by the velocity form of the Verlet algorithm.

Upon decreasing temperature, different regimes can be identified by the incoherent intermediate scattering function (or self density correlator) $F_s(q, t)$ for the small particles (Fig. 1). At high temperatures ($T > 2.3$), both small and big particles are in a liquid state. When the temperature is lowered, we observe a transition around $T \sim 2.3$ where the big particles form a crystalline matrix while the small particles are still in the liquid phase. At this point, we observe the manifestation of a plateau in $F_s(q, t)$ for the small particles (Fig. 1). We stress that it results from the formation of the crystal. Further decrease of the temperature leads to an increase of the height of the (oscillatory) plateau that corresponds to an increasing lo-

calization of the small particles at intermediate times. The long-time decay of $F_s(q, t)$ is non-exponential. This is due to the hopping motion of the small particles from a given to another site in the sub-lattice of the crystalline matrix of big particles. The temperature dependence of the characteristic decay time τ_s of $F_s(q, t)$ to zero is rather weak for temperatures $2.3 > T > 0.1$ (essentially τ_s increases linearly with temperature. However, for lower temperatures τ_s increases strongly with temperature and eventually at $T = 0.01$ the small particles are trapped on the time scale of the simulation.

In the talk, we analyze the dynamics further by means of localization lengths, diffusion constants, and the van Hove correlation function $G(r, t)$, and we compare the results to those for other types of systems where mobile particles move in an immobile environment.

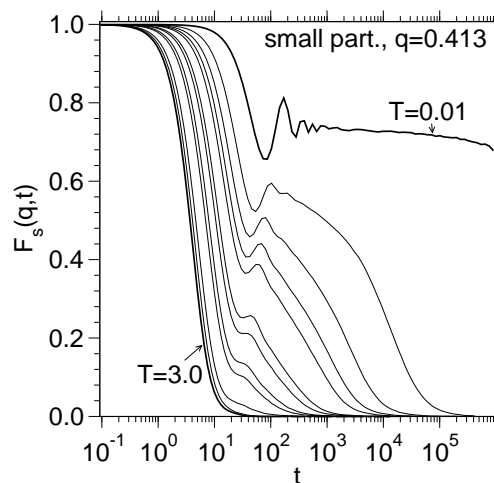


FIG. 1: Time dependence of the incoherent intermediate scattering function $F_s(q, t)$ of small particles for different temperatures $T = 3.0, 2.5, 2.0, 1.0, 0.8, 0.5, 0.4, 0.2, 0.15, 0.1, 0.05, 0.01$. The wave-vector $q = 0.413$ corresponds to the location of the main peak in the static structure factor $S_{bb}(q)$.

* Corresponding author: kikuchi@uni-mainz.de

[1] A. Imhof and J.K.G. Dhont, Coll. Surf. A **122**, 53 (1997); Phys. Rev. E **52**, 6344 (1995); Phys. Rev. Lett. **75**, 1662 (1995).

Mode-coupling theory for the liquid-glass transition of a fluid confined in a disordered porous matrix

Vincent Krakoviack*

*Laboratoire de Chimie, UMR 5182, École Normale Supérieure de Lyon,
46 allée d'Italie, 69364 Lyon cedex 07, France*

We report on an extension of the mode coupling theory (MCT) for the liquid-glass transition to a class of models of confined fluids, the so-called quenched-annealed (QA) binary mixture. In this model, the fluid particles (the annealed component) evolve in a disordered array of immobile interaction sites (the quenched component).

The resulting equations are similar to those describing the bulk, except for the presence of a linear term in the memory function. Such a term makes continuous (type A) ideal glass transitions possible, in addition to the standard discontinuous (type B) scenario met in the bulk.

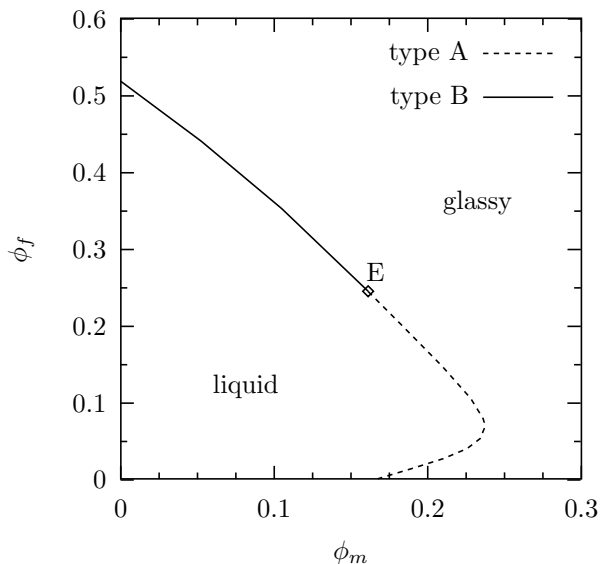


FIG. 1: Dynamical phase diagram of a hard sphere fluid confined in a matrix of identical hard spheres frozen in an equilibrium configuration. ϕ_f and ϕ_m denote respectively the fluid and matrix compacities. Point E is the common endpoint of the type A and type B transition lines. From Ref. [1].

Thanks to some peculiarities of the static correlations in QA systems, the present theory allows a simple and rigorous discussion of the relation between statics and dynamics in confinement and a direct illustration of possible inconsistencies between statics and dynamics resulting from the approximations involved in deriving the MCT. A formal illustration of the difference between self-induced and quenched disorder in fluid systems can be obtained as well.

We then present the different dynamical scenarios which are obtained when the theory is applied to simple model systems ruled by excluded volume interactions only. The corresponding dynamical phase diagrams are computed, which show new and nontrivial transition scenarios, including reentrant glass transitions and different topologies of the bifurcation manifold, with a variety of higher order singularities. For instance, Fig. 1 shows the dynamical phase diagram of one of the simplest models, which reproduces the topology of the bifurcation diagram of the schematic F_{12} model, with its degenerate A3 endpoint (denoted by E).

Partial account of the present research can be found in Refs. [1] and [2].

* Corresponding author: vincent.krakoviack@ens-lyon.fr

- [1] V. Krakoviack, Phys. Rev. Lett. **94**, 065703 (2005).
- [2] V. Krakoviack, J. Phys.: Condens. Matter **17**, S3565 (2005).

Polymer chain in a quenched random medium: slow dynamics and ergodicity breaking

V. G. Rostiashvili,* A. Milchev, G. Migliorini, and T.A. Vilgis
Max Planck Institute for Polymer Research
10 Ackermannweg, 55128 Mainz, Germany

The Langevin dynamics of a self-interacting chain embedded in a quenched random medium is investigated by making use of the generating functional method and one-loop (Hartree) approximation. We have shown how this intrinsic disorder causes different dynamical regimes. Namely, within the Rouse characteristic time interval the *anomalous diffusion* shows up. The corresponding subdiffusional dynamical exponents have been explicitly calculated and thoroughly discussed. For the larger time interval the disorder drives the center of mass of the chain to a trap or frozen state provided that the Harris parameter, $(\Delta/b^d)N^{2-\nu d} \geq 1$, where Δ is a disorder strength, b is a Kuhnian segment length, N is a chain length and ν is the Flory exponent. We have derived the general equation for the non-ergodicity function $f(p)$ which characterizes the amplitude of frozen Rouse modes with an index $p = 2\pi j/N$. It has been shown that the functional structure of the equation for $f(p)$ is related with the Götze's F_{12} -model. The numerical solution of this equation has been implemented (see Fig. 1) and shown that the different Rouse modes freeze at the same critical disorder strength $\Delta_c \sim N^{-\gamma}$ where the exponent $\gamma \approx 0.25$ and does not depend on the solvent quality.

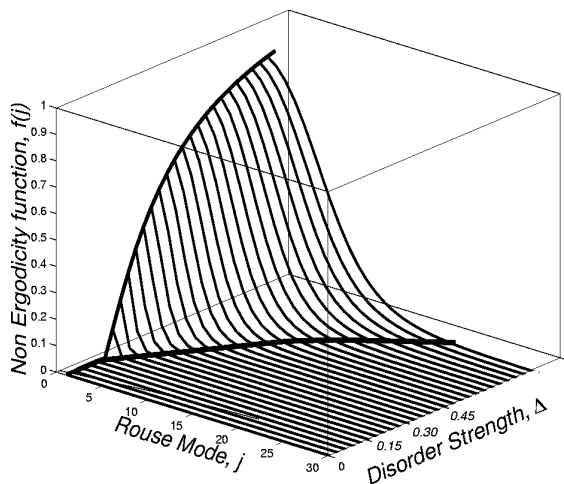


FIG. 1: 3D - Bifurcation diagram. The freezing of the modes appears above a critical value of $\Delta_{cr} \approx 0.13$.

We also have tested these predictions through the use of a Monte Carlo (MC) simulation. For this end the off-lattice bead-spring model of a self-avoiding

polymer chain immersed in a 3-dimensional quenched random medium has been used. The chain center of mass mean-squared displacement as a function of time reveals two crossovers which depend both on chain length N and on the degree of Gaussian disorder Δ . The first crossover from normal to anomalous diffusion regime is found at short time τ_1 and observed to vanish rapidly as $\tau_1 \propto \Delta^{-11}$ with growing disorder. The second crossover back to normal diffusion, τ_2 , scales as $\tau_2 \propto N^{2\nu+1}g(N^{2-3\nu}\Delta)$ with g being some scaling function. The diffusion coefficient D_N depends strongly on disorder and drops dramatically at a *critical dispersion* $\Delta_c \propto N^{-2+3\nu}$ of the disorder potential (see Fig. 2) so that for $\Delta > \Delta_c$ the chain center of mass is practically frozen. These MC-findings agree pretty well with our theoretical predictions.

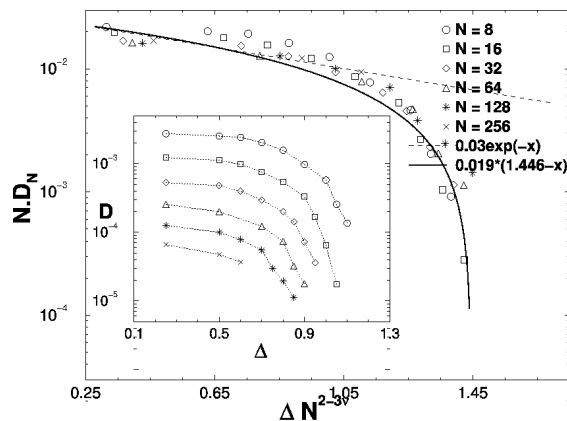


FIG. 2: Diffusion coefficient D_N/D_R as a function of the scaled degree of disorder $x = \Delta N^{2-3\nu}$ for chains of length $8 \leq N \leq 256$. Dashed line denotes the simple Markovian diffusion prediction $ND_N \propto \exp(-x)$, a full line is a best fit with $ND_N \propto (x_c - x)$. Unscaled data is shown in the inset.

* Corresponding author: rostiash@mpip-mainz.mpg.de

- [1] G. Migliorini, V.G. Rostiashvili and T.A. Vilgis, Eur. Phys. J. B **33**, 61 (2003).
[2] A. Milchev, V.G. Rostiashvili and T.A. Vilgis, Europhys. Lett. **68**, 384 (2004).

Elastic models for viscous liquids

Jeppe C. Dyre, Niels Boye Olsen, T. Christensen

Department of Mathematics and Physics (IMFUFA), "Glass and Time" – DNRF Centre for Viscous Liquid Dynamics, Roskilde University, Postbox 260, DK-4000 Roskilde, Denmark

This paper deals with phenomenological models for the non-Arrhenius average relaxation time of glass-forming liquids. Here, a phenomenological model is a model which predicts the relaxation time activation energy from a macroscopic quantity. We first briefly discuss four models where the activation energy is controlled by: 1) the configurational entropy (Adam-Gibbs model); 2) the free volume; 3) the energy; 4) the instantaneous elastic moduli [1]. The latter models, which go back in time the 1940's and 1950's and exist in many versions, may be termed "elastic" models.

After giving an overview of various problems with the first three kinds of models the paper goes on to discuss the elastic models in more details. It is argued that in the simplest approximation the elastic models are all equivalent.

We discuss the apparently puzzling property of elastic models that the long-time relaxational properties are predicted by short-time elastic constants; it is argued that this is entirely possible and not counterintuitive. It is also shown that the elastic models predict a connection between thermodynamics and fragility: more fragile liquids are predicted to have higher excess specific heats. Although this is qualitatively obeyed, the effect is too large to quantitatively explain the experimental findings. Finally, we discuss the experimental situation more generally.

* Corresponding author: dyre@ruc.dk

[1] J. C. Dyre, *Nature Mater.* 3, 749 (2004).

Self-Confinement Effects in Extremely Diluted Polymer Blends

 A. Arbe,^{1,*} M. Tyagi,² J. Colmenero,² B. Frick,³ and R. Stewart³
¹Unidad Física de Materiales (CSIC-UPV/EHU), San Sebastián, Spain

²Donostia International Physics Center, San Sebastián, Spain

³Institut Laue-Langevin, Grenoble, France

How are the dynamical processes of a polymer affected by blending with another polymer? This question –the dynamic miscibility– is particularly interesting in the case of the α -relaxation when the polymers involved show very different T_g -values. Experimental studies indicate a clear dynamic heterogeneity: though affected by blending, the two α -relaxation processes can still be distinguished. The "self-concentration" –the chain connectivity enhances the concentration of the polymer over the bulk concentration in the relevant cooperative volume– is the main ingredient of the Lodge/McLeish (LML) model [1], that gives account for the experimental observations in a large number of blends above the average T_g of the blend, $\langle T_g \rangle$. However, recently a different phenomenology has been found in blends with small concentration of the low- T_g component. First, dielectric studies close and below $\langle T_g \rangle$ detected a relaxation process slower than the localized motions inducing the secondary relaxations [2]. That process was attributed to rather localized, weakly cooperative motions of the fast component resulting from the topological constraints imposed by the almost frozen chains of the high- T_g component. Furthermore, a combined quasielastic neutron scattering (QENS) and MD-simulations study on 25%PEO/75%PMMA (PEO: poly(ethylene oxide); PMMA: poly(methyl methacrylate)) suggested that the presence of the hardly moving PMMA matrix leads to the creation of little pockets of mobility where PEO can move [3].

Here we present a QENS study of the dynamics of PEO in a blend with poly(vinyl acetate) (PVAc) (20%PEO/80%PVAc). As the PVAc component was deuterated, neutrons revealed selectively the PEO motions. The T -range investigated (270 K to 400 K) covered the region of $\langle T_g \rangle$. At $T \gg \langle T_g \rangle$ (375 K and 400 K) the behavior could be compatible with the LML predictions ("equilibrium" behavior). However, strong deviations are found at 350 K and below. The spectra were analyzed in terms of log-normal distributions of relaxation times. Extremely broad distributions are revealed approaching $\langle T_g \rangle$. Interestingly, even at 350 K, the momentum transfer (Q)-dependent width of the distribution shows a clear deviation from the typical entropy-driven (Rouse) behavior. The consequent sudden increase of the average relaxation time with respect to the expected Rouse behavior indicates the freezing of the Rouse modes. From the Q -value where this deviation occurs a confinement size of about 1 nm is deduced, as it was reported for PEO in PMMA [3]. This size would decrease with decreasing T , indicating a stronger and stronger dynamical confinement when the slow phase approaches $\langle T_g \rangle$. Furthermore, a flattening of the characteristic timescales

at Q -values above $\approx 1 \text{ \AA}^{-1}$ is observed that clearly reveals signatures of localization. Fig. 1 shows the constant- Q timescale found at high Q (τ^*) for PEO in both blend systems. τ^* should be characteristic for the localized motions taking place within the confined regions. The typical length scales of the localized motions would be of about 2.5 \AA close to $\langle T_g \rangle$. Clear deviations from "equilibrium" can be seen below 350 K. Moreover, once the slow component becomes frozen for the timescale of PEO, the localized process is independent of the nature of the rigid phase surrounding the fast blend component.

We have characterized the self-confinement phenomenon induced by the freezing of the majority slow component in thermodynamically miscible blends. Selectivity of QENS with deuteration is essential to shed light in this recently discovered effect.

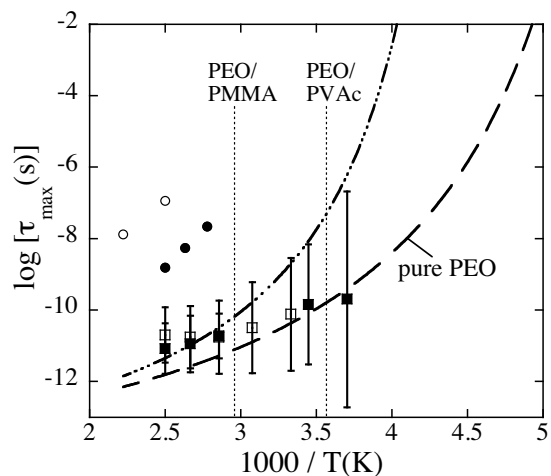


FIG. 1: T -dependence of the time of the maximum of the distribution function. Squares: τ^* for PEO in the blend with PVAc (full symbols) and with PMMA (empty symbols). Dashed line: pure PEO at $Q = 1.5 \text{ \AA}^{-1}$; dashed-dotted line: LML prediction. Vertical lines through τ^* : width of the distribution (FWHM). Dotted vertical lines: location of $\langle T_g \rangle$. Circles: timescales of the other component at $Q = 1 \text{ \AA}^{-1}$: PVAc (full) and PMMA (empty).

* Corresponding author: waparnea@sc.ehu.es

- [1] T. P. Lodge and T. C. B. McLeish, *Macromolecules* **33**, 5278 (2000).
- [2] C. Lorthioir, A. Alegría, J. Colmenero, *Phys. Rev. E* **68**, 031805 (2003).
- [3] A.-C. Genix, A. Arbe, F. Alvarez, J. Colmenero, L. Willner and D. Richter, *Phys. Rev. E* **72**, 031808 (2005).

Rubber-like dynamics in sulfur above the λ -transition temperature

G. Monaco,^{1,*} L. Crapanzano,¹ R. Bellissent,² W. Crichton,¹
D. Fioretto,^{3,4} M. Mezouar,¹ F. Scarponi,^{3,4} and R. Verbeni¹

¹European Synchrotron Radiation Facility, Boîte Postale 220, 38043 Grenoble, France

²Centre d'Etudes Nucleaires de Grenoble, DRFMC/SPSMS/MDN, 6 rue Horowitz, 38054 Grenoble, France

³Dipartimento di Fisica, Università di Perugia, Via A. Pascoli, 06123 Perugia, Italy

⁴INFM CRS-SOFT, c/o Università di Roma "La Sapienza", P. A. Moro 2, 00185 Roma, Italy

At 432 K and ambient pressure, liquid sulfur undergoes a rather peculiar reversible transition between a yellow pale, low-viscosity liquid and a reddish, high-viscosity one. This transition, known as λ -transition, is marked by an anomalous behavior in many physical properties, in particular by an increase in shear viscosity by at least four orders of magnitude [1] and a λ -like singularity in the temperature dependence of the heat capacity [2]. This transition is generally attributed to a reversible polymerization process: the S_8 units of the low-temperature molecular liquid tend to open above the transition temperature T_λ and to polymerize, thus giving rise to a solution of polymers in monomeric S_8 molecules.

From a theoretical point of view, the λ -transition is described in terms of a second order phase transition which includes nonclassical critical effects [3]. However, this theory fails to describe quantitatively the anomalies experimentally detected at T_λ [4]. As a matter of fact, the λ -transition in sulfur, despite being studied for more than one century and being considered the prototype of equilibrium polymerizations [4], still requires some effort to be really understood.

modulus in sulfur below and above the λ -transition temperature.

We have performed an inelastic x-ray scattering (IXS) study of the high-frequency acoustic dynamics of sulfur across T_λ [5]. The combination of these high-frequency data with lower frequency, literature ones indicates that the elastic moduli are characterized by a glass-like plateau in the THz frequency range for both liquid phases and - for the high-temperature, polymeric solution only - by an additional, rubber-like plateau in the sub-kHz frequency range, as schematically shown in Fig. 1. Thus, while the dynamics of the molecular liquid is similar to that of simple liquids, the dynamics of the high-temperature phase is strongly affected by entanglement coupling among polymeric chains.

* Corresponding author: gmonaco@esrf.fr

[1] R.F. Bacon, and R. Fanelli, *J. Am. Chem. Soc.* **65**, 639 (1943).

[2] F. Feher, and E. Hellwig, *Z. Anorg. Allg. Chem.* **294**, 63 (1958).

[3] J.C. Wheeler, S.J. Kennedy, and P. Pfeuty, *Phys. Rev. Lett.* **45**, 1748 (1980).

[4] S.C. Greer, *J. Phys. Chem. B* **102**, 5413 (1998).

[5] G. Monaco, L. Crapanzano, R. Bellissent, W. Crichton, D. Fioretto, M. Mezouar, F. Scarponi, R. Verbeni, *Phys. Rev. Lett.* (in press).

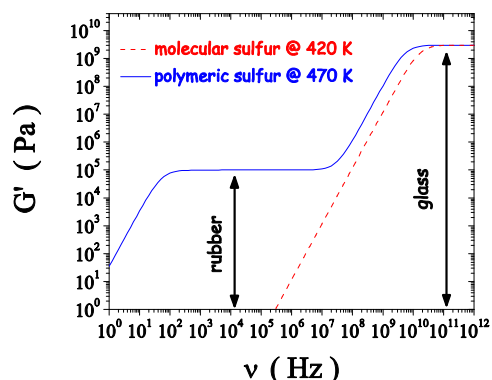


FIG. 1: Sketch of the frequency dependence of the shear

Emergence and establishment of the corset effect in mesoscopic polymer melt layers: A crossover from bulk to confined dynamics.

Ravinath Kausik^{*1}, Carlos Mattea¹, Rainer Kimmich¹, Nail Fatkullin², Nicola Hüsing³

¹Sektion Kernresonanzspektroskopie, Universität Ulm, 89069 Ulm, Germany

²Department of Physics, Kazan State University, 420008 Kazan, Russia/Tatarstan

³Abteilung Anorganische Chemie I, Universität Ulm, 89069 Ulm, Germany

Polymer chain dynamics changes dramatically from bulk to mesoscopically confined melts [1]. The Rouse and Renormalized Rouse theories describe the behaviour of bulk polymers while the Tube or Reptation theory explains the dynamics of confined polymers [2].

We have investigated the emergence of the confinement effect on Rouse polymers at micrometer thick layers which is a consequence of the **Corset Effect** [2]. This effect has also been explored by packing polymer in 4nm small pores. The chain dynamics have been probed using field cycling NMR relaxometry as the predominant technique supplemented by rotating frame relaxometry.

The corset effect implies that the chain modes are affected by walls many random coil diameters away. The effect is due to the chain uncrossability and the finite size of the system reducing the free volume fluctuations in confined samples. Small systems cannot be subject to large molecular fluctuations. Since the low compressibility typical for liquids does not allow for large free volume fluctuations, conformational chain rearrangements are largely suppressed.

Micrometer scale polymer layers were prepared by the following technique and their spin lattice dispersion curves compared with the bulk values.

Driven with a motor, a thin polyimide tape was led at constant velocity in the range from 1 to 10 mm/s through a dilute solution of the polymer and wound on a thin glass rod. On the way from the solution to the sample roll the solvent in the adsorption layer is volatilized, so that the tape is finally covered by a dry film of the polymer [3]. The thickness of this layer can be controlled by varying the concentration of the solution keeping the velocity of the motor constant [4],[5]. Micrometer thick polymer melt layers were prepared using this principle and field cycling NMR relaxometry used to investigate the emergence of deviation from bulk dispersion indicating the corset effect [6].

In the other extreme, completely established corset effect corresponding to reptation dynamics were exhibited as expected in the dispersion curves of polymer packed inside 4nm porous vycor glass. The signatures of the tube/reptation model of the spin lattice relaxation time, both with respect to the molecular weight and frequency were satisfied. The vycor glasses were covered by a layer of tri-methyl siloxy groups and the effect of adsorption, leading to an increase of spin lattice relaxation times in 4nm small pores and the absence of such an effect in 1 μ m large pores have been demonstrated.

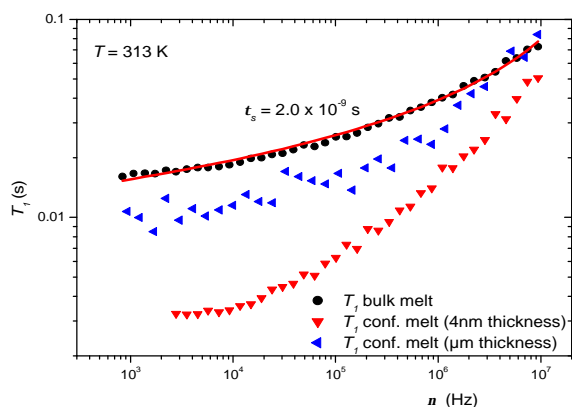


FIG. 1: Frequency dependence of fluorine spin lattice relaxation times for bulk and samples confined in micrometer and nanometre length scales.

* Corresponding author: ravinath.kausik@uni-ulm.de

[1] R. Kimmich, N. Fatkullin, *Advan. Polym. Sci.* 170 (2004) 1.

[2] C. Mattea, N. Fatkullin, E. Fischer, U. Beginn, E. Anordo, M. Kroutieva, R. Kimmich, *Appl. Magn. Reson.* 27 (2004) 371.

[3] Sherwood, M. H., Schwickert, B. *Polymer Preprints* (2003).

[4] Landau L. D. and Levich B., *Acta Physicochim. USSR*,17(1942) 42.

[5] Derjaguin B.V., *Acta Physicochim. USSR*, 20(1943) 349.

[6] Ravinath Kausik, Carlos Mattea, Nail Fatkullin and Rainer Kimmich, submitted.

Phase Diagram and Glass Transitions in Oppositely Charged Colloids.

Jose B. Caballero,^{1,*} Antonio M. Puertas,¹ and M. E. Cates²

¹*Department of Applied Physics, University of Almeria, 04120 Almeria, Spain*

²*School of Physics, The University of Edinburgh,
Kings Buildings, Mayfield Road, Edinburgh EH9 3JZ, U. K.*

In this contribution, we study the colloidal analog of the ionic fluid [1] (Restricted Primitive Model, RPM) using computer simulations, i.e. a symmetrical mixture of oppositely charged colloids. Experimental works are focused on the crystal phases [2].

The system is composed of a 1:1 binary mixture of N spherical particles of equal diameter; $N/2$ bearing surface potential $+\phi$ and $N/2$ with $-\phi$. The mixture is immersed in a continuous medium characterized by its dielectric constant, ϵ , in presence of an electrolyte. The electrostatic interactions are modeled using the well-known DLVO effective potential between the colloidal particles and the dispersion forces were not considered. Thus the total potential is given by:

$$U(r) = \begin{cases} \infty, & r \leq \sigma \\ \pi\epsilon\sigma\phi_1\phi_2 \cdot \exp\{-\kappa(r - \sigma)\}, & r > \sigma \end{cases} \quad (1)$$

Where σ is the diameter of the particles, κ is the inverse Debye length and ϕ is the surface potential. Obviously, this is the first approximation to the whole problem, because the small ions are not taken into account but an effective interaction between the macromolecules. The aim is to obtain the phase diagram and glass transitions in this system varying the salt concentration, i.e. the range of the interaction.

The gas-liquid coexistence curve was obtained combining Gibbs Ensemble and Grand Canonical Monte Carlo simulations. As in ionic fluids, this model undergoes a gas-liquid transition in the low T -low ρ region; where high correlations between oppositely charged colloids arise. The critical temperature presents a non monotonic behavior with the interaction range, what can be rationalized considering charge correlations. On average, each charged colloid is surrounded by a layer of oppositely charged particles, followed by a layer of similarly charged colloids and so on. Therefore, when the salt concentration is increased, the attractive term is shortly screened (because the opposite charged particles are in contact); contrary, the repulsive contributions are strongly screened since longer distances separate unequal colloids. The system, thus, gains energy upon increasing $\kappa\sigma$, resulting in an increase of the critical

temperature (opposite to the behavior of monocomponent systems). At high enough κ , the repulsive interactions are completely screened, T_c decreases as in a monocomponent system, since only the first layer of particles (with opposite charge) interacts, leaving a maximum at $\kappa\sigma \approx 10$. An island of phase separation (gas-liquid) is then predicted for this model.

Next, using NVT Molecular Dynamics simulations, we have studied the non ergodic lines for this model system. Now, polydisperse samples are equilibrated at high temperatures and quenched down to sub-critical conditions where the system is phase separated. At the highest temperatures studied, the system undergoes a thermodynamic gas-liquid transition. At lower temperatures, however, arrested phase separation is observed, and further quenches do not produce denser liquids, as it is thermodynamically expected. We identified the point where the glass line intercepts the gas-liquid transition and studied the dynamics in this region. Properties of the mean square displacement and the correlation functions fulfill the universal predictions of the ideal Mode Coupling Theory (MCT). Also we found similarities between our viscous liquid and that of hard-spheres, and therefore, interpret this non ergodic line as a repulsive glass. At deeper quenches a ramified percolating cluster is observed. Now permanent bonds are formed although there is plenty of free space to move. In this case, the dynamics of the system is similar to that which was reported for an attractive glass showing interesting dependences with the density of the sample. The same behavior was noticed for all the $\kappa\sigma$ studied.

We can summarize that two different arrested phase separated states exist in our model presenting different rheological properties: one which is dominated by the steric repulsion between the particles and the other one which is formed due to the formation of permanent bonds.

* Corresponding author: jcaballe@ual.es

[1] J. B. Caballero et al., J. Chem. Phys. **121** 2428 (2004).

[2] M. E. Leunissen et al., Nature **80**, 235 (2005).

**Homogeneous nucleation kinetics of model charged sphere suspensions:
a Different Route into the Glassy State?**

Hans-Joachim Schöpe

Institut für Physik, Universität Mainz, Staudinger Weg 7, D-55099 Mainz

Colloidal suspensions have acquired a model system status in experimental research on the fundamentals of solidification. Most work so far was performed on hard sphere suspensions. Here we investigated the kinetics of homogeneous nucleation from a shear melt for a model system of deionised aqueous suspensions of charged spheres and compare the results with hard spheres. With the aid of nearly index matched perfluorinated particles of low polydispersity we extended previous studies into the regime of large meta-stability and nucleation dominated solidification. With increasing particle number density n the solidification time determined by the appearance of a finite shear modulus decreased from minutes to milliseconds. Nucleation rate densities J were derived from the width of the principal peak in the static structure factor as measured by light scattering after complete solidification. J was observed to increase approximately exponentially with n as expected from classical nucleation theory in the absence of a kinetic glass transition. Additional measurements of the elastic and dynamic behaviour, however, show that for the largest concentrations the sample properties are glass-like. Thus an amorphous state is kinetically stabilised via a different route as compared to hard spheres.

Infrared Photon Correlation Spectroscopy: a novel experimental technique for the investigation of dynamics in viscous liquids

Tullio Scopigno*

INFN CRS-SOFT, c/o Università di Roma "LaSapienza", I-00185, Roma, Italy

Dynamic light scattering is a well established, robust technique, for the investigation of dynamics in colloidal systems, polymers and glass forming materials. Originally, visible light from a laser source has been utilized as probe, with some limitations due to absorption in non transparent samples and multiple scattering in dense suspensions. More recently, the use of highly collimated X-ray beams become possible (XPCS), thus extending this technique at higher values of momentum transfer.

We present here a novel experimental setup to perform dynamic light scattering with infrared radiation ($\lambda = 1064$ nm). Advantages and drawbacks in comparison to the conventional photon correlation spectroscopy with visible and X-ray light will be discussed, and a flavor of the recent experimental investigations carried out so far will be given. These include: i) **absorption-induced convection effects in colloidal systems:** Colloidal suspension in water, decalin and tetralin have been investigated. Due to the infrared absorption from the solvent, the sample heating induces convective motion of the beads, resulting in a non-trivial, non-exponential decaying autocorrelation function.

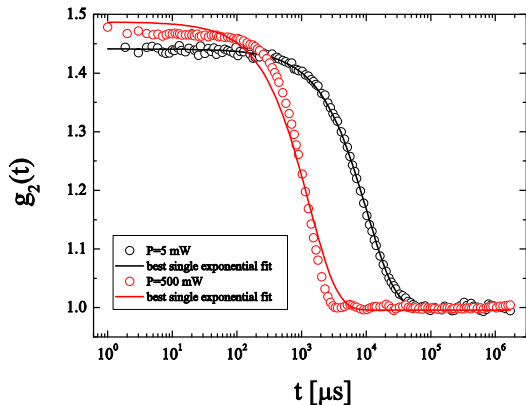


FIG. 1: PMMA suspension in Decalin/Tetralin solvent. We show here the omodine autocorrelation function as measured with IRPCS. With 500 mW incident power the deviation from a simple exponential behavior testifies of absorption-induced convection effects. On reducing the power the exponential decay typical of brownian motion is restored.

ii) **structural relaxation in non transparent glass formers:** Binary and ternary Chalcogenide glass-formers of different compositions and pure Selenium, presenting absorption and photo-induced effects from visible light, have been studied. The structural relaxation has been investigated in the supercooled region down to the glass transition temperature, thus determining the fragility.

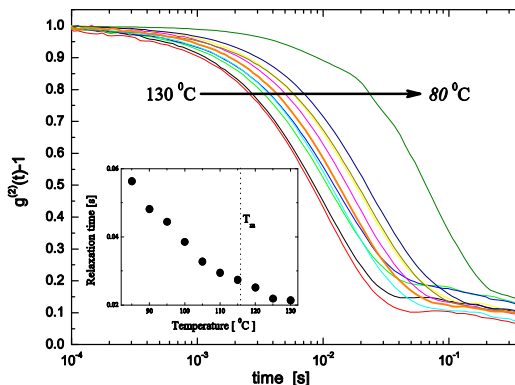


FIG. 2: Autocorrelation function of supercooled sulphur at different temperatures, from $T = 130$ °C down to $T = 80$ °C, in steps of 5 °C. Inset: Structural relaxation time.

iii) **liquid-liquid transition in polymeric fluids:** Liquid Sulphur present a liquid-liquid phase transition at around $T = 159$ °C. Preliminary visible light scattering data show a complex relaxation pattern in that temperature region [1]. We report here dynamic light scattering data with Infrared light, discussing the emerging picture.

* Corresponding author: tullio.scopigno@phys.uniroma1.it

[1] S.N. Yannopoulos et al. private communication.
 [2] S.G.J. Mochrie et al., Phys. Rev. Lett. 78, 1275 (1996).

Universality in the Vibrational Spectra of Amorphous Systems

Gurpreet S. Matharoo^{1,2,*} and Subir K. Sarkar¹

¹*School of Physical Sciences, Jawaharlal Nehru University, New Delhi 110067, India*

²*Department of Physics, St. Francis Xavier University, Antigonish, NS, B2G 2W5, Canada*

We perform extensive numerical computations on the vibrational spectra of amorphous systems. We deal with isolated amorphous clusters and with the bulk amorphous systems. With both these systems, we generate inherent structures which are the local minima of the Potential energy landscape(PEL) or surface(PES). In amorphous clusters, we vary the number of particles to investigate the effects of finite size on various properties whereas, for the bulk amorphous systems we use periodic crystals where we vary the number of particles in the unit cell. The interaction potential is also varied in both the cases to study the possible universality. At each local minima, we calculate the vibrational spectra using standard techniques for both the systems and look for some universal features in them.

For amorphous clusters, we find that over a large central region of the vibrational spectrum, the integrated density of states can be described by the same functional form, containing only one scale of frequency in all the cases and the spectral fluctuations are described by the Gaussian orthogonal ensemble of the Random matrices to an extra ordinarily high degree of accuracy [1, 2].

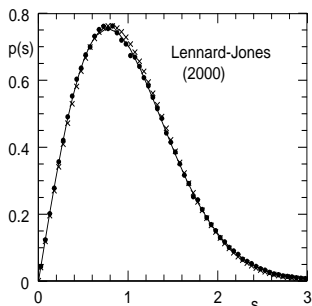


FIG. 1: Probability density $[p(s)]$ for the normalized nearest neighbor spacing (s) for Lennard-Jones Potential. Filled circles: Our data. Crosses: Wigner's surmise for GOE. Continuous line: Exact prediction for the GOE.

For bulk amorphous systems, at constant pressure, using techniques of Monte Carlo simulations and the Conjugate Gradient method of minimization we

demonstrate the change in nature of the vibrational spectrum as one goes from crystalline state to completely amorphous states and there are indeed certain limiting conditions in which the normalized density of states assume a universal shape *over the entire spectrum*. The analysis with the bulk systems gives a detailed picture of how excess vibrational modes develop in both low frequency and high frequency domains of the spectrum, the accumulation in the low frequency domain is the reason behind the existence of 'Boson peaks'[3]. In these calculations, we have not used any specific model of disorder. Once the choice of the potential is made, there is no need to make any further approximation.

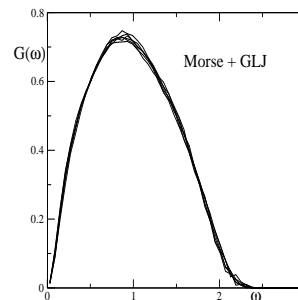


FIG. 2: Convergence of the Normalized density of states ($G(\omega)$) vs. normalized frequency (ω) to a universal shape over the whole spectrum for some selected cases of Morse potential and Generalized Lennard-Jones(GLJ) potential.

GSM thanks CSIR, India for the financial support.

-
- * Corresponding author: gurpreet@stfx.ca
 [1] S. K. Sarkar, G. S. Matharoo and A. Pandey, Phys. Rev. Lett. **92**, 215503 (2004).
 [2] G. S. Matharoo, S. K. Sarkar and A. Pandey, Phys. Rev. B **72**, 075401 (2005).
 [3] W. Schirmacher, G. Diezemann, and C. Ganter, Phys. Rev. Lett. **81**, 136 (1998).

A Transient Grating study of the molecular glass former *m*-toluidine down to the vicinity of its glass transition temperature

A. Azzimani ⁽¹⁾, C. Dreyfus ⁽¹⁾, and R.M. Pick* ⁽¹⁾, A. Taschin ⁽²⁾, P. Bartolini ⁽²⁾ and R. Torre ⁽²⁾

(1) IMPMC, Univ. P et M. Curie, Paris, (F)

(2) LENS, Università di Firenze, Firenze, (I)

A full theory of Heterodyne Detected Transient Grating (HD-TG) experiments in Supercooled Molecular liquids has been recently formulated that takes into account retardation effects in each term appearing in the generalised Navier Stokes equations [1]. The TG signal can be expressed as the sum of responses corresponding respectively to a thermal absorption, H , an electrostrictive effect, a , and the anisotropic part of the molecular polarisability, b . and detected either by density (proportional to a), or to orientational (proportional to b) modulations. When $H \gg a \gg b$ (condition C) only two independent response functions, the isotropic and anisotropic responses, can be measured by careful selection of the polarisation.

Such measurements have been performed at LENS, on *m*-toluidine, from 315 K down to 195 K= T_g +7 K. Detailed analysis of the data shows that:

- Condition C is fulfilled and the corresponding ratios have been determined;
- Both the relaxation contributions to the specific heat at constant volume, $C_V(t)$, and to the thermal pressure coefficient, $\beta(t)$, are necessary to give a consistent description of the signal whatever the ratio of the longitudinal α -relaxation time, τ_L , to the heat diffusion time;

- For $\omega_B \tau_L > 1$ (where ω_B is the longitudinal phonon pulsation), the description of the isotropic signal requires an important stretching of the α relaxation process, this stretching increasing with decreasing temperature. At still lower temperatures ($\omega_B \tau_L \gg 1$) this α relaxation process alone no longer provides a proper description of the full relaxation process: in the vicinity of $T \approx 1.1 T_g$, different processes, taking place in different time windows, have to be taken into account; the shortest one exhibits a quasi-logarithmic decay.

- The relaxation time, τ_μ , of the rotation-translation coupling function is detected through the anisotropic signal. To a good accuracy, τ_μ is equal to the rotational relaxation time, τ_R ; it does not scale with τ_L and exhibits a much smaller stretching.

* Corresponding author: cor@moka.ccr.jusieu.fr

[1] R.M. Pick et al., EPJB **39**, 69 (2004)

Correlation of primary relaxations and high-frequency modes in supercooled liquids

A. Nowaczyk,¹ B. Geil,¹ M. Winterlich,¹ G. Hinze,² G. Diezemann,² R. Böhmer¹

¹*Experimentelle Physik III, Universität Dortmund, 44221 Dortmund, Germany*

²*Institut für Physikalische Chemie, Universität Mainz, 55099 Mainz, Germany*

The question regarding a possible correlation of the time scales of primary and secondary relaxations in supercooled liquids is addressed quantitatively. It is shown how this question can be answered using spin-lattice relaxation weighted stimulated-echo experiments.

The theoretical expressions relevant for the description of such experiments in the presence of correlation effects are analyzed by Monte Carlo integration for various correlation scenarios also including exchange processes which are the hallmark of dynamical heterogeneity. The results of these numerical simulations provide clear signatures that allow one to distinguish uncorrelated from differently correlated cases. Since modified spin-lattice relaxation effects occur in the presence of non-exponential magnetization recovery it is shown how to correct for them in first order.

The experiments are performed using deuterium NMR somewhat above the calorimetric glass-transition of substances such as ortho-terphenyl, D-sorbitol, and ortho-carborane. It found that supercooled liquids exhibit a correlation regarding the time scales of primary and secondary relaxation.

Acknowledgement: The financial support for this project is provided by the Graduiertenkolleg 298 (Dortmund).

* Corresponding author: roland.bohmer@uni-dortmund.edu

Cole-Cole Dynamics in Molecular and Colloidal Liquids

Matthias Sperl*

Duke University, Physics Department, Box 90305, Durham, NC 27708, USA

Within mode-coupling theory (MCT) a Cole-Cole-like law is derived for the susceptibility spectra [1],

$$\chi_q(\omega) = \chi_{0q}^{cc} / \left[1 + (-i\omega/\omega_q^c)^a + \hat{K}_q^{cc} (-i\omega/\omega_q^c)^{2a} \right], \quad (1)$$

for wave vectors q . For vanishing correction, $\hat{K}_q^{cc} = 0$, one recovers the leading-order result: the Cole-Cole function [2].

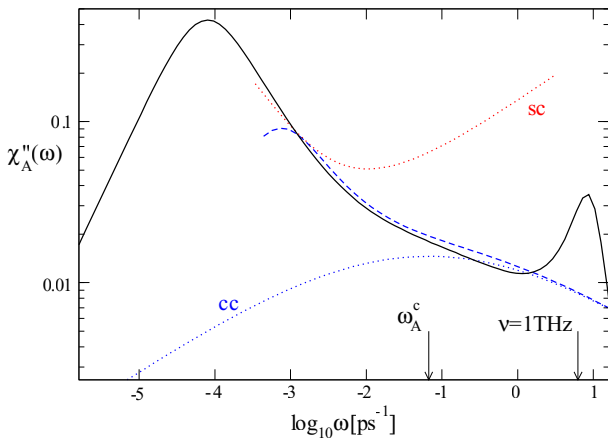


FIG. 1: Wing in the spectrum for BZP for $T = 251\text{K}$ (full line) [1, 3]. The dotted line *sc* displays the scaling-law approximation. The dotted line *cc* shows the first line of Eq. (1); the dashed line is the equivalent of *cc* for a finite distance from the critical point. The Cole-Cole frequency $\omega_A^c = 0.067\text{ps}^{-1}$ is indicated by an arrow.

Cole-Cole peaks following Eq. (1) are identified in experimental data. For molecular glass formers one finds three scenarios. For $0.4Ca(NO_3)_2 \cdot 0.6K(NO_3)$ (CKN) ω^c is so high that only the low-frequency part of the Cole-Cole peak is relevant which is equivalent to the well-known power law ω^a . For the second example, salol, the leading-order result in Eq. (1) describes the spectra better than the ω^a law for two orders of magnitude in frequency. Finally, for benzophenone (BZP), the scaling laws like ω^a fail in the relevant frequency windows, and Eq. (1) must be used instead to explain the data [3]. The existence of a Cole-Cole peak gives rise to a wing in the spectrum as shown in Fig. 1. This wing is explained by leading-order asymptotic formulas equivalent to the first line of Eq. (1).

In colloidal systems, the equivalent of Eq. (1) is identified in data for the mean-squared displacement of the hard-sphere system [4]. In contrast to the power-law solution t^{-2a} , the Cole-Cole formula can explain the full range of relaxation, cf. Fig. 2.

Further examples for Cole-Cole dynamics include the incoherent scattering function for hard spheres, correlation functions for binary hard-sphere mixtures, and the dipole correlator for the hard-dumbbell system.

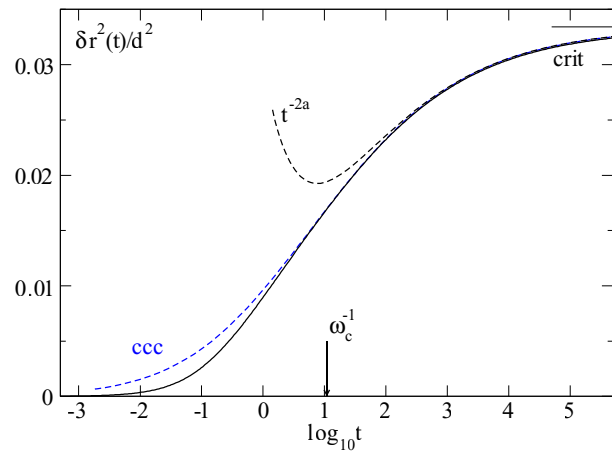


FIG. 2: Cole-Cole law in the mean-squared displacement (MSD) for the hard-sphere system [4]. The full line shows the MSD at the critical point. The dashed line (t^{-2a}) displays the power-law approximation, (*ccc*) the approximation by Eq. (1).

Part of this work is carried out together with W. Götze. This work is supported by DFG SFB 513, DFG Grant No. SP 714/3-1, NSF-DMT0137119, and NSF-DMS0244492.

* Corresponding author: msperl@duke.edu

[1] W. Götze and M. Sperl, to be published

[2] K. S. Cole and R. H. Cole, J. Chem. Phys. **9**, 341 (1941).

[3] W. Götze and M. Sperl, Phys. Rev. Lett. **92**, 105701 (2004).

[4] M. Sperl, Phys. Rev. E **71**, 060401 (2005).

The exponential distribution of the landscape energy-barriers and the fast dynamics of glassy polymers : evidences from high-field Electron Paramagnetic Resonance of molecular guests

V.Bercu,¹ M.Martinelli,² C.A.Massa,² L.A.Pardi,² and D.Leporini^{3,*}

¹Dipartimento di Fisica "Enrico Fermi", Università di Pisa, Largo B. Pontecorvo 3, I-56127 Pisa, Italy, Istituto per i processi Chimico-Fisici, via G.Moruzzi 1, I-56124 Pisa, Italy

² IPCF-CNR, via G.Moruzzi 1, I-56124 Pisa, Italy

³Dipartimento di Fisica "Enrico Fermi", Università di Pisa, and SOFT-INFM-CNR, Largo B. Pontecorvo 3, I-56127 Pisa, Italy

Particular interest and a current subject of strong controversy is the so called fast dynamics of glasses, occurring in the time window $1 - 10^2$ ps with several studies carried out by neutron [1–3], light [4] and Raman scattering [5] and high-field Electron Paramagnetic Resonance (HF-EPR) [6–8]. The scattering techniques observe that on heating above the onset temperature T_f ($T_f < T_g$) : i) the dynamics of glass-forming systems deviates from the harmonic behavior and quasielastic scattering starts to accumulate in the low frequency range of $S(Q, \omega)$; ii) the atomic mean-squared displacement starts to deviate from the linear temperature dependence.

The microscopic origin of the fast dynamics is still a question open to a strong controversy. The role of carbon-carbon *torsional* barriers to drive the fast dynamics of glass-forming polymers was pointed out [1]. In the particular case of polystyrene (PS, $T_f = 175 \pm 25K$ [2, 3]) the onset of the fast dynamics was ascribed to the change of the *librational* dynamics of the side-chain phenyl ring .

The reorientation of the paramagnetic guest molecule TEMPO (spin probe) in glassy PS [6–8] and polybutadiene is studied by high-field Electron Paramagnetic Resonance spectroscopy at three different Larmor frequencies (95, 190 and 285 GHz). For PS two different regimes separated by a crossover region are evidenced (see fig.1). Below 180K the rotational times are nearly temperature-independent with no apparent distribution. In the temperature range 180 – 220K a large increase of the rotational mobility is observed with widening of the distribution of correlation times which exhibits two components: i) a delta-like, temperature-independent component representing the fraction of spin probes w which persist in the low-temperature dynamics; ii) a strongly temperature-dependent component, to be described by a power-distribution, representing the fraction of spin probes $1-w$ undergoing activated motion over an *exponential* distribution of barrier heights $g(E)$ [6, 9]. Above 180K a steep decrease of w is evidenced. The shape and the width of $g(E)$ do not differ from the reported ones for PS [4, 5] within the errors. The large increase of the rotational mobility of the spin probe at $T \geq 180K$ is ascribed to the onset of the fast dynamics detected by neutron scattering at $T_f = 175 \pm 25K$ [2, 3, 7, 8].

The evidence that the deep structure of the energy landscape of PS exhibits the exponential shape of the energy-barriers distribution agrees with results

from extreme-value statistics and the trap model by Bouchaud and coworkers [9].

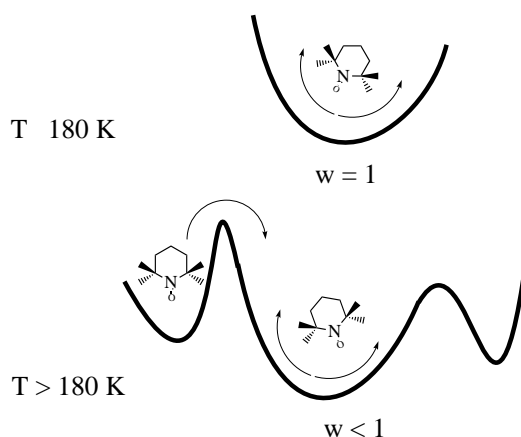


FIG. 1: The exploration of the orientational energy landscape by TEMPO in PS. $T \leq 180K$: all molecules are trapped ($w = 1$). Orientation correlations are lost via non-activated entropic-like pathways. $T > 180K$: a fraction of the molecules equal to $1 - w$ rotate by activated jumps over the exponentially-distributed energy barriers.

* Corresponding author: dino.leporini@df.unipi.it

- [1] J.Colmenero, A.Arbe, Phys.Rev.B **57**,13508 (1998) .
- [2] T.Kanaya, K.Kaji, Adv.Polym.Sci. **154** , 87(2001).
- [3] B. Frick, U. Buchenau, and D. Richter, Colloid Polym. Sci. **273**, 413 (1995).
- [4] N.V.Surovtsev, J.A.H.Wiedersich, V.N.Novikov, E.Rössler, A.P.Sokolov, Phys.Rev.B **58**, 14888 (1998).
- [5] A.P.Sokolov, V.N.Novikov, B.Strube, Europhys.Lett. **38**, 49(1997).
- [6] V.Bercu, M.Martinelli, C.A. Massa, L.A. Pardi and D.Leporini, J. Phys.:Condens. Matter **16**, L479 (2004).
- [7] V.Bercu, M.Martinelli, C.A. Massa, L.A. Pardi and D.Leporini, "The onset of the fast dynamics in glassy polystyrene observed by the trapping of guest molecules: a high-field Electron Paramagnetic Resonance study", Europhysics Letters, in press (DOI: 10.1209/epl/i2005-10290-0) .
- [8] V.Bercu, M.Martinelli, C.A. Massa, L.A. Pardi and D.Leporini, "Signatures of the fast dynamics in glassy polystyrene: first evidence by high-field Electron Paramagnetic Resonance of molecular guests", Journal of Chemical Physics, in press.
- [9] J -P.Bouchaud, M.Mezard, J.Phys.A: Math.Gen. **30**, 7997(1997).

How localized mutations in RC protein will improve the relation between the whole structure, functional activity and atomic mobility?

C. Alba-Simionesco^{*1}, V. Derrien¹, P. Sebban¹, S. Dmitrief¹, B. Frick², J. Teixeira³

¹ LCP, Bât 349, UMR 8000, Université de Paris-sud, 91405 Orsay cedex, France

² I.L.L., 38042 Grenoble, cedex, France

³ L.L.B., CEN-Saclay, France

Proteins have a glass transition distinct from the folding transition, at much lower temperature, and at which the internal atomic mobility becomes frozen on the experimental time scale. Functional activity and atomic mobility both requiring thermal fluctuations, they both decrease exponentially fast as T is lowered. The coincidence of those decreases does not warrant a relation between the two phenomena. Only by varying at least one external parameter in addition to T can one hope to probe this relation. In this study, the dynamical transition of a membrane protein, -the reaction centre (RC's) protein of the Rhodobacter Sphaeroides considered as an excellent model to study at a molecular level processes in energy-converting proteins-, is revealed by inelastic neutron scattering and localized mutations have been used for the first time as the additional parameter. Thus the aim of the present work is to understand what are the key structural and dynamical elements that ensure fast and efficient electron transfer and control its rate on a native protein and its mutants. Localized mutations - 2 residues as compared to 848 of the protein- affect the structure, consequently the electrostatic interaction around the active core of the protein, and changes the rate constant of the first electron transfer. We answered the question of whether or not the characteristic structural changes induced by these very localized mutations associated with the function of the protein, modify its overall dynamics observed by quasielastic neutron scattering experiments at the nano-pico seconde time scale. While the dynamical transition temperature remains identical within the error bars, the anharmonic regime in the mean square displacement of hydrogen atoms as revealed by backscattering experiments is significantly different between the native protein and its mutants and confirmed by the dynamical structure factor measured by time-of-flight technique. No solvent effect is involved here, since the native RC and the mutants are all in D₂O at the same concentrations. The apparent anti-correlation, namely, the more mobile the inside of the protein at a given T, the less efficient the electron transfer, is the novel and striking result that will be discussed. As a conclusion, we will comment on recent inelastic neutron

scattering experiments under high pressure on the dynamical transition in condensed matter involving different systems such as a protein, amorphous polymers and molecular glassforming liquids.

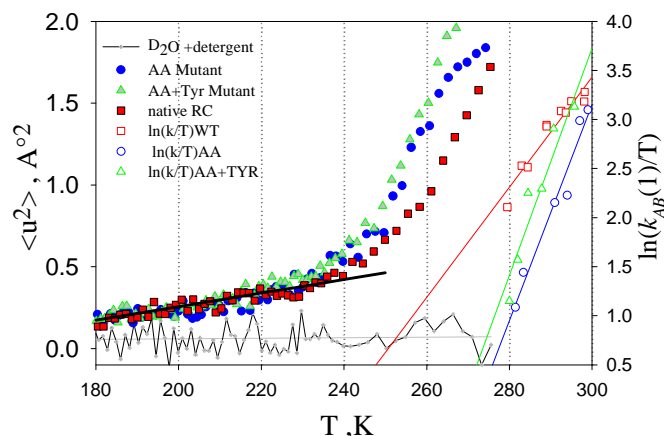


FIG. 1: mean-square-displacement as a function of temperature, $\langle u^2 \rangle$ in \AA^2 , of the native RC protein, the 2 mutants (AA and AA+TYR) and the solvent (D₂O +detergent) compared to the T-dependence of the enzymatic activity, *i.e.* the constant rate of the first electron transfer $k_{AB}(1)$ between the quinones, measured by laser-induced absorbance change spectroscopy

* Corresponding author: Christiane.Alba-Simionesco@lcp.u-psud.fr

[1] Elber, R., and M. Karplus. 1987. *Science*. 235:318–321; Frauenfelder, H., S. G. Sligar, and P. G. Wolynes. 1991. *Science*. 254:1598–1603; Parak, F.G., Rep. Prog. Phys., 66, 103-129,(2003).
 [2] Caliskan G., Kisliuk G., Tsai A., Soles, C.L., Sokolov A.P.,J. Chem. Phys., Vol. 118, No. 9, 2003
 [3] Doster W., Cusak, S., Petry, W., *Nature*, 337, 754-756

The effect of intramolecular architecture on the sub- T_g dynamics of some engineering thermoplastics

S. Arrese-Igor^{a,*}, I. Quintana^b, A. Arbe^a, A. Alegría^{a,b}, J. Colmenero^{a,b,c}, and B. Frick^d

^aUnidad de Física de Materiales CSIC-UPV/EHU, Apartado 1072, 20080 San Sebastián, Spain

^bDepartamento de Física de Materiales UPV/EHU, Apartado 1072, 20080 San Sebastián, Spain

^cDonostia International Physics Center, Pasco Manuel Lardizabal 4, 20018 San Sebastián, Spain and

^dInstitut Laue-Langevin, BP 156X, 38042 Grenoble Cedex 9, France

We have investigated the dynamics of phenylene rings (PR) in glassy polyethersulfone (PES), polysulfone (PSF), phenoxy (PH), and polycarbonate (PC) below its glass transition temperature by means of neutron scattering (NS) techniques. The last three polymers consist of bisphenol-A (BPA) units linked by molecular groups of different nature: diphenyl sulfone group in PSF, carbonate group in PC, and an aliphatic chain in PH (Fig. 1). Comparing them we aim at deciphering the influence of the linking group between PR on their dynamics and on secondary relaxations. NS is an excellent technique to characterise the motions at a molecular level as it provides spatial information and selective labelling through atomic deuteration. In this particular case the deuteration of proton positions other than those in aromatic rings has allowed to study the ring motion in an isolate way. In addition, a relatively wide dynamic range has been covered thanks to the combination of two different types of neutron spectrometers, time of flight ($\approx 3 \cdot 10^{-13} - 3 \cdot 10^{-11} s$) and backscattering ($\approx 10^{-10} - 10^{-9} s$).

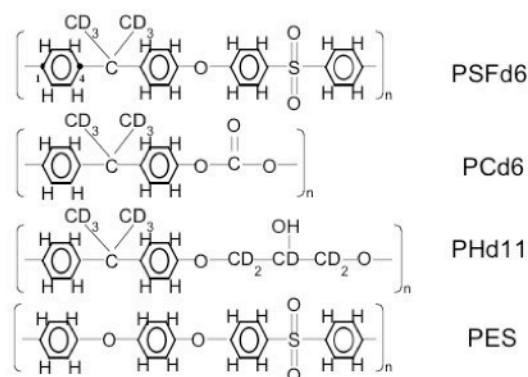


FIG. 1: Molecular formulae.

As a consequence of the different linking groups between PR, PES, PSF, PES, PH, and PC exhibit differentiated dynamics. On the one hand, PR within the four polymers perform: i) fast oscillations of increasing amplitude with temperature and mean activation energy $\sim 0.2eV$; and ii) *flips* (180° rotations) of mean activation energy $\sim 0.41 - 0.46eV$; both motions around $C1C4$ axis, and with broadly distributed characteristic times [1-4]. However, the oscillation amplitudes are very similar for PES, PC, and PSF, whereas in PH are slightly smaller at low tempera-

tures. The origin of this reduced mobility could be a better packing of the local structure in PH due to the higher flexibility of the aliphatic chain [3]. On the other hand, the PR in PC are more mobile and, in addition to the motions observed for PES, PSF and PH, also exhibit $\sim 90^\circ$ rotations [4].

After characterising the PR dynamics we have tried to relate the molecular motions seen by NS with the γ -relaxations observed in these polymers by spectroscopic techniques. The conclusion is that the various features of the γ -relaxation of PC, PH, PSF, and PESF can be well rationalised in terms of the sum of different contributions coming from the motion of their constituent molecular groups. From a molecular point of view the four polymers exhibit nearly equal ring flips. From a spectroscopic point of view they all have a common relaxation component at 170 K at 1 Hz. Therefore, our results support the very close relation between *flips* and the γ -relaxation process, however, this is not the only molecular motion reflected in the relaxation, but for each polymer the relaxation process is also influenced by the nature of the linking group between BPA units. The presence of mobile molecular groups different from PR between BPA units in PC and PH, leads to new observable contributions to the γ -relaxation. In the case of PC the second contribution has revealed to be correlated with the extra motion of PC's PR, i.e. $\sim 90^\circ$ rotation. In the case of PH the additional component of the γ -relaxation is related to the motion of the aliphatic chain. Finally, the γ -relaxation in PSF and PES, which merely consist of the repetition of Ph-X-Ph type structures, do not seem to be composed of more than one process, what is quite reasonable bearing in mind that we do not expect the behaviour of the two Ph-X-Ph structures to differ from each other considerably.

* Electronic address: waaarirs@ehu.es

- [1] I. Quintana, A. Arbe, J. Colmenero, B. Frick. *Macromolecules* **38**, 3999 (2005).
- [2] S.Arrese-Igor, A. Arbe, A. Alegría, J. Colmenero, B. Frick. *J. Chem. Phys.* **120**, 423 (2004).
- [3] S.Arrese-Igor, A. Arbe, A. Alegría, J. Colmenero, B. Frick. Submitted to *Macromolecules*.
- [4] S.Arrese-Igor, A. Arbe, A. Alegría, J. Colmenero, B. Frick. *J. Chem. Phys.* **123**, 014907 (2005).

Center of mass diffusion in viscous liquids: A third diffusion constant?

N. P. Bailey,* T. B. Schröder, and J. C. Dyre

Center for Glass and Time, Dept. of Mathematics and Physics, Roskilde University, Roskilde, Denmark

There are commonly considered to be two independent diffusion constants characterizing diffusion within a liquid. The self-diffusion constant D_s quantifies the long-time motion of individual particles according to $D_s = \lim_{t \rightarrow \infty} \langle \Delta \mathbf{r}(t) \rangle^2 / 6t$. The coherent diffusion constant D_{coh} quantifies the decay of the dynamical structure factor at long wavelengths, that is, the decay of density fluctuations, according to $S(q, t) = S(q) \exp(-D_{coh} q^2 t)$. A third type of diffusion constant has been postulated to play a role in the highly viscous regime of supercooled liquids[1]. This has been termed the “center-of-mass diffusion constant”, D_{CM} ; it characterizes the long-time behavior of the center of mass of the system: $D_{CM} = \lim_{t \rightarrow \infty} \langle \Delta X(t) \rangle^2 / 2Nt$, where N is the number of particles and X is the sum of their x -coordinates. In the highly viscous regime the total momentum cannot be considered a constant, because changes of momentum can readily be transmitted from the container walls to any point in the fluid, for example the location of a flow event. A natural assumption would be that $D_{CM} \sim D_s \sim D_{coh}$; the diffusion constants are said to be “coupled”. Arguments in Ref.[1] suggest that these relations between the diffusion constants could break down in the highly viscous regime, in a manner simi-

lar to the break-down of the Stokes-Einstein relation. The latter has been observed in computer simulations, and we are undertaking a careful program of simulation to study these three quantities. D_{CM} is an unusual quantity to calculate in simulations, particularly since it requires that periodic boundary conditions not be used, hence the initial part of the work involves efforts to determine it: to determine what time scale is necessary for the diffusive regime to be observed, what the effects of finite system size are, etc. The system we use is a metallic alloy, Mg-Cu, with a many-body interatomic potential, supercooled (always in equilibrium) until the relaxation time is of the order of tens of nanoseconds. In one direction atoms at the ends of the simulation cell are frozen to create “walls”, and the system is simulated at constant energy and volume. Initial results for D_{CM} , as well as the other two diffusion constants, will be presented.

* Corresponding author: nbailey@ruc.dk
 [1] J. C. Dyre, Phys. Rev. E **72**, 011501 (2005).

Positron annihilation lifetime spectroscopy and dynamics of glycerol and the cluster model of viscous liquids

Josef Bartoš^{1*}, O.Šauša², J.Krištiak²

¹Polymer Institute of SAS, 842 36 Bratislava,

²Institute of Physics of SAS, 842 28 Bratislava, Slovak Republic

The structure and dynamics of supercooled liquids represent one of very actual topics of condensed matter physics. Evidently, our understanding of the basic phenomenon of disordered systems, i.e. the liquid to glass transition, depends on the detailed explanation of the factors controlling the evolution of structure and a slowing down of the dynamics as a function of decreasing temperature.

Traditionally, the structure of the liquid state is measured by x-rays or neutron diffraction techniques. In general, smooth and weak variations in the structure factor $S(Q)$ on cooling are observed for van der Waals systems such as ortho-terphenyl and cis-trans-1,4-poly(butadiene)[1]. In contrast, in some associated liquids [2], such as glycerol and m-toluidine, the so-called pre-peak in $S(Q)$ evolves on supercooling the liquid sample. On the basis of Monte Carlo (MC) and molecular dynamics (MD) simulations this pre-peak effect is attributed to a clustering of several molecules being responsible for the medium - range order [3].

Recently, positron annihilation lifetime spectroscopy (PALS) is becoming an effective method for microstructural characterization of disordered systems. This is due to its ability of a direct detection and measurement of the local regions of lowered electron density the so-called free volume [4]. Some phenomenological correlations between the free volume parameters extracted from the ortho-positronium (o-Ps) annihilation data and the macroscopic rheological or/and dielectric relaxation data have been found [5].

Several theoretical models of the liquid state have been offered to explain the dynamical slowing-down on cooling a liquid. However, only a few models attempted to address the structure and dynamics of liquids simultaneously. One of them is the two-order parameter (TOP) model of the liquid - glass transition [6] based on the idea about the competition between the long-range density ordering tendency of the constituent particles and the short-range bond ordering trend due to the possibility to form certain local stable favored structures (clusters) of non-crystalline symmetry.

This contribution is focused on a verification of the TOP model to describe both the structural and dynamical aspects of liquid glycerol (GL). The former is represented by the o-Ps lifetime, τ_3 , from PALS investigation closely related to the free volume micro-structural parameters as [7]. The latter consists in the possibility to describe the temperature dependence of the relaxation time over a very wide temperature range [8] including both the normal low viscosity liquid above the melting point, T_m , as well as the viscous supercooled liquid state below T_m by means of the modified Vogel - Fulcher - Tamman - Hesse (MVFTH) eq. [6]. The fitting parameters of the MVFTH eq. for glycerol are used for subsequent fitting the PALS data. FIG.1

shows the result of such a fit of the o-Ps lifetime, $\tau_3(T)$, in terms of $F(T)$ function stemming from the MVFTH eq. Thus, the simultaneous descriptions of both the free volume microstructure and dynamic data of GL over wide temperature ranges within the TOP model can be achieved. In conclusion, the physical picture behind the TOP model, i.e., the slowing down in the dynamics due to the evolution of solid-like domains in the normal liquid - like structures appears to be valid for weakly H-bonded glycerol, at least.

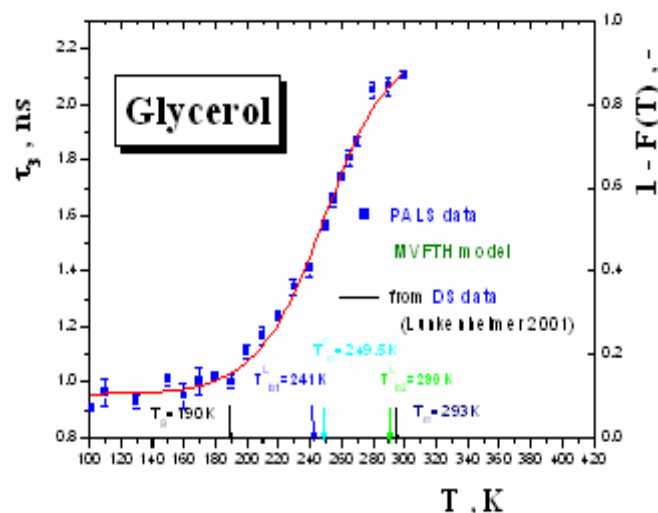


FIG1. PALS data fit in terms of the TOP model

Acknowledgements: The authors thank the VEGA, Slovakia for financial support of this project by the VEGA grant 2/6035/06 (JB) and (JK)

* Corresponding author: upolbrts@savba.sk

- [1] E.Bartsch et al., Chem.Phys. **169**,373 (1993); B.Frick et al., Europhys.Lett. **9**,557 (1989)
- [2] D.C.Champeny et al., Mol.Phys. **58**,337 (1986); M.Descamp et al. Progr. Theor.Phys.Suppl. **126**, 207 (1997)
- [3] D.Morineau, C.Alba-Simionesco, J.Chem.Phys **109**, 8494 (1998); R.Chelli et al.J.Chem Phys. **119**, 357 (2003); J.Blieck et al.Chem.Phys. **317**,253 (2005)
- [4] J.Bartoš in *Encyclopedia of Analytical Chemistry*, Wiley,Chichester 2000 p. 7968.
- [5] J.Bartoš et al. J.Non-Cryst.Solids **307-310**, 417 (2002)
- [6] H.Tanaka, J.Non-Cryst.Solids **351**,3371, 3385 and 3396 (2005)
- [7] J.Bartoš et al., J.Phys.-Cond.Matter **13**,11 473 (2001)
- [8] P.Lunkenheimer,A.Loidl,Chem.Phys.**284**,205 (2002)

A molecular dynamics simulation study of the segmental relaxations in model polymer blends.

Dmitry Bedrov* and Grant D. Smith

Department of Materials Science & Engineering, University of Utah, Slat Lake City, Utah, USA

Molecular dynamics simulations of model miscible polymer blends consisting of chemically realistic 1,4-polybutadiene (CR-PBD) (slow component) and PBD chains with reduced dihedral barriers (LB-PBD) (fast component) have been performed in order to study the influence of blending on segmental relaxation processes. We find that blending with a slow (high glass transition temperature, or T_g) component significantly increases the separation between the α - and β -relaxations of the fast (low T_g) component, which may be unresolvable or nearly unresolvable in the pure melt.

In Fig.1 we show the normalized dielectric loss as a function of frequency for the components and total of the blend with 25% concentration of the LB-PBD component. Also shown are the dielectric losses for pure CR-PBD and LB-PBD melts weighted by 0.75 and 0.25, respectively. The weighting of the pure melts response facilitates comparison with the response of individual components in the blend. Examination of Fig.1 shows that, first, the dielectric response of the LB-PBD component in the blend shows two distinct peaks consistent with the split between the α - and β -relaxations. The position of the high frequency peak coincides with the peak position of dielectric loss in the pure LB-PBD melt, which consists of contributions of two processes that are separated only by about an order of magnitude in frequency yielding a single broad peak. The low frequency (α -relaxation) process for the LB-PBD component of the blend shows up as a very broad process in the frequency range that overlaps the response of the CR-PBD component in the blend. Hence upon blending the high-frequency process (β -relaxation) of the LB-PBD component is only weakly affected while the low-frequency α -relaxation moves to much lower frequencies and broadens significantly. For the CR-PBD component the dielectric loss upon blending becomes narrower and shifts to higher frequencies. Finally, for the total blend the dielectric response consists of two clear peaks: 1) a low-frequency peak due to relaxation of the CR-PBD component and α -process of the LB-PBD component and 2) a high-frequency peak due to β -process of the LB-PBD component.

Based on these observations we interpret the high-frequency loss observed in numerous dielectric spectroscopy studies of miscible polymer blends that is apparently uninfluenced by blending as being due to the intrinsic β -relaxation of the fast component and not due to concentration fluctuations and/or structural heterogeneities within the blend. In other words, instead of assuming that some fraction of the fast component is not affected upon blending due to presence of the pure melt-like local environments we

believe that a *fraction of the relaxation* of the fast component (the β -relaxation) is not affected by blending and contributes *homogeneously* to the high-frequency response of the blend, while the contribution from the α -relaxation is shifted to lower frequencies with increasing fraction of the slow component.

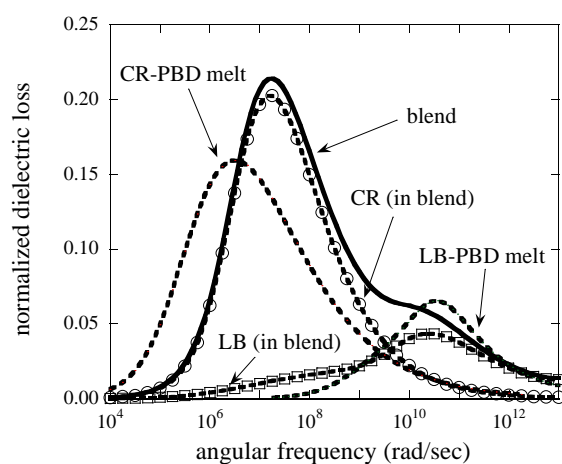


FIG. 1: Dielectric loss as a function of frequency for the LB-PBD/CR-PBD blend and its components for the 25% LB-PBD concentration at 198K. Also shown are dielectric losses for neat LB-PBD and CR-PBD melts scaled by their composition in the blend

We further investigate the segmental relaxations by examining torsional autocorrelation functions, dipole moment autocorrelation function, and dielectric response for each component and for the blend as a function of temperature and concentration.

* Corresponding author: bedrov@tacitus.mse.utah.edu

Relaxation behavior, physical aging and crystallization kinetics of amorphous acetaminophen

M. Beiner* and T.R. Gopalakrishnan

Martin-Luther-Universität Halle-Wittenberg, FB Physik, D-06099 Halle/Saale, Germany

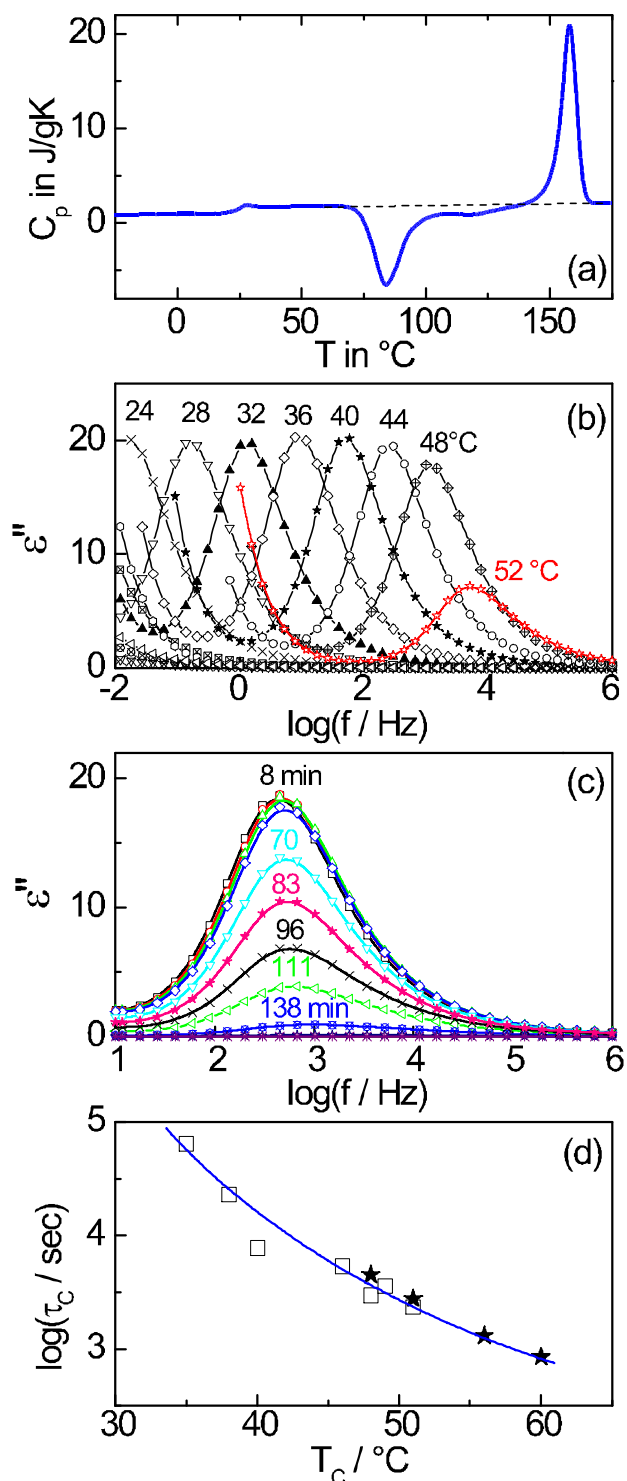
In the recent years there is increasing interest in the properties of amorphous pharmaceuticals. We have studied in detail the relaxation and crystallization behavior of amorphous acetaminophen produced by rapid quenching. DSC heating curves for this sample (Fig.1a) show a pronounced glass transition at $T_g=23^\circ\text{C}$ before spherulites are formed during the cold crystallization process at temperatures around $T_c=85^\circ\text{C}$. Weak exothermal contributions in the range $110\text{--}130^\circ\text{C}$ indicate a solid-to-solid transition to another polymorphic state which finally melts at $T_m\sim 158^\circ\text{C}$. In order to get more detailed information about the relaxation behavior of amorphous acetaminophen we have investigated the dynamic glass transition (α) between T_g and T_c by dielectric spectroscopy (Fig.1b). A weak secondary relaxation (β) has been identified in ϵ'' isotherms measured at temperatures below T_g . The crystallization kinetics will be described based on isothermal crystallization experiments by dielectric spectroscopy at temperatures between 25°C and 55°C . We observed that isothermal crystallization affects mainly the α relaxation strength $\Delta\epsilon$ while shape and position of the α peak in ϵ'' isotherms are nearly unaffected (Fig.1c). This shows that the situation can be approximated by a two phase model. Obviously, dielectric online measurements are a powerful tool to study the crystallization kinetics. The dielectric results are consistent with data from calorimetric measurements detecting the change of the strength of the thermal glass transition Δc_p after different periods of isothermal crystallization at T_c . Characteristic crystallization times τ_c obtained by both methods are nearly identical (Fig.1d). The results of isothermal annealing experiments below T_g will be presented and the influence of the equilibrium to non-equilibrium transition at T_g on the crystallization kinetics will be discussed. Furthermore, the results will be incorporated in the recent discussion about possible connections between dynamic heterogeneities and spherulitic growth.

Acknowledgement. We are grateful for financial support by Sachsen-Anhalt (CoE "Nanostructured Materials").

* Corresponding author: beiner@physik.uni-halle.de

[1] T.R. Gopalakrishnan and M. Beiner, Letters in Drug Design & Discovery, to be published.

FIG. 1: (a) DSC heating curve (+10K/min) and (b) dielectric loss isotherms for amorphous acetaminophen prepared by rapid quenching. (c) Dielectric loss curves measured after different periods t_c of isothermal crystallization at $T_c=46^\circ$. (d) Half times τ_c as obtained from isothermal crystallization measurements at T_c by dielectrics (squares) and DSC (stars). The τ_c value corresponds to that time where 50% of the material is crystalline.



On the interpretation of dynamic data in molecular glass formers

U. Buchenau*, M. Ohl and A. Wischnewski

Institut für Festkörperforschung, Forschungszentrum Jülich, Postfach 1913, 52425 Jülich, Germany

Using literature data, we confirm the recently observed splitting of time scales within the α -process close to the glass transition [1] and in the range of validity of the mode coupling theory [2]. Fig. 1 shows this splitting in glycerol over the whole temperature range.

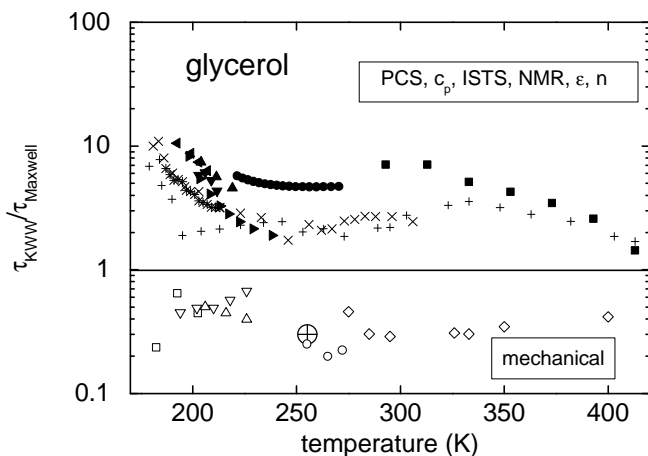


FIG. 1: Kohlrausch relaxation times in glycerol, normalized to the Maxwell time as described in the text. The lower group are mechanical shear, longitudinal and compression data, the upper group photon correlation spectroscopy, heat capacity, NMR, transient grating, neutron spin-echo at the first sharp diffraction peak and dielectric data. References will be given in the full paper.

The data in Fig. 1 have been reevaluated in terms of Kohlrausch functions in order to have the same functional form for all of them. The resulting relaxation time τ_{KWW} is divided by the Maxwell time $\tau_{Maxwell} = \eta/G_{\infty}$, taking the viscosity η and the infinite frequency shear modulus G_{∞} from measurements [3,4].

Note that this splitting of time scales is not the two-stage scenario of the mode coupling theory; both time scales move with the Maxwell time. In ref. [2] the shorter time scale was identified with the α -process of the mode coupling theory.

The idea of two different time scales (or an initial and final stage of the same process) is further supported by the different shape of the relaxation functions for the two groups of Fig. 1. The mechanical data have a decidedly larger stretching ($\beta_{KWW} \approx 0.4..0.5$) than the heat capacity, the dielectric constant and the neutron spin-echo signal ($\beta_{KWW} \approx 0.55..0.7$).

In order to explain these results, we postulate that the excess potential energy of a given configuration at a given temperature decays to zero via its fraction r of long range shear energy. r is considered to remain constant during the decay process. If the decay of the shear energy were exponential, the configurational decay would be also exponential with the relaxation time $\tau_{Maxwell}/r$. The case of a non-exponential decay is less trivial, but can be treated numerically. As it turns out, a Kohlrausch function for the shear decay provides again to a good approximation a Kohlrausch function for the configurational decay. With $\beta_{KWW} = 0.45$ for the shear and an assumed $r = 0.2$, one gets the observed factor of ten in the time scale and a $\beta_{KWW} = 0.61$ for the upper group in Fig. 1, in good agreement with experimental facts.

We thank Ernst Rössler and Peter Lunkenheimer for supplying their dielectric data and for helpful discussions.

* Corresponding author: buchenau-juelich@t-online.de

- [1] K. Schröter and E. Donth, *J. Non-Cryst. Solids* **307-310**, 270 (2002).
- [2] A. Brodin, M. Frank, S. Wiebel, G. Shen, J. Wuttke and H. Z. Cummins, *Phys. Rev. E* **65**, 051503 (2002).
- [3] K. Schröter and E. Donth, *J. Chem. Phys.* **113**, 9101 (2000).
- [4] F. Scarponi, L. Comez, D. Fioretto and L. Palmieri, *Phys. Rev. B* **70**, 054203 (2004).

Temperature, Density, Connectivity effect on Dynamics of Viscous Liquids

Simone Capaccioli^{1,2*}, Daniele Prevosto¹, Mauro Lucchesi¹, Pierangelo Rolla¹
¹Dipartimento di Fisica, Università di Pisa, Largo Pontecorvo 3, I-56127, Pisa, Italy
²CNR-INFM, CRS SOFT, Piazzale Aldo Moro 2, I-00185 Roma, Italy

Supercooled or overpressed liquids conventionally attain the glassy state at temperature T_g where structural relaxation time $t_a \sim 100$ s. On approaching T_g from the liquid side, different systems show qualitatively different T dependencies of t_a , classified by the concept of steepness index or “fragility” [1], defined as $m = \partial \log(t_a) / \partial (T_g/T) |_{T=T_g}$. Prototypical examples of fragile (high m) systems are van der Waals molecular liquids, like o-terphenyl, whereas strong (low m) glass-formers are characterized by strong covalent directional bonds, forming space-filling networks (like silica); hydrogen-bonded systems (like glycerol) have intermediate m values [1]. On the other hand, according to the energy landscape (EL) framework, two effects are convoluted in the isobaric T-dependence of t_a : changes in thermal energy which determine the accessible region of the EL and changes of the EL itself, due to the variation of density r with T . Only measurements at different pressures and temperatures can disentangle these effects. An isothermal compression, in fact, changes only density and so the EL profile, but keeps the thermal energy level constant. Recent results indicate that both T and r contributions are important, and, in the absence of specific interactions such as H-bonding [2,3], equivalent. Usually experiments can assess isobaric fragility $m_P(P)$, turning out to be a constant or a decreasing function of pressure for common glass-forming systems [2,3]. Anyway, from the point of view of EL framework, the isochoric fragility m_V (i.e. evaluated at constant r) is more fundamental. Since a master-plot for all the data $t_a(T,P)$ is often obtained vs. the scaling factor $G_r = r^n/T$ [3-4], the quantity m_V is density independent and characteristic of the material and it can be obtained as:

$$m_V = m_P / (1 - nT_g r^{-1} \partial r / \partial T) \quad (1)$$

In the present study dynamics of molecular (OTP, TPCM, BIBE, DPVC, poly-alcohols, epoxies) and oligomeric (PPG, polystyrene, polyisobutylene) glass-forming systems were studied by dielectric spectroscopy at different T (120-400 K) and P (0÷700 MPa) from the liquid to the glassy state, covering a time-scale range of 10 decades. Available equations of state allowed to assess r . Additional insights came from molecular dynamics simulations on oligomeric systems [4]. For most of the systems all the data $t_a(T,P)$ collapsed on a master-curve once scaled against the factor $G_r = r^n/T$ (see Fig.1). Eq.(1) was verified for all glass-formers under study. For van-der-Waals liquid an inverse correlation between n and m_V was found, enabling to build-up a “fragility normalized” master-curve for the α -dynamics of a number of different systems. On the other hand, fragility of H-bonded systems strongly increased with P, with a transition from intermediate to fragile behavior maybe related to some change of the H-bonding structure. Oligomeric systems were found

strong or fragile depending on connectivity, steric hindrance and specific interactions between monomers. Their fragility m_P and scaling parameter n were found molecular weight dependent: a rationale for this behavior was found by evaluating the relative effect of intramolecular and intermolecular energy barriers. Overall, empirical links emerge between m , a macroscopic dynamic property, and the microscopic interactions among the particles constituting the system, namely intermolecular potentials, connectivity, rigidity. Knowledge of $t_a(T,r)$ and available calorimetric and expansivity data enabled the comparison between dynamics and thermodynamics: the results were analyzed in the framework of models based on the statistical properties of the potential energy landscape [5] and according to the Adam–Gibbs relation, connecting t_a to configurational entropy S_c [6]. A density scaling law for S_c was found. Finally, the correlation between fragility of supercooled liquids and the T-dependence of nonergodicity factor [7] in the glassy state was successfully checked also for high pressure data.

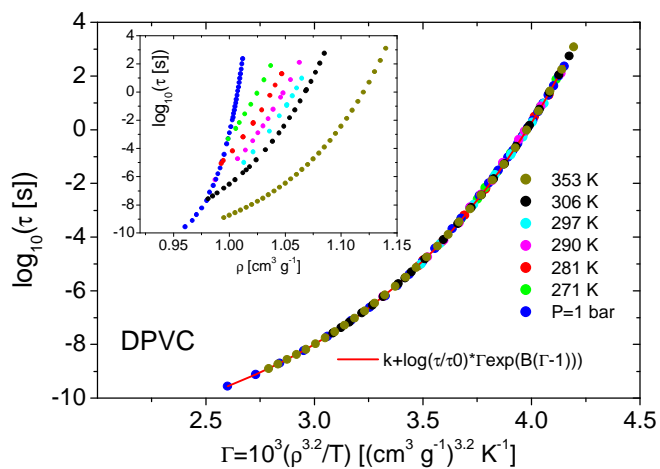


FIG. 1: Relaxation map vs. density (inset) and vs. scaling factor Γ (main figure) for diphenylenevinylcarbonate (DPVC)

* Corresponding author: capacci@df.unipi.it

[1] C.A. Angell, Science, **267**, 1924 (1995).
 [2] C. Alba-Simionesco et al., Eur. Lett., **68**, 58 (2004); C. Dreyfus et al., Eur. Phys. J. B, **42**, 309 (2004).
 [3] R. Casalini, C.M. Roland, cond-mat/0403622 and Phys. Rev. B, **71**, 014210 (2005).
 [4] A.Barbieri, S.Capaccioli, D.Leporini, J.Chem.Phys., **120**, 437 (2004)
 [5] G. Ruocco et al., J. Chem. Phys., **120**, 10666 (2004)
 [6] D. Prevosto et al., Phys. Rev. B, **67**, 174202 (2003).
 [7] T. Scopigno, et al., Science, **302**, 849 (2003).

Investigation of the dynamic and sub-ambient transition relationships in frozen sucrose solutions: differential scanning calorimetry and neutron scattering analysis.

D Champion^{*a}, C Loupiac^a, G. Roudaut^a, D. Simatos^a and JM Zanotti^b

^a *Laboratoire d'Ingénierie Moléculaire et Sensorielle de l'Aliment et des Produits de Santé – ENSBANA Université de Bourgogne F-21000 Dijon.*

^b *Laboratoire Léon Brillouin CEA-CNRS. CEA Saclay, F-91191 Gif Sur Yvette. France.*

Dynamic studies of low temperature supercooled or glassy carbohydrates are of importance for the food industry. The use of the glass transition temperature (T_g) for the stability prediction or the temperature sensitivity of foodstuffs has been widely described in literature [1-2].

However, in the case of frozen products, the change in dynamics above T_g and the melting of ice both contribute to the decrease in viscosity, enhancing molecular mobility. Moreover, DSC thermograms of carbohydrate solutions in presence of freezable water shows a non-classical shape, different from that observed with low water content solutions. For instance, the maximally freeze concentrated sucrose solutions obtained from a 50% sucrose solution, show two baseline shifts in the temperature areas where the glass transition is expected, according to the state diagram (Fig. 1).

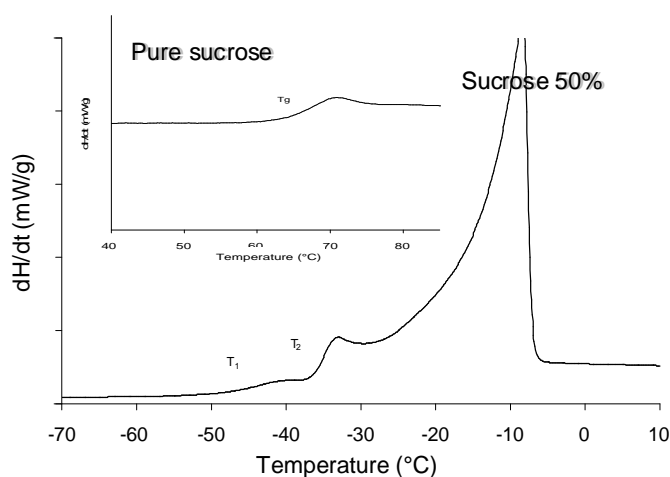


FIG. 1: Comparison of the DSC results between a pure glassy sucrose and the cryo-concentrated sucrose solution.

The nature of these two thermal events still is the subject of debates but the current trend seems to assign the lower temperature transition (midpoint: T_1), at around -45°C to the glass transition of the maximally freeze-concentrated glass. The higher temperature transition (midpoint: T_2), at around -35°C , may correspond to the onset of ice crystal melting although it exhibits strong second order behavior similar to the glass transition process [3-4]. In fact, depending on the freezing protocol used to prepare sample, the thermal behavior of these transitions can be changed.

The purpose of the present study is to clarify the nature of these events, in order to better identify the temperature of onset mobility in frozen solutions.

To this end, sucrose solutions were annealed at temperature above T_1 to promote the maximally freeze concentration and then aged at different temperatures. The DSC analysis showed different patterns as a function of the aging temperature. For aging temperatures of -35°C or -50°C , the glass transition showed two steps as for non-aged sample. However, only one transition was detected after an aging period of 3 h at -40°C (between the two transitions). Then, this transition exhibited a high enthalpy excess that may correspond to the merging of the two transitions.

Whatever the physical significance of these transitions: glass transition or ice melting, they both induce an increase in molecular mobility. Quasielastic neutron scattering experiments were carried out to determine the dynamics in these solutions in picosecond range.

Sucrose solutions were investigated by neutron scattering with the same thermal treatments used for DSC measurements in order to analyse the changes in the transition temperatures as a function of aging conditions. Using H_2O and D_2O as solvent for our sucrose solutions, we were able to better characterize the high temperature transition attributed to water/ice or to sucrose in annealed samples. By comparison of our DSC and neutron scattering results, we tried to attribute the physical meaning of the transitions.

References

- [1] D. Simatos, G. Blond and M. Le Meste *Cryo-Letters* **10**, 77 (1989).
- [2] Y. Roos, M. Karel and J. L. Kokini, *Food Technology* **95** (1996).
- [3] S. A. Knopp, S. Chongprasert and S. L. Nail, *J. Thermal Anal.* **54**, 659 (1998).
- [4] S. R. Aubuchon, L. C. Thomas, W. Theuerl and H. Renner, *J. Thermal Anal.* **52**, 53 (1998).

* Corresponding author: dominique.champion@u-bourgogne.fr

Measurements of the Poisson ratio and fragility of glass-forming liquids

T. Christensen^{*}, A. Budtz, A. Bacher, D. E. Nygaard and N. B. Olsen

Department of Mathematics and Physics (IMFUFA)

“Glass and time” – Danish National Research Foundation Centre for Viscous Liquids Dynamics

Roskilde University, Postbox 260,

DK-4000 Roskilde, Denmark

Recently much attention has been given to models and phenomenology of glass-forming liquids that correlates fast and slow degrees of freedom [1], [2], [3]. In particular the Poisson ratio has been correlated with fragility. We present data on shear - and bulk modulus obtained by the techniques of the piezoelectric transducers PBG [4] and PSG [5] on a number of glass-forming liquids. Hereby the Poisson ratio can be found. Furthermore the PSG also gives the temperature dependence of shear viscosity and thereby the fragility. The validity of the conjectured relation is discussed.

^{*} Corresponding author: tec@ruc.dk

[1] V. N. Novikov and A. P. Sokolov, *Nature* **431**, 961 (2004)

[2] J. C. Dyre, *Nature Materials* **3**, 749 (2004)

[3] J. C. Dyre, T Christensen and N. B. Olsen, e-print: cond-mat/0411334.

[4] T. Christensen and N. B. Olsen, *Phys. Rev.* **B49**, 15396 (1994)

[5] T. Christensen and N. B. Olsen, *Rev. Sci. Instrum.* **66**, 5019-5031

Colloidal Systems with Competing Interactions: a Monte Carlo Study

Andrea Corsi* and Luciano Reatto

Dipartimento di Fisica, Università degli Studi di Milano, via Celoria 16, 20133 Milan, Italy

We present a study of a tridimensional suspension of colloidal particles that interact through an effective potential composed of a short-range attractive part complemented by a longer ranged repulsive tail.

The long-range repulsion can arise from screened electrostatic interactions or from effective interactions that are associated to the presence of other species in the solution. The presence of the short-range attraction, instead, can be achieved by the addition of short non-adsorbing polymers which are able to modify the effective colloid-colloid interactions through depletion mechanisms. The length scale of these attractions is usually of the order of a few percent of the size of the colloidal particles.

Experiments [1, 2] and simulations [3, 4] have shown that such systems tend to form aggregates characterized by sizes and shapes that strongly depend on the balance between the attractive and repulsive parts of the potential.

We have compared different Monte Carlo techniques in order to determine which one is the most promising to study this kind of systems. The range of the repulsive portion of the interaction has been limited by applying a spherical cutoff to the interaction poten-

tial, cutoff that has been usually chosen to be limited to a few times the value of the colloid diameter.

We study the formation of stable equilibrium structures as a function of temperature and density as well as of the specific form of the repulsive and attractive portions of the potential between particles. We present results on both the structural and thermodynamic properties of the observed structures.

We acknowledge support from MRTN-CT-2003-504712.

* Corresponding author: andrea.corsi@fisica.unimi.it

- [1] A. Stradner, H. Sedgwick, F. Cardinaux, W. C. K. Poon, S. U. Egelhaaf and P. Schurtenberger, *Nature* **432**, 492 (2004)
- [2] A. I. Campbell, V. J. Anderson, J. S. van Duijneveldt and P. Bartlett, *Phys. Rev. Lett.* **94**, 208301 (2005).
- [3] A. Imperio and L. Reatto, *J. Phys.: Condens. Matter* **16**, S3769 (2004)
- [4] F. Sciortino, S. Mossa, E. Zaccarelli and P. Tartaglia, *Phys. Rev. Lett.* **93**, 055701 (2004).

Molecular Correlation Functions for Uniaxial Ellipsoids in the Isotropic State

Cristiano De Michele*

Dipartimento di Fisica and INFM-CRS Soft, Università di Roma "La Sapienza", P.le Aldo Moro 2, 00185 Roma, Italy

Antonio Scala

*Dipartimento di Fisica and INFM-CRS SMC,
Università di Roma "La Sapienza", P.le Aldo Moro 2, 00185 Roma, Italy*

Rolf Schilling

Johannes-Gutenberg-Universität Mainz, D-55099 Mainz, Germany

Francesco Sciortino

Dipartimento di Fisica and INFM-CRS Soft, Università di Roma "La Sapienza", P.le Aldo Moro 2, 00185 Roma, Italy

The structure of *simple* liquids can be characterized by the density-density correlator $g(r)$ or by its Fourier transform, the static structure factor $S(q)$. Strong efforts have been made to derive analytical tools for the calculation of these quantities, since $g(r)$ or $S(q)$ allow one to calculate several thermodynamical quantities, e.g. the equation of state. Among the most prominent theoretical approaches are the Percus-Yevick (PY), the hypernetted chain (HNC) and other more elaborate integral equations [1], that well reproduce "exact" results evaluated from simulations or experiments for models of simple liquids when the number density is not too large.

For *molecular* liquids, structural information becomes more diverse due to the presence of the orientational degrees of freedom and of their interactions with the translational ones. Expansion of the angular dependent microscopic density with respect to spherical harmonics and Wigner functions for linear and arbitrary molecules, respectively, leads to a generalization of $S(q)$ to tensorial correlators $S_{\lambda\lambda'}(\mathbf{q})$. Several analytical approaches have been proposed to calculate these correlations functions [2–6, 8–12], and in particular integral equation theories (such as PY and HNC) have been extended to molecular liquids [1, 13]. Latter ones, in our opinion, proved to be superior with respect to other techniques [15, 17, 18] but, as compared to simple liquids, their quality for anisotropic particles has been less intensively investigated and the debate on the orientational structural properties is not quite settled.

Therefore we have applied a newly developed event-driven MD-algorithm [21] to perform event-driven molecular dynamics simulations [20] of a system composed by uniaxial hard ellipsoids for different values of the aspect-ratio and packing fraction. We compare the molecular orientational-dependent structure factors previously calculated within the Percus-Yevick approximation [19] with the numerical results. The agreement between theoretical and numerical results

is rather satisfactory. We also show that, for specific orientational quantities, the molecular structure factors are sensitive to the particle shape and can be used to distinguish prolate from oblate ellipsoids. A first-order theoretical expansion around the spherical shape and a geometrical analysis of the configurations confirms and explains such an observation.

* Electronic address: cristiano.demichele@phys.uniroma1.it

- [1] J. P. Hansen and I. R. McDonald, *Theory of Simple Liquids* (Academic Press, 1986), 2nd ed.
- [2] R. Pynn, Solid State Comm. **14**, 29 (1974).
- [3] R. Pynn, J. Chem. Phys. **60**, 4579 (1974).
- [4] A. Wulf, J. Chem. Phys. **67**, 2254 (1977).
- [5] J. D. Parsons, Phys. Rev. **A19**, 1225 (1979).
- [6] S. D. Lee, J. Chem. Phys. **87**, 4972 (1987).
- [7] S. D. Lee, J. Chem. Phys. **89**, 7036 (1987).
- [8] M. Baus, J.-L. Colot, X.-G. Wu, and H. Xu, Phys. Rev. Lett. **59**, 2184 (1987).
- [9] J. F. Marko, Phys. Rev. **A39**, 2050 (1989).
- [10] A. Chamoux and A. Perera, J. Chem. Phys. **104**, 1493 (1996).
- [11] A. Chamoux and A. Perera, Mol. Phys. **93**, 649 (1998).
- [12] G. Rickayzen, Mol. Phys. **95**, 393 (1998).
- [13] C. G. Gray and K. E. Gubbins, *Theory of molecular fluids*, vol. 1 (Clarendon Press, 1984).
- [14] A. Perera, P. G. Kusalik, and G. N. Patey, J. Chem. Phys. **87**, 1295 (1987).
- [15] J. Talbot, A. Perera, and G. N. Patey, Mol. Phys. **70**, 285 (1990).
- [16] J. W. Perram, J. L. M. S. Wertheim, and C. O. Williams, Chem. Phys. Lett. **105**, 277 (1984).
- [17] J. Ram and Y. Singh, Phys. Rev. **A44**, 3718 (1991).
- [18] J. Ram, R. C. Singh, and Y. Singh, Phys. Rev. **E49**, 5117 (1994).
- [19] M. Letz and A. Latz, Phys. Rev. E **60**, 5865 (1999).
- [20] D. C. Rapaport, *The Art of Molecular Dynamics Simulation* (Cambridge University Press, 2004).
- [21] C. De Michele and A. Scala, in preparation.

Topological Fluctuation Approach to Structure and Dynamics of Liquids

Takeshi Egami*

Oak Ridge National Laboratory, Oak Ridge, TN 37831
and University of Tennessee, Knoxville, TN 37996, USA

Formulating a microscopic theory of dynamics of liquids is challenging because the many-body nature of the problem deeply frustrates traditional approaches. The problem is exacerbated by the complexity of the liquids studied by experimentalists. We propose to circumvent this difficulty by adopting a novel approach and applying it to simple atomic liquids. The starting point of this approach is to consider the dynamics of a network of atomic connectivity (topology). In metallic liquids the metallic bonds are cut and formed at a high rate, resulting in the fluctuation of local topology of atomic connectivity. We will then make a connection between the local topology and the local energy landscape through the concept of atomic level stresses [1]. The amplitude of local topological fluctuations expressed in terms of the atomic level strains is proportional to $T^{1/2}$ at high temperatures, but the system deviates from this relationship at lower temperatures because of topological frustration, which defines the glass transition [2,3]. We derived the expression of the glass transition temperature in terms of the local atomic volume, bulk modulus and Poisson's ratio. It was tested against the data on 35 metallic glasses for which these data are available, with excellent agreement ($\pm 4\%$). We have also explained the relationship between the liquid fragility and Poisson's ratio recently discovered by Novikov and Sokolov [4] as shown in Fig. 1. Unlike other successful theories this theory is microscopic, and requires virtually no fitting parameter. In this talk we will discuss details of our theory, verification by molecular dynamics simulation, and its relationship to the mode-coupling theory.

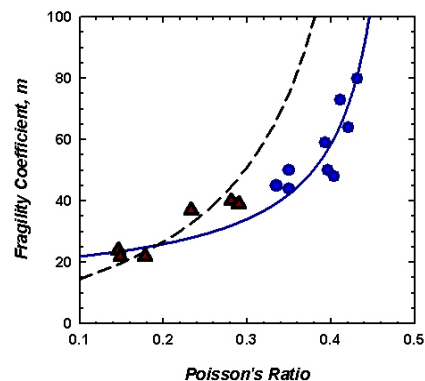


FIG. 1: The dependence of the liquid fragility on Poisson's ratio: Data on metallic alloy liquids (circles) and covalent liquids (triangles), and our theory (solid curve).

This work was supported by the Office of Basic Energy Sciences, U.S. Department of Energy under contract DE-AC05-00OR-22725 with UT-Battelle, LLC.

* Corresponding author: first.author@institution.edu

- [1] T. Egami, K. Maeda and V. Vitek, *Phil. Mag.* **A41**, 883 (1980).
- [2] T. Egami and D. Srolovitz, *J. Phys. F: Metal Phys.* **12**, 2141 (1982).
- [3] S.-P. Chen, T. Egami and V. Vitek, *Phys. Rev. B* **37**, 2440 (1988).
- [4] V. N. Novikov and A. P. Sokolov, *Nature*, **431**, 961 (2004).

The Reptation Model in light of Thermodynamics.

Nail Fatkullin* and Rainer Kimmich

Kazan State University, Physics Department, 420008, Kazan, Russia/Tatarstan
 Universität Ulm, Sektion Kernresonanzspektroskopie, 89069 Ulm, Germany

The reptation concept was introduced by de Gennes [1] with the aim to explain thermal motions of a long polymer chain in the presence of fixed obstacles. The “tube” was suggested by Edwards as an interpretation of the enhanced modulus of rubber [2]. The unification of the two formalisms by Doi and Edwards led to the “tube/reptation” model [3], which nowadays is considered as the standard phenomenological description of polymer chain dynamics [4].

The tube/reptation model appears to be quite persuasive and can be explained using relatively simple mathematics. Qualitatively it gives reasonable explanations for several experimental findings. On the other hand, substantial discrepancies between certain model predictions and experimental observations must be stated. Examples can be found in a recent review article and in the literature cited in it [5].

Actually, one faces a situation similar to the phenomenological van der Waals equation of state for dense gases and liquids. The reasoning leading to the van der Waals equation is also easily understood. The formalism is based on simple mathematics and qualitatively renders the main features of the gas-to-liquid phase transition. Nevertheless, apart from dilute gases no real system can be described precisely by the van der Waals equation. Keeping this rather rough, but meaningful analogy in mind, the purpose of the present study is to find a time region, where the tube/reptation model can provide a more accurate description of reality.

Based on a relation between the mean squared fluctuation of the number of segments in a given volume element and the isothermal compressibility of the polymer system, it follows straightforwardly that the tube/reptation model predicts fluctuations larger than permitted by thermodynamics on the time scale $t \gtrsim \tau_R$, where τ_R is the Rouse relaxation time.

There is a discrepancy intrinsic to the postulates of the standard tube/reptation model: On the one hand, interactions between the probe chain and neighboring chains are essential. Chain motions are supposed to be extremely anisotropic and restricted to tubes for times $t \ll \tau_1$. This can only be the consequence of *strong* interchain interactions. On the other hand, macromolecules are supposed to move in a diffusive way inside their own tubes without any substantial mutual correlation. This anticipates *weak* intermolecular interactions.

Obviously, in order to reach more realistic polymer dynamics models, dynamical correlations of different polymer chains must be taken into account.

The same conclusion can be drawn from the recently discovered and qualitatively explained “corset effect” [6,7], which also reveals the importance of intermolecular dynamical correlations in polymer melts even between chains separated by distances much larger than the Flory radius.

This work was supported by the Volkswagen-Stiftung (1/74602), RFBR and CRDF.

* Corresponding author: Nail.Fatkullin@ksu.ru

- [1] P.G. de Gennes, *J.Chem.Phys* **55**, 572 (1971).
- [2] S.F. Edwards, *Proc.Phys.Soc* **92**, 9 (1967)
- [3] M.Doi, S.F.Edwards, *J.Chem.Soc.Faraday Trans. II*, **74**, 1789 (1978).
- [4] M. Doi, S.F. Edwards, *The Theory of Polymer Dynamics*, 1986, Clarendon, Oxford.
- [5] R.Kimmich, N.Fatkullin, *Advan. Polym. Sci* **170**, 1 (2004).
- [6] C.Mattea, N.Fatkullin, E.Fischer, U.Beginn, E.Anoardo, M. Kroutieva, R.Kimmich, *Appl.Magn.Res*, **27**,371 (2004).
- [7] N.Fatkullin, R.Kimmich, E.Fischer, C.Mattea, U.Beginn, M.Kroutieva, *New Journal of Phys* **6**, 46 (2004).

Effect of Pressure on the Segmental Relaxation and the Crystallization in pODMA-*b*-*pt*BA-*b*-pODMA Triblock Copolymers

A. Gitsas and G. Floudas*

Department of Physics and Foundation for Research and Technology-Hellas, Biomedical Research Institute (FORTH-BRI), University of Ioannina, P.O. Box 1186, 451 10 Ioannina, Greece

Recently, we reported on the phase behavior of the poly(*n*-octadecyl methacrylate)-*b*-poly(*tert*-butyl acrylate)-*b*-poly(*n*-octadecyl methacrylate) (pODMA-*b*-*pt*BA-*b*-pODMA) triblock copolymer in bulk and on surfaces [1] using small-angle X-ray scattering (SAXS) and atomic force microscopy (AFM), respectively. pODMA undergoes side-chain crystallization [2] below ~285 K (with a melting temperature (T_m) of 300 K), whereas *pt*BA is an amorphous polymer with a glass temperature (T_g) at 320 K. Based on the disordered state structure factor we extracted the temperature dependence of the interaction parameter χ on temperature as $\chi = 0.12 + 38/T$ giving rise to the following phase diagram (Fig. 1).

The melt phase diagram of the copolymer consists of different phase regions depending on the copolymer composition. The lamellar phase is the dominant one, with smaller regions of hexagonally packed cylindrical and cubic phases. The majority of the copolymers lie in the strong segregation limit (SSL), as demonstrated by $\chi \gg 10$ and the dependence of the domain spacing on the total molecular weight as $d \sim M^{0.64}$ [1]. In this system there exists self-organization in multiple length scales: between the two blocks and inside the pODMA domain because of side-chain crystallization.

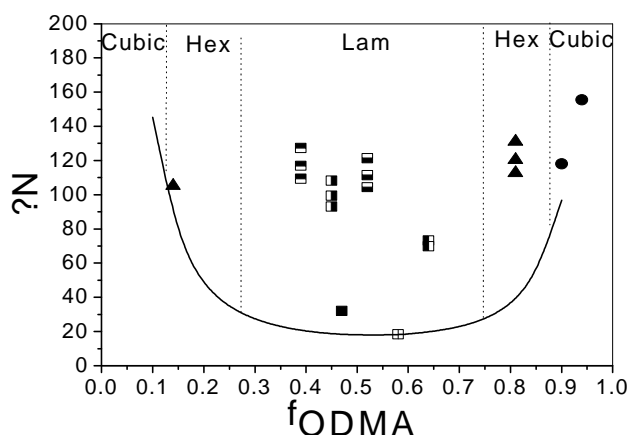


FIG. 1: Bulk phase diagram based on the SAXS results. The symbols correspond to the different block copolymer compositions measured at different temperatures, resulting in the different χ values shown. The vertical lines give the approximate positions of the phase boundaries. The solid line separates the ordered from the disordered region as predicted from the mean field theory (MFT).

Earlier works have shown a strong effect of thermodynamic confinement on polymer crystallization with different regimes (breakout, templated and confined crystallization) [3]. The aim of the present work [4] is to examine the effect of pressure on the dynamics of the two blocks forming the nanophases. Three compositions were examined: (i) pODMA forming hexagonally packed cylinders confined by the glassy, *pt*BA matrix ($f_{\text{pODMA}}=0.14$, Fig. 2), (ii) equal amount of both blocks forming a lamellar nanophase and (iii) pODMA as the majority phase surrounding *pt*BA in cylindrical nanodomains ($f_{\text{pODMA}}=0.81$). For this purpose we have employed temperature and pressure dependent broadband dielectric spectroscopy (BDS) and investigated the effect of pressure on the segmental relaxation of the amorphous and the semi crystalline block.

The most interesting effect was obtained for $f_{\text{pODMA}}=0.14$, where the presence of the nanodomain affects the T_g of the pODMA restricted amorphous phase (RAP). In particular, the T_g increased by ~40 K. On the other hand, the pODMA T_m and the *pt*BA T_g had similar values and pressure dependencies to the pure components ($dT_g/dP \sim 0.5$ K/MPa and $dT_m/dP \sim 0.16$ K/MPa, respectively).

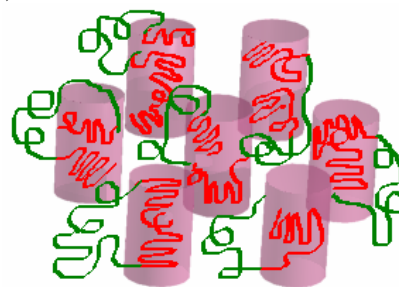


FIG. 2: Schematic representation of hexagonally packed pODMA cylinders (red) within the *pt*BA matrix (green). Parts of the pODMA chains are crystallized while the remaining chains form the restricted amorphous phase.

* Corresponding author: gfloudas@cc.uoi.gr

- [1] W. Wu, J. Huang, S. Jia, T. Kowalewski, K. Matyjaszewski, T. Pakula, A. Gitsas and G. Floudas, *Langmuir* **21**, 9721 (2005).
- [2] M. Mierzwa, G. Floudas, P. Stepanek and G. Wegner, *Physical Review B* **62**, 14012 (2000)
- [3] Y. L. Loo, R. A. Register and A. J. Ryan, *Macromolecules* **35**, 2365 (2002)
- [4] A. Gitsas, G. Floudas, T. Pakula and K. Matyjaszewski, in preparation (2005)

Combining Helium and Neutron Spin Echo to Clarify Surface Effects in Benzene Dynamics in Graphitic Mesopores

P. Fouquet,^{1,*} H. Hedgeland,² A. P. Jardine,² G. Alexandrowicz,²
W. Allison,² J. Ellis,² G. Dosseh,³ and C. Alba-Simionesco³

¹*Institut Laue-Langevin, BP 156, 38042 Grenoble Cedex 9, France*

²*Cavendish Laboratory, Madingley Road, Cambridge CB3 0HE, U.K.*

³*Universite Paris 11, Laboratoire Chimie Physique, CNRS, UMR 8000, 91405 Orsay, France*

We present a new approach to gain a deepened understanding of surface contributions to the dynamics of viscous liquids confined in mesoporous materials. In mesoporous confinements a large fraction of molecules interacts with the wall of the matrix. These molecules give a significant contribution to the overall dynamics of the confined liquid [1]. However, without a sensible quantification of the interaction potentials it is difficult to reach a good theoretical description of the dynamics. We aim to solve this problem by studying the dynamics of molecules confined in matrices with increasing pore size and adsorbed on surfaces. As a prototype study for our approach we have measured the diffusion of benzene molecules on HOPG and exfoliated graphite surfaces as well as in activated carbon fibers using helium and neutron spin-echo spectroscopy (HeSE and NSE, respectively).

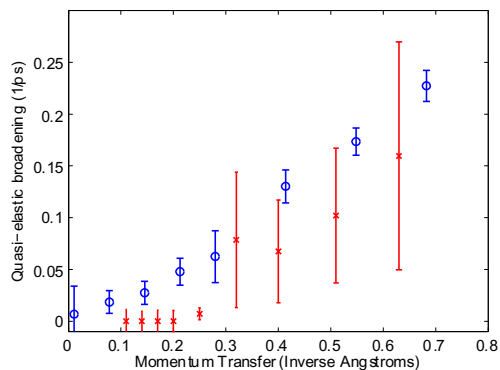


FIG. 1: Quasi-elastic broadening obtained with HeSE (circles) and NSE (crosses) for 0.5 mono-layers benzene on a graphite surface.

For neutron scattering, the spin-echo technique has been developed into a routine tool since its invention in the 1970's [2]. Furthermore, recent signal improvements for the NSE spectrometers at ILL allow to study sub-monolayer coverages on samples with high specific surface areas, e.g. exfoliated graphite. A strictly surface sensitive variant of this technique has been realized by the introduction of HeSE [3, 4]. The latter technique uses a set-up which is very similar to NSE, however, instead of neutrons HeSE uses ³He atoms as

probe particles. ³He atoms have a nuclear magnetic moment similar to neutrons, but due to their electronic shell they do not penetrate into the samples.

HeSE being a novel technique, it was essential for our research to first verify the consistency of the results of HeSE and NSE, since both techniques need to be used in parallel. An ideal system for this test was found to be benzene on graphite surfaces, since graphite surfaces are available in high quality both for pure surface studies (HOPG) and for neutron scattering studies using exfoliated graphite with a specific surface area of several 10 m² per gramme. The measurements (Fig. 1) show a good agreement on the molecule diffusion time scales for HeSE and NSE, confirming the future transferability of results between the two techniques. For this graph the broadening was derived as $\Gamma = 1/\tau$ from fitting a simple exponential decay to the measured spin echo curves without the need of any further assumptions. The large NSE error bars emphasize the need to use HeSE for further advancements in this field. The results also agree with molecular dynamics calculations.

As a follow on the dynamics of benzene liquid in activated carbon fibers (ACF) were studied using NSE. The surface structure of ACFs is very similar to exfoliated graphite, but surface-surface distances are strongly reduced to between 1 and 2 nm. Here we found a very broad distribution of relaxation times due to the different dynamics of molecules close to and far away from the matrix wall.

* Corresponding author: fouquet@ill.fr

- [1] C. Alba-Simionesco, G. Dosseh, E. Dumont, B. Frick, B. Geil, D. Morineau, V. Teboul and Y. Xia, *Eur. Phys. J. E* **12**, 19 (2003).
- [2] F. Mezei (Ed.), *Neutron Spin Echo*, Lecture Notes in Physics, Vol. 122, Springer, Berlin, 1980.
- [3] A.P. Jardine, S. Dworski, P. Fouquet, G. Alexandrowicz, D.J. Riley, G.Y.H. Lee, J. Ellis and W. Allison, *Science* **304**, 1790 (2004).
- [4] P. Fouquet, A.P. Jardine, S. Dworski, G. Alexandrowicz, W. Allison and J. Ellis, *Rev. Sci. Instrum.* **76**, 053109 (2005).

Structure and Dynamics in Poly(methyl methacrylate) close and above the Glass Transition

A.-C. Genix^{*1}, A. Arbe², F. Alvarez^{2,3}, J. Colmenero^{1,2,3}, A. Wischnewski⁴, D. Richter⁴
and B. Farago⁵

¹ Donostia International Physics Center (DIPC), San Sebastián - SPAIN

² Consejo Superior de Investigaciones Científicas, Unidad de Física de Materiales CSIC-UPV/EHU, San Sebastián - SPAIN

³ Universidad del País Vasco, Departamento de Física de Materiales UPV/EHU, San Sebastián - SPAIN

⁴ Forschungszentrum Jülich (FZJ), Institut für Festkörperforschung, Jülich – GERMANY

⁵ Institut Laue-Langevin (ILL), Grenoble - FRANCE

During the last years a great deal of effort has been made in order to understand the atomic motions in supercooled liquids in connection to the phenomenon of the glass transition. In addition to the anomalous diffusion behind the α or structural relaxation, localized motions –possibly responsible for the secondary relaxations– have been identified in glass forming polymers by neutron scattering (NS) and also recently by molecular dynamics (MD) simulation [1]. The combination of these two techniques is by now one of the most powerful tool to disentangle the behavior of complex polymer melts.

Poly(methyl methacrylate) (PMMA) is a very well known glass-forming polymer that displays a complicated dynamics close and above the glass transition temperature ($T_g \sim 400\text{K}$) [2]. In particular, a complex and likely cooperative secondary β -relaxation has been reported. Moreover, the static structure factor $S(Q)$ of PMMA also shows a complex behavior (see Fig. 1). In this work, we have combined fully atomistic MD-simulation with NS-experiments in order to unravel both the local structure and the dynamics in PMMA. The agreement found between simulation and experiments validates the simulation cell as a realistic representation of our system. Then, we have taken advantage of the simulation to go beyond the experimental possibilities.

In the first part of this study, MD-simulation together with the measurements of five different partial structure factors which could be accessed by neutron polarization analysis and different partial deuteration levels were used to unveil the structural peculiarities of the PMMA chains. The pair correlations obtained from the MD-simulation were grouped according to the 3 different structural units of the PMMA monomer, i.e., main chain (MC), ester side group (SG) and α -methyl group (MG). Fig. 1 displays the 6 partial correlation functions together with their sum. In this figure all atoms are weighted equally thus the sum is the true structure factor. A close inspection of the MC/MC and MC/SG correlation functions led to the conclusion that the PMMA melt displays a strong local ordering where the main chain and the side groups are anti-correlated over the average distance between the main chains, $d = 2\pi/Q_{\max} \approx 8.4\text{\AA}^{-1}$. This observation reminds on the nanophase separation that has been reported for higher order poly(di-n-alkyl methacrylate)s [3]. Furthermore, the simulations also point out the strong correlations that exist between the backbones (the MC/MC peak is six times above the average high Q limit of 0.27), indicating strong local ordering.

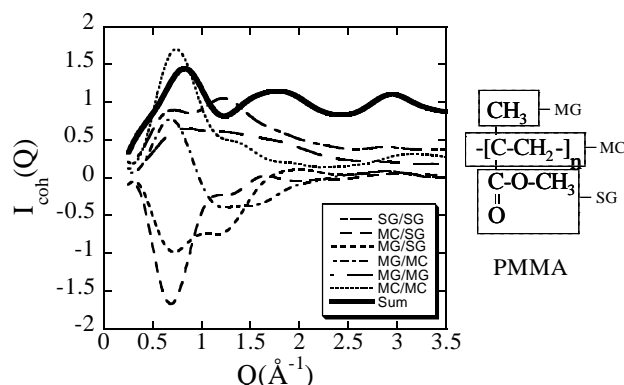


FIG. 1: Different partial structure factors into molecularly determined groupings for PMMA. $S(Q)$ is displayed by the line.

Moving to the dynamics of PMMA, backscattering experiments through the self motions of the hydrogens have allowed the characterization of the relaxation involving the main chain in the α -process. Then, neutron spin echo was used to investigate the dynamic structure factor. It shows that around the 2 first peak positions of $S(Q)$, the dynamics display similar temperature dependence and are dominated by the overall $\alpha\beta$ -process in our t, T -window. In parallel, the MD-simulations show that the dynamics at the second maximum of $S(Q)$ is dominated by the correlations SG/SG (mainly ester methyl group) and MG/MG (see Fig. 1). As well, we learned from simulations that the SG-hydrogens move significantly faster in PMMA than the ones from main chain and α -methyl group [4]. Finally, close to T_g the self part of the van Hove correlation function of the SG-hydrogens displays a clear double peak revealing the occurrence of well defined localized motions (jumps), with a rather large amplitude of about 6\AA and fast timescale ($\sim 10\text{ns}$).

This study has allowed to unravel the complex dynamics of PMMA at a molecular level.

* Corresponding author: swxgegec@sw.ehu.es

- [1] J. Colmenero, A. Arbe, F. Alvarez, A. Narros and M. Monkenbusch, D. Richter, Europhys. Lett. **71**, 262 (2005).
- [2] R. Bergman, F. Alvarez, A. Alegría and J. Colmenero, J. Chem. Phys. **109**, 7546 (1998).
- [3] M. Beiner, Macromol. Rapid Commun **22**, 869 (2001).
- [4] A.-C. Genix, A. Arbe, F. Alvarez, J. Colmenero, L. Willner, D. Richter, Phys. Rev. E **72**, 31808 (2005).

Mechanical Spectroscopy of Na₂O-Al₂O₃-SiO₂ Melts.

Katarzyna Gniazdowska* and Sharon L. Webb

Mineralogy Department, Georg-August-University, 37077 Göttingen, Germany

The structure of silicate melts can be described as a function of the changes in their physical and thermodynamic properties with changing composition. The heat capacity, shear modulus, shear viscosity and relaxation rate of a series of Na₂O-Al₂O₃-SiO₂ melts were measured. The combination of these measurements and calculated parameters was then used to address the question of the structure of these melts. There are seven Na₂O-Al₂O₃-SiO₂ melts with a constant value of 66.7 mol% SiO₂. They have all been made by fusing the component oxides at high temperature (to 1600°C).

The micropenetration technique has been used to measure viscosity (range between 10⁸ and 10¹³ Pa s). The melt sample is ~3 mm thick and has ~8 mm diameter. A sapphire sphere (diameter r_s~2 mm) is pushed into the melt with an applied force F. These parameters are used to calculate the viscosity η (Eq. 1).

$$h = \frac{0,1875 \cdot F \cdot t}{\sqrt{r_s} \cdot \sqrt{l^3}} \quad (1)$$

where t - time (s), l - distance of the micropenetration (m).

A forced oscillation technique is used to determine the shear properties of the Na₂O-Al₂O₃-SiO₂ melts and the dependence of their shear moduli and viscosities on frequency and temperature (Fig. 1). The principles of the measuring method are based on rotational deformation [1].

The torsion machine has been built in the Mineralogy Department, University of Göttingen. The frequency range is between 1 and 0.001Hz. Temperatures up to 1000°C can be achieved. The shear modulus depends on the frequency (Fig. 2).

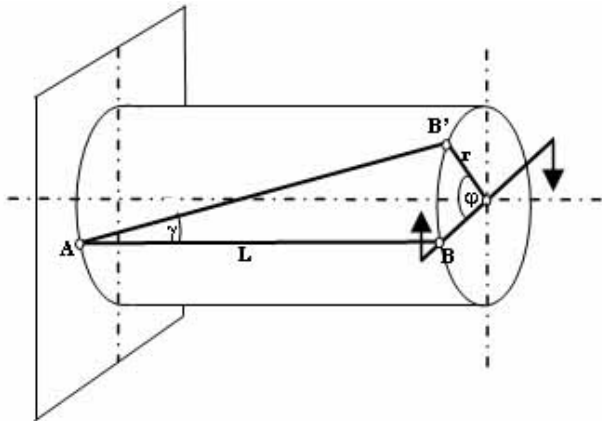


FIG. 1: Schematic diagram of a long cylinder to which a twisting force is applied.

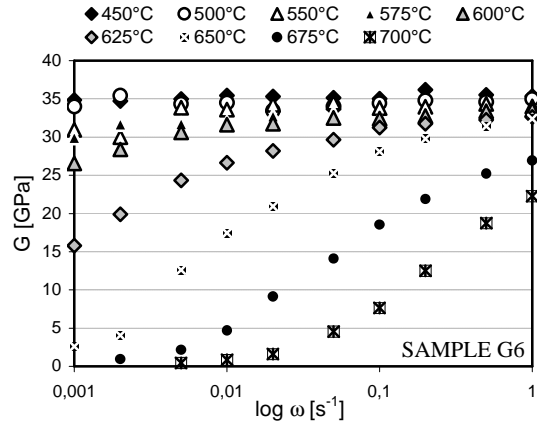


FIG. 2: Plot of the relationship between shear modulus G and log frequency (sample G6).

A plot of the real and imaginary shear modulus as a function of log normalised frequency was created from all of the data for each sample at different temperatures (Fig. 3). In this way, the behaviour of the melt (circles in Fig. 3) can be compared to the simple viscoelastic model (lines in Fig. 3).

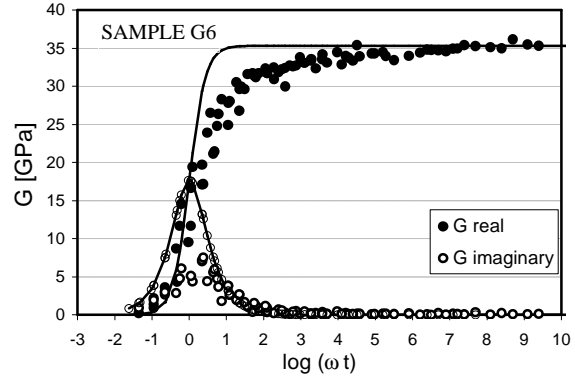


FIG. 3: Plot of real and imaginary shear modulus as a function of log normalised frequency (sample G6).

The frequency dependence of the shear modulus changes with changing composition and especially the Na/Al ratio. The range of G for investigated samples is between 30 and 37 GPa.

* Corresponding author: kgniazd@gwdg.de

[1] W. F. Riley, L. D. Sturges and D. H. Morris, Mechanics of materials, 272-344 (1999).

Sensitivity of arrest in mode-coupling glasses to low- q structure

M. J. Greenall,* Th. Voigtmann, P. Monthoux, and M. E. Cates
 SUPA, School of Physics, The University of Edinburgh,
 JCMB King's Buildings, Edinburgh EH9 3JZ, United Kingdom

We quantify, within mode-coupling theory [1], the sensitivity of arrest in a glass-former to its structure. Our approach mirrors one widely used in superconductivity theory (following [2]): we study the functional derivative $\delta F(q)/\delta S(q')$, with $F(q)$ the nonergodicity parameter of the glass [1], and $S(q)$ the static structure factor of the glass-forming liquid.

When the glass formation is dominated by inter-particle repulsion, we find a strong sensitivity to structure at wavevectors *below* the structure factor peak at $q_0 \approx 2\pi/d$: an increase in $S(q_0/2)$ *lowers* $F(q)$ over a wide q -range (Fig. 1). Such low- q structure corresponds to density modulations on length scales of order $2d$, and has been seen in recent experiments and simulations on glass-formers including silica melts and aromatic compounds [3–6].

By considering $\delta F(q)/\delta g(r)$, which describes the response of the glass to changes in the liquid radial distribution function $g(r)$, we explain this low- q sensitivity in terms of packing effects. The ‘trough’ in the functional derivative at $q' \approx q_0/2$ (Fig. 1) appears in this real-space result (Fig. 2) as a modulation of period $\approx 2d$, negative for $r < d$ and positive for $r > d$. The negative section tells us that adding structure to a system *within* the (effective) hard-sphere diameter; that is, softening the particles, will lower the degree of

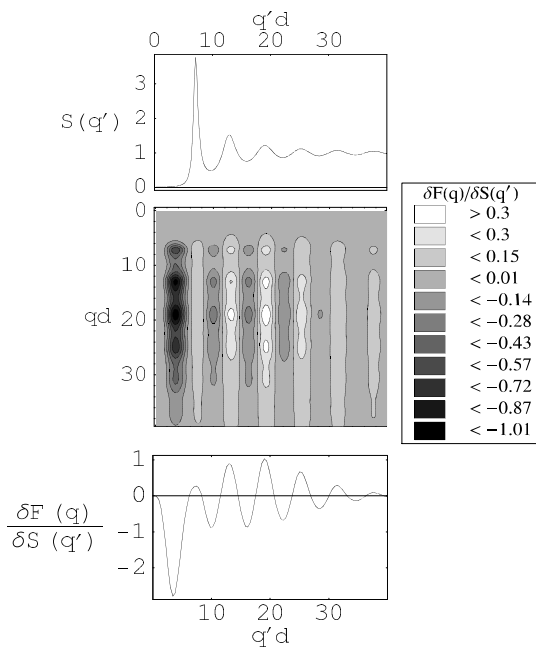


FIG. 1: Hard-sphere system (particle diameter d), just within the glass. Top panel: structure factor; middle panel: $(\delta F(q)/\delta S(q'))_{\text{reg}}$; bottom panel: cut through derivative at $qd = 19$. (The ‘same-mode’ contribution $(\delta F(q)/\delta S(q'))_{\text{sing}}\delta(q - q')$ is omitted here.)

arrest over a wide range of length scales. The positive part of the modulation ($d < r < 2d$) shows that the glass will be strengthened by adding structure *in between* the first- and second-nearest-neighbour peaks, forming a ‘caged cage’.

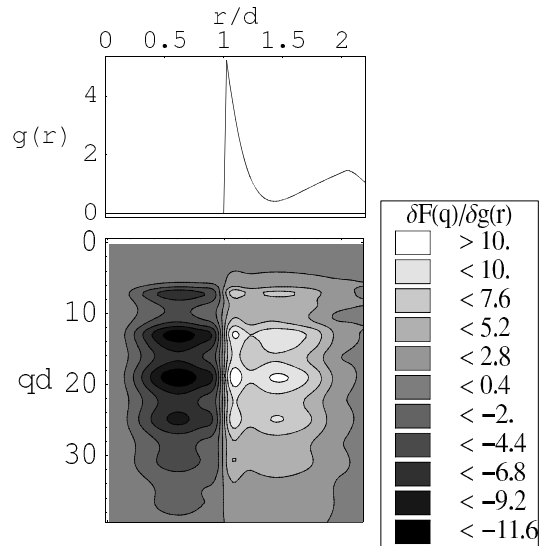


FIG. 2: Upper panel: radial distribution function; lower panel: $(\delta F(q)/\delta g(r))_{\text{reg}}$. System as above.

This strong sensitivity to packing effects is much weaker in ‘attractive’ glasses (see e.g. [7]) where bonding is more important. Here, the depth of the trough in $\delta F(q)/\delta S(q')$ falls by a factor of ≈ 100 . The near-vanishing of the low- q sensitivity in these systems is a non-trivial prediction, and might thus be relatively specific to the MCT picture of the glass transition.

This work was funded by EPSRC grant GR/S10377.

- * Corresponding author: martin.greenall@ed.ac.uk
 [1] W. Götze and L. Sjögren, Rep. Prog. Phys. **55**, 241 (1992).
 [2] G. Bergmann and D. Rainer, Z. Phys. **263**, 59 (1973).
 [3] L. Comez, S. Corezzi, G. Monaco, R. Verbeni and D. Fioretto, Phys. Rev. Lett. **94**, 155702 (2005).
 [4] S. Corezzi, D. Fioretto and J. M. Kenny, Phys. Rev. Lett. **94**, 065702 (2005).
 [5] A. Meyer, J. Horbach, W. Kob, F. Kargl and H. Schober, Phys. Rev. Lett. **93**, 027801 (2004).
 [6] L. Fabbian *et al.*, Phys. Rev. E **60**, 5768 (1999).
 [7] K. N. Pham *et al.*, Science **296**, 104 (2002); J. Bergenholtz and M. Fuchs, Phys. Rev. E **59**, 5706 (1999); K. Dawson *et al.*, Phys. Rev. E **63**, 011401 (2001)

Indications for a slow β -relaxation in strong and fragile metallic glasses

Jörg Hachenberg* and Konrad Samwer

I. Physikalisches Institut, Universität Göttingen, Friedrich-Hund-Platz 1, 37077 Göttingen, Germany

The elastic moduli of a strong and a fragile metallic glass are investigated by mechanical spectroscopy. The double-paddle oscillator and the dynamic mechanical analyzer are used to investigate thin films and melt spun bands of $Zr_{65}Al_{7.5}Cu_{27.5}$ and $Pd_{77}Cu_6Si_{17}$ at 5.4 kHz and in the low Hz band. In the vicinity of the glass-transition, a Havriliak-Negami fitting function in temperature domain is used to model the α -relaxation. The measured data clearly deviate from the model for both systems. A secondary relaxation has to be taken into account to achieve a suitable fit. Our experimental results provide evidence that a slow β -relaxation, existing in both strong and fragile amorphous metals, can be regarded as a universal property also of metallic glasses.

The α -relaxation is then fitted with a Havriliak-Negami function, transformed into temperature domain [2]. A clear misfit between 630 K and 650 K occurs (excess wing) that has also been observed for $Zr_{65}Al_{7.5}Cu_{27.5}$ [2] resulting from an additional slow β -relaxation. Both cases will be compared and discussed within recent MD simulations and analytic models, bridging the gap between atomic vibrations and cooperative shear transformation zones [3, 4].

The authors would like to thank P. Rösner, P. Lunkenheimer, A. Loidl and W.L. Johnson for many stimulating discussions. This work is supported by the Deutsche Forschungsgemeinschaft, Graduiertenkolleg 782 and SFB 602, TP B8.

* Corresponding author: joerg.hachenberg@phys.uni-goettingen.de

- [1] P. Lunkenheimer, U. Schneider, R. Brand, A. Loidl, *Contemp. Phys.* **41**, 15 (2000).
- [2] P. Rösner, K. Samwer, P. Lunkenheimer, *Europhys. Lett.* **68** (2), 226 (2004).
- [3] H. Teichler, *Phys. Rev. E* **71**, 031505 (2005).
- [4] W. L. Johnson, K. Samwer, *Phys. Rev. Lett.* (2005) in press.

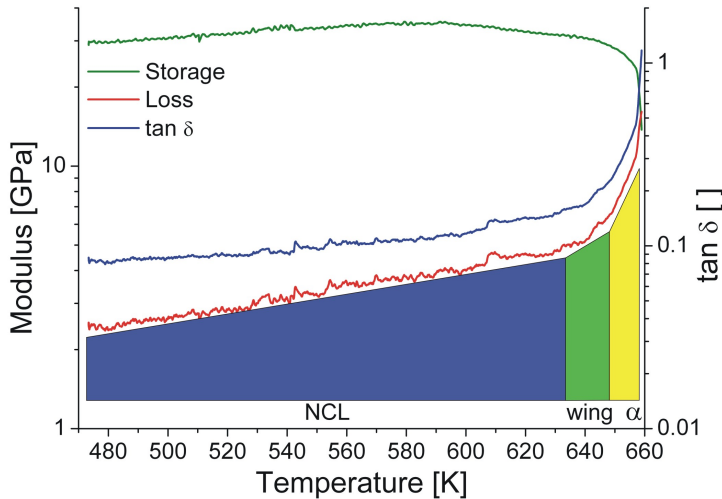


FIG. 1: Storage and loss modulus and $\tan \delta$ of $Pd_{77}Cu_6Si_{17}$ from a temperature scan at 5 K/min, 1 Hz and constant strain amplitude of 0.04 %. The coloration highlights the regions of the nearly constant loss (NCL), the excess wing (wing), and the α -relaxation (α)

Figure 1 presents an exemplary temperature scan at 5 K/min and 1 Hz using extensional spectroscopy of a melt spun strip of $Pd_{77}Cu_6Si_{17}$. There are three characteristic regions shown: Below 640 K the loss is dominated by a slight increase, called the nearly constant loss [1]. In this temperature range, the storage modulus increases slightly, due to physical aging up to 600 K. Above 640 K a pronounced relaxation sets in, that is divided into the excess wing and the α -relaxation.

Measurements of the Frequency-Dependent Bulk Modulus of Supercooled Liquids

B. Igarashi^{*}, T. Christensen, N.B. Olsen, and J.C. Dyre

*Department of Mathematics and Physics (IMFUFA), DNRF Centre for Viscous Liquid Dynamics, Roskilde University,
Postbox 260, DK-4000 Roskilde, Denmark.*

A method for measuring the frequency-dependent adiabatic bulk modulus of a liquid by measuring the electrical impedance of a spherical piezoelectric shell containing the liquid was presented some time ago [1]. Recent measurements will be reported for several supercooled liquids with temperatures near the glass transition, describing relaxational behaviors of

bulk moduli as frequency is varied continuously between 1 Hz and 20 kHz.

^{*} Corresponding author: brig@ruc.dk

[1] T. Christensen and N.B. Olsen, *Phys. Rev. B* **49**, 15396 (1994).

A new oscillating cup viscometer for temperatures up to 2500 K

M. Kehr ^{1*}, W. Hoyer ¹ and I. Egry ²

¹ *Technische Universität Chemnitz, Institut für Physik, D-09107 Chemnitz*

² *Deutsches Zentrum für Luft- und Raumfahrt, Institut für Raumsimulation, D-51147 Köln*

Values of the viscosities of liquid metals are of importance for technical as well as for scientific use. Several methods are known for measuring these values [1]. For alloys at higher temperatures the method of the oscillating cup is the most commonly employed one.

Based on the experience with this type of viscometers at medium temperatures a new high-temperature viscometer was constructed. The objective was to extend the measuring range to higher melting alloys, such as nickel- or iron-based alloys. With the new viscometer a maximum temperature of 2500 K is possible. The temperature is reached by using a graphite tube furnace and is measured by using a C-type thermocouple and a pyrometer. Due to the special design of the heater an excellent uniformity of temperature distribution in vertical as well as in radial direction could be reached. Special care was taken to shield the torsion wire against the heat. Starting from room temperature at the beginning of the measurement, the temperature of the wire does not rise above 40°C during the measurement.

Torsional oscillations are excited and the torsional angle $f(t)$ is detected by using a laser and a position sensitive detector (PSD). To get the values of oscillation period and logarithmic decrement, a damped harmonic oscillation function is fitted to the measured values of $f(t)$ by using a Marquardt-Levenberg algorithm [2].

From the knowledge of the size of the crucible, mass of the sample, moment of inertia of the pendulum and from the measured logarithmic decrement the viscosity is calculated. The analysis is based on the working formulas of either Roscoe [3] or Beckwith, Kestin, Newell [4].

Measurements are carried out under argon atmosphere at a pressure of 1000 mbar. The sample is held in cups made from either alumina or boron nitride. Graphite cups are still under testing. First measurements were performed on several pure elements.

*Corresponding author: mirko.kehr@physik.tu-chemnitz.de

[1] T. Iida, R.I.L. Guthrie, "The Physical Properties of Liquid Metals", Oxford: Clarendon Press, 1988

[2] W.H. Press, S.A. Teukolsky, W.T. Vetterling, B.P. Flannery, "Numerical Recipes for C 2nd Edition", Cambridge University Press, 1992

[3] R. Roscoe, Proc. Phys. Soc. **72** 576-584 (1958)

[4] J. Kestin, G.F. Newell, Z. Angew. Math. Phys. **8** 433-449 (1957)

High frequency acoustic wave study of glasses and liquids

Christoph Klieber^{*1)}, Tina Hecksher²⁾, Emmanuel Peronne³⁾, and Keith A. Nelson¹⁾

1) Department of Chemistry, Massachusetts Institute of Technology, Cambridge, MA 02139, USA

2) Department of Mathematics and Physics, Roskilde University, 4000 Roskilde, Denmark

3) CNRS-Universite Pierre et Marie Curie, 75015, France

We present results from liquid and glass samples obtained with a recently developed technique for generation and detection of ultrahigh frequency, tunable acoustic waves. Acoustic wave generation is accomplished through the use of a novel reflection-based pulse shaper [1]. Pulse sequences are generated by multiple passes through a retroreflecting system. The output waveform is a sequence of 7 pulses in a roughly Gaussian envelope with repetition rate tunable between 2-2000 GHz.

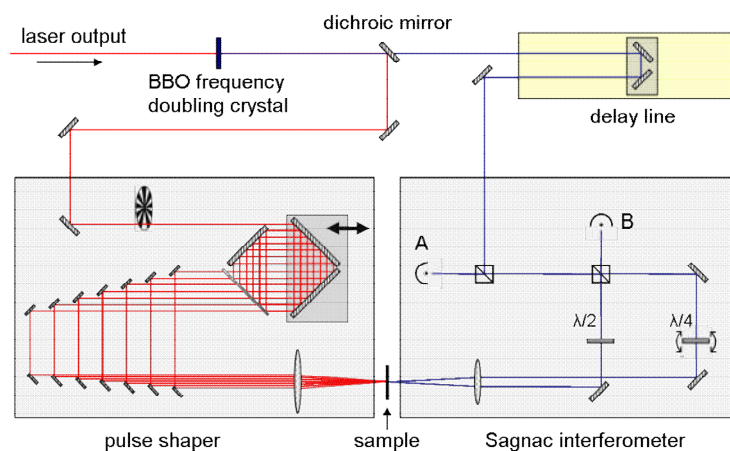


Figure 1 – Schematics of the pulseshaper and the Sagnac interferometer.

Acoustic waves with frequencies up to 500 GHz and corresponding wavelengths as short as 10 nm are generated at one side of a sample and are detected at the other side by a low-noise Sagnac interferometer [2]. A schematic illustration of the setup is shown in figure 1.

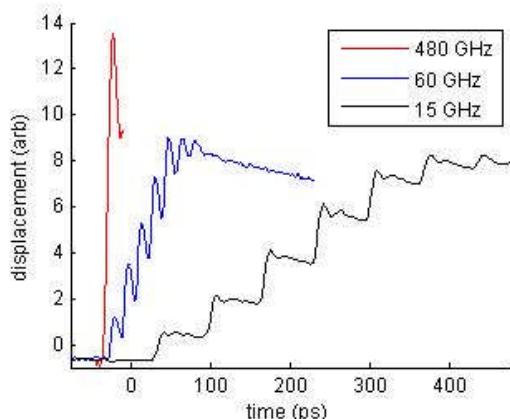


Figure 2 – 3 different frequencies generated on a 20 nm aluminum film deposited on sapphire.

Signals from a bare aluminum film are shown in figure 2. The narrowband acoustic waves appear as small oscillations superimposed on the rise that reflects the broadband envelope of excitation pulses.

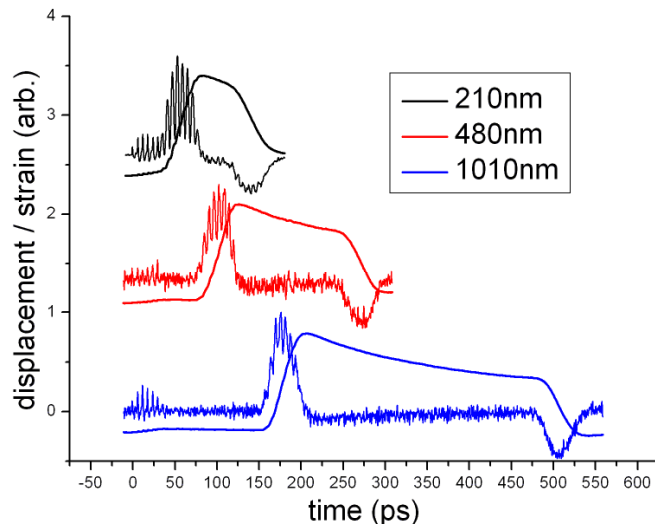


Figure 3 – Raw data for SiO₂ at 165 GHz at 3 different thicknesses. The smooth curves show the displacement and the strongly modulated curves are the corresponding strain (the derivative of the displacement). Data have been normalized and vertically shifted.

Figure 3 shows propagation of 165 GHz waves through 3 different thicknesses of silica glass (SiO₂). Both the initial arrival of the acoustic pulses after a single traversal through the sample is seen as a rise in signal level, and an acoustic “echo” after an additional round trip through the same is seen as a fall in signal level due to inversion of the unipolar acoustic wave upon reflection at the back surface. The corresponding strain (derivative of the displacement) is plotted on top of the displacement and clearly shows the arrival of each high-frequency acoustic cycle.

Phonon mean free path results from silica glass (SiO₂) at 10-300 K differ sharply from earlier reports [3], suggesting a reevaluation of the models of glassy behavior that have been used to rationalize them.

Studies are under way of glass-forming liquids, whose complex elastic moduli and relaxation dynamics can be determined in the GHz frequency range.

* Corresponding author: cklieber@mit.edu

[1] J.D.Choi et al, Appl. Phys Let. **87**, 384 (2005).

[2] J.Y. Dusquesne, B. Perrin, Phys. Rev B **68**, 134205 (2003)

[3] Zhu et al, Phys. Rev. B **44**, 172 (1995).

A binary two-dimensional colloidal glass former: local analysis of amorphous structure and heterogeneous dynamics

Hans König^{1,2,*}

¹*Institute of Physics, Johannes-Gutenberg University Mainz, 55099 Mainz, Germany*

²*Department of Physics, University of Konstanz, 78457 Konstanz, Germany*

Colloidal suspensions are excellent model systems to study questions according to structures or local relaxation processes in solid physics. Here, the intriguing interplay between local amorphous micro-structures and the corresponding heterogeneous micro-dynamics is considered from normal liquids up to strongly supercooled liquids. Therefore, video-microscopically measured time-dependent particle coordinates of binary colloidal 2D glass former with repulsive dipole interaction are investigated [1].

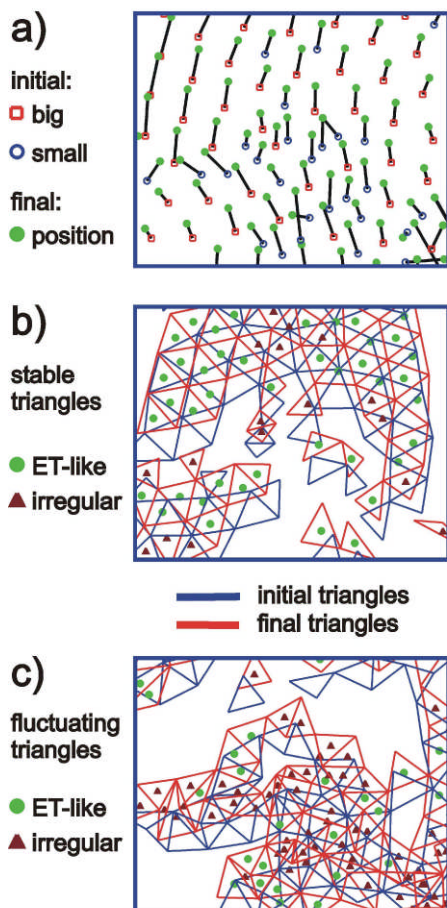


FIG. 1: Cooperative movements of fast particles in a supercooled liquid. a) 2-time trajectories. Stable (b) and fluctuating TNNP (c) compared with ET-like TNNP.

At the glass transition temperature, the long-time relaxations freeze or the cage effect becomes stable although no discontinuous change of the amorphous structure occurs. However, the solidification must directly be connected with the microscopic particle configurations since the cage around each particle, which is formed by its neighbors, become stable. Up to now,

no model as well as no theory allows to link the local amorphous structure with heterogeneous dynamics. In this contribution, a novel description of the microscopic structure and the local dynamics in a 2D binary colloidal glass former is introduced using the geometric properties of triangles of nearest neighboring particles (TNNP). These triangles allow considering the local particle configurations, i.e. the cages, and their time-dependent variations, giving a stability criterion of local structures, directly in the monolayer and by averaged functions.

For high temperatures we find a normal liquid. In this case, the TNNP are irregular and their shape fluctuates with time. For low temperatures a supercooled liquid is found. Crystallite clusters (CC) of stable elementary triangles (ET) form, which may be viewed as tiny crystal nuclei. The ET are idealized triangles, which are local density-optimized packed. We find exactly one ET for each 3-particle combination of the two kinds of colloids. Touching CC of different kinds of ET-like TNNP are local density-optimized termed as multi crystallite clusters (MCC). These clusters are surrounded by liquid-like irregular triangles. In strongly supercooled systems MCC often move cooperatively resulting in heterogeneous dynamics. Therefore, ET-like TNNP seem to be related to a stability criterion for local cages. At the glass transition temperature we expect that the different clusters conglomerate and form a stable frame through the whole system. We call this local explanation of the glass transition concept of local density-optimized crystallite clusters.

Additionally, the description of the local amorphous structure by TNNP and ET allows to understand the characteristic features of the partial radial pair-distribution functions [2]. Nevertheless, further local investigations in glass formers are necessary. Colloidal glass formers with other particle interactions and in 3D are therefore very good candidates.

The author thanks K. Zahn, G. Maret, R. Haussmann, U. Gasser, and J. Horbach for discussions, the SFB 513 of the Deutsche Forschungsgemeinschaft for financial support and the Marie Curie Network No. MRTN-CT-2003-504712.

* Corresponding author: koenigh@uni-mainz.de

[1] H. König, R. Hund, K. Zahn, G. Maret, *Eur. Phys. J. E*, DOI: 10.1140/epje/e2005-00034-9 (2005).

[2] H. König, *Europhys. Lett.* **71**, 838 (2005).

Corrections to mean field behavior of ultrathin polymer films

T. Kreer,* J. Wittmer, H. Meyer, A. Johner, and J. Baschnagel
Institut Charles Sadron, 6 Rue Boussingault, 67083 Strasbourg, France

A. Cavallo
Institut für Physik, Johannes Gutenberg Universität, Staudinger Weg 7, D-55099 Mainz

In order to test recent theoretical predictions [1] on the static and dynamical properties of (quasi) two-dimensional polymer films we perform computer simulations of a lattice (bond-fluctuation) and an off-lattice (bead-spring) model.

Ultrathin polymer films are involved in many systems of great interest, such as polymer coated surfaces or lubricated contacts between solids. A theoretical description of such confined polymers would therefore be a basis of understanding a variety of problems related to tribology, membrane physics etc.

In a recent theoretical approach Semenov and Johner consider two distinct models [1]: (1) strictly two-dimensional polymers, where the chains cannot intersect [so-called self-avoiding walks (SAWs)], and (2) ultrathin films, where the chains can perform small excursions into the third dimension [so-called self-avoiding trails (SATs)]. While in model (1) the chains are forced to stay separated, model (2) allows for entanglements between the chains.

Already in 1986 Duplantier has shown [2] that in strict two dimensions (model 1) the chains are segregated and described by non-classical critical exponents. The surface line is of fractal dimension $5/4$, which is smaller than the fractal dimension of a classical random walk [1]. Thus, unlike in the classical Rouse description, the polymers relax along their surface, revealing a smaller dependence of the relaxation times on chain length N than expected by the classical picture. For SATs, where overlaps between different chains are allowed, theory predicts mean-field behavior with logarithmic corrections [1]. As an example, Fig. 1 shows the deviation of the lateral chain extension, characterized by the radius of gyration, R_{gx} , from mean-field behavior (ρ is the monomer density, h the film thickness, and b_e the segment length). Note that the data is compared to theory without using any adjustable parameter. The non-mean-field behavior leads to long range ($1/r^4$) concentration fluctuations. Unlike the classical reptation prediction, where the relaxation time scales like $\tau \sim N^3$, Semenov and Johner predict

$$\tau \sim \exp \left[\frac{N}{N_e} \frac{c}{b^4 h^2 \rho^2} \right], \quad (1)$$

where N_e represents the entanglement length of the melt, c is a constant, and b is the renormalized segment length. Thus, the relaxation time should depend exponentially on N . Since concentration fluctuations are also relevant in three-dimensional systems [4], a confirmation of Eq. (1) is thus of great interest for a general understanding of polymer dynamics.

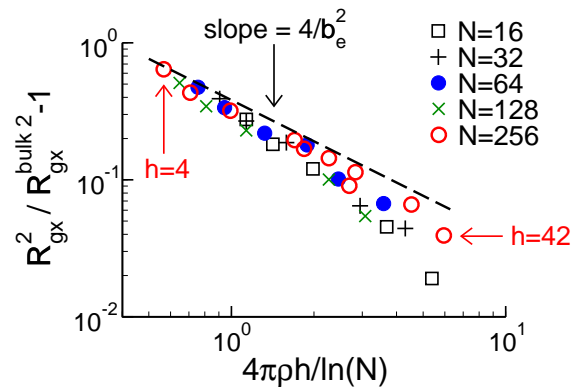


FIG. 1: Squared radius of gyration in x -direction parallel to the walls divided by its bulk value as a function of monomer density ρ , film thickness h and inverse logarithmic chain length N . The dashed line represents the theoretical expectation for $h \ll R_g^{\text{bulk}}$ (≈ 15 for $N = 256$). $b_e = 3.2$ is the bulk value of the effective segment length. Data from bond-fluctuation model taken from Ref. [3].

This work is partially financed by the DFG under project number Kr 2854/1-1.

* Corresponding author: tkreer@ics.u-strasbg.fr

- [1] A.N. Semenov and A. Johner, *Eur. Phys. J. E* **12**, 469 (2003).
- [2] B. Duplantier, *J. Phys. A* **19**, L1009 (1986).
- [3] A. Cavallo, M. Müller, J.P. Wittmer, A. Johner, and K. Binder, *J. Phys.: Cond. Mat.* **17**, S1697 (2005).
- [4] J.P. Wittmer et al., *PRL* **93**, 147801-1 (2004).

Mechanical contraction method applied to simulation of random packings of cylinders.

T. V. Kruglov* and A. P. Philipse

*Van't Hoff Laboratory for Physical and Colloid Chemistry, Debye Institute, University of Utrecht, Padualaan 8, 3508
TB Utrecht, The Netherlands*

Wide ranges of colloids are composed of anisotropic particles varying in shape from thin plates to long rods. The packing density of those particles is largely unresolved issue. Most recently simulations on packings of spherocylinders, ellipsoids and cut spheres were done. Simple cylinders however present much greater challenge in terms of their implementation in simulation algorithm.

We applied recently developed mechanical contraction method to simulate random packings of cylindrical particles as a function of their aspect ratio. We found that packing density has two maxima at aspect ratios above and below one.

* Corresponding author: T.V.Kruglov@chem.uu.nl

Effects of potential shape on dynamics and structure of dense fluids

Erik Lange^{1,*}, Jose B. Caballero², and Matthias Fuchs¹, Antonio M. Puertas²
¹University of Konstanz, Germany and
²University of Almeria, Spain

Hard spheres are a popular tool to simplify complex systems. This is particularly true when modelling fluids. On the experimental side the medium of choice are colloidal suspensions since their pair interaction can be manipulated and can be tuned to be close to the hard sphere interaction — but not quite.

Computer simulations reflect this situation with a variety of different interaction potentials. We use apart from the true hard sphere potential also the following approximation of a repulsive interaction:

$$U(r) = \epsilon \left(\frac{\sigma}{r} \right)^n,$$

with the exponential chosen in a range from $n = 12$ to $n = 36$.

Our goal in this study is to give some indication on how to answer the following question: what effect does the steepness of the repulsive pair interaction have on the structure and dynamics of a fairly dense fluid[1]?

In a preliminary study we have overcome the first difficulty: that is to find a meaningful mapping. We introduce the dimensionless parameter

$$\Gamma = \rho \sigma^3 \left(\frac{\epsilon}{K_B T} \right),$$

and scale to $\Gamma/\Gamma_{freezing}$. In addition we choose the mean particle distance $\rho^{-1/3}$ as length scale. This has the distinct advantage to bypass the problem of defining an effective particle radius.

The resulting static structure factors not only confirmed the Verlet-Hansen criterion[2] (value of first peak equal) but also showed an overall similarity of the curves including the position of the first peak.

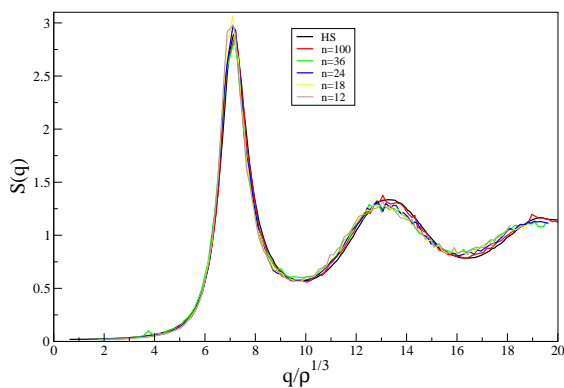


FIG. 1: Comparing the static structure factor of systems with different pair interaction. All systems are very close to freezing (99 percent of the critical density).

Mode coupling theory suggests that such a strong resemblance in the structure factor

$$S_q = \frac{1}{N} \sum_{ij} \exp [i(\mathbf{q} \cdot (\mathbf{r}_i - \mathbf{r}_j))]]$$

would entail a similar long time dynamics[3] for any of the systems concerned. We were able to confirm this by investigating the diffusion coefficient.

$$D = \frac{1}{6} \frac{d \langle r^2 \rangle}{dt}.$$

At high densities the diffusion showed a remarkable universality. However at lower densities this is not the case. In fact: the structure factors displayed noticeable differences at these densities already.

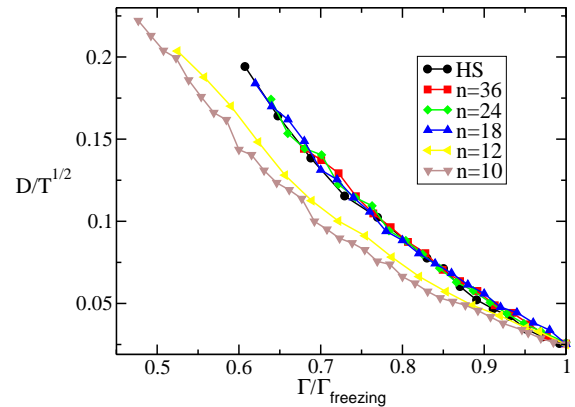


FIG. 2: The diffusion coefficient illustrates the fact that at higher densities the potential shape does not have a strong effect on the long time dynamics. At lower densities this is not true anymore.

In a further step we compare the intermediate scattering function, viscosities and the stress tensor in order to be able to answer the posed question more fully.

* Corresponding author: erik.lange@uni-konstanz.de
[1] D. M. Heyes and A. C. Branka Thoma, JCP **122**, 234504 (2005).
[2] J. P. Hansen and L. Verlet, Phys. Rev. **184**, 151 (1969).
[3] W. Götze and L. Sjögren, Rep. Prog. Phys. **55**, 241 (1992).

Light scattering study of the scaling of the alpha relaxation time in supercooled liquids

A. Le Grand¹, C. Dreyfus¹, J. Gapinski², A. Patkowski² and W. Steffen³

(1)IMPMC, Université P. et M. Curie, Paris, France, (2)Univ A. Mickiewicz, Poznan, Poland (3)Max Planck Institut for Polymer, Mainz, Germany

Estimating the relative importance of density and temperature in the change of the dynamical properties of a liquid near its glass transition is a long-lasting problem. Recently, results obtained through dielectric and light scattering measurements at variable temperature and pressure give new insights into this problem. We shall consider here mainly light scattering results.

In a first study[1] performed on the glassforming liquid OTP the analysis shows that the relaxation time depends on a single control parameter, product of a function of density by the inverse temperature. This observation is extended to other glassforming molecular liquids[2]. An expression of the relaxation time depending on this control parameter is given. It allows to describe results obtained in experimental and simulated supercooled

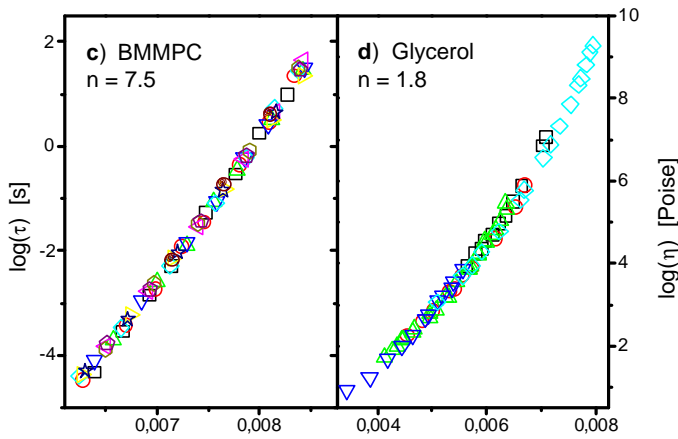


Figure 1 scaling of the α relaxation in BMMPC and glycerol

* Corresponding author:
catherine.dreyfus@impmc.jussieu.fr

[1] C. Dreyfus, A. Aouadi, J. Gapinski, M. Matos-Lopes, W. Steffen, A. Patkowski and R.M. Pick; Phys. Rev. E 68, 011204(2003).

[2] C. Dreyfus, A. Aouadi, J. Gapinski, M. Matos-Lopes, W. Steffen, A. Patkowski and R.M. Pick; Phys. Rev. E 68, 011204(2003).

A manifestation of the Ostwald step rule: Molecular-dynamics simulations and free-energy landscape of the primary nucleation of polyethylene single-molecules in dilute solution

L. Larini and D. Leporini*

Dipartimento di Fisica "Enrico Fermi", Università di Pisa, Largo B.Pontecorvo 3, I-56127 Pisa, Italy and INFN-CRS SOFT, Largo B.Pontecorvo 3, I-56127 Pisa, Italy

Numerical results from extensive MD simulations of the crystallization process of a single polyethylene chain with $N = 500$ monomers were performed [1].

The crystalline polymers arrange in an ordered way a large number of connected monomers. The backbone of a single polymer chain is folded inside the lamella to form the so-called stems, i.e. straight chain portions perpendicular to the basal surfaces of the lamella where the loops connecting the stems are localized. Fig.1 shows typical conformations.



FIG. 1: Snapshots of the molecular conformations involving the disappearance of two stems.

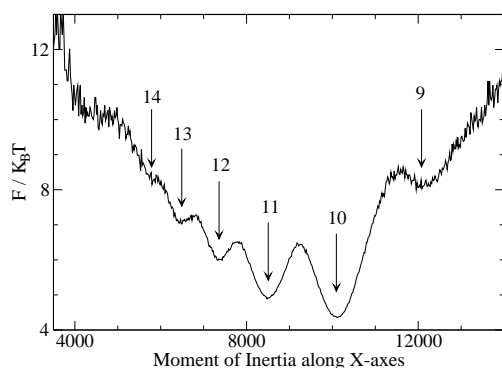
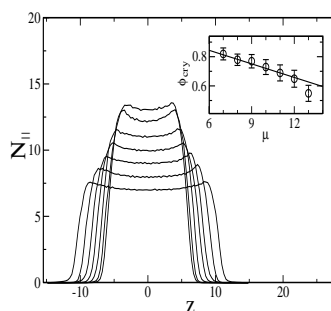


FIG. 2: Free energy landscape at $T=9$. The labels mark the number of stems of the crystalline structures corresponding to the minima.

The folding process involves several intermediate ordered *metastable* states [1, 2] - as evidenced by the several local minima of the free-energy landscape (Fig.2) - being characterized by a different number of stems μ in strong analogy with the experiments [3] and ends up in a well-defined long-lived lamella with ten stems arranged into a regular, hexagonal pattern. This behaviour may be seen as a *microscopic* manifestation

of the Ostwald step rule [1, 4]. For the different



μ	m	m^*
7	14.0	14.43
8	12.2	12.12
9	10.25	10.33
10	8.75	8.9
11	7.5	7.73
12	6.25	6.75
13	5.0	5.92

FIG. 3: Left: the number of intersections of the chain with a plane perpendicular to the z axis parallel to the aligned stems for different metastable crystalline states. The number of stems $\mu = N_{\parallel}(0)$ is in the range 7-13. Inset: The crystalline fraction ϕ_{cry} vs. the number of stems. The superimposed line is the theoretical prediction [1]. Right: comparison between the number of Kuhn segments of each stem from the simulation, m , and the model, m^* , assuming that all the metastable crystals have loops with four Kuhn segments.

metastable crystals Fig.3 (left) shows the number of intersections of the polymer chain with a plane perpendicular to the z axis being parallel to the stems.

The interconversion between the different metastable crystals involve surface rearrangements leading to the creation/disappearance of stems. Fig. 1 shows the disappearance of two stems.

Remarkably, the loops connecting the stems of the different metastable crystals have the same number of Kuhn segments , $\lambda = 4$ [1]. Evidence is gained by investigating both the crystalline fraction of the metastable structures, i.e. the relative fraction of monomers in the stems (see inset of Fig.3) and the length of the stems m (see the table in Fig.3).

* Corresponding author: dino.leporini@df.unipi.it
 [1] L. Larini, D. Leporini, J. Chem. Phys. **123**, 144907 (2005).
 [2] L. Larini, A. Barbieri, D. Prevosto, P.A. Rolla, D. Leporini, J. Phys.: Condens. Matter **17**, L199 (2005).
 [3] G. Ungar, J. Stejny, A. Keller, I. Bidd, M.C. Whiting, Science **229**, 386 (1985).
 [4] W. Ostwald, Z. Phys. Chem. Stoichiom. Verwandtschaftsl. **22**, 289 (1897). (2005).

Local and chain dynamics in miscible polymer blends: A Monte Carlo simulation study

Jutta Luettmmer-Strathmann*

Department of Physics, The University of Akron, Akron, OH 44325-4001

Local chain structure and local environment play an important role in the dynamics of polymer chains in miscible blends. In general, the friction coefficients that describe the segmental dynamics of the two components in a blend differ from each other and from those of the pure melts. In addition, recent experiments on miscible blends well above the glass transition have shown interesting differences between the dynamics on the scale of the shortest Rouse segment and dynamics on the scale of a chemical bond. In this work, we investigate polymer blend dynamics with Monte Carlo simulations of a generalized bond-fluctuation model, where differences in the interaction energies between non-bonded nearest neighbors distinguish the two components of a blend. Simulations employing only local moves and respecting a non-bond crossing condition were carried out for blends with a range of compositions, densities, and chain lengths. The results for the self-diffusion coefficients presented in Fig. 1 show that the blends investigated here have long-chain dynamics in the crossover region between Rouse and entangled behavior. In order to investigate the scaling of the self-diffusion coefficients, characteristic chain lengths N_c are calculated from the packing length of the chains. These are combined with a local mobility μ determined from the acceptance rate and the effective bond length to yield characteristic self-diffusion coefficients $D_c = \mu/N_c$. We find that the data for both melts and blends collapse onto a common line in a graph of reduced diffusion coefficients D/D_c as a function of reduced chain length N/N_c , see Fig. 2. The composition dependence of dynamic properties is investigated in detail for melts and blends with chains of length twenty at three different densities. For these blends, we calculate friction coefficients from the local mobilities and consider their composition and pressure dependence. The friction coefficients determined in this way show many of the characteristics observed in experiments on miscible blends.

In a smaller set of simulations, we also explore the effects of chain stiffness on local mobility and characteristic chain length of blend components.

Acknowledgments

Financial support through the National Science Foundation (NSF DMR-0103704) and the Research Corporation (CC5228) is gratefully acknowledged.

* Corresponding author: jutta@physics.uakron.edu

[1] W. Hess, *Macromolecules* **19**, 1395 (1986)

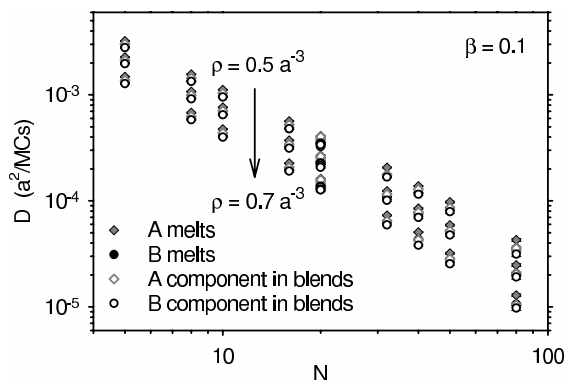


FIG. 1: Self diffusion coefficients as a function of chain length for all melts and blends considered in this work. The filled and open symbols represent simulation results for melts and blends, respectively, while diamonds and circles stand for chains of type A and B, respectively. The results represent three different monomer densities, $\rho = 0.5a^{-3}$, $\rho = 0.6a^{-3}$, and $\rho = 0.7a^{-3}$. In this graph, results for the B melts are hidden by the symbols for blend results.

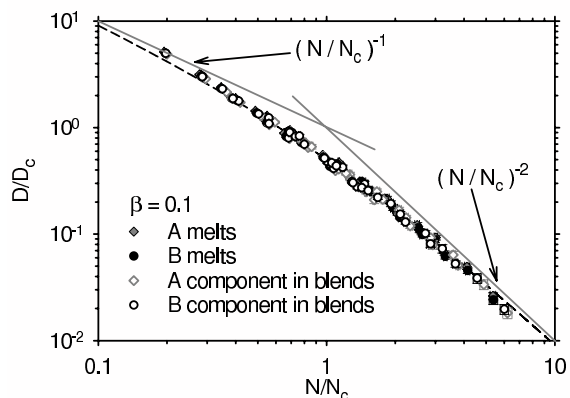


FIG. 2: Scaling representation of the self-diffusion coefficients for all melts and blends considered in this work. The dashed line represents the crossover function of Hess [1] while the gray solid lines represent the limiting power laws of the Rouse and reptation models.

From local dynamics to bulk mechanics of amorphous polymers: molecular dynamics simulation

Alexey Lyulin* and M.A.J. Michels

Group Polymer Physics, Eindhoven Polymer Laboratories and Dutch Polymer Institute, Technische Universiteit Eindhoven, P.O. Box 513 5600 MB Eindhoven, The Netherlands

In order to investigate the possible polymer-specific effects in the glassy dynamics we have performed a molecular dynamics (MD) simulation of the segmental orientational mobility of the low-molecular-weight glass-former, isopropylbenzene (iPB), atactic polystyrene (PS) and bisphenol A polycarbonate (PC) at an isotropic atmospheric pressure and in a wide temperature range.

The choice of iPB was motivated by the fact that its typical time scale of the orientational relaxation is within the simulated time window, which allow us to separate different relaxational processes with sufficient precision.

We also simulate the mechanical behaviour of PS and PC under the uniaxial deformation. We see the experimentally observed [1] strain-softening and strain-hardening phenomena (FIG. 1) and try to find possible links of the different bulk mechanics with the difference of the mobility on the segmental level. Constant pressure – constant temperature (NPT) MD algorithms have been implemented both in isotropic state and under the influence of the uniaxial mechanical deformation [2].

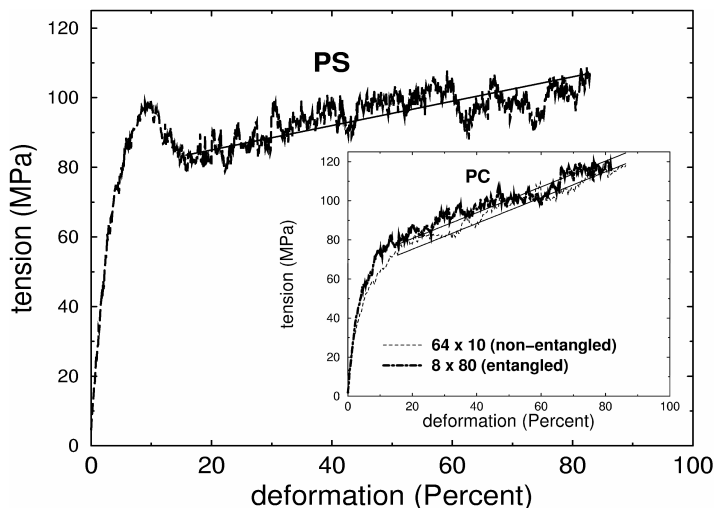


FIG. 1: Stress-strain behaviour of a non-entangled PS melt and two specimens of PC of different molecular weight at $T = 300\text{K}$. Strain softening is clearly seen for a PS sample, and is clearly absent for PC. The straight lines are the least-square fits of the data in the strain-hardening regime.

For all simulated compounds in the non-deformed state the analysis of the distribution functions of the characteristic orientational relaxation times for the second order autocorrelation functions (Legendre polynomials) reveals the existence of three different relaxation processes: initial ballistic process at very short times, followed by the b relaxation (motions within the cage) and, finally, the relaxation of the cage itself. This final relaxation which is a collective a -relaxation process above T_g is changed into some activated process below T_g , with very different activation energies for polymer- and low-molecular-weight glasses. b relaxation is an activated process which continues below T_g , and merges with a process at high temperature.

The mode-coupling theory (MCT) was used to fit the data. The predictions of the MCT are non-universal, and depend on the specific chemical structure. The value of the critical exponent is $g \sim 1$ for iPB and increases significantly for polymers. Significant changes of the local mobility have been observed under the deformation.

This work is the part of the research program of the Dutch Polymer Institute (projects 180 and 487). High Performance Computing Centre SARA in Amsterdam is acknowledged for providing the generous amount of the necessary CPU time.

* Corresponding author: a.v.lyulin@tue.nl

- [1] H. G. H. van Melick, L. E. Govaert, H. E. H. Meijer, *Polymer* 44, 2493 (2003).
- [2] A.V. Lyulin, B. Vorselaars, M.A. Mazo, N.K. Balabaev, M.A.J. Michels, *Europhys. Lett.* 71, 618 (2005).

Viscoelastic properties of polymer melts from equilibrium simulations

H. Meyer* and J. Baschnagel
Institut Charles Sadron, CNRS UPR 22, 67083 Strasbourg, France

We present results from molecular-dynamics simulations of a bead-spring model which aim at a complete characterization of the polymer and melt dynamics. From the simulations we do not only determine (standard) single-chain properties, such as mean-square displacements (MSDs), intrachain dynamic structure factor, end-to-end relaxation, etc., but also collective dynamic properties, such as the intermediate coherent scattering function and the shear modulus. We decompose these collective dynamic correlation functions into intrachain and interchain parts, and we show that a pure single-chain approach is insufficient to understand the dynamics of our model.

The model is a bead-spring model where non-bonded interactions are modeled with a purely repulsive potential $U_{nb}(r) = \epsilon((\sigma_0/r)^9 - (\sigma_0/r)^6) + \epsilon_m$ which has been used in a crystallizable polymer model [1]. The bonds are modeled with a harmonic bond potential $U_b(r) = k(r - r_0)^2$ with $r_0 = 0.97\sigma_0$. U_{nb} is not applied to bonded nearest neighbors. This separation allows for an easy decomposition of bonded and nonbonded contributions. This model is qualitatively similar to the Kremer-Grest model whose shear modulus has recently been examined up to chain-length $N = 120$ [2]. Figure 1 shows that entanglement effects are apparent only for much longer chains.

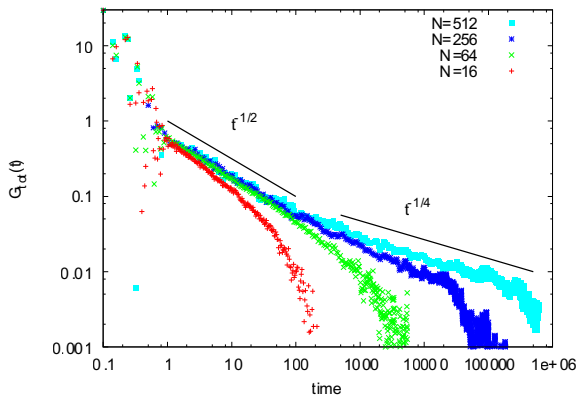


FIG. 1: Time dependent shear modulus $G(t)$ for different chain lengths at melt density $\rho = 0.84$. For short times, strong oscillations due to bond vibrations are present. At intermediate times, Rouse behaviour with power law $t^{-1/2}$ is seen and longer chains show a cross-over to $t^{-1/4}$ predicted for contour length fluctuations.

In equilibrium simulations, the shear modulus is calculated as the time auto-correlation function of the off-diagonal elements of the pressure tensor $P_{\alpha\beta}$ ($\alpha, \beta = x, y, z$):

$$G(t) = \frac{V}{k_B T} \langle P_{\alpha\beta}(t) P_{\alpha\beta}(0) \rangle \quad (1)$$

This quantity is extremely difficult to obtain with reason-

able statistics. The main reason is that it is a collective quantity which is not self-averaging. There is only one value per time step (or 3: xz, xy, yz), and this value is fluctuating strongly due to liquid properties at melt density. The polymer signal is 3-4 orders of magnitude weaker. One needs to correlate several 10^7 values to get reasonable data up to the terminal relaxation shown in figure 1.

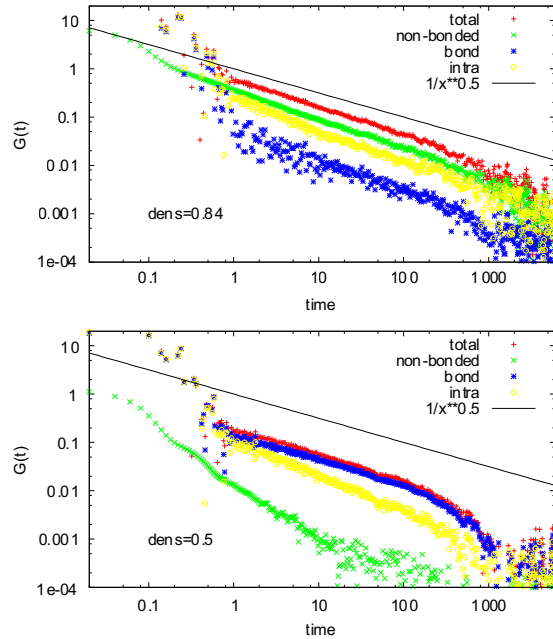


FIG. 2: Time dependent shear modulus for two different densities (top: melt $\rho = 0.84$, bottom: semi-dilute $\rho = 0.5$). Each graph shows the total $G(t)$ as well as the partial correlation functions of the contribution from bonded and non-bonded interactions. The relative contribution of bonded and nonbonded interactions is inverted when passing from the dense to the semi-dilute system. The intra part alone is apparently underestimating the correlations of the melt.

Figure 2 shows an example of the shear modulus $G(t)$ for chains $N = 64$ at two different densities. The contribution from bonded and nonbonded interactions as well as the contribution from intra-chain interactions only is shown. It is clear that the single chain-approach is apparently not sufficient to describe the viscoelasticity of the melt.

* Corresponding author: hmeyer@ics.u-strasbg.fr
 [1] H. Meyer and F. Müller-Plathe, J. Chem. Phys. **115**, 7807 (2001).
 [2] S. Sen, S. K. Kumar, and P. Keblinski, Macromolecules **38**, 650 (2005).

Locally preferred structure of model liquids

Stefano Mossa^{1,*} and Gilles Tarjus²

¹*European Synchrotron Radiation Facility, B.P. 220, F-38043 Grenoble, Cedex France*

²*Laboratoire de Physique Théorique de la Matière Condensée, Université Pierre et Marie Curie, 4 place Jussieu, Paris 75005, France*

Experimental [1] and numerical [2] work on bulk liquids confirms the tendency to form local order of icosahedral symmetry. This fact prompts two matters. First, the competition between extension of a local order and global constraints, associated with periodic tiling of the space, gives rise to geometrical frustration [3] which can be connected to the dynamic slowing down in supercooled liquids [4]. Second, the nature of local icosahedral order, although well understood in the case of isolated clusters [5], still needs to be clarified in the case of bulk liquids. Indeed, for small isolated clusters, the energetics is dominated by surface effects; the outermost atoms of an isolated cluster have a reduced number of interacting neighbors compared to the inner atoms or to atoms in bulk liquid. One may then ask if the preference for icosahedral order in a 13-atom cluster does not merely result from such surface effects.

It is evident from the above considerations that the concept of a “locally preferred structure” in bulk liquids needs a firm footing. Here we review our general method [6] to identify the “locally preferred structure” in bulk liquids. The latter is determined numerically as the ground state of the effective (free) energy landscape of small clusters embedded in a liquid-like mean-field environment. In this way the surface effects present in isolated clusters are minimized without introducing full blown geometrical frustration which hinders the manifestation of icosahedral order.

Our procedure is tested on a system of N atoms interacting via the Lennard-Jones potential $v(r) = 4\epsilon \left((\sigma/r)^{12} - (\sigma/r)^6 \right)$. The atoms are placed in a cavity of radius R_C that we envisage as surrounded by bulk liquid made of the same atoms and characterized, at the chosen temperature T and density ρ , by a known pair distribution function $g(r; T, \rho)$. The outside liquid is therefore essentially considered as a continuum, as in a mean-field type of description [7]. The mean-field-like potential energy acting on a given atom of the cluster at position \mathbf{r} due to the liquid outside a cavity of radius R_C is then given by

$$\mathcal{W}(r; R_C) = \frac{\rho}{2} \int_{|\mathbf{r}'| > R_C} d^3\mathbf{r}' g(|\mathbf{r} - \mathbf{r}'|) v(|\mathbf{r} - \mathbf{r}'|). \quad (1)$$

With the external potential so defined, one can determine the ground-state configuration of an N -atom cluster in a liquid-like environment (at given T and ρ) by searching the global minimum of the total energy

$$\mathcal{U}(\{\mathbf{r}_j\}_{1,\dots,N}; R_C) = \sum_{i < j=1}^N v(|\mathbf{r}_i - \mathbf{r}_j|) + \sum_{j=1}^N \mathcal{W}(r_j; R_C) \quad (2)$$

with respect to variations of the positions of the N atoms and of the cavity radius R_C . The procedure

for finding the ground state uses the basin-hopping optimization method [8]. The resulting energy per particle when plotted as a function of the size of the cluster shows a sharp minimum at $N = 13$ (see Fig. 1), lower than the corresponding bulk energy per particle and corresponding to an icosahedral structure. This allows us to confirm, without any a priori input, that the locally preferred structure in a bulk liquid is an icosahedral arrangement of thirteen atoms.

We finally describe how to deal with molecular systems and report some results about the Lewis and Wahnström model of ortho-terphenyl [9].

* Corresponding author: mossa@esrf.fr

- [1] A. Di Cicco *et al.*, Phys. Rev. Lett. **91**, 135505 (2003).
- [2] J. P. K. Doye, J. Chem. Phys. **119**, 1136 (2003).
- [3] J. F. Sadoc and R. Mosseri, “*Geometric Frustration*”, (Cambridge University Press, Cambridge, 1999).
- [4] G. Tarjus *et al.*, preprint cond-mat/0509127.
- [5] F. C. Frank, Proc. Roy. Soc. A **215**, 43 (1952).
- [6] S. Mossa and G. Tarjus, J. Chem. Phys **119**, 8069 (2003); preprint cond-mat/0510576.
- [7] Some care is needed in applying mean-field approaches [6]; when considering the interaction between cavity atoms and outside liquid one should treat differently the attractive component, which can be simply described by a mean-field type of approximation, and the short-range repulsive one, which accounts for the exclusion effect creating the cavity.
- [8] D. J. Wales and J. P. K. Doye, J. Phys. Chem. A **101**, 5111 (1997); J. P. K. Doye and D. J. Wales, Phys. Rev. Lett. **80**, 1357 (1998).
- [9] L. J. Lewis and G. Wahnström, Phys. Rev. E **50**, 3865 (1994).

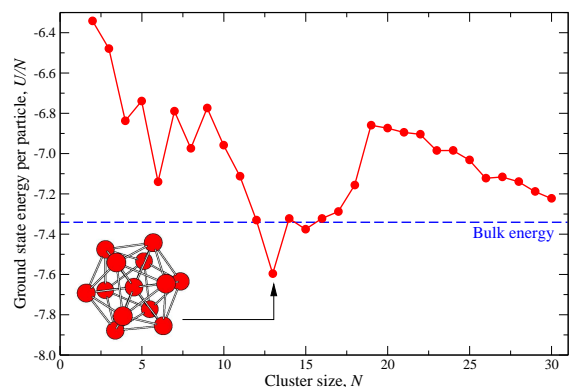


FIG. 1: Ground state energy per atom of N -atom clusters embedded in a liquid-like environment. The horizontal line is the corresponding bulk energy per atom. Note the clear minimum at $N = 13$.

Localized motions in 1,4-Polybutadiene close to the glass transition: Fully atomistic molecular dynamics simulations and neutron scattering results

*A. Narros⁽¹⁾, F. Alvarez^(1,2), A. Arbe⁽²⁾, J. Colmenero^(1,2,3), M. Monkenbusch⁽⁴⁾, D. Richter⁽⁴⁾ and B. Farago⁽⁵⁾

(1) Departamento de Física de Materiales (UPV/EHU), Apdo. 1072, 20080 San Sebastián, Spain

(2) Unidad de Física de Materiales (CSIC-UPV/EHU), Apdo. 1072, 20080 San Sebastián, Spain

(3) Donostia International Physics Center, San Sebastián, Spain

(4) Institut für Festkörperforschung, Forschungszentrum Jülich GmbH, D-52425 Jülich, Germany

(5) Institut Laue-Langevin, BP 156, 38042 Grenoble Cedex 9, France

1,4-polybutadiene (PB) is one of the most investigated polymeric glass formers. At low temperatures (about 20 K above the glass transition temperature, $T_G = 178$ K), aside of the alpha-relaxation many additional processes were identified experimentally - from dielectric spectroscopy, damping of the longitudinal Brillouin modes, depolarized Raman scattering and NSE [1,2,3]. Furthermore recent computer simulations have also contributed to the dynamic study of this polymer [4,5].

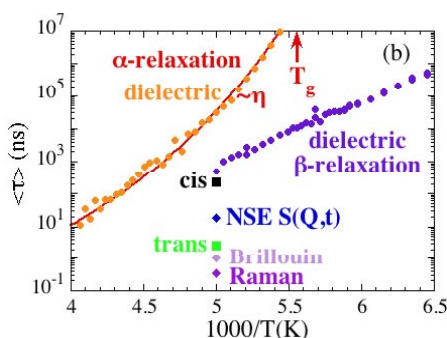


FIG 1: Compilation of the time scales identified for this polymer by different methods. The technique used is specified near the corresponding experimental point(s) in the same color.

It was to explore the possibility of unravelling this puzzling relaxation map [see Fig. 1], that we have performed MD-simulations of a realistic model of 1,4-polybutadiene. The simulations were carried out at 200 K, 220 K, 240 K, 260 K and 280 K, that is above but close to T_G , and extend until 1 microsecond for the lowest temperature. The good agreement obtained from the direct comparison of the dynamic structure factor at different Q-values with NSE results validates the simulations. Therefore, we can calculate from them dynamic magnitudes that cannot be directly measured and distinguish different parts of the system to be separately studied.

A direct investigation of the self part of the van Hove correlation function in the real space, $G_S(r,t)$, and particularly of the cis and trans units, reveals the presence of well defined hopping processes which are not evident in the $F_S(Q,t)$ behaviour. The jump distance involved results to be of the order of 2 Å [5]. This feature is just hidden in the reciprocal space. We have analyzed the real space data of the cis and trans units, $G_S(r,t)$, fitting them to an occurrence of hopping processes and sublinear diffusion assigned to the structural relaxation [5][see Fig. 2]. As can be seen in Fig. 1 the different behaviours we have obtained for the two studied species can help in the understanding of the different dynamic results of the several techniques shown above.

We have also qualitatively observed the thermal activation of these hopping processes which quantitative analysis is being currently performed.

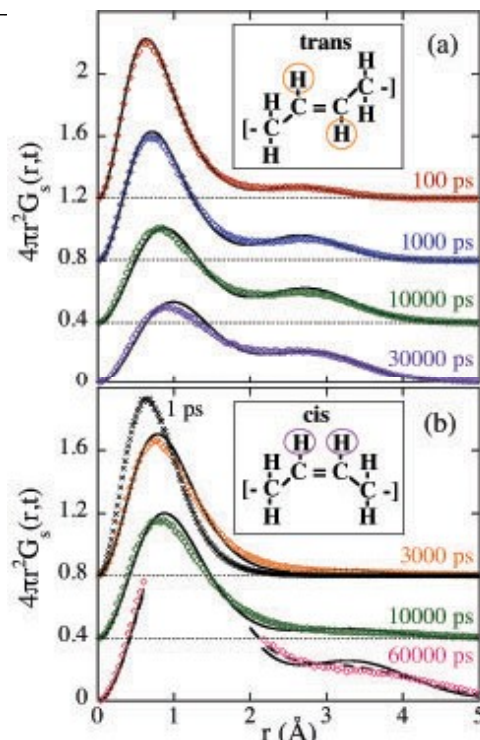


FIG. 2: Self part of the density pair correlation function for the double-bond hydrogens of the trans units (a) and the cis units (b) at 200K and different times as indicated. For clarity, the origins are shifted to the levels displayed by the horizontal dotted lines. For comparison in (b) we also display the results at $t = 1$ ps. (x). The solid lines show the description obtained by the proposed model [5]. For $t = 60000$ ps. in (b) we have magnified the curves to show the effect of a distribution of jump distances on the quality of the data description (dashed line).

*Corresponding author: wabnagoa@sc.ehu.es

[1] A. Arbe, D. Richter, J. Colmenero and B. Farago, Phys. Rev. E 54 (1996) 3853
 [2] A. Aouadi, M. J. Lebon, C. Dreyfus, B. Strube, W. Steffen, A. Patkowski and R. M. Pick, J. Phys.: Cond. Mat. 9 (1997) 3803
 [3] Y. Ding, V. N. Novikov and A. P. Sokolov, J. Of Polym. Sci. Part B: Polym. Phys. 42 (2004) 994.
 [4] A. Narros, A. Arbe, F. Alvarez, J. Colmenero, R. Zorn, W. Schweika, and D. Richter Macromolecules (ASAP).
 [5] J. Colmenero, A. Arbe, F. Alvarez, A. Narros, M. Monkenbusch, D. Richter, Europhys. Lett. 71 (2005) 262.

Of equilibrium clusters fluids and fluid clusters

K. Seelos, M. Nunez-Portela, R. Goldberg, T. Palberg*

Institute of Physics, University of Mainz

* Corresponding author: Thomas.Palberg@uni-mainz.de

Charged colloidal spheres interact via a long ranged repulsive screened Coulomb interaction. They are known to display an interesting phase behavior in both bulk equilibrium and in confinement, where fluid, crystalline or glassy phases have been reported.

Introduction of additional short ranged attractive interactions (e.g. by adding a second much smaller component) may further induce gelation, attractive glasses or an equilibrium cluster phase [1,2]. In these cases entropy drives local phase separation and the formation of large sphere aggregates. For sufficiently charged large spheres, however, the route to the gel state appears to be blocked by the accumulation of cluster charge [3]. Thus finite size clusters become stable. Experiments confirm this general picture so far for charged sphere/polyelectrolyte and charged sphere/neutral polymer mixtures [4].

We here report on a the phase behavior and the cluster statistics in a highly asymmetric *binary charged sphere mixture*. The larger component is a moderately polydisperse Polystyrene latex sphere of 1130nm diameter, the smaller is a highly charged monodisperse latex sphere of 68nm diameter. We observe cluster formation over a wide range of mixing ratios and total concentrations. In most cases at low salt concentration clusters formed display rod-like or chain-like morphologies. Interestingly, with decreasing salt concentration the clusters become ever more mobile and a fast monomer exchange dynamic is observed. On the other hand the cluster dynamics may become arrested by the first order crystallization transition of the smaller component occurring at increased small sphere concentration.

At larger salt concentrations clusters in general become more spherical but still appear to be very mobile and to display pronounced exchange dynamics. At very large concentrations of both small and large particles and of salt a continuous transition from a cluster fluid (separate clusters assuming fluid like inter-cluster structure) to a state which may be more accurately described as a fluid of spheres displaying mobile holes.

The difficulties to characterize these structures by light scattering and microscopy are discussed and preliminary results are presented.

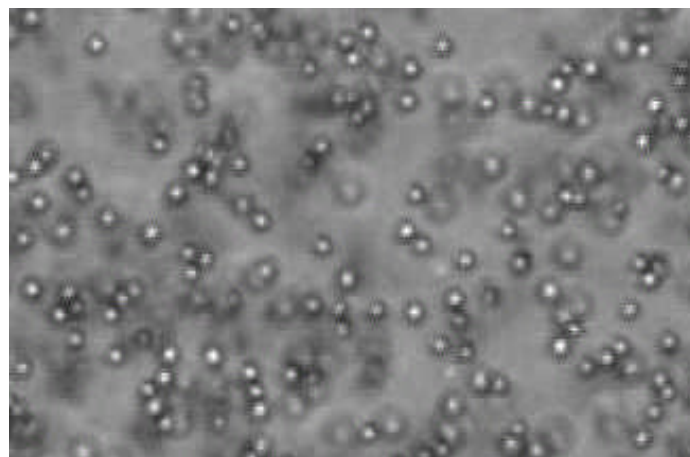


FIG. 1: equilibrium clusters from a binary charged mixture prepared from particles of a size ratio of 0.06 at a background salt concentration of $5 \times 10^{-6} \text{ mol l}^{-1}$. The number densities here were adjusted to be $n_{1130} = 1.8 \times 10^{16} \text{ m}^{-3}$ and $n_{68} = 4 \times 10^{19} \text{ m}^{-3}$. Note the open structure of the formed clusters, which appear to be highly mobile aggregates with strong internal dynamics.

[1] S. Scortino, S. Mossa, E. Zaccarelli, P. Tartaglia, *Phys. Rev. Lett.* **93**, 055701 (2004).
 [2] G. Foffi, F. Sciortino, E. Zaccarelli, P. Tartaglia, *J. Phys.: Condens. Matter*, **16**, S3791 (2004).
 [3] J. Groenewoldt, W. Kegel, *J. Phys. Chem B* **105**, 11702 (2001).
 [4] H. Sedgwick, S. U. Egelhaaf, W. C. K. Poon, *J. Phys.: Condens. Matter* **16**, 4913 (2004).

Confinement Effects on the Slow Dynamics of a Simulated Supercooled Polymer Melt

Simone Peter, Hendrik Meyer, and Jörg Baschnagel
*Institut Charles Sadron, 6 rue Boussingault, 67083 Strasbourg, France**

We present results from molecular-dynamics simulations for a model of non-entangled short polymer chains in a free standing and a supported film geometry. We investigate the influence of the confinement on the static and the dynamic properties of the melt.

The mean-square displacements (MSD) of the monomers $g_0(t)$ are used to analyze the dynamics of the systems. We find that the monomers at the free surface are faster not only in comparison to the bulk, but also with respect to the slightly accelerated dynamics at the supported surface (see figure 1). We determine a relaxation time τ from g_0 via $g_0(\tau) = 1$. τ may be fitted by a power law to extract the characteristic temperature T_c of mode-coupling theory. In agreement with the qualitative observations from figure 1 we find a decrease in T_c with decreasing film thickness and an overall stronger effect for the free standing films. T_c for a free standing film and a supported film of half the thickness are comparable.

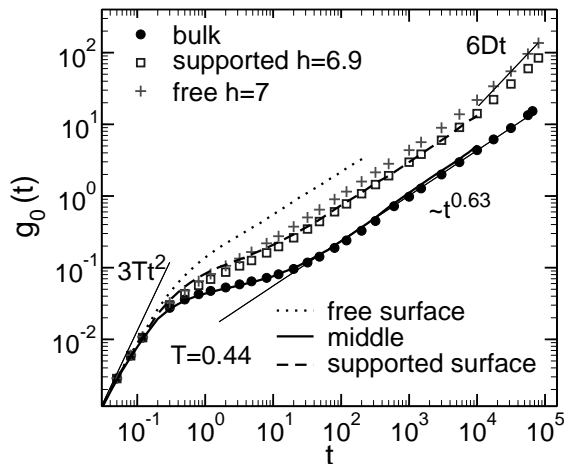


FIG. 1: Monomer MSD $g_0(t)$ parallel to the film interface versus t at temperature $T = 0.44$ and pressure $p = 0$; the bulk values are indicated by closed circles, the averages of the supported film of thickness $h = 6.9$ (rectangles) and the free film ($h = 7$: crosses). The full line indicates the MSD in the middle of the film, the dashed line at the supported surface and the dotted line at the free surface. The width of the slabs was $\Delta y = 2$. $g_0(t)$ is multiplied by $\frac{2}{3}$ for all films to account for the difference in spatial directions between the bulk and the film.

By measuring the film thickness $h(T)$ on cooling at a constant rate we can calculate the thermal expansion coefficient $\alpha = \frac{1}{h} \frac{\partial h}{\partial T}$. T_g is identified with the inflection point of α as shown in figure 2. For the films considered in our study T_c coincides with T_g within

the error bars. $T_c(h)$ can be described well by a fit to equation $T_c(h) = \frac{T_c^{\text{bulk}}}{1+h_0/h}$ [1]. The value of the fitting parameter h_0 is almost twice as large for the free standing film in comparison with the supported film.

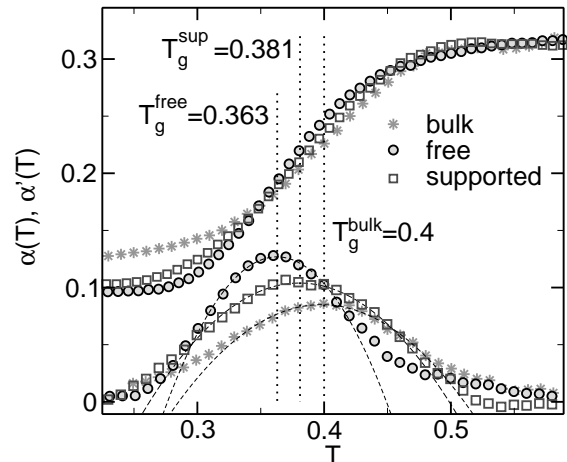


FIG. 2: For the bulk (stars), a supported (rectangles) and a free film (circles) the thermal expansion coefficient α is shown. The first derivative $\alpha' = \partial\alpha/\partial T$ is also displayed. The dotted lines indicate T_g identified with the inflection point of the thermal expansion coefficient. The dashed lines show the parabola used to determine the maximum of α' . The cooling rate was 2×10^{-5} per τ at $p = 0$ and the films contained $n = 576$ chains. α' was divided by 10 for clarity.

We find that the first maximum of the static structure factor S_q is smaller in the films than in the bulk when the same temperatures are compared. By contrast, the intrachain structure factor remains essentially unchanged by the confinement. This implies that the confinement alters the intermolecular packing: The “cage” around a monomer cannot “tighten” so quickly, as it is possible in the bulk. Since this effect becomes more pronounced with decreasing h , we can understand why the dynamics is faster in the films than in the bulk. An immediate consequence of this is that $T_c(h)$ decreases with h , in agreement with the depression of T_g .

* Corresponding author: peter@ics.u-strasbg.fr
 [1] J. Baschnagel and F. Varnik, *J. Phys.: Condens. Matter* **17**, R851 (2005)

Intermediate Range Order and Transport Processes in Viscous Aluminum Silicates: Molecular Dynamics Simulations

Patrick Pfeleiderer,* Jürgen Horbach, and Kurt Binder
Institut für Physik, Johannes-Gutenberg-Universität Mainz, Staudingerweg 7, 55099 Mainz

Glassforming mixtures of SiO_2 and Al_2O_3 with different compositions are investigated by molecular dynamics (MD) computer simulations. These systems form tetrahedral network structures, i.e. both Al and Si are fourfold coordinated by oxygens. In all compositions we find that Al prefers a different, denser packing of tetrahedra involving threefold-coordinated O atoms. The result is a microphase-separated system in which alumina-rich regions form a percolating network through the SiO_2 structure. This intermediate-range order appears as prepeaks in the partial static structure factors near 0.5^{-1} . We study how these

structural properties influence dynamical quantities such as diffusion constants, the Debye-Waller factor, and wave-vector dependent relaxation times. In the temperature range under investigation, i.e. for $T > 2000$ K, structural relaxation can be well described by mode-coupling theory.

* Corresponding author: pfleider@uni-mainz.de

Attractive glasses: quantitative comparison with MCT and aging

Oliver Henrich,¹ Antonio M. Puertas,^{2,*} Matthias Fuchs,¹ and Michael E. Cates³

¹*Fachbereich Physik, University of Konstanz, D-78457 Konstanz, Germany*

²*Group of Complex Fluids Physics, Department of Applied Physics, University of Almeria, 04120 Almeria (SPAIN)*

³*SUPA, School of Physics, The University of Edinburgh, JCMB Kings Buildings, Mayfield Road, Edinburgh EH9 3JZ, UK*

Two glasses have been identified in colloidal systems with short range attractions: a repulsive one at high density, lead by volume exclusion and similar to atomic glasses, and an attractive glass at moderate densities, driven by the attractions among particles. This scenario was predicted by Mode Coupling Theory (MCT), and corroborated by simulations and experiments [1]. The connection between the attractive glass and colloidal gels is still unclear, as they both occur inside the liquid-gas spinodal, and the interplay of dynamical arrest with phase separation is yet unknown.

In attractive glasses, since the density is not too high (it can be as low as $\rho \sim 0.5$), the formation of the bonds induces structural heterogeneities; the system is a network of particles with voids and tunnels. In the structure factor, this is noted as a peak at low q , which grows the higher the attraction strength. This feature is absent in repulsive glasses, and causes stronger dynamic heterogeneities in attractive ones.

We will perform here, in a system where the phase separation is hindered, a quantitative test of the MCT predictions. The structure factors from the simulation are used as input to MCT, and we study the effects of polydispersity and the long-range repulsive barrier in the potential (introduced to forbid crystallization and liquid-gas separation, respectively). Polydispersity kills off the high- q oscillations in $S(q)$, resulting in a glass transition similar to the repulsive one when this $S(q)$ is used in MCT. The repulsive barrier, on the other hand, responsible for the low- q peak in $S(q)$, makes the modes at this low- q the slowest ones, but leave the properties of the transition unaltered.

Although the transition point from MCT is at lower temperature than in the simulation, the quantitative comparison of the non-ergodicity parameters f_q , critical amplitudes h_q and time scale τ_q agree satisfactorily, in particular at large wavevectors, where the effect of the prepeak is less noticed. As an important side remark, we note that the transition is driven by the high- q oscillations, i.e. the attraction between particles, with little effect coming from the low- q prepeak.

Next, we study the aging of the system at different states in the non-ergodic region. In agreement

with the behaviour of repulsive (atomic) glasses, the density correlation functions can be scaled to overlap the decay from the plateau, with the time scale following a power-law with the waiting time. The non-ergodicity parameters grow as the quench is made deeper into the glass, following a square-root dependence with the distance to the transition. Furthermore, the non-ergodicity parameters oscillate in phase with the structure factor. However, in the attractive glass, aging implies the build up of the network of particles, and thus, structural evolution.

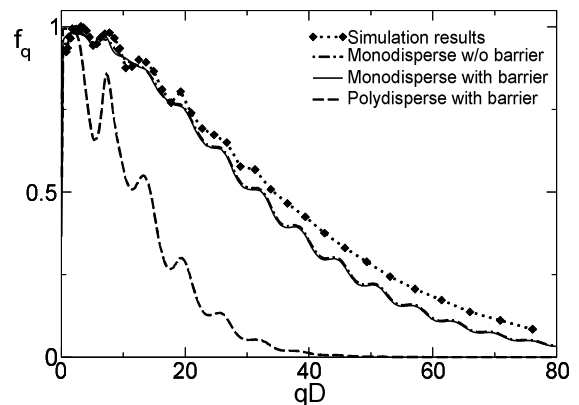


FIG. 1: Comparison of the non-ergodicity parameters from the simulations and MCT using different $S(q)$ as inputs

All of the results presented here show that the attractive glasses predicted by MCT are indeed obtained in colloidal systems with short-range attractions, provided the phase transitions are hindered. The transition is driven by bond formation, and the only effect of the repulsive barrier is to forbid liquid-gas separation. Additionally, we show that this glass behaves as a standard glass also in the non-ergodic region, where MCT cannot be applied.

* Corresponding author: apuertas@ual.es
 [1] K. Pham et al. Science **296**, 104 (2002).

Dynamics of Less Viscous Liquids as Described by Mode-Coupling Theory

Walter Schirmacher*

Techn. Univ. München, Phys.-Dept. E13, D-85747 Garching, Germany

Harald Sinn

Argonne National Laboratory, 9700 S. Cass Avenue, Argonne, IL 60439, USA

By comparison to experimental and simulation data it is shown that mode-coupling theory, which is known to give a good description of the relaxational dynamics of viscous liquids in the liquid-glass transformation regime, does also describe the non-viscous regime at higher temperatures fairly well.

It is by now well known that mode-coupling theory (MCT) gives a good and detailed account of the sophisticated and non-trivial dynamic blocking phenomena which occur in the vicinity of the liquid-glass transformation regime [1]. The key role in the descrip-

MCT version is the static structure factor $S(q)$ and known parameters like temperature, mass and density. As in all versions of MCT, there are no adjustable parameters.

We therefore became interested in the question as to whether the liquid dynamics in the less viscous regime away from the glass transition can also be described in terms of the "glass MCT". In fact, using the measured static structure factor as input, we found in the case of liquid titanium that the dynamical structure factor predicted by MCT shows almost perfect agreement to recent inelastic X-Ray diffraction data obtained at the Advanced Photon Source at the Argonne National Laboratory [3].

As the the static structure factor of simple liquids can be well described in terms of hard spheres the effective packing fraction η is the relevant density parameter of simple liquids. If the hard-sphere diameter σ is used as length scale and the isothermal sound velocity, divided by σ , i. e. $\omega_0 = \frac{v_{iso}}{\sigma} = \sqrt{\frac{k_B T}{m S(q=0)}} / \sigma$ as frequency scale, η remains as the only parameter of the theory.

In FIG. 1 we have plotted the memory function as calculated by MCT for different values of η . It is remarkable that it shows a two-step decay as, in fact, found in experimental and simulation data of several liquid metals [4]. It can be seen that the slow part of the decay gradually approaches the regime where, eventually at a critical value of η the non-ergodic plateau appears.

Work supported by the US Department of Energy, Office of Basic Energy Sciences, under Contract No. W-31-109-ENG-38.

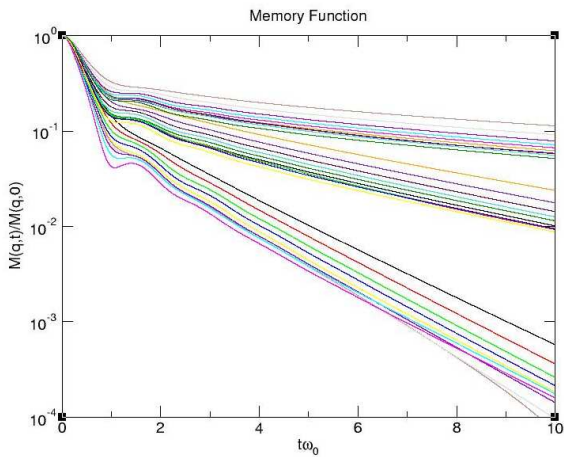


FIG. 1: Memory functions for the hard-sphere like model for packing fractions $\eta = 0.40$ (bottom curves), $\eta = 0.45$ (intermediate curves) and $\eta = 0.49$ (top curves). The q values are (essentially from bottom to top) $\sigma q = 0.9, 0.18, \dots, 8.1, 9.0$, where σ is the hard-sphere diameter, $\eta = (\pi/6)\rho\sigma^3$ and ρ is the number density.

tion of the so-called cage effect is played by the memory function $M(q, t)$ in the generalized Langevin equation for the density fluctuation correlator $\phi(q, t)$. Precursors of this theory were versions of MCT in which memory functions corresponding to current fluctuations were considered and which have been applied successfully for describing the microscopic density and current fluctuations of simple liquids [2]. However, the implementation of this theory is rather cumbersome, as it involves detailed knowledge of the interatomic potentials. In contrast, the only input to the present

* Corresponding author: wschirma@ph.tum.de

- [1] W. Götze, in *Liquids, Freezing and the Glass Transition*, J.-P. Hansen, D. Levesque, J. Zinn-Justin, Eds., North-Holland, Amsterdam 1991.
- [2] J. Bosse, W. Götze and M. Lücke, *Phys. Rev. A* **17**, 434 (1978); *ibid.*, **17**, 447 (1978); *ibid.*, **18**, 1176 (1978).
- [3] A. Said *et al.*, to be published
- [4] T. Scopigno, G. Ruocco, F. Sette, *Rev. Mod. Phys.* **77**, 881 (2005).

Application of the Ruin & Recreate Approach to Physical Models

Johannes J. Schneider*

Institute of Physics, Johannes Gutenberg University of Mainz, Staudinger Weg 7, 55099 Mainz, Germany

In this article, the application of the Ruin & Recreate optimization approach to the ground state search for physical systems is discussed.

When performing computer simulations of a physical system, often the knowledge of the ground state of the considered system is required. For example, order parameters for the description of phase transitions are used which map the current configuration onto the ground state of this system.

For complex systems, the ground state can often not be achieved via analytical calculations or a ground state search with exact optimization algorithms, as these often require calculation times which grow exponentially with the system size. Therefore, heuristic algorithms have to be used which lead to very good configurations and hopefully also to the global optimum of the system.

Most of these heuristic algorithms use the Local Search approach: the algorithm starts with a randomly chosen configuration, which is iteratively altered by the application of so-called small moves. These moves change the configuration only slightly in order to let the tentative new configuration stay in the neighborhood of the previous configuration.

This approach is surely sufficient for most simple problems. However, it turned out that this approach was e.g. unable to get to the global optimum of a simple network optimization problem. Therefore, we developed a new approach called Ruin & Recreate [1]: here we destroy the system to some larger extent, i.e., we remove some parts from the configuration. Then we rebuild a new configuration for the whole system by starting from the remaining configuration of the subsystem and reinserting the removed pieces according to a proposed rule-set. These rules shall guarantee that the move ends up at a good configuration for the overall system. The resulting configuration is then to be accepted or rejected by the acceptance criterion of the underlying optimization algorithm.

The Ruin & Recreate approach was first developed for network creation models, the Traveling Salesman Problem, and for vehicle routing problems [1]. For these problems, it turned out that two approaches for the Ruin part of the moves lead to good results:

- First of all, there is the Random Ruin, i.e., some pieces of the configuration are randomly picked and removed from the system.
- Secondly, there is the Radial Ruin, which takes some neighborhood relation into account and removes one center piece and all other pieces in some neighborhood of the center piece from the system.

However, not in all models, an obvious neighborhood relation is given: for example, in the SK-model for

spin glasses, all spins interact with each other via an interaction matrix J containing Gaussian random numbers. No locations of the spins are given. But one can overcome this problem and define a distance d_{ij} between two spins i and j via the strength J_{ij} of the interaction between them as $d_{ij} = 1/|J_{ij}|$. Thus, two spins are the closer together the stronger the interaction between them is. This approach leads to better results for the SK model than the common Local Search approach [2].

A further problem occurs when applying the Ruin & Recreate method to systems in which particles can be moved to new positions and in which not only the ground state is of interest but also the behavior at some given temperature: here the Ruin & Recreate moves have to obey to the condition of detailed balance, such that a thermal equilibrium can be reached at each temperature. This can e.g. be done by performing a local optimization run based on small moves, in which a part of the system is heated up to some temperature and then cooled down to the global temperature of the outside system. During this local optimization run, all particles outside the chosen local system part which is to be altered remain unchanged. Here one faces the problem that if the global temperature is already rather small, such that the system is e.g. crystalline, the “hot” particles might run outside the chosen part and not be able to return to it such that they form defects in the crystalline structure. Here additional penalty terms have to be introduced which ensure that the particles basically stay within the chosen part and also that the temperature the particles “feel” is equal to the global temperature. For this purpose, these added penalty terms have to be reduced in size when the local temperature approaches the global temperature. When the local temperature finally reaches the global temperature, the penalty terms should vanish. The coordinated decrease of the penalty terms is rather difficult to realize, there is only a narrow regime between destroying the crystalline structure and destroying detailed balance.

Finally, I would like to thank the Materialwissenschaftliches Forschungszentrum in Mainz, Germany for financial support.

* Electronic address: schneidj@uni-mainz.de;
URL: <http://www.staff.uni-mainz.de/schneidj>

[1] G. Schrimpf, J. Schneider, H. Stamm-Wilbrandt, and G. Dueck, *J. Comp. Phys.* **159**, 139 (2000).
[2] J. Schneider, *Effiziente parallelisierbare physikalische Optimierungsverfahren*, PhD thesis (University of Regensburg, Germany, 1999).

Diffusion in Metallic Glass and their Melts: Aging and Heterogeneity

H. R. Schober* and M. Kluge
Institut für Festkörperforschung, Forschungszentrum Jülich, 52425 Jülich, Germany

We report results of molecular dynamics simulations of a binary Lennard-Jones system at zero pressure in the undercooled liquid and glassy states. We first follow the evolution of diffusivity and dynamic heterogeneity with temperature and show their correlation. In a second step we follow the aging of a quenched glass. As diffusivity decreases with aging, heterogeneity increases. We conclude that the heterogeneity is a property of the inherent diffusion of the relaxed state. The variations with aging time can be explained by annealing of quenched defect structures. This annealing has the same decay constants for both diffusivity and heterogeneity of both components.

As an example, Fig. 1 shows the diffusion coefficients for both components of the binary Lennard-Jones glass at zero pressure at $T = 0.32 \epsilon/k$, i. e. just below the mode coupling critical temperature.

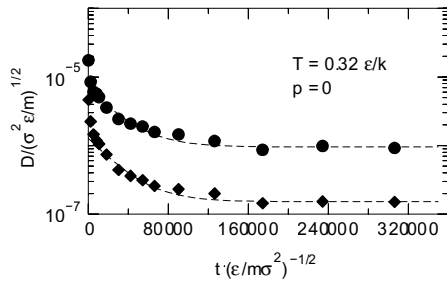


FIG. 1: Aging of the diffusion coefficients in a binary Lennard-Jones glass at $T = 0.32 \epsilon/k$. The dashed lines show the fit with an inherent plus a defect diffusion [?].

The aging behavior is consistent with the assumption that the diffusivity is the sum of two terms

$$D(t) = D_{\text{inh}} + D_{\text{def}} c_{\text{def}}(t) \quad (1)$$

where D_{inh} is a time independent inherent diffusion coefficient, D_{def} is a defect mediated diffusion constant and $c_{\text{def}}(t)$ is the defect concentration. If the defects are slowly annealed, with some rate α_{def} during the aging at constant temperature, we get

$$D(t) = D_{\text{inh}} + D_{\text{def}} c_{\text{def}}(0) e^{-\alpha_{\text{def}} t}. \quad (2)$$

The same decay constant α_{def} describes the slowing down of diffusion with aging for both components.

Further more the analogous law

$$\alpha_2(t) = \alpha_2^{\text{inh}} + \alpha_2^{\text{def}} c_{\text{def}}(0) e^{-\alpha_{\text{def}} t}. \quad (3)$$

describes the increase of the maximal non-Gaussianity, which measures the dynamic heterogeneity, with the same value of α_{def} .

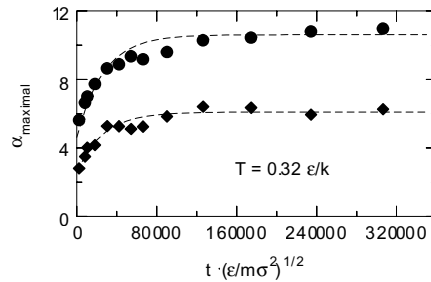


FIG. 2: Aging of the maximal non-Gaussianity in a binary Lennard-Jones glass at $T = 0.32 \epsilon/k$. The dashed lines show the fit with an inherent plus a defect heterogeneity [1].

During aging the glass densifies. We show that this process is much slower. It affects the atomic mobility much less than the above process. This is related to the observed small activation volumes of diffusion [2].

We will discuss aging for different temperatures above and below T_c and T_g . We will also look at effects on correlation functions.

* Corresponding author: H.Schober@fz-juelich.de
 [1] H. R. Schober, J. Phys. Chem. Chem. Phys. **6**, 3654 (2004).
 [2] H. R. Schober, Phys. Rev. Lett. **88**, 145901 (2002).

Simulations of an energy landscape model for glass forming liquids in three dimensions

Esben F. Pedersen, Ulf R. Pedersen, Tina Hecksher, Jeppe C. Dyre, and Thomas B. Schröder*

*Department of Mathematics and Physics (IMFUFA),
Glass & Time - Danish National Research Foundation Centre for Viscous Liquid Dynamics,
Roskilde University, Postbox 260, DK-4000 Roskilde, Denmark*

We present results from extensive computer simulations of a three-dimensional lattice gas model for viscous liquids [1]. The model is characterized by each particle having its own random energy landscape. The equilibrium dynamics of the model were investigated by continuous time Monte Carlo simulations at two different densities at a range of temperatures. At high densities and low temperatures the model captures the important characteristics of viscous liquid dynamics. We thus observe non-exponential relaxation in the

self part of the density auto-correlation function, and fragility plots of the self-diffusion constant and relaxation times show non-Arrhenius behavior.

* Corresponding author: tbs@ruc.dk
[1] U.R. Pedersen, T. Hecksher, J.C. Dyre, and T.B. Schröder, cond-mat/0511147 (2005).

Ultra fast processes for solvent evaporation in thin polymer films below T_g

Mireille Souche* and Didier Long

Laboratoire de Physique des Solides, Batiment 510, Université Paris Sud, 91405 Orsay, France

The solvent diffusion coefficient D in a solvent-polymer system can be much larger than the ratio a^2/τ_α , where a is one monomer length (about 0.5 nm) and τ_α is the dominant relaxation time measured e.g. by broadband dielectric spectroscopy [1, 2]. The discrepancy can be by up to 6 orders of magnitude and more. We propose here that the solvent diffusion is dominated by path in the liquid with fast relaxation time. It allows to quantitatively explain the discrepancy between D and τ_α^{-1} . Then, we apply this model to describe solvent evaporation of a polymer film with thickness of order a few micrometers. As a consequence of the presence of these fast paths, we show that such a film can dry within an accessible experimental time, even at temperatures well below the glass transition temperature. Our results qualitatively explain corresponding experimental results on PMMA films performed at room temperature [3].

The discrepancy between solvent diffusion and α -relaxation is reminiscent of other experiments in which it has been shown that the dynamics in liquids in the Williams Landel Ferry regime and down to the glass transition is strongly heterogeneous [4]. When considering the diffusion of a single fluorescent molecule in a pure liquid, such as ortho-terphenyl or a polystyrene melt, Ediger et al, Fujara et al, have shown that the diffusion coefficient is decoupled from the dominant relaxation time of the liquid, and that it is larger by up to 3 orders of magnitude as one would expect from the Stokes law. It has been proposed recently that the dynamical heterogeneities in such liquids are due to density fluctuations, which allowed to explain the amplitude of dynamical heterogeneities, the amplitude of the violation of the Stokes law, and also the shift of relaxation time in ultra-thin films as compared to the bulk [5, 6]. We extend here some aspects of this model to study the solvent diffusion in polymer-solvent mixtures.

We propose indeed that dynamical heterogeneities in solvent-polymer mixtures exist also, and that they are due to the solvent concentration fluctuations. The corresponding dominant scale is determined by considering the amplitude of these fluctuations, as a function of the considered scale, and their lifetime, which is also scale-dependent. From this and the known plasticizing effect of the solvent, we deduce the relaxation time distribution, which is significantly larger than for liquids in the bulk. In particular it allows to explain

the amplitude of the ratio Da^2/τ_α , and the fact that it can be as large as 10^6 , and more when cooling the system further. Then, we consider a polymer film in equilibrium with a non-zero solvent vapor pressure, such that the system is above the glass transition. By reducing the solvent activity in the surrounding atmosphere, the solvent evaporates. The relaxation dynamics of the film is described by two coupled equations: 1- a Fokker-Planck equation, which governs the evolution of the polymer volume fraction distribution, and 2- a differential equation, which governs the overall evaporation rate of the solvent. The latter is controlled by a time scale which is the product of the fast time controlling solvent diffusion by a geometrical factor l/a^2 where l is the film thickness. Typically, for films of one micrometer thickness, this factor is of order 10^6 . We show, that, by reducing the solvent activity down to zero, the solvent can totally evaporate in an accessible experimental time, even at temperatures well below the polymer glass transition temperature. This is a consequence: 1- of the presence of the fast path 2- of the film being out equilibrium, and in a dynamical state which is much faster than the one it would have at equilibrium. Both aspects are essential to explain the corresponding experimental features. Another striking feature of our results is that the time scale associated with solvent evaporation can be non monotonous in this kind of experiments.

In conclusion, we show here that dynamical heterogeneities are essential for understanding solvent diffusion close to and below T_g . The dynamical heterogeneities are even larger in polymer-solvent systems than in pure liquids. Taking them into account is essential for describing solvent evaporation.

* Corresponding author: souche@lps.u-psud.fr

- [1] A.-C. Dubreuil, F. Doumenc, B. Guerrier, D. Johannsmann and C. Allain, *Polymer* **44**, 377-387 (2003).
- [2] P.K. Davis, R.P. Danner, J.L. Duda and I.H. Romdhane, *Macromolecules* **37**, 9201-9210 (2004).
- [3] F. Doumenc, B. Guerrier and C. Allain, submitted for publication (2005).
- [4] M.D. Ediger, *Annu. Rev. Chem.* **51**, 99 (2000).
- [5] D. Long and F. Lequeux, *EPJ E* **4**, 371-387 (2001).
- [6] S. Merabia, D. Long, *EPJ E* **9**, 195-207 (2002).

Dynamics in aqueous nano- and microdroplets: optimization of dielectric heating

J.Tsuwi*¹, C.Holtze², R.Sivaramakrishnan³, K.D.Kramer³, M.Antonietti⁴, F.Kremer¹

¹Institute for Experimental Physics I, University of Leipzig, Linnéstraße 5, 04103 Leipzig, Germany

²Experimental Soft Condensed Matter Group, 40 Oxford St. Harvard University, MA 02138, U.S.A

³Department of Physics, Free University Berlin, Arnimallee 14, 14195 Berlin, Germany

⁴Max Planck Institute of Colloids and Interfaces, Department of Colloid Chemistry, Research Campus Golm, D-14424 Potsdam, Germany

The dynamics in aqueous NaCl nano- and microdroplets dispersed in oil is analyzed in the frequency range 1MHz – 4GHz. The droplet sizes ranged from diameters of 125nm to 3.6µm produced in the spherical geometry by employing the inverse miniemulsion preparation technique. The miniemulsions showed one broad dielectric loss peak whose frequency position and intensity is found to dependent in a non-trivial way to the size of the droplets (Fig.1).

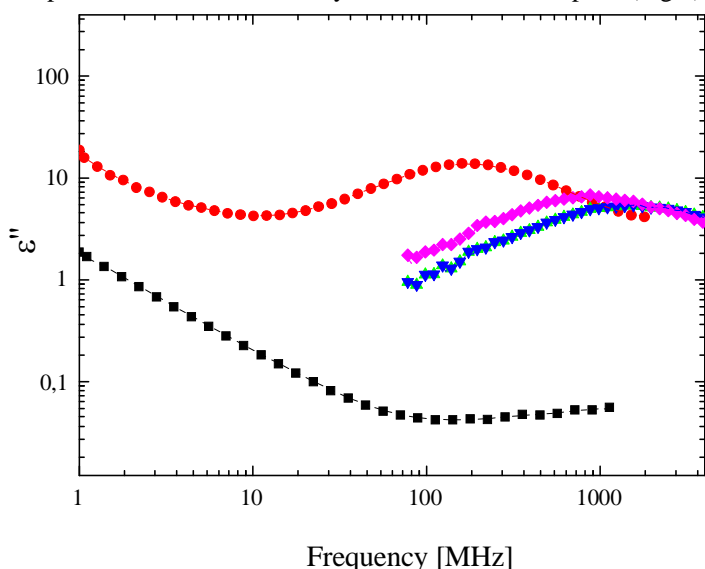


FIG.1. Frequency dependent dielectric loss of aqueous 1M NaCl spherical droplets of different diameter sizes: 125nm (square), 256nm (circle), 600nm (up triangle), 2100nm (down triangle) and 3600nm (diamond).

The analysis of data is discussed in the context of Maxwell-Wagner polarization mechanism. At droplet sizes of less than 150nm, the dispersion peak cannot be resolved because the droplet size is too small to allow effective charge separation. At larger droplet sizes, single-size effects dominate with observable absorption and shifts in the peak position. When size of droplet is explicitly reflected in the existing heterogeneous mixture models, the frequency of maximum absorption changes by 63MHz. Generally, the frequency of peak maxima for the various miniemulsions investigated is found to be lower than predicted from theory.

Fig.2 shows the dielectric loss intensity and frequency of maximum position taken from Fig.1 and plotted as a function of droplet size. Both intensity and frequency are seen to have a maximum however they do not overlap. Between the two maxima, a new maximum is found at 1.592 GHz which both size and intensity are optimized with values of 589.82nm droplet diameter and 13 respectively.

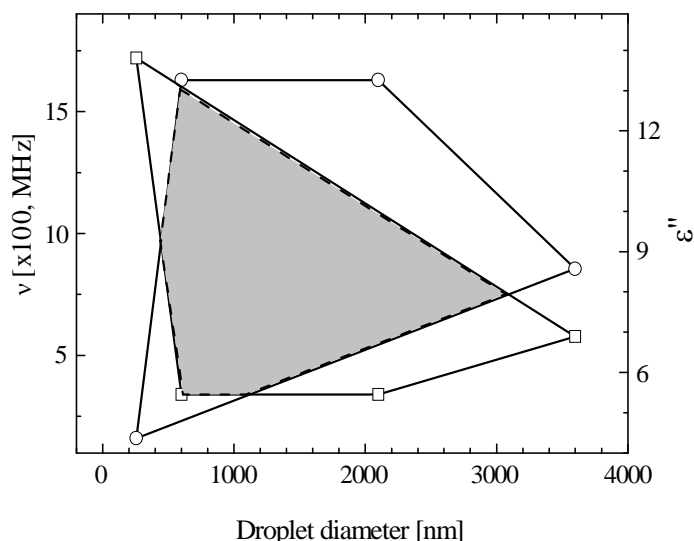


FIG 2. Size dependence dielectric intensity ϵ'' (squares) and the corresponding frequency of maximum peak (circles). The area enclosed by each type of symbol covers all possible values attainable with an interpolated droplet size. The overlapping region (shaded) gives the range of sizes for which intensity and absorption frequency are interlinked.

The information obtained from this study not only allows the simple adjustment of heating rates (for example in microwave enhanced chemical reactions) by structural control in multiphase emulsions and dispersions, but also is relevant in maximizing or minimizing RF and microwave damping of radar signals.

*corresponding author: tsuwi@physik.uni-leipzig.de

References

- [1] Holtze C, Antonietti M, Sivaramakrishnan R., Kramer K. D., Tsuwi J., Kremer F. *submitted*.
- [2] Tsuwi J., Holtze C, Antonietti M, Sivaramakrishnan R., Kramer K. D., Kremer F. *submitted*.
- [3] Tsuwi J., Holtze C, Antonietti M, Sivaramakrishnan R., Kramer K. D., Kremer F. *in preparation*.
- [4] Antonietti, M.; Landfester, K. *Prog. Polym. Sci.* 2002, 27, 689-757
- [5] J. Sjöblom; H. Førdedal; T. Skodvin, *J. Disp. Sci. and Techn.* 1999, 20, 921-943.

On the Q-Dependence of the Atomic Motions in the α -Relaxation Range. A neutron scattering study of short chain analog of poly(vinyl acetate).

M. Tyagi^{1,*}, A. Alegria², F. Alvarez², J. Colmenero^{1,2}, M. Monkenbusch³, and B. Frick⁴
¹ Donostia International Physics Center, Paseo Manuel de Lardizabal, 4, 20018 San Sebastian, Spain
² Departamento de Física de Materiales and Centro Mixto CSIC-UPV/EHU, Facultad de Química, Apartado 1072, 20080 San Sebastian, Spain
³ Institut für Festkörperforschung, Forschungszentrum, Juelich, Germany and
⁴ Institut Laue Langevin, BP 156, 38042, Grenoble Cedex 9, France

Polymeric systems and low molecular weight glass forming liquids (LMGFL) exhibit a series of universal features. One of these universal features shared among polymers and LMGFL is the so-called anomalous diffusive regime observed in the intermediate Q -range which is reflected by the shape of the intermediate scattering function $S(Q, t)$ and particularly by the momentum transfer (Q) dependence of characteristic times observed by incoherent neutron scattering. This regime has been studied very well in polymers and it has been well established that the characteristic times follow a power law in Q as $\tau_{KWW} = \tau_0 Q^{-2/\beta_{KWW}}$ where β_{KWW} is stretching shape parameter for $S(Q, t)$. At higher Q values (above $Q \approx 1 \text{ \AA}^{-1}$) polymer dynamics shows a crossover to non-Gaussian regime where Q dependence of characteristic times approximately follows $\tau \approx Q^{-2}$ law. However, in very low Q -regime (or equivalently at higher spatial scales) the LMGFL are expected to show normal diffusive processes related with the displacement of center of mass of the entire molecule. This behavior is prevented in polymers because of chain connectivity and rather a crossover to Rouse regime is expected which characterizes Brownian dynamics of ideal Gaussian chain in melt. In this work, we present our recent findings obtained by combined neutron spin echo (NSE) and Backscattering (BS) measurements on a fully protonated trimer of vinyl acetate (which is a short chain analog of poly(vinyl acetate)) to explore the possible crossover regimes in LMGFL. The scattering functions $S(Q, t)$ were directly measured in the low- Q regime at $Q=0.08, 0.14, 0.20$ and 0.28 \AA^{-1} by NSE (FRZ-Juelich) at $350K$. The measured spectra were analyzed in terms of stretched exponential Kohlrausch-Williams-Watts (KWW) function to obtain the shape parameters and characteristic times. The dynamic scattering functions, $S(Q, \omega)$, measured by BS (IN16, ILL-Grenoble) were analyzed in terms of the Fourier transform of KWW functions. The scattering functions observed by NSE show sub-linear diffusive motions ($S(Q, t) \approx \exp[-(t/\tau_{KWW})^{\beta_{KWW}}]$) for Q values ranging between 0.14 - 0.28 \AA^{-1} . This result is well supported by BS in the overlapping range of Q and found to extend until $Q=0.5 \text{ \AA}^{-1}$ for all the temperatures ($270K$ - $350K$) measured by backscattering. In polymers, stretching exponent is found to be weakly dependent on temperature and, hence, power exponent in the Q dependence of characteristic times remains more or less same for all temperatures. How-

ever, in LMGFL stretching exponent is strongly temperature dependent and hence power exponent should vary strongly with temperature. It was interesting to see that power law is full-filled for all stretching parameters at different temperatures (Fig.1). The non-Gaussian regime is also exhibited by trimer sample in the Q -range 0.7 - 1.9 \AA^{-1} . This regime is fundamentally different from purely diffusive regime where characteristic times also follow the Q^{-2} law. In the purely diffusive regime, scattering function $S(Q, t)$ should be a simple exponential. This is found to be the case in our NSE measurements at the lowest- Q value. In addition, the Q -dependence of time scales at this value showed a weaker dependence (than in sub-linear diffusive regime). The exponential behaviour of $S(Q, t)$ followed by weaker Q -dependence of momentum transfer indicates a crossover to purely diffusive regime somewhere between 0.08 - 0.14 \AA^{-1} . Molecular dynamics simulation is also in progress to get a deeper insight of molecular mechanism involved and will be presented at the conference. In addition, results will be compared with our recent results on its polymer counterpart, namely, poly(vinyl acetate)[1].

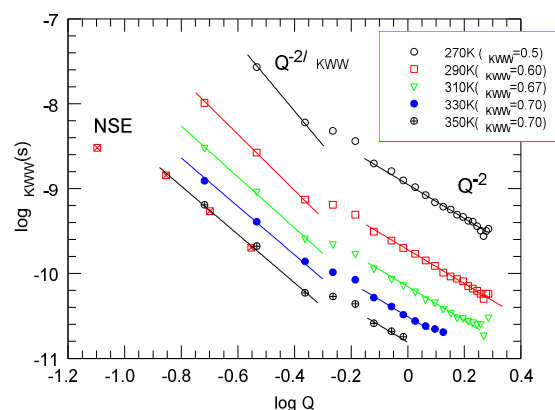


FIG. 1: The momentum transfer dependence of characteristic times in trimer sample.

* Corresponding author: swxytyym@sc.ehu.es

[1] M. Tyagi, A. Alegria and J. Colmenero, J. Chem. Phys. **122**, 244909 (2005).

Single molecule as a probe for local density fluctuations and structural relaxation in polymers.

R.A.L. Vallée,* M. Baruah, J. Hofkens, N. Boens, and M. Van der Auweraer
*Department of Chemistry, Katholieke Universiteit Leuven,
 200F Celestijnenlaan, 3001 Heverlee, Belgium*

D. Beljonne

Laboratory for Chemistry of Novel Materials, University of Mons, Place du Parc, 20, 7000 Mons, Belgium

The structural relaxation behavior of glass-forming liquids is a field of intense research[1–4]. Above the glass transition temperature T_g (the temperature below which the system of interest becomes an amorphous solid), the behavior is dominated by the so-called α -relaxation process. In ensemble experiments, the relaxation decays in a nonexponential manner, according to the stretched exponential (Kohlrausch-Williams-Watts, KWW) function: $\phi(t) = f_0 e^{-(t/\tau_K)^\beta}$, where τ_K is the relaxation time and $0 \leq \beta \leq 1$ is the stretching parameter. The average relaxation time $\tau_C = \frac{\tau_K}{\beta} \Gamma(\frac{1}{\beta})$, where Γ denotes the gamma function, of this process increases as the transition temperature is approached. Extensive ensemble measurements [3–5] have suggested that the dynamics near the glass transition is spatially heterogeneous. Because they allow bypassing the ensemble averaging intrinsic to bulk studies, Single Molecule Spectroscopy (SMS) constitutes a powerful tool to assess the dynamics of heterogeneous materials at the nanoscale level [6–8]. Recently, single molecule rotational motion has been used to probe the heterogeneous dynamics in polymers near their glass transition [9]. On the basis of these SMS studies, the nonexponential relaxation seen in ensemble experiments has been interpreted as the result of ensemble averaging over many molecular environments, each of which having its own exponential relaxation, as confirmed by formal analysis taking properly into account all optical parameters [10, 11]. We have shown that the fluorescence lifetime of single molecules with quantum yield close to unity is highly sensitive to changes in local density occurring in a polymer matrix [12–14]. A clear correlation was established between the radiative lifetime distributions measured for single molecules and the local fraction of surrounding holes.

Here, we show that this local fraction of holes is independent of the molecular weight of the polymer, in the glassy state. It increases once the system is brought in the supercooled regime. These results provide a firm microscopic confirmation of the densification of the system as T_g is approached and point to the importance of the mobility of voids in order to explain the dependence of T_g on M_n in the glassy state. In the supercooled regime, we demonstrate that the α -relaxation process, as probed by each single molecule, is best fitted with a single exponential function, with

an average relaxation time that increases as T_g is approached. By reconstructing the ensemble in two different ways, we recover the expected nonexponential decay. We are able to attribute it to spatially heterogeneous dynamics, and can discriminate between the influence of local changes in density and packing from other effects.

The authors are grateful to the University Research Fund of the K.U.Leuven for GOA 2001/2, IDO-grant IDO/00/001, and a postdoctoral fellowship to M. B. The Fonds voor Wetenschappelijk Onderzoek Vlaanderen is thanked for a postdoctoral fellowship for R. V. and for grants G.0320.00 and G.0421.03. The continuing support through IAP-V-03 is gratefully acknowledged. D. B. is a research associate of the Fonds National de la Recherche Scientifique.

* Electronic address: renaud.vallee@chem.kuleuven.be

- [1] P. G. Debenedetti, F. H. Stillinger, *Nature* 410, 259 (2001).
- [2] C. A. Angell, K. L. Ngai, G. B. McKenna, P. F. McMillan, S. W. Martin, *J. Appl. Phys.* 88, 3113 (2000).
- [3] M. D. Ediger, *Annu. Rev. Phys. Chem.* 51, 99 (2000).
- [4] H. Sillescu, *J. Non-Cryst. Solids* 243, 81 (1999).
- [5] K. Schmidt-Rohr, H. Spiess, *Phys. Rev. Lett.* 66, 3020 (1991).
- [6] W. E. Moerner, M. Orrit, *Science* 283, 1670 (1999).
- [7] X. S. Xie, J. K. Trautman, *Annu. Rev. Phys. Chem.* 49, 441 (1998).
- [8] F. Kulzer, M. Orrit, *Ann. Rev. Phys. Chem.* 55, 585 (2004).
- [9] L. A. Deschesnes, D. A. Vanden Bout, *Science* 292, 255 (2001); L. A. Deschesnes, D. A. Vanden Bout, *J. Phys. Chem. B* 106, 11438 (2002).
- [10] G. Hinze, G. Diezemann, Th. Basché, *Phys. Rev. Lett.* 93, 203001 (2004).
- [11] C.-Y. J. Wey, Y. H. Kim, R. K. Darst, P. J. Rossky, D. A. Vanden Bout, *Phys. Rev. Lett.* 95, 173001 (2005).
- [12] R. A. L. Vallée, N. Tomczak, L. Kuipers, G. J. Vancso, N. F. van Hulst, *Phys. Rev. Lett.* 91, 038301 (2003).
- [13] R. A. L. Vallée, M. Van der Auweraer, F. C. De Schryver, D. Beljonne, M. Orrit, *ChemPhysChem*, 6, 81 (2005).
- [14] R. A. L. Vallée, P. Marsal, E. Braeken, S. Habuchi, F. C. De Schryver, M. Van der Auweraer, D. Beljonne, J. Hofkens, *J. Am. Chem. Soc.*, 127, 12011 (2005).

On the critical behavior of the specific heat in glass-formers

L. A. Fernández,¹ V. Martín-Mayor,¹ and P. Verrocchio^{2,*}

¹Departamento de Física Teórica I, Universidad Complutense, Av. Complutense, 28040 Madrid, Spain

²Dipartimento di Fisica, Università di Trento, via Sommarive 14, 38050 Povo, Trento, Italy

The glass-transition differs from standard phase transitions in that the equilibration time of glass-formers (polymers, supercooled liquids, colloids, granulars, super-conductors, ...) diverges without apparent dramatic changes in their structural properties. Reconciling these two faces is a major challenge for condensed matter physics.

A general mechanism producing a divergence of the equilibration time of an homogeneous system at finite temperature is the divergence of a correlation length (*critical slowing down*). Since static quantities do not seem to reveal fluctuations over large length scales close to the glass-transition, it has been suggested that dynamic functions, such as time-correlators, must be rather studied (*dynamic heterogeneities* scenario).

Here we report numeric simulations at odds with the previous scenario. Exploiting a fast Monte-Carlo algorithm which reduces of a factor ~ 200 the relaxation time, we find in a fragile glass-forming liquid large scale fluctuations of the specific heat, a static function[1]. Moreover, the infinite-volume specific heat shows a power-law divergence. This suggests that the dynamical features of the glass-transition might be ascribed to critical slowing down arising from a continuous phase transition. The difficulty in recognizing it is due to the fact that standard experiments are not devised to detect spatial fluctuations in the energy density.

A large correlation-length can be detected through Finite-Size effects. In Fig. 1(a) we show the specific heat dependence on the size of the simulation box, L . Down to $T = 0.921T_{mc}$ (T_{mc} being the mode-coupling temperature) no finite-size effects are detected. However, for $T = 0.897T_{mc}$, a noticeable growth of the specific-heat is found up to $L \sim 4\text{nm}$, which is then a rough estimate of the correlation-length. This length is well above the interaction range (a fews \AA). Consistently, Fig. 1(b) shows that at $T = 0.897T_{mc}$ the time-correlator of the energy decays more slowly as L grows. Studying the critical behavior in the infinite-volume specific heat (Fig.1(c)) is difficult due to the presence of a large non-critical background. Fortunately, the background is described by the Rosenfeld-Tarazona law, $T^2C_V \propto T^{8/5}$. From $T \sim T_{mc}$ to beyond $10T_{mc}$ the $T^{8/5}$ law is extremely accurate (Fig.1(c)), while at lower temperatures *devi-*

ations start to be significant. Such deviations point toward the existence of a critical point, since they show a power-law divergence over two decades (Fig.1(d)).

From our simulations potential energy, rather than density, fluctuations emerge as the best candidates for the study of this critical phenomenon. While measurements of the frequency dependence of the specific heat are an appealing possibility to estimate the energy re-

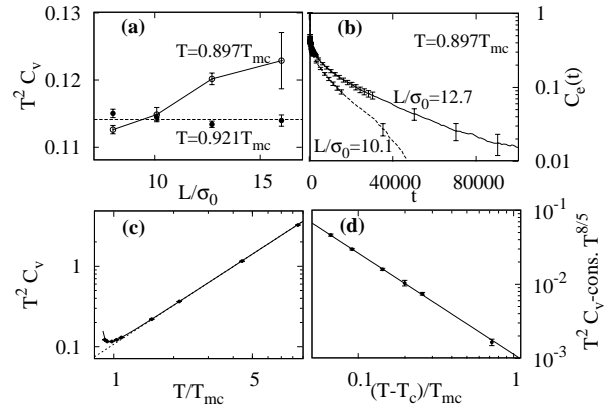


FIG. 1: Panel (a): the specific heat is a growing function of the simulation box size, until the system becomes much larger than the correlation length. This is visible for $L < 12\sigma_0$ ($\sigma_0 = 3.5\text{\AA}$ in Argon units) at $T = 0.897T_{mc}$, but not at $T = 0.921T_{mc}$. The correlation length grows quickly close to T_c , which is confirmed by the time correlator for the potential energy (b). Panel (c): infinite volume specific-heat vs. temperature. The dotted line is the $T^{8/5}$ Rosenfeld-Tarazona law. Deviations from the $T^{8/5}$ law can be fitted by a critical divergence (full line in (d)).

laxation time, the correlation-length could be studied by Finite-Size Scaling of the specific-heat and of relaxation times in films or in larger pores than previously used to confine glass-formers.

* Corresponding author: paolo.verrocchio@unitn.it
 [1] L.A. Fernandez, V. Martin-Mayor, P. Verrocchio, cond-mat/0504327

Influence of Angular Potentials on the Crystallization of Model Polymer Chains

Thomas Vettorel,* Hendrik Meyer, and Jörg Baschnagel
Institut Charles Sadron, CNRS
 6 rue Boussingault, 67083 Strasbourg, France

We used a simplified polymer model which allows an efficient and accurate description of crystallization of polymers. Going one step further than usual united-atom models, we resume all atoms of a monomer into one sphere. The coarse-graining is performed to map results from atomistic simulations of poly(vinyl alcohol) onto the parameters of our simpler model CG-PVA [1, 2]: Connectivity, an excluded-volume interaction which contains no attractive part and, most importantly, an angular potential accounting for specific properties of the polymer. These angles result from two consecutive dihedral angles on the atomic scale (hence the three minima corresponding to trans-trans, trans-gauche and gauche-gauche torsions of the backbone, see fig. 1). The relation between the angular potential and other quantities such as the radius of gyration is non-trivial with this three-state model.

We varied the depths of minima and heights of barriers in the angular potential (fig. 1 presents the original CG-PVA potential as well as two variations, $x4$ and $x8$; the figure also displays the corresponding phase diagrams). One can observe that for the $x4$ potential, the second minimum is shallower, which favours the states in which bond angles are stretched. This makes crystallization easier: T_{cryst} is higher in that case than for CG-PVA. For $x8$ on the contrary, the angular potential being closer to the original one, but still the two phase diagrams are different (a lower fraction of stretched states can be observed for $x8$, which results in a more frustrated structure and a lower T_{cryst}).

Using the different polymer models created in modifying the angular potential, we tried to point out some correlations between measured quantities, including the characteristics of the potentials and the related probability distributions. For most cases, no clear conclusion can be drawn. However, there is a definite correlation between the trans-trans fraction (measured as the probability to find an angle $\theta > 150^\circ$) in

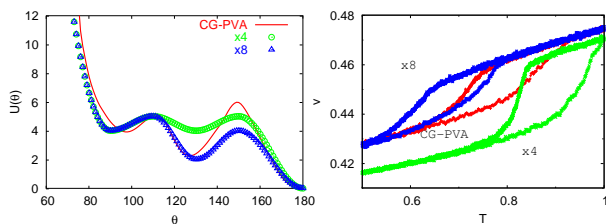


FIG. 1: Phase diagrams obtained by continuous cooling at rate $5 \cdot 10^{-6} \tau^{-1}$ (right) for the models with the corresponding angular potentials (left)

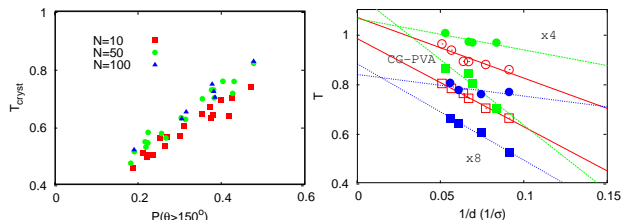


FIG. 2: Crystallization temperature vs. probability of stretched angle for the different angular potentials used, and for different chain lengths (left); Crystallization (squares) / Fusion (circles) temperature vs. inverse stem length (right)

the melt at high temperature and the crystallization temperature (see fig. 2). This means that the conformation far from the transition seems to strongly influence the crystallization process. Thus, the folds being strongly present in the melt prevent the crystal from having a long extension along the chain axes.

Crystallization can also be studied during an isothermal relaxation simulation (fig. 2): It is then possible to determine an average length d for the crystalline parts of the chains for a given supercooling (below some limit crystallization temperature). As expected, d is inversely proportional to the supercooling. These crystallization and melting lines have been already discussed earlier [3] and are used by Strobl to support his picture of intermediate phases [4]. It is interesting that these lines are present in this simple model where no mesomorphic phase is expected and this point deserves further investigation.

- * Corresponding author: vettorel@ics.u-strasbg.fr
- [1] H. Meyer and F. Müller-Plathe, *J. Chem. Phys.* **115** (2001) 7807;
 - [2] H. Meyer and F. Müller-Plathe, *Macromolecules* **35** (2002) 1241;
 - [3] A. Keller, G. Goldbeck-Wood and M. Hikosaka, *Faraday Discuss.*, 1993, **95**, 109-128
 - [4] G. Strobl, *Eur. Phys. J. E*, 3:165, 2000

Collective Single Particle Jumps Below The Glass Transition: A Computer Simulation

Katharina Vollmayr-Lee*

*Institut für Theoretische Physik,
Universität Göttingen, Friedrich-Hund-Platz 1,
D-37077 Göttingen, Germany*

and

*Department of Physics, Bucknell University,
Lewisburg, Pennsylvania 17837, USA*

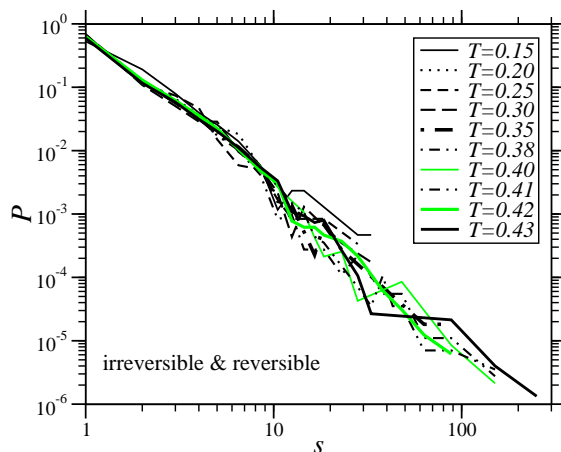


FIG. 1: Log-log plot of the distribution of cluster sizes of simultaneously (irreversible and reversible) jumping particles.

We study a binary Lennard-Jones mixture below the glass transition via molecular dynamics simulations. To investigate the dynamics of the system we define single particle jumps via their single particle trajectories [1]. We find two kinds of jumps: “reversible jumps,” where a particle jumps back and forth between two or more average positions, and “irreversible jumps,” where a particle does not return to any of its former average positions, i.e. successfully escapes its cage. We present as a function of temperature the number of jumps, jump size and waiting time between jumps. With increasing temperature particles undergo more jumps, the ratio of irreversible to reversible jumps increases, and the jump size increases. The waiting time between successive jumps however is independent of temperature.

To study how the single particle jumps are correlated in time and space we investigate (I) clusters of simultaneously jumping particles and (II) tempo-

rally extended clusters, i.e. clusters of jump events for which the jumping particles are spatially nearby and the jumps occur at consecutive times. We find highly collective jump processes: For cases (I) and (II) we find that up to 100–300 single particle jumps are spatially and temporally correlated. In case (II) up to 25 consecutive times (of 125 for the whole simulation run) are involved. These most collective processes happen at the beginning of the simulation run but even at later times up to 50 jumping particles are spatially and temporally correlated. To investigate how typical these highly correlated jump processes are, we present the distribution of cluster sizes $P(s)$. As shown in Fig. 1 for case (I), we find $P(s) \sim s^{-\tau}$ with $\tau \approx 2.5$ in case (I) and $\tau \approx 2.3$ in case (II). In comparison, Donati et al. [2] find above the glass transition such a power law only for their lowest temperature. In contrast we find that $P(s)$ is temperature independent (see Fig. 1). We also find that $P(s)$ is independent of the waiting time. By studying the average coordination number within the clusters as a function of the cluster size, we find that the shape of the clusters is string-like.

I would like to thank K. Binder and A. Zippelius for hospitality, financial support and for their helpful discussions. I also thank J. Horbach and B. Vollmayr-Lee for helpful discussions. I gratefully acknowledge financial support from SFB 262 and DFG Grant No. Zi 209/6-1.

* Corresponding author: kvollmay@bucknell.edu

[1] K. Vollmayr-Lee, J. Chem. Phys. **121**, 4781 (2004).

[2] C. Donati, S. C. Glotzer, P. H. Poole, W. Kob, and S. J. Plimpton, Phys. Rev. E **60**, 3107 (1999).

Non-Gaussian aspects in glassy systems

Bart Vorselaars,* Alexey V. Lyulin, and M.A.J. Michels

*Group Polymer Physics, Eindhoven Polymer Laboratories,
Technische Universiteit Eindhoven, P.O. Box 513, 5600 MB Eindhoven, The Netherlands*

Glasses are in between solids and liquids. Their long-time relaxation, often exceeding the experimental time scale is typical for a solid, while their disordered non-crystalline structure is typical for a normal liquid. The question is in what way this disordered structure has its influence on the dynamics of the particles the glass consists of.

In this paper we look at the non-Gaussian behaviour of the dynamics. The non-Gaussianity of the dynamics is usually expressed in terms of the (second) time-dependent non-Gaussian parameter $\alpha_2(t)$, which is a measure of the variance of the mean square translational displacement, when compared to the Gaussian case. As an example, the self part of the van Hove function of a purely diffusive particle has a Gaussian shape and the parameter equals 0. So a non-zero value of $\alpha_2(t)$ indicates non-Gaussian behaviour. This is often interpreted as an effect of the cooperative and heterogeneous nature present in glasses.

Using molecular dynamics we simulate a typical polymer glass former, atactic polystyrene (PS). It is seen that this material indeed shows non-Gaussian be-

haviour close to the glass transition.

To interpret this non-Gaussian behaviour, we study a simple model, in which the cage-effect is incorporated. It consists of a particle moving in a periodic external field. The motion of the particle is governed by the Langevin equation. This equation is solved numerically.

The results are compared with the molecular simulation results for PS and for low-molecular weight compounds. It turns out that the behaviour is very similar, thereby suggesting that the underlying mechanism of the non-Gaussian dynamics is the same, both for low-molecular weight systems and polymer glass-formers. Moreover, by analyzing the results of the simple model, it is possible to explain some features of the bell-shaped main peak of $\alpha_2(t)$.

* Corresponding author: B.Vorselaars@tue.nl

Configurational Heat Capacity of Aluminosilicate Melts

Sharon L. Webb*

Mineralogy Department, Georg-August-University, 37077 Göttingen, Germany

The relationship between a melt's structure and its physical properties (density, viscosity, shear modulus, compressibility) has been used as a rich source of information on melt structure and how silicate melts flow; and as a basis for discussing changing physical properties of melts with changing composition, temperature and pressure. The mechanism by which melts flow determines their viscosity and the energy required for viscous flow to occur. While the basic flow mechanism is the exchange of Si-O bonds, changes in melt structure introduce pre- and post-Si-O bond exchange structures that have varying bond energies, timescales and probabilities.

Although the description of flow mechanisms in binary alkali-silicate melts is clear; that for multi-oxide compositions quickly becomes very complex. It is not clear whether alkaline-earths with their 2+ charge can charge-balance two oxygens. The addition of aluminium to melts creates the need for a charge-balancing cation for the tetrahedrally co-ordinated Al^{3+} . With the presence of both X^+ and Y^{2+} atoms there are questions about which atom is preferred as the charge balancer and which will form non-bridging oxygen bonds.

These questions can be answered by determining the physical properties of melts as a function of composition in combination with structural information from NMR and Raman, X-ray or other spectroscopic techniques. The effect of the addition of each new atom on the melt structure needs to be addressed individually in order to unravel the relationship between physical properties and structure.

The $Na_2O-Al_2O_3-SiO_2$ and $CaO-Al_2O_3-SiO_2$ systems are used as analogues for the more complex natural magmatic systems of the earth. This study addresses the structure of peraluminous ($Al > Na + Ca$) and peralkaline ($Al < Na + Ca$) $Na_2O-CaO-Al_2O_3-SiO_2$ melts and the change in structure with composition via determination of their shear viscosity and heat capacity.

The structural changes occurring as a function of composition in these melts can be addressed in terms of their heat capacity, configurational heat capacity and configurational entropy at a viscosity of 10^{12} Pa s. The configurational heat capacity (c_p^{conf}) is determined from

the difference between the liquid (c_{pl}) and the glass (c_{pg}) heat capacity at the glass transition temperature.

To a first approximation c_{pg} can be calculated from a linear summation of the c_{ps} of the oxide components. Similarly, if there are no anomalous changes in melt structure upon heating through T_g , the c_{pl} will be a linear sum of the contributions of the component oxides [1]. Configurational entropy $S_{conf}(T_g)$ can be calculated from viscosity data obtained in the range $10^9 - 10^{13}$ Pa s [2]. The compositional variation in $B/S_{conf}(T_g)$ for some $Na_2O-Al_2O_3-SiO_2$ and $CaO-Al_2O_3-SiO_2$ melts with 67 and 50 mol% SiO_2 respectively are presented in Figure 1. The viscosity and heat capacity data for both series of melts indicate a change in melt structure at the $Na_2O+CaO = Al_2O_3$ composition.

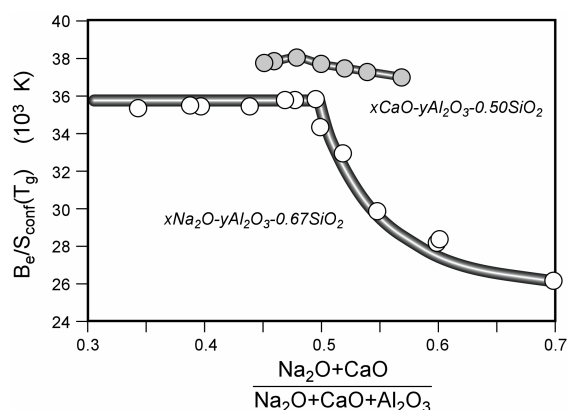


Figure 1. Configuration entropy data for a series of $Na_2O-Al_2O_3-SiO_2$ and $CaO-Al_2O_3-SiO_2$ melts as a function of composition. Data from [3], [4] and [5].

* Corresponding author: swebb@gwdg.de

- [1] P. Richet and Y. Bottinga, *Geochim. Cosmochim. Acta.*, **49**, 471 (1985)
- [2] M. J. Toplis, *Am. Mineral.*, **83**, 480 (1998)
- [3] S. L. Webb et al., *Am. Mineral.*, **89**, 812 (2004)
- [4] M. J. Toplis et al., *Am. Mineral.*, **82**, 979 (1997)
- [5] M. J. Toplis and D.B. Dingwell, *Geochim. Cosmochim. Acta.*, **68**, 5169 (2004).

Random packing of spherical and non-spherical particles

Alan Wouterse* and Albert Philipse

Van 't Hoff laboratorium, Debye Institute, Utrecht University, The Netherlands

The effect of particle shape on the packing of particles was studied using a recently developed simulation method [1]. We investigated random packing density for monodisperse shapes in a wide range of aspect ratios for the existence of a density maximum for near-spheres and a limiting packing law for high aspect ratio particles (See Fig. 1).

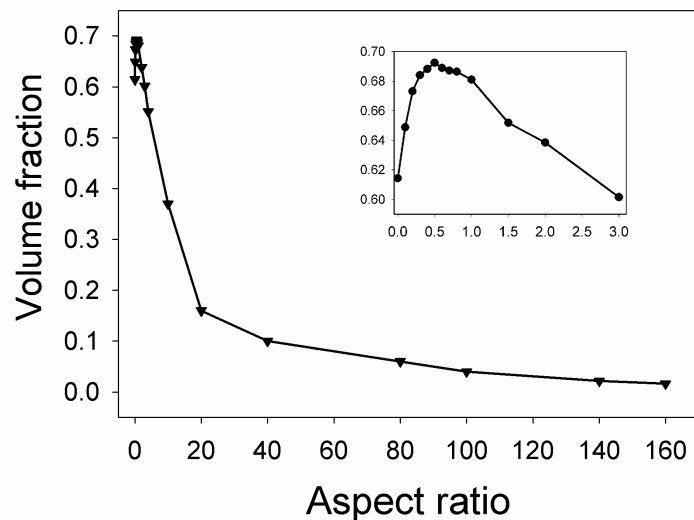


FIG. 1: Volume fractions of random rod packings as a function of aspect ratio

This study shows the importance of the geometrical shape on physical properties of particle packings.

It is expected that the same geometrical effects that play a role in random packing also play a roll in glassy systems and viscous liquids containing non-spherical particles. For high aspect ratio the particles form entangled networks which can dramatically increase the viscosity of a fluid, whereas a slight shape deformation may substantially decrease the viscosity of a hard-sphere glass.

Not only shape variation but also size variation can influence the properties of a random packing. To this end bidisperse sphere packings were studied [2]. Besides the already known triangular density distribution we found that bidisperse packings show properties which can be defined by local contact numbers [3].

* Corresponding author: a.wouterse@chem.uu.nl

[1] S. R. Williams and A.P. Philipse, *Phys. Rev. E* **67**, 051301 (2003).

[2] K. de Lange Kristiansen, A. Wouterse, A.P. Philipse, *Physica A* **358**, 249-262 (2005).

[3] A. Wouterse, M. Plapp, A. P. Philipse, *J. Chem. Phys.* **123**, 054507 (2005).

Structure and diffusion in viscous surfactant mesophases.

Anand Yethiraj,^{1,*} Donatella Capitani,² Nicholas E. Burlinson,³ and E. Elliott Burnell³

¹*Department of Physics and Physical Oceanography,
Memorial University of Newfoundland, Canada.*

²*Institute of Chemical Methodologies, CNR, Italy.*

³*Department of Chemistry, University of British Columbia, Canada.*

The diffusion of both water and surfactant components in aqueous solutions of the nonionic surfactant $C_{12}E_6$ which includes hexagonal, cubic, lamellar, and micellar mesophases has been studied by pulsed-field-gradient NMR [1].

NMR spectra were obtained in unaligned and shear-aligned samples in all of these phases. In these samples, significant memory effects were observed on temperature cycling across phase transitions.

Spectra and diffusion coefficients were also obtained via NMR in the hexagonal and lamellar phases in oriented monodomain samples that were magnetically aligned by slow cooling from the micellar phase in an 11.7 T magnet.

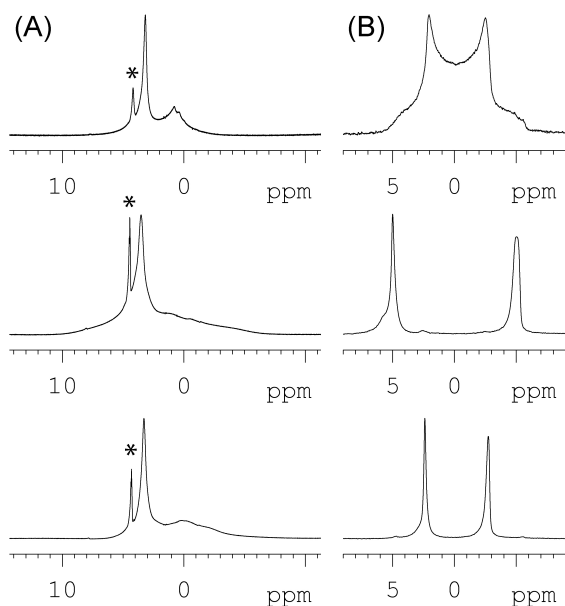


FIG. 1: (A) ¹H and (B) ²H spectra in powder sample (top), and in samples that had been magnetically pre-oriented parallel (middle) and perpendicular (bottom) to the B_0 NMR magnetic field. In pulsed gradients, the attenuation of the “parallel” and “perpendicular” spectra yield anisotropic diffusion coefficients.

These samples did not display memory effects. Measured water and soap diffusion coefficients in the

NMR-isotropic cubic and (high-water-content) micellar phases as well as diffusion anisotropy measurements in the magnetically aligned hexagonal phase were quantitatively consistent with the constituent structures of these phases being undulating surfactant cylinders with radius around 2 nm, with only the fraction of surface-associated water varying with the water-soap molar ratio.

The values of the water and soap diffusion coeffi-

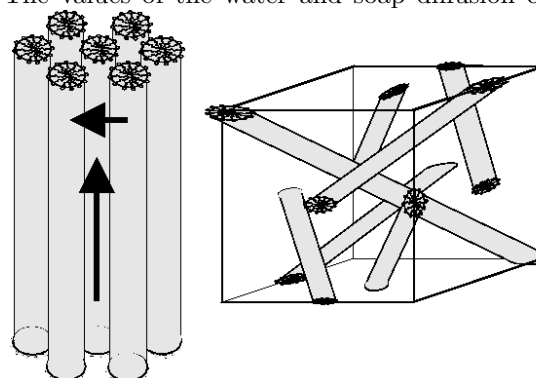


FIG. 2: The hexagonal (left), cubic (right) and micellar phases are all thought to be composed of cylindrical building blocks. Diffusion anisotropy measurements yield quantitative values for structure sizes. In particular, the hexagonal and micellar phases are consistent with being composed of undulating cylinders with radius 2nm.

coefficients in the oriented lamellar phase suggest an increase in defects and obstructions to soap diffusion as a function of increasing water content, while those in the low-water-content micellar phase rule out the presence of inverse micelles.

This work is being supported by the National Science and Engineering Research Council of Canada (NSERC).

* Corresponding author: anand@physics.mun.ca

[1] A. Yethiraj, D. Capitani, N.E. Burlinson, E.E. Burnell, *Langmuir*, **21**, 3311 (2005).

List of participants

Page numbers in **bold face** indicate authors with oral presentations; page numbers in normal print indicate the corresponding author of a poster presentation; page numbers in *italic* indicate co-authors.

Name	Page
Christiane Alba-Simionesco, Paris, France	67, 82
Michael Allen, Warwick, UK	
Roberta Angelini, Roma, Italy	48
Arantxa Arbe, San Sebastian, Spain	55 , 68, 83, 100
Silvia Arrese-Igor, San Sebastian, Spain	68
Nicholas P. Bailey, Roskilde, Denmark	69
Adriano Barra, London, UK	
Josef Bartoš, Bratislava, Slovak Republic	70
Jörg Baschnagel, Strasbourg, France	27 , 91, 98, 102, 114
Dmitry Bedrov, Salt Lake City, USA	26, 71
Mario Beiner, Halle, Germany	72
Ludovic Berthier, Montpellier, France	18
Rut Besseling, Edinburgh, Scotland	34
Kurt Binder, Mainz, Germany	103
Giulio Biroli, Paris, France	17 , 18, 24
Roland Böhmer, Dortmund, Germany	63
J.P. Bouchaud, Gif-sur-Yvette, France	24
Joe Brader, Konstanz, Germany	
Uli Buchenau, Jülich, Germany	73
Jose B. Caballero, Almeria, Spain	58 , 93
Daniele Cangialosi, San Sebastian, Spain	29
Simone Capaccioli, Pisa, Italy	74
Horacio E. Castillo, Athens, Ohio, USA	46
Andrea Cavagna, Rome, Italy	25
Dominique Champion, Dijon, France	75
David Chandler, Berkeley, USA	22
Tage Christensen, Roskilde, Denmark	54, 76, 87
Juan Colmenero, San Sebastian, Spain	29, 33, 55, 68, 83, 100, 111
Andrea Corsi, Milano, Italy	77
Gregor Diezemann, Mainz, Germany	49 , 63
Catherine Dreyfus, Paris, France	62, 94
Jeppe C. Dyre, Roskilde, Denmark	54 , 69, 87, 108
Nail Fatkullin, Kazan, Russia/Tatarstan	57, 80

Erhard W. Fischer, Mainz, Germany	
Peter Fouquet, Grenoble, France	82
Thomas Franosch, München, Germany	50
Matthias Fuchs, Konstanz, Germany	27, 36, 37, 41 , 93, 104
Emanuela Del Gado, Napoli, Italy	40
Juan Garrahan, Nottingham, UK	22
Burkhard Geil, Dortmund, Germany	63
Anne-Caroline Genix, San Sebastian, Spain	83
Antonis Gitsas, Ioannina, Greece	81
Katarzyna Gniazdowska, Göttingen, Germany	84
Roy Goldberg, Mainz, Germany	101
Martin Greenall, Edinburgh, UK	85
Jörg Hachenberg, Göttingen, Germany	86
Henrik Hansen, Roskilde, Denmark	
Tina Hecksher, Roskilde, Denmark	89, 108
Oliver Henrich, Konstanz, Germany	36, 37 , 104
Andreas Heuer, Münster, Germany	20
Gerald Hinze, Mainz, Germany	63
Felix Höfling, Berlin, Germany	50
Jürgen Horbach, Mainz, Germany	31, 51, 103
Hsiao-Ping Hsu, Mainz, Germany	
Sara Iacopini, Mainz, Germany	
Francesca Ianni, Rome, Italy	35
Brian Igarashi, Roskilde, Denmark	87
Svetlana Jungblut, Mainz, Germany	
Ravinath Kausik, Ulm, Germany	57
Mirko Kehr, Chemnitz, Germany	88
Norio Kikuchi, Mainz, Germany	51
Christopher Klieber, Cambridge, USA	89
Walter Kob, Montpellier, France	40
Hans König, Mainz, Germany	90
Vincent Krakoviack, Lyon, France	52
Torsten Kreer, Strasbourg, France	91
Kurt Kremer, Mainz, Germany	42
Tim Kruglov, Utrecht, The Netherlands	92
Erik Lange, Konstanz, Germany	93
Luca Larini, Pisa, Italy	95
Heine Larsen, Roskilde, Denmark	
Alexandre Lefevre, Gif-sur-Yvette	23
Dino Leporini, Pisa, Italy	65 , 95
Martin Letz, Mainz, Germany	
Valentin Levashov, Knoxville, USA	79
Jutta Luettmmer-Strathmann, Akron, USA	96
Alexey Lyulin, Eindhoven, The Netherlands	97, 116

Gurpreet S. Matharoo, Antigonish, Canada	61
Simone Melchionna, Rome, Italy	
Andreas Meyer, München, Germany	30
Hendrik Meyer, Strasbourg, France	<i>27, 91, 98, 102, 114</i>
Cristiano De Michele, Rome, Italy	78
Kenneth Mølbæk, Roskilde, Denmark	
Giulio Monaco, Grenoble, France	56
Angel Moreno, San Sebastian, Spain	33, 39
Stefano Mossa, Grenoble, France	99
Arturo Narros Gonzalez, San Sebastian, Spain	100
Kristine Niss, Paris, France	
Niels Boye Olsen, Roskilde, Denmark	<i>54, 76, 87</i>
Thomas Palberg, Mainz, Germany	101
Wolfgang Paul, Mainz, Germany	
Esben F. Pedersen, Roskilde, Denmark	<i>108</i>
Ulf R. Pedersen, Roskilde, Denmark	<i>108</i>
Simone Peter, Strasbourg, France	102
Patrick Pfeleiderer, Mainz, Germany	103
Robert M. Pick, Paris, France	62
Wilson Poon, Edinburgh, Scotland	34, 38
Antonio M. Puertas, Almeria, Spain	<i>58, 93, 104</i>
Laurence Ramos, Montpellier, France	47
David R. Reichman, New York, USA	21
Vakhtang Rostiashvili, Mainz, Germany	53
Rolf Schilling, Mainz, Germany	78
Walter Schirmacher, München, Germany	105
Johannes Schneider, Mainz, Germany	106
Herbert R. Schober, Jülich, Germany	107
Hans-Joachim Schöpe, Mainz, Germany	59
Thomas B. Schrøder, Roskilde, Denmark	<i>69, 108</i>
Tullio Scopigno, Rome, Italy	60
Klemens Seelos, Mainz, Germany	<i>101</i>
Iliia Sergueev, Grenoble, France	28
Grant D. Smith, Salt Lake City, USA	26, 71
Jens-Uwe Sommer, Mulhouse, France	43
Mireille Souche, Paris, France	109
Matthias Sperl, Durham, USA	64
H. W. Spiess, Mainz, Germany	44
Gilles Tarjus, Paris, France	19, 99
Yulia Trukhina, Mainz, Germany	
Julius Tsuwi, Leipzig, Germany	110
M. S. Tyagi, San Sebastian, Spain	<i>55, 111</i>
Renaud Vallée, Universiteit Leuven, Belgium	112
Fathollah Varnik, Düsseldorf, Germany	36

Paolo Verrocchio, Trento, Italy	113
Thomas Vettorel, Strasbourg, France	114
Michael Vogel, Münster, Germany	32
Thomas Voigtmann, Edinburgh, Scotland	31, 85
Katharina Vollmayr-Lee, Göttingen, Germany	115
Bart Vorselaars, Eindhoven, The Netherlands	116
Sharon L. Webb, Göttingen, Germany	84, 117
Alan Wouterse, Utrecht, The Netherlands	118
Yefeng Yao, Mainz, Germany	44
Leonid Yelash, Mainz, Germany	
Anand Yethiraj, St. John's, NL, Canada	119
Emanuela Zaccarelli, Roma, Italy	39
Michaela Zamponi, Jülich, Germany	45
Jochen Zausch, Mainz, Germany	